

UC Irvine

UC Irvine Electronic Theses and Dissertations

Title

Characterization and Source Apportionment of Greenhouse Gas Emissions in the Los Angeles Megacity

Permalink

<https://escholarship.org/uc/item/5f14m7qp>

Author

Vizenor, Nicholas Matthew

Publication Date

2018

Peer reviewed|Thesis/dissertation

UNIVERSITY OF CALIFORNIA,
IRVINE

Characterization and Source Apportionment of Greenhouse Gas Emissions in the Los Angeles
Megacity

DISSERTATION

submitted in partial satisfaction of the requirements
for the degree of

DOCTOR OF PHILOSOPHY

in Chemistry

by

Nicholas Vizenor

Dissertation Committee:
Professor Donald R. Blake, Chair
Professor Barbara J. Finlayson-Pitts
Professor Sergey Nizkorodov

2018

DEDICATION

To

Michael Hutter and Romuald “Ray” Hutter

You both inspired me as a child to explore the world of science and engineering. You taught me how to speak up for myself and defend what I know to be right. I miss you both dearly, and I know that we would have had many great discussions about my thesis and the current state of science as I progressed through this grad school process.

TABLE OF CONTENTS

	Page
LIST OF FIGURES	vii
LIST OF TABLES	xii
ACKNOWLEDGMENTS	xiv
CURRICULUM VITAE	xv
ABSTRACT OF THE DISSERTATION	xviii
CHAPTER 1: Introduction and Background	1
1.1 The Science of Climate Change	1
1.1.1 The Greenhouse Effect	1
1.1.2 Anthropogenic Greenhouse Gas Emissions	2
1.1.3 Evidence for Climate Change	3
1.1.4 Current Regulations and Predicted Future Scenarios	5
1.2 Greenhouse Gases	7
1.2.1 CO ₂ : Sources and Sinks	7
1.2.2 Methane	11
1.2.2.1 Anthropogenic Methane Sources	13
1.2.2.1.1 Methane from Anaerobic Bacteria	13
1.2.2.1.1.1 Agriculture	14
1.2.2.1.1.2 Waste Management	15
1.2.2.1.2 Fossil Methane	16
1.2.2.1.3 Pyrogenic Methane	18
1.2.2.2 Methane from Natural Sources	18
1.2.3 Halocarbons	19
1.2.3.1 Chlorofluorocarbons	19
1.2.3.2 Hydrochlorofluorocarbons	20
1.2.3.3 Hydrofluorocarbons	22
1.2.3.4 Fourth Generation Refrigerants	22
1.3. The Fossil Fuel Industry	23
1.3.1 Coal	23
1.3.2 Oil	23
1.3.3 Natural Gas	24
1.3.3.1 Sources of Leakage in Production and Transmission	24
1.4 .The South Coast Air Basin	28
1.4.1 Geographical and Meteorological Background	28
1.4.2 History of Air Quality and Emissions in the SoCAB	30
1.4.3 Recent Greenhouse Gas Emissions Regulations and Studies	32
1.4.4 Oil and Natural Gas in the SoCAB	34
1.5 References	36

CHAPTER 2: Methods	44
2.1 Sampling Site	44
2.2 Project Description	44
2.3 Gas Chromatography Analysis	48
2.4 Creation and Use of Working Standards	54
2.5 Detection and Quantitation of new HFCs	55
2.6 Autosampler Offgassing Test	58
2.7 Precision Test	59
2.8 Historical Data	59
2.9 References	60
CHAPTER 3: Trends in SoCAB Hydrocarbon Mixing Ratios and Emissions	61
3.1 Data Overview	61
3.2 Wind Direction and Speed Data	62
3.3 Enhancement Analysis	69
3.3.1 Selection of Background Values	69
3.3.2 Alkane Enhancement Results	72
3.3.3 Enhancement Ratio Analysis	73
3.3.3.1 Ethane to Methane Ratio	73
3.3.3.2 Propane to Ethyne	78
3.3.3.3 Isopentane to <i>n</i> -pentane	79
3.4 Seasonal Variation	81
3.4.1 Carbon Monoxide	81
3.4.2 Other Species	82
3.5 Conclusions	85
3.6 References	86
CHAPTER 4: Using Positive Matrix Factorization for Source Apportionment	89
4.1 Positive Matrix Factorization Background and Theory	89
4.2 Positive Matrix Factorization Analysis	91
4.2.1 Data Filtering	91
4.2.2 Positive Matrix Factorization Inputs	92
4.2.3 Analysis of Number of Factors	94
4.3 Results from Seasonal Analysis	95
4.3.1 Summer	95
4.3.2 Fall	100
4.3.3 Winter	103
4.3.4 Spring	107
4.4 Results from Full Two Year Mt. Wilson Data Set	112
4.4.1 Source Identification and Analysis	112
4.4.2 Biogenic Emissions Factor	116
4.4.3 Vehicular Emissions Factors	118
4.4.4 Industrial Solvent Use	120
4.4.5 Light Alkanes Factor: Oil and Gas Production Source	120
4.4.6 Natural Gas Factor	121

4.4.7 Bacterial Methane	122
4.4.8 Issues with Ethene and Propene	124
4.5 Discussion of PMF Utility in the SoCAB	126
4.6 References	128
CHAPTER 5: Further Natural Gas Analysis	131
5.1 Natural Gas Composition Testing	131
5.1.1 Collection and Gas Chromatography Analysis	131
5.1.2 Results	134
5.1.3 Discussion	135
5.2 Quantifying Natural Gas Emissions in the SoCAB	139
5.3 Natural Gas Leakage Studies	143
5.3.1 UCI Indoor Sampling Study	143
5.3.1.1 Background	143
5.3.1.2 Methods and Site Description	144
5.3.1.3 Results and Discussion	145
5.3.2 SoCalGas Leakage Map Study	147
5.3.2.1 Background of Pipeline Leaks in Cities	147
5.3.2.2 SoCalGas Leak Map and Study Details	148
5.3.2.1 Results and Discussion	151
5.4 Aliso Canyon Natural Gas Leak	152
5.4.1 Determination of Porter Ranch Influenced Samples	153
5.4.2 Analysis of Influenced Samples	157
5.5 Conclusions	158
5.6 References	159
CHAPTER 6: Top-down Emissions Estimates of Hydrocarbons in the SoCAB	161
6.1 Background and History of Emissions Estimates	161
6.2 Calculating Emissions Estimates	162
6.2.1 Top-down Estimate Calculations	162
6.2.2 CARB's CO Estimate	163
6.3 Results and Discussion	166
6.3.1 Enhancement Plots and Correlations	166
6.3.2 Hydrocarbon Emissions Estimates	171
6.3.2.1 Comparing Methane and Ethane Emissions Estimates	172
6.3.2.2 Hexane Emissions Estimate	173
6.4 Combining PMF and Emissions Estimates for Inventory Creation	174
6.6 References	176
CHAPTER 7: Emissions Estimates and Analysis of Refrigerant Halocarbons	179
7.1 Statistical Analysis and Calculation of Emissions Estimates	179
7.2 Results	179
7.2.1 Banned First Generation CFCs	186
7.2.2 HCFC-22	188
7.2.3 HCFC-141b	191
7.2.4 HCFC-142b	192

7.2.5 HCFC Replacements	193
7.3 Conclusions	195
7.4 References	196
CHAPTER 8: Conclusions	198

LIST OF FIGURES

		Page
Figure 1.1	Law Dome ice core concentration of CO ₂ since the beginning of the Common Era. The vertical line represents the beginning of the Industrial Revolution. The last data point shown is from 1955.	3
Figure 1.2	Nine year rolling average of fraction of the contiguous United States land that experienced an extreme precipitation event	5
Figure 1.3	Infrared spectra of the three most prevalent greenhouse gases in the atmosphere: water, carbon dioxide and methane. Spectra from NIST Chemistry WebBook	8
Figure 1.4	Law Dome ice core concentration of methane since the beginning of the Common Era. The vertical line represents the beginning of the Industrial Revolution. The last data point shown is from 1955.	13
Figure 1.5	Price and consumption of natural gas in the United States since 2005. Due to advances in fracking and shale gas technology, natural gas prices have continued to drop despite increased demand. Data for plot taken from Energy Information Administration.	17
Figure 1.6	Monthly average atmospheric concentrations of various halocarbons as seen at Trinidad Head, CA. Plot was created with data from the AGAGE Network	21
Figure 1.7	Map of the western United States with the Southern California region outlined. In the lower map, the South Coast Air Basin is outlined in red. Outlined in black are the active oil fields in the SoCAB. The blue circles represent SoCalGas natural gas storage wells. The black triangle represents Mt. Wilson, where the air sampling study took place.	29
Figure 2.1	The greater South Coast Air Basin as seen from the Mt. Wilson sampling site at various times of day and the year. The top left image shows the extent to which the marine layer can infiltrate the region. The top right image shows the marine layer breaking up later that same day, and the bottom image shows a summer afternoon in which one can see to the coast.	45
Figure 2.2	Schematic of the autosampler setup that was used at the Mt. Wilson site. Shown are 8 of the 32 canisters and lines. Each line has its own pneumatic valve that allows for the filling of one canister at a time..	47

Figure 2.3	Schematic of the parallel gas chromatography system used to analyze carbon monoxide and carbon dioxide. To detect CO via FID, the CO must first be catalytically converted to methane.	49
Figure 2.4	Schematic of the parallel 5 column gas chromatography system used to analyze VOCs	51
Figure 2.5	Single ion monitoring chromatograms from the DB-5 MS column of newly detected HFCs. In the top chromatogram is the peak representing HFC-227ea. In the middle chromatogram is the peak representing HFC-245fa. In the bottom chromatogram is the peak representing HFC-365mfc. The ions being monitored were m/z 151, m/z 115, and m/z 133 respectively.	57
Figure 3.1	Wind rose plot of winds arriving at the Mount Wilson sampling site at the start of each daytime sample during the full two years of the study. The radial axis represents the fraction of the time the wind was blowing from a given direction, and the speed is color coded. Meteorological data was taken from the nearby Clear Creek weather station five miles east of Mt. Wilson	64
Figure 3.2	Wind rose plot of winds arriving at the Mount Wilson sampling site at the start of each daytime sample during the full two years of the study separated by season. The radial axis represents the fraction of the time the wind was blowing from a given direction, and the speed is color coded. Meteorological data was taken from the nearby Clear Creek weather station five miles east of Mt. Wilson	65
Figure 3.3	HYSPLIT back trajectories starting from the base of the San Gabriel Mountains in front of Mt. Wilson that are representative of the trajectories commonly found in each season. In a vast majority of cases, air masses passed through the SoCAB before reaching the mountains.	68
Figure 3.4	Seasonally averaged background methane mixing ratios taken from the two Mt. Wilson data sets. The background methane mixing ratio rose 8.5 ± 1.9 ppb/yr over the span between the two studies.	72
Figure 3.5	Ethane to methane enhancement ratios seen at Mt. Wilson over the two year year sampling period. A slight overall increase is noted along with significant variation day to day. Average error in each ratio is $\pm 0.12\%$. due to error propagation.	75
Figure 3.6	HYSPLIT back trajectory analysis for May 26, 2015 in which the four samples collected at Mt. Wilson varied substantially in ethane to methane enhancement ratios despite showing the same trajectory to the site.	77

Figure 3.7	Correlation plot of isopentane and n-pentane enhancements in SoCAB influenced samples seen at Mt. Wilson. There appear to be a variety of sources of pentanes to the region.	80
Figure 3.8	Seasonality of isoprene emissions as seen at Mt. Wilson, CA over the full two years of sampling. Due to the increased temperatures and more intense daylight, isoprene emissions spike in the summer months.	84
Figure 4.1	Relationship between the experimental Q value and the number of factors selected for a PMF analysis of the full two year Mt. Wilson data set	94
Figure 4.2	Profiles of the six factors resolved from positive matrix factorization of the summer SoCAB influenced samples.	96-97
Figure 4.3	A) Normalized contributions of oil and gas production and gasoline liquids factors to the samples collected at Mt. Wilson in summer 2014 and summer 2015. B) Normalized contributions of the natural gas factor during the same time period.	99
Figure 4.4	Profiles of the five factors resolved from positive matrix factorization of the fall SoCAB influenced samples.	101-102
Figure 4.5	Profiles of the five factors resolved from positive matrix factorization of the winter SoCAB influenced samples including the transient industrial source.	104-105
Figure 4.6	Profiles of the six factors resolved from positive matrix factorization of the spring SoCAB influenced samples including the transient industrial source.	108-109
Figure 4.7	Profiles of the seven factors resolved from positive matrix Factorization of the SoCAB influenced samples for the two full years of sampling	113-115
Figure 4.8	Relationship between the normalized contribution of the biogenic factor from PMF analysis and the mixing ratio of isoprene in a given sample. The positive correlation confirms the determination of the factor as being biogenic in nature.	117
Figure 5.1	Top: Chromatogram of a natural gas sample run on the Db-1 column of the NMHC system described in Chapter 2. Bottom: A portion of the above chromatogram zoomed in 50x. All retention times are in minutes.	133

Figure 5.2	Correlation between the percentage of propane and ethane in natural gas samples collected in the SoCAB.	137
Figure 5.3	Composition of natural gas collected once a month in canisters and the average monthly reported composition of the natural gas at the Playa del Rey Storage Facility as reported by SoCalGas.	137
Figure 5.4	Trends seen in ethane to methane ratios in the South Coast Air Basin and in natural gas supplied to the region.	142
Figure 5.5	Sample of SoCalGas operated and published natural gas leakage map of part of Tustin, CA. The sites marked in green are those that are being monitored and the sites in blue are those that are slated to be repaired.	149
Figure 5.6	Correlation plots of methane and ethane mixing ratios versus carbon monoxide mixing ratios seen in daytime samples during the Mt. Wilson sampling period plotted with 95% confidence ellipses and the median in red	154
Figure 5.7	HYSPLIT back trajectory from the base of Mt. Wilson showing that their mass had passed over the Aliso Canyon blowout at 34.31 N 118.55 W	155
Figure 6.1	California Air Resources Board estimated inventories for CO Emissions in the South Coast Air Basin based on base year 2008 and 2012.	165
Figure 6.2	Correlation and enhancement plots of methane and ethane versus CO seen at the Mt. Wilson sampling site. Errors in the slope and y-intercept are 95% confidence intervals.	170
Figure 7.1	Temporal patterns of HCFC-22 mixing ratios as seen at Mt. Wilson during the 2007-2008 sampling campaign.	182
Figure 7.2	Temporal patterns of HCFC-141b mixing ratios as seen at Mt. Wilson during the 2007-2008 sampling campaign.	183
Figure 7.3	Temporal patterns of HCFC-142b mixing ratios as seen at Mt. Wilson during the 2007-2008 sampling campaign.	184
Figure 7.4	Temporal patterns in the mixing ratios of the three most emitted HCFCs as seen at Mt. Wilson during the 2014-2016 campaign. The vertical dotted line denotes the beginning of the lowered cap on HCFC consumption by the EPA, and the black horizontal line is the seasonal average seen at Trinidad Head, CA, part of the AGAGE Network.	185

Figure 7.5	CFC-11 mixing ratio enhancements show no distinct seasonality in emissions when considering the two year Mt. Wilson data set presented here.	187
Figure 7.6	Enhancement plots of the three HCFCs studied here with carbon monoxide in both the 2007 (left) and 2014 (right) campaigns.	189
Figure 7.7	Temporal patterns in the mixing ratios of HFC-365mfc at Mt. Wilson during the 2014-2016 campaign. HFC-365mfc is the main industrial replacement for HCFC-141b. The results presented here are still exploratory, and so error on any given data point is $\pm 50\%$. The vertical dotted line denotes the beginning of the lowered cap on HCFC consumption by the EPA, and the black horizontal line is the seasonal average seen at Trinidad Head, CA, part of the AGAGE Network.	195

LIST OF TABLES

		Page
Table 1.1	Global warming potentials and atmospheric lifetimes for selected greenhouse gases that will be discussed in this work as described over a 20 and 100 year period.	11
Table 2.1	Statistical overview of the hydrocarbons and halocarbons used in analysis herein as measured by gas chromatography	53
Table 2.2	Overview of HCFCs and HFCs detected for the first time on our analytical system and their presence in our working standard as well as in global background samples	56
Table 3.1	Overview of mixing ratio results for selected hydrocarbon species from the daytime samples collected during the two year Mt. Wilson sampling project. Nd stands for not detected and means that at least one sample fell below our detection limits for that species. The 2007 daytime average mixing ratio is included for reference. IQR stands for interquartile range and is the difference between the mixing ratio at the 75th percentile and the 25th percentile.	62
Table 3.2	Average daytime enhanced mixing ratios for alkanes as seen from the same sampling site at Mt. Wilson during two different sampling intensives. The previous study ran from April 2007-February 2008, sampling every hour for a week during each of the 4 seasons. The reported errors are the 1σ uncertainties in the mean.	73
Table 3.3	Average daytime enhanced mixing ratios for carbon monoxide across the eight seasons of sampling at Mt. Wilsons. The reported errors are the 1σ uncertainties in the mean.	82
Table 3.4	Average daytime enhanced mixing ratios for species which showed summer values significantly higher than the rest of the year. The reported errors are the 1σ uncertainties in the mean.	84
Table 4.1	Averaged normalized contributions of emissions sources as determined via PMF analysis for the spring season by month shown with standard deviation	110
Table 4.2	Averaged normalized contributions of emissions sources as determined via PMF analysis for the full Mt. Wilson data set by season shown with standard deviation	119
Table 4.3	Samples influenced by petrochemical production in the SoCAB and the mixing ratios of select hydrocarbons in the samples	125

Table 5.1	Composition of natural gas collected once a month in canisters from the SoCAB	135
Table 5.2	Results from the UCI pilot study on indoor natural gas leakage. Errors shown are based on precision of individual measurements and error propagation	146
Table 5.3	Results from the pilot study into locations marked by SoCalGas as being potential or known points of natural gas leakage in the SoCAB	150
Table 5.4	Mixing ratios of selected alkanes and meteorological conditions for the four samples determined to have been influenced by the Aliso Canyon natural gas leak. The error in a given mixing ratio is based off of the stated precision in Table 2.1. The error associated with the averages is the standard error of the mean	156
Table 6.1.	California Air Resources Board estimated inventories for CO emissions in the South Coast Air Basin based on base year 2008 and 2012 by sector and how the estimate has changed.	166
Table 6.2	Enhancement slopes for hydrocarbons versus carbon monoxide ($\pm 1\sigma$ standard error) for the Mt. Wilson data set along with the percentage of the species associated with tailpipe emissions	167
Table 6.3	Hydrocarbon emissions rates for the period of June 2014 through May 2016 for the SoCAB as reported in Gg per year. Also included are literature estimates for previous studies of the region. Note that the CO estimate used in the current study is from an updated inventory as compared to the older studies.	171
Table 6.4	Methane and ethane emissions inventories based on positive matrix factorization results and total emissions estimates calculated using the CARB CO inventory for 2015. The ranges associated with each sector fraction are the results from displacement analysis ($dQ_{max}=4$).	175
Table 7.1	Summary of mixing ratios of first, second and third generation refrigerants seen in daytime samples collected at Mt. Wilson during the 2014-2016 campaign and the 2007 campaign (in parentheses).	180
Table 7.2	Annual SoCAB emissions estimates for the three most emitted HCFCs and the major replacement, HFC-134a, during both Mt. Wilson sampling campaigns and Barletta et al. which was an airborne sampling mission over the SoCAB that took place in May 2010.	190

ACKNOWLEDGMENTS

I would like to extend great appreciation and thanks to my research advisor Dr. Don Blake. Don, you have been a constant source of positive support and encouragement. In times when I found myself overwhelmed or out of my comfort zone, you always seemed to find a moment to pull me aside and let me know that I was doing a great job. If I had a question that stumped you as well, you always knew exactly to reach out to and always followed up with me. Thank you for believing in me and aiding me through this process

Thank you to Professors Sergey Nizkorodov and Barbara Finlayson-Pitts, members of my dissertation committee, for their support and advice throughout my graduate school career. You both challenged me to be a better scientist, but always in a supportive and uplifting manner.

Thank you to Professor Shane Ardo for encouraging me and helping me through the difficult transition to grad school and navigating my first quarter. You believed in me even during some of the most difficult moments of quantum mechanics. Holy Bananas!

To the technical staff of the Rowland-Blake lab including Simone Meinardi, Gloria Liu, and Brent Love, thank you! You are all the backbone that holds this lab together. Your technical advice, support, and time made this dissertation possible.

Thank you to Barbara Chisholm! Without you, I would be lost in a sea of receipts and bureaucracy. Your knowledge of the university and its many departments and practices has proved invaluable to me over the years. Your life advice will always stick with me!

To all members of the Rowland-Blake lab, past and present, thank you! Those of you whom I interacted with on a daily basis made grad school and life running cans more bearable!

To my fiancée Tory Doolin, I cannot express enough how lucky I am to have you in my life. I don't know how I would have made it through without your support, love, and encouraging smile. I am so excited to get to marry you next year!

To the Game Night crew! Thank you for being a weekly reprieve from the grind of academia. Having a group of friends as awesome as you all to commiserate about grad school and life with has been unbelievably beneficial.

Finally, to my parents and grandmother, I would not be where I am today without your love and support. You encouraged me as I began to explore science. You were always just a phone call away when I needed some guidance. You instilled in me many values that have shaped who I am today as a person and a scientist including integrity, humility and a strong work ethic! Thank you so much! I love you.

This work was funded largely by the California Air Resources Board.

CURRICULUM VITAE

Nicholas Vizenor

nvizenor@uci.edu

B47 Rowland Hall • University of California, Irvine • Irvine, CA 92617 • (530) 514-5892

EDUCATION

University of California, Irvine

Ph.D. in Chemistry (March 2018)

Dissertation Title: “Characterization and Source Apportionment of Greenhouse Gas Emissions in the Los Angeles Megacity”

California State University, Fresno

B.S. Chemistry (May 2013)

Summa Cum Laude with University and Departmental Honors

RESEARCH EXPERIENCE

Graduate Student Researcher - University of California, Irvine

2014-2018

Advisor: Dr. Donald Blake

Collection and Analysis of Whole Air Samples from Polluted and Remote Atmospheres

- Collected whole air samples at both ground based sites in Los Angeles and aboard NASA airborne missions around the Pacific Rim
- Analyzed samples for over 70 volatile organic compounds via three separate gas chromatography systems
- Designed and carried out a monthly sampling plan to collect air samples representative of the Los Angeles Basin over a two year study
- Conducted source apportionment of methane and ethane emissions in Los Angeles using positive matrix factorization to determine methane and ethane sources
- Calculated emissions estimates for CFCs and their replacements in Los Angeles
- Led pilot study to detect indoor natural gas leaks around UC, Irvine campus in collaboration with Dr. Jack Brouwer in the Department of Engineering
- Worked with Mothers Out Front activist group to attempt to detect natural gas pipeline leaks throughout Orange County
- Authored white paper for the City of Irvine on the issues facing the city over the next 100 years as a result of climate change. This paper was instrumental in the city council voting to approve a feasibility study for Community Choice Energy
- Analyzed large data sets using Excel, IGOR, R, and SPSS
- Authored annual reports to the California Air Resources Board with updates on data

Field Campaigns Participated In:

Student Airborne Research Project (SARP) – 2014
Front Range Pollution and Photochemistry Experiment (FRAPPE) – 2014
Wintertime Investigation of Transport, Emissions, and Reactivity (WINTER) – 2015
Korea-US Air Quality (KORUS-AQ) – 2016
Atmospheric Tomography Mission (ATom) - 2016-2017
UCI Global Monitoring Network 2014-2017

Undergraduate Researcher - California State University, Fresno 2011-2013

Advisor: Dr. Alam Hasson

Kinetic and Mechanistic Studies of Isoprene Hydroxynitrates with Atmospheric Radicals

- Conducted smog chamber experiments aimed at determining rate constants of isoprene hydroxynitrate compounds with atmospheric oxidants such as ozone and chlorine
- Determined possible mechanism pathways for the reactions based on product yield
- Utilized analytical techniques such as FT-IR and PTR-MS
- Interned at the National Center for Atmospheric Research during summer of 2012

Teaching Experience

University of California, Irvine

Head Lecture Teaching Assistant, Preparatory Chemistry Fall 2016

Laboratory Teaching Assistant, Analytical Chemistry Fall 2013 and Spring 2015

Laboratory Teaching Assistant, General Chemistry Spring 2014

Laboratory Teaching Assistant, Advanced Instrumental Analysis Winter 2014 and Winter 2017

California State University, Fresno

Private Tutor, General and Organic Chemistry 2012-2013

Departmental Tutor, General Chemistry 2011

Publications

Wunch, D.; Toon, G. C.; Hedelius, J. K.; **Vizenor, N.**; Roehl, C. M.; Saad, K. M.; Blavier, J.-F. L.; Blake, D. R.; Wennberg, P. O. Quantifying the Loss of Processed Natural Gas within California's South Coast Air Basin Using Long-Term Measurements of Ethane and Methane. *Atmospheric Chemistry and Physics* 2016, 16 (22), 14091–14105.

Hormaza-meija, A.; MacKinnon, M.; **Vizenor, N.**; Blake, D.R.; Brouwer, J. Consideration of Methane Emissions from Customer-side Infrastructure Sources. (In Review)

Kuwayama, T.; Charrier-Klobas J.; Chen, Y.; Vizenor, N.; Blake, D.R.; Pongetti, T.; Sander, S.; Croes, B.; Herner, J. Source Apportionment of Ambient Methane Enhancements in Los Angeles, California to Evaluate Emission Inventory (In Preparation)

Vizenor, N. and Blake, D.R. Evidence for the success of EPA phase outs of hydrochlorofluorocarbons as seen in an urban atmosphere. (In Preparation)

Presentations

“Methane: Sources of the Other Greenhouse Gas in Los Angeles” Oral Presentation at the UCI Grad Slam. Semifinalist. February 2018

“Climate Change and Community Choice Energy in the City of Irvine” Poster Presentation at the UCI Environmental Research Poster Symposium. December 2017

“Sherry Rowland and the Montreal Protocol” Guest Lecturer in History 21C: Modern World History, Climate and Disaster. July 2017

“Source Apportionment of Methane and Ethane in the South Coast Air Basin: The Role of Natural Gas Leakage” Poster Presentation at the 34th Informal Symposium on Kinetics and Photochemical Processes in the Atmosphere. May 2017

“Quantifying Methane Emissions in Los Angeles” Oral Presentation at the UCI Associated Graduate Students Symposium. April 2017. Won People’s Choice Award.

“Is Your Kitchen Leaking Methane? A Pilot Study at UCI” Oral Presentation with John Stansberry and Alejandra Hormaza-meija at the Science and Societal Impacts of Air Quality and Climate Issues: Past, Present, and Future Symposium. April 2017

“The Emission of Unburned Natural Gas in the South Coast Air Basin” Poster Presentation at the 33rd Informal Symposium on Kinetics and Photochemical Processes in the Atmosphere. March 2016

“A Kinetic Study of the Reactions of Isoprene Hydroxynitrates in the Troposphere” Oral Presentation at the Central California Research Symposium. Awarded Best Oral Presentation April 2013

“Kinetic and Mechanistic Study of Isoprene 4,1-hydroxy Nitrate” Poster Presentation at the 30th Informal Symposium on Kinetics and Photochemical Processes in the Atmosphere March 2013

Awards and Honors

NASA Group Achievement Award for Participation in KORUS-AQ August 2017

Michael E. Gebel Award May 2017

Excellence in Environmental Chemistry Research

Climate Action Training Program Member January 2017

Multidisciplinary group of ten graduate student scholars whose research goals are related to climate change. Received training in data visualization and scientific communication as well as funding for a summer internship

Chemistry Department Outstanding Undergraduate April 2013

Stanley and Frances Zeigler Physical Chemistry Scholarship May 2012

Downing Science Scholarship May 2012

ABSTRACT OF THE DISSERTATION

Characterization and Source Apportionment of Greenhouse Gas Emissions in the Los Angeles
Megacity

By

Nicholas Vizenor

Doctor of Philosophy in Chemistry

University of California, Irvine, 2018

Professor Donald R. Blake, Chair

Short lived greenhouse gases are an immediate target for reductions in climate policy planning. To understand to what extent legislation to limit greenhouse gas emissions is working, monitoring projects are necessary. In this work, whole air samples were collected downwind of the Los Angeles megacity over the course of two years between June 2014 and May 2016. Samples were analyzed via gas chromatography instruments to quantify over 70 volatile organic compounds with limits of detection on the single part per trillion level.

Unlike larger hydrocarbons, the daytime average mixing ratio for both methane and ethane did not decrease in the region since a previous study in 2007 suggestive of continued natural gas leakage. Using monthly ethane to methane enhancement ratios and natural gas composition of gas delivered to the region showed that $72 \pm 16\%$ of all excess methane emitted in the SoCAB was due to natural gas leakage. This result is significantly higher than the fraction due to natural gas in previous bottom-up inventories in the region.

Positive matrix factorization was applied to the data set to aid in apportionment of hydrocarbons to various sources in the region. A seven factor result was obtained in which natural gas, oil and gas refining, biogenic, industrial sources, BTEX, gasoline liquids and tailpipe

emissions were matched to source profiles. Via this analysis, 59% (57-65%) of the methane seen in the SOCAB was due to the leakage of unburned natural gas. This agrees well with the result obtained using the composition of delivered gas and two recent studies of the region using other data sets.

Finally, several classes of refrigerants which are potent greenhouse gases were studied. The emission of banned chlorofluorocarbons was noted to have completely stopped in the region. Hydrofluorochlorocarbons are currently being phased out and so emissions estimates were calculated and compared to older data sets to show that regulations are working to limit their emission. HCFC-142b emissions were noted to have dramatically stopped during the sampling period as the result of a phase down rule that went into place on January 1, 2015.

CHAPTER 1: Introduction and Background

1.1 The Science of Climate Change

1.1.1 The Greenhouse Effect

The atmosphere above earth is separated into five different layers. All of life on earth exists in the lowest layer of the atmosphere, the troposphere, which stretches from the surface of the Earth to roughly 12 km up. Earth is warmed by electromagnetic radiation from the sun. The incoming solar radiation at the top of the atmosphere is equal to 342 W per square meter of the Earth's surface.¹ This radiation can have several different fates. First, the radiation can be reflected back out in the upper atmosphere by clouds or particles present in the air. It can also be absorbed by molecules present in the atmosphere such as carbon dioxide (CO₂) and water vapor. If the radiation reaches the surface of the earth, a small fraction will be reflected back to the atmosphere but most will be absorbed by the earth. This absorption of the solar radiation by the Earth is what causes heating of the planet during daytime hours.¹ During both the day and night, the earth emits some of this absorbed energy at a longer wavelength in accordance with the Stefan-Boltzmann law.² Assuming no interaction with the atmosphere, this would result in the effective temperature of the earth being -19°C.¹

In the atmosphere, certain gases exist that absorb infrared (IR) radiation spectrum (wavelengths on the order of 10⁻⁶ m) at resonant frequencies of their vibrational modes. These gases that readily absorb energy in the IR region of the spectrum are known as greenhouse gases (GHGs). To absorb in the IR portion of the spectrum, the gas must have a vibrational mode that changes the dipole of the molecule. All molecules with three atoms or more have such a mode.³ While 99% of the molecules in the atmosphere are nitrogen, oxygen, or argon, IR inactive compounds, the remaining fraction includes many species capable of acting as greenhouse

gases.⁴ The presence of these gases in the atmosphere keep enough of the outgoing radiation in the troposphere to raise the average temperature of the Earth to 15°C.

1.1.2 Anthropogenic Greenhouse Gas Emissions

While water vapor, ozone (O₃), and CO₂ have been present in the atmosphere long before humans came into existence, modern civilization has begun to add GHGs to the atmosphere at an alarming rate. Since people discovered that the burning organic matter produced heat that could be harnessed for power, they have been releasing CO₂ into the atmosphere as a product of combustion. The scale at which this emission took place for most of human history was not enough to affect the overall concentration of CO₂ in the atmosphere. However, since the Industrial Revolution began in the 1800s, the emission of CO₂ has increased dramatically as technology and civilization has advanced in both the mining of and use of fossil energy.¹ The use of coal, and later oil, to power modern civilization has emitted enough CO₂ to begin to truly affect the balance of life on earth. Carbon dioxide is the most emitted anthropogenic greenhouse gas and is used to show historical context for what has happened since the Industrial Revolution. Historical CO₂ atmospheric concentrations are determined by measuring the concentration of gas trapped in ice cores collected in Antarctica.⁵ Figure 1.1 shows that since the beginning of the Common Era (Year 1 A.D.), atmospheric CO₂ concentrations remained relatively constant with some fluctuation. However, since the Industrial Revolution atmospheric CO₂ concentrations have skyrocketed. Recently, tropospheric CO₂ reached a concentration of 400 parts per million (ppm) at Mauna Loa observatory, which is used as the basis for modern clean remote air sampling.⁶ The emission of CO₂ and other GHGs by modern humanity has altered the greenhouse potential of the troposphere and has the Earth already starting to heat up.

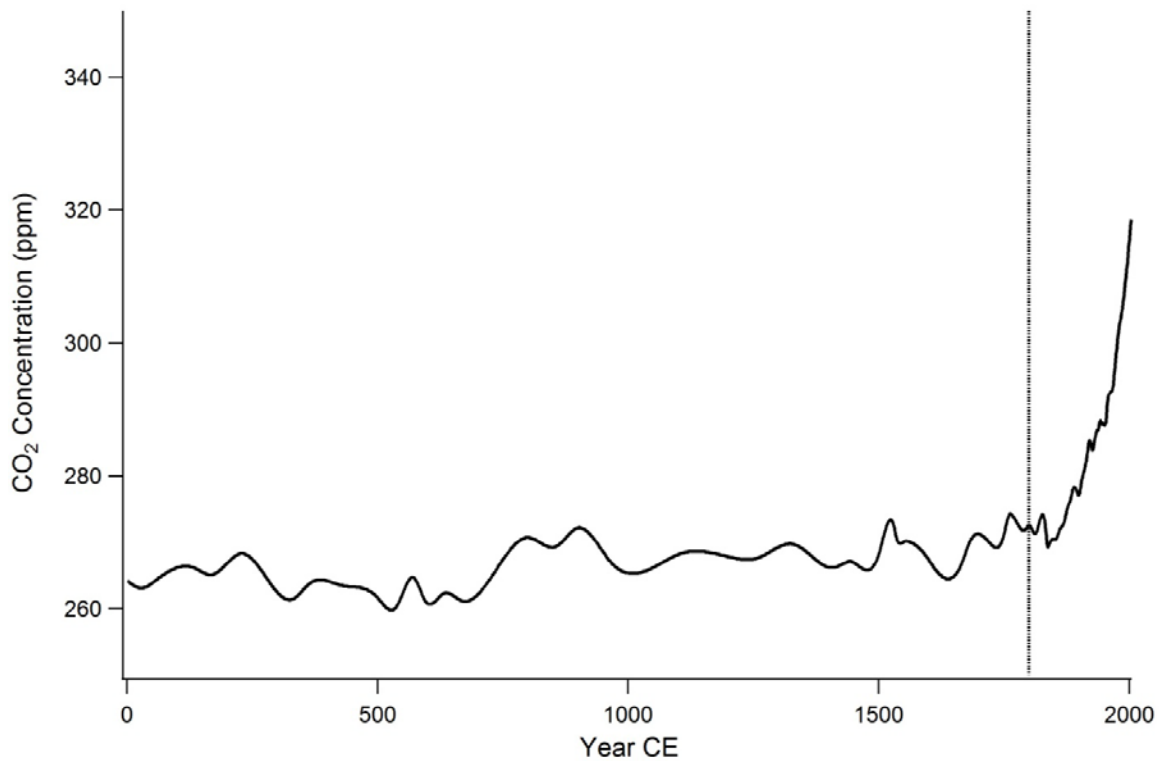


Figure 1.1. Law Dome ice core concentration of CO₂ since the beginning of the Common Era. The vertical line represents the beginning of the Industrial Revolution.⁵ The last data point shown is from 1955.

1.1.3 Evidence for Climate Change

The increase in GHG concentrations in the atmosphere is only half of the evidence required to show that global climate change is occurring. The other half is actual temperature increase from the excess heat trapped. Over the last thirty years, the Earth has begun to see a rising global temperature. Since 1880, the average daytime high on Earth has risen 1.4°F with two thirds of that rise occurring since the 1970s.⁶ For a local example, in Irvine, CA, between 1970 and 1989, the average daytime high recorded was 73.0 °F. Over the next twenty years, the average increased to 74.1°F.⁷ While a one degree change may not seem like a lot, that change happened on a 20 year time scale over which climate patterns should be stable.

By trapping excess heat in the troposphere, climate change will affect normal weather patterns in various regions and results in abnormal weather patterns. For many parts of the world, this translates to a warmer and drier climate. For others, more rain is expected due to increased water vapor in the atmosphere. Regional extreme weather conditions are becoming more likely.¹ Increased water vapor can lead to more intense rain storms that society is not prepared for. Parts of the United States are already suffering from these intense rainstorms. Figure 1.2 shows that there has been an increase in the last twenty years in the area of the U.S. that has experienced an extreme precipitation event.⁸ In Southern California, the most dangerous extreme weather condition is extreme heat, which is defined as a day where the daytime high is above the 98th percentile for daytime highs between April and October, based on historical data. The number of extreme heat days in Irvine rose from 89 to 102 during the two twenty year periods from 1961-1980 and 1981-2000.⁹

The correlation between increased global temperature and greenhouse gas concentrations in the atmosphere is proven to be a casual effect via atmospheric models. These models allow scientists to determine to what extent climate change is being caused by anthropogenic emissions. In the latest Intergovernmental Panel on Climate Change report, the results of several different modeling methods are shown where different effects on global climate are varied individually while all others are held constant. The models agree that more than half of the temperature anomaly since 1951 has been caused by anthropogenic greenhouse gas emissions and minimal change due to volcanoes or solar forcing.¹⁰ A more recent study showed that without the increase in atmospheric greenhouse gas concentrations the likelihood of the record temperatures seen in the last decade is 600 to 130,000 times lower.¹¹ These studies and others

show that there is no other likely explanation for the change in climate seen globally in the last 60 years.

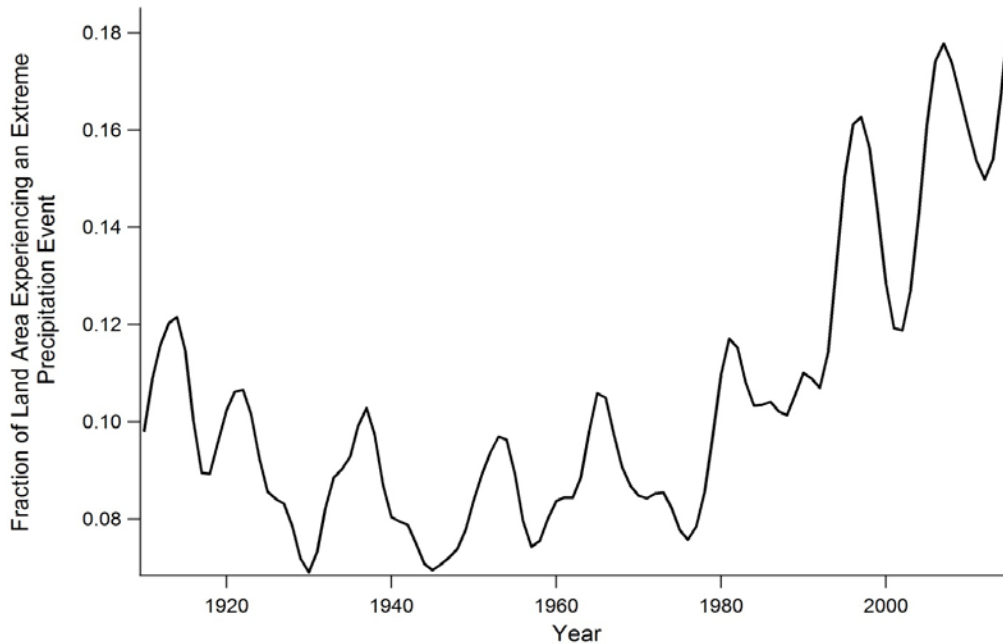


Figure 1.2 Nine year rolling average of fraction of the contiguous United States land area that experienced an extreme precipitation event.⁹

1.1.4 Current Regulations and Predicted Future Scenarios

To understand to what extent climate will continue to change in the future and how much of that is based on anthropogenic CO₂, climate scientists use models based on historical records and simulated emissions estimates. These emissions estimates can vary based on when humanity will react to the emission of CO₂ and try to limit it. This allows for a series of models that vary in the extent that humans try and wean themselves off fossil fuels. Two often used emissions scenarios are the Representative Concentration Pathways (RCP) 4.5 and RCP 8.5.¹² The numbers in these models represent the radiative forcing as a result of GHG emissions by the year 2100. Radiative forcing has the units of watts per square meter of the earth, which shows how much extra energy is being trapped due to increase atmospheric concentrations of GHGs.¹

The RCP 4.5 is a realistic possible future in which humanity does start to scrutinize CO₂ GHGs and emissions actually peak in 2040. In each subsequent year, emissions decrease and eventually stabilize in the year 2070 at emissions levels half of that seen in the year 2000.¹³ RCP 8.5 is also a realistic scenario in which CO₂ emissions continue to increase at the current rate all the way through the end of the century.¹² What the outputs of these models show is that the extent of climate change can still be decided by our future actions. These models were used on Irvine, CA as an example of what the future is predicted to be like on a local level.⁷ In the near term (out to 2030), temperatures increase in both models. However, by midcentury, the outputs of RCP 4.5 and RCP 8.5 diverge in terms of average highs for Irvine, CA. In RCP 4.5 the average high is modeled to be 76.8°F and in RCP 8.5 the average temperature is almost a full degree higher, 77.6°F.⁷ These temperatures are both over three degrees higher than the 1970-1989 period, showing the extent to which anthropogenic emissions have already begun to change the climate. By the end of the century, the effect of anthropogenic emissions becomes even more apparent. In RCP 4.5 the average high in Irvine between 2080 and 2099 will be 78.1°F; in RCP 8.5 it will be 81.2°F.⁷ The half degree rise between 2050 and 2100 in RCP 4.5 is promising. To some extent, damage to the climate has already been done, but it is still possible to prevent further climate change that may be devastating.

If prevention is going to occur, it will take global cooperation and collaboration to come up with ways to limit GHG emissions. Despite skeptics continuing to stir the pot and denying factual sciences, in the last decade or so, global policy has caught up to the state of climate science and the first steps towards GHG reductions have begun. In 2016, parties of the United Nations came together to enact the Paris Agreement. This agreement, although having no enforcement power, has nations of the world agreeing to reducing their GHG emissions

proportionally to keep the global average temperature from rising more than 2°C above baseline. How those emissions goals are to be met is left to each nation.¹⁴ Popular plans to reduce GHG emissions include cap and trade which slowly lowers the limit on total CO₂ emissions allowed and subsidies for renewable energy sources which reduces the demand for fossil fuel.¹⁵ To understand if these methods are effective and if they will work for a given nation or state it is important to study the different types of GHGs and what the sources of these gases are.

1.2 Greenhouse Gases

1.2.1 CO₂: Sources and Sinks

As mentioned above, an important greenhouse gas is CO₂, which is emitted along with water in the combustion of organic matter. Despite only accounting for 0.04% of the molecules that make up air, it has a strong greenhouse effect due to its strong IR absorption bands. The spectrum of CO₂ is shown in Figure 1.3.^{4,16} A strong IR absorption band exists for CO₂ around 2400 cm⁻¹ which occurs where water vapor does not absorb. The IR absorption spectrum of water vapor is also shown in Figure 1.3. Strong absorption in regions of the spectrum where water vapor does not absorb make for effective greenhouse gases. In an atmosphere void of greenhouse gases, IR radiation would flow directly out of the troposphere at those wavelengths. Instead due of the presence of these species, there is an increased chance that the radiation will be trapped by a GHG. Although, CO₂ only absorbs at very discrete wavelengths it is the intensity and location of the absorption that make it an effective GHG.

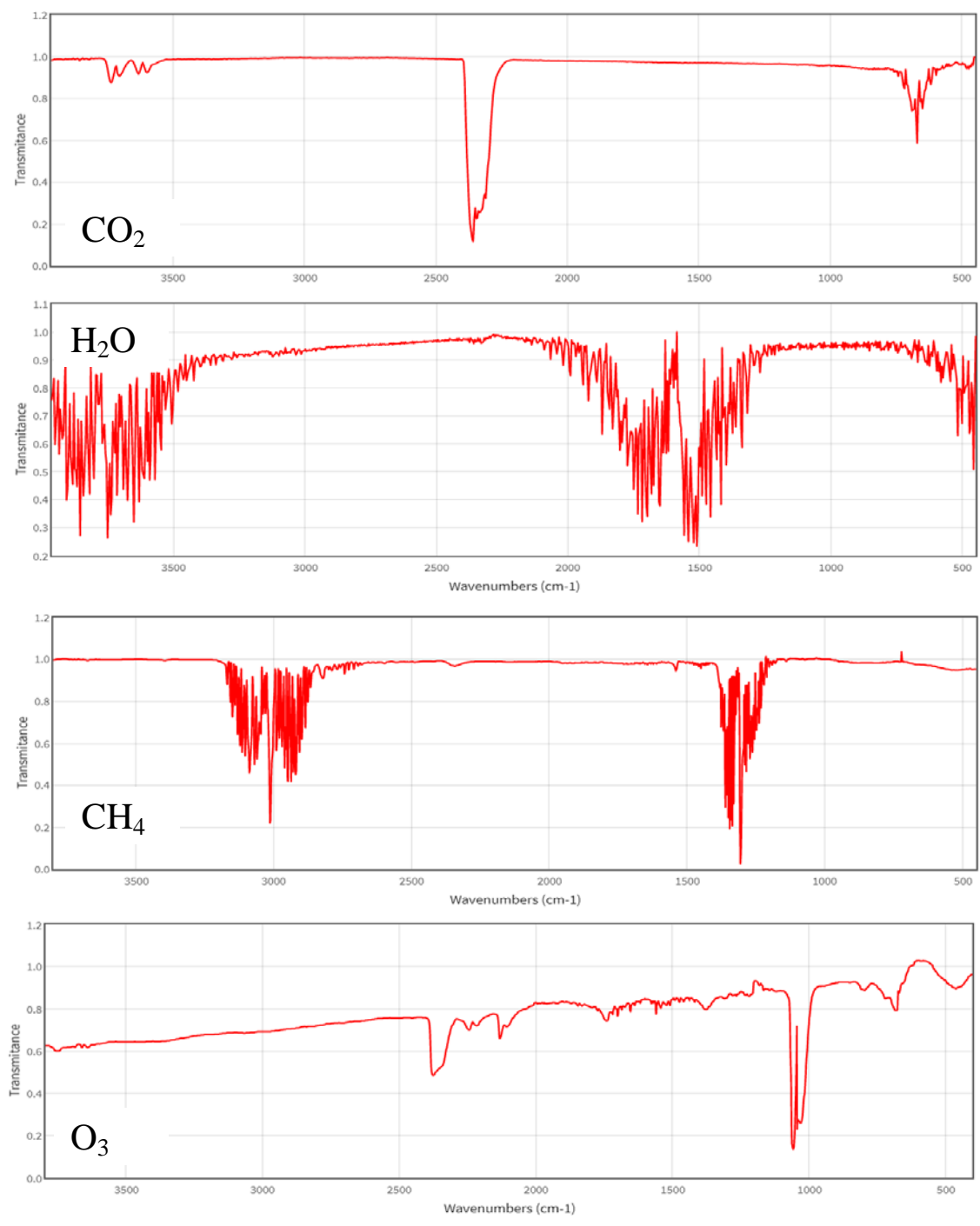


Figure 1.3. Gas phase infrared spectra of the four most prevalent greenhouse gases in the atmosphere: water, carbon dioxide, ozone, and methane. Spectra from NIST Chemistry WebBook¹⁵

To compare the potency of different greenhouse gases, scientists have developed a metric called the global warming potential (GWP). Global Warming Potentials are calculated by factoring in the wavelength integrated optical absorption of the gas and its atmospheric lifetime, to be able to compare the potency of a given mass of two different gases. The GWP system is a relative scale where the amount of energy that is trapped in the atmosphere due to a given mass of CO₂ is set to be equal to unity. Therefore, any GWP larger than one is more potent and should be of concern if present in the atmosphere. Global warming potentials can vary depending on the time scale specified.

For CO₂, the main removal process from the atmosphere is by its natural sinks as part of the carbon cycle. Carbon dioxide in the atmosphere is largely regulated by its uptake by plants to be used in photosynthesis. Studies have shown that in the short term, plants respond to increased CO₂ positively and grow rapidly. However, in the longer term, there is actually a decrease in photosynthesis due to a lack of available nitrogen.¹⁷ The argument cannot be made that plants will respond accordingly and regulate our CO₂ emissions. Another major sink of CO₂ is uptake by the oceans. Dissolved CO₂ in ocean water is in equilibrium with carbonic acid. As more CO₂ is added to the atmosphere, Le Chatlier's principle says that more carbonic acid will be produced in the ocean, lowering the pH. This acidification creates its own problems by causing the dissolution of calcium carbonate found in coral.¹⁸ Carbon dioxide can also be taken up on land by alkaline rocks in the form of carbonates. It is estimated that 65-80% of excess CO₂ emitted to the atmosphere is removed over centuries to two millennia by the ocean with the remaining being left for longer periods and being able to affect climate on a millennial scale.¹⁹ Because CO₂ has natural sinks, its global warming potential is significantly lower than what it could be.

Globally, in 2015, 36,000 Tg of CO₂ were emitted to the atmosphere as estimated by the European Commission's Emissions Database for Global Atmospheric Research, of which the United States was responsible for 14%.²⁰ The Environmental Protection Agency (EPA) has estimated that the United States emitted 5633 Tg of CO₂ in 2014, which was up 1% from 2013 but down 9% from 2005.²¹ The decrease since 2005 was in part due to state and federal regulations that aim to minimize greenhouse gas emissions. At the federal level, most of these regulation efforts fall under the Clean Air Act which after a challenge from the state of Massachusetts, was determined by the Supreme Court to include greenhouse gases under its jurisdiction.²² Efforts put forth by the EPA under the act to limit GHG emissions include automobile efficiency standards and source production standards for oil refineries.²³ These regulations still allow for states to enact their own more stringent policies should they so choose (to be discussed later), but set the minimum for the United States as we begin to attempt to limit our CO₂ emissions.

The other GHGs that will be discussed here do not have sinks in the earth or ocean and are thus a heavy focus when it comes to limiting GHG emissions. A list of GHGs to be discussed in this dissertation along with their 20 year and 100 year GWPs and atmospheric lifetimes is shown in Table 1.1. The GWPs shown in the table are as reported by the Intergovernmental Panel on Climate Change in their latest Assessment Report.²⁴ It becomes clear when comparing the 20 year and 100 year assessments how much of a role the atmospheric lifetime of a gas plays. The presence of hydrogen atoms in these molecules lowers their atmospheric lifetimes and therefore GWPs by orders of magnitude. This result is due to the main chemical removal process in the atmosphere for these gases being reaction with the hydroxyl radical OH. The hydroxyl radical is the main oxidant for gases in a clean atmosphere.¹ For gases without soil or oceanic

sinks, their atmospheric lifetimes are calculated relative to their reaction with the hydroxyl radical. Total emissions of these gases are much lower than that of CO₂. The EPA estimates that of all GHG emissions in 2015, 84% by CO₂ equivalents were CO₂.²¹ However, due to CO₂ being the end product of combustion that is used to meet our energy needs, legislators often turn their attention to the gases that make up the other 16% as targets for reduction as their emission is not as widespread or the gases have available replacements.

Table 1.1 Global warming potentials and atmospheric lifetimes for selected greenhouse gases that will be discussed in this work as described over a 20 and 100 year period.

Compound	Formula	20 Year GWP in IPCC AR5 ²⁴	100 Year GWP in IPCC AR5 ²⁴	Atmospheric Lifetime
Carbon dioxide	CO ₂	1	1	>200 yrs
Methane	CH ₄	84	28	12.4
CFC-12	CCl ₃ F	10800	10,200	100
CFC-11	CCl ₂ F ₂	6900	4,660	45.0
HFC-134a	CH ₂ FCF ₃	3710	1300	13.4
HFC-152a	CHF ₂ CH ₃	506	138	1.5
HCFC-22	CHF ₂ Cl	5280	1760	11.9
HCFC-141b	CH ₃ CCl ₂ F	2550	782	9.2
HCFC-142b	CH ₃ CClF ₂	5020	1980	17.2
HCFC-225ca&cb	CF ₃ CF ₂ CHCl ₂ / CF ₂ ClCF ₂ CHClF	469/1860	127/525	1.9/5.9
HFC-43-10mee	CF ₃ CF ₂ (CFH) ₂ CF ₃	4310	1650	16.1
HFC-227ea	CF ₃ CFHCF ₃	5360	3350	38.9
HFC-236fa	CF ₃ CH ₂ CF ₃	6940	8060	242.
HFC-245fa	CF ₃ CH ₂ CHF ₂	2920	858	7.7
HFC-365mfc	CF ₃ CH ₂ CF ₂ CH ₃	2660	804	8.7
HFO-1234yf	CH ₂ CF ₂ CF ₃	1	<1	0.029

1.2.2 Methane

The next most emitted GHG behind CO₂ is methane (CH₄). Methane is the simplest hydrocarbon and is a gas at room temperature. Methane's lack of a strong biologic or geologic sink like CO₂, means that its main removal process is chemical reaction and due to its size and stability, it has an atmospheric lifetime over 12 years.¹ Further, methane absorbs in regions of

the IR spectrum where CO₂ does not absorb at all (Figure 1.3).¹⁶ Climate skeptics are quick to point out that the absorption bands of methane overlap with those of water vapor and ozone which are more prevalent in the atmosphere. Skeptics then argue that we really should not even care about methane emissions since water vapor is natural and completely dwarfs any effect of methane.²⁵ This argument is a misunderstanding of the greenhouse effect. Emitting methane to the atmosphere increases the total GHG concentration which in turn increases radiative forcing. It is also worth noting how intensely it absorbs compared to water at the overlapping bands. More importantly, methane has an absorption band around 3000 cm⁻¹ that does not overlap with that of water vapor at all. These facts give methane its GWP of 84 over a 20 year timescale.²⁴

Like CO₂, global methane concentrations have risen dramatically since the beginning of the Industrial Revolution (Figure 1.4). Pre-industrially, the atmospheric concentration of methane fluctuated between 600 and 700 ppb. Since the mid-1800s, the concentration has increased to nearly 1.9 ppm as of 2015.²⁶ Since the Industrial Revolution, the emission of methane accounts for 20% of the warming seen by GHGs.²⁷ More recently, there have been some unexpected changes in the global methane concentration. During the 1980s, global methane concentrations showed a nearly linear year after year increase averaging 12 ppb yr⁻¹.²⁸ In the 1990s, this rate slowed, but still showed an overall increase. However, data starting in 1999 show a much more erratic methane trend. Between 1999 and 2007, global methane concentrations leveled off around 1.8 ppm. In the year 2000, the concentration actually decreased from the previous year.²⁸ The cessation in increased methane was surprising to scientists and no conclusive result as to what caused the pause has been found. Theories include a decrease in emissions from rice paddies and natural gas to an increased concentration of the hydroxyl radical.^{27,29} Since 2007, global background levels have begun to rise steadily once again. This

increase is well accepted to largely be a result of increased production of natural gas and the mining of shale gas (discussed in greater detail later).³⁰ An estimate of global emissions is difficult due to scale and lack of reporting, and so most are done on a regional or hemispherical scale. Saunio et al.³¹ attempted a global inventory on a decade long time scale. They estimated that between 2003 and 2012, average methane emissions were 558 (540-568) Tg yr⁻¹. They note the large uncertainty in certain emissions categories and how emissions are changing.³¹ This analysis shows one of the biggest challenges in reducing methane emissions. There are a wide variety of sources, both anthropogenic and biogenic making apportionment to sources difficult. It is clear that there is more work to be done to determine the contributions to the total methane budget. To do so, it is important to understand what these sources are and how they release methane to the atmosphere.

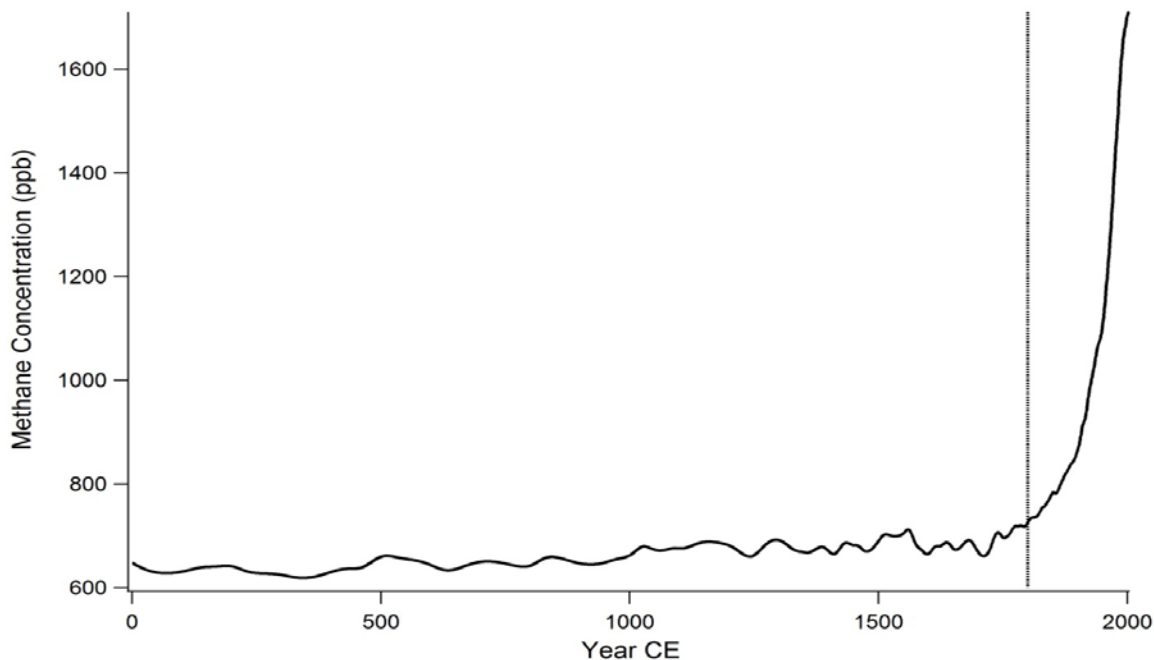


Figure 1.4. Law Dome ice core concentration of methane since the beginning of the Common Era. The vertical line represents the beginning of the Industrial Revolution.⁵ The last data point shown is from 1955.

1.2.2.1 Anthropogenic Methane Sources

1.2.2.1.1 Methane from Anaerobic Bacteria

Methane is released to the atmosphere from bacteria known as methanogens. These bacteria reduce CO₂ or acetic acid to methane as the last step in their respiration cycle. They do not require oxygen to respire and thus are often found underground. They work to breakdown waste products in the soil as part of the carbon cycle.^{32,33} Methanogens occur naturally, however methane emission related to their life cycle can be traced to various anthropogenic sources.

1.2.2.1.1.1 Agriculture

Agricultural production accounts for 52-84% of global methane emissions.³⁴ The two biggest methane producers within agriculture are rice paddies and ruminant digestion. Rice paddies are a significant source of anthropogenic anaerobic methane emissions in Southeast Asian countries where rice is the dominant production crop. The main method of harvesting rice is through the flooding of the fields creating a nutritious environment for anaerobic digestion. It was recently estimated that 14% of the globally emitted methane is from rice paddies.³⁵ Recently, a study has shown that going forward, increased CO₂ concentrations and increased daytime highs due to climate change will increase the amount of methane released from rice paddies while at the same time slightly decreasing rice yield. This will have the effect of making rice less environmentally friendly as significantly more methane will be released per pound.³⁶ Naturally occurring swamps and wetlands also contain large amounts of methanogens and have a strong seasonal dependence with emissions peaking in late summer.³⁷

More prominent in the United States is methane tied to beef and dairy production. Due to the presence of methanogens in the stomachs of cattle, the offgassing of digestive gases from cow belching and has become an increasingly important methane source. These methanogens

live in a symbiotic relationship with the ruminant by breaking down cellulose in grasses into digestible fatty acids.³⁸ Some of these fatty acids are broken down even further and end up being emitted as methane. About 26% of the gas found in the rumen of a cow is methane.³⁹ An estimated 15% of all methane emissions globally come from ruminant (cows, goats, and sheep) digestion.³² The cost of production of both dairy products and beef has increased over the last several years due to the increased cost of water due to drought, however demand for both has continued.⁴⁰ Demand for dairy is projected to increase over the coming decade.⁴¹ Due to this demand, ways to minimize methane release from cattle in feedlots and dairies is an active area of research. Possible solutions range from adding legumes to the forage to milking cows for eighteen months before calving as opposed to the usual twelve to reduce unproductive cattle and energy costs.^{42,43}

1.2.2.1.1.2Waste Management

Another segment of methane from anaerobic digestion comes from the collection of organic waste. Most notable is the landfill and the buried anthropogenic waste. The waste management sector produces roughly one fifth of the world's methane by one estimate.⁴⁴ This methane is emitted in combination with other gases known together as landfill gas. This gaseous mixture is predominantly methane and CO₂. The CO₂ is released from bacteria that respire aerobically. They use some of the methane from deeper underground along with organic waste near the surface as a food source and off gas CO₂.⁴⁴ The ability for methanotrophs to limit the amount of methane emitted from landfills has been a source of a great deal of scientific pursuit. Studies have shown that the ratio of methane to CO₂ released from a landfill can be affected by moisture content, pH, soil composition, temperature, and cover plants.³³ It is also worth noting that while often lumped in with cattle offgassing, the emission of methane from waste lagoons on

dairies and feedlots is a contributing source to emissions from the agricultural sector.⁴⁵

Collecting the methane from waste lagoons and using it as biogas has been proposed as far back as the 1970s and has become a secondary source of income for some dairy farmers and ranchers.⁴⁶

1.2.2.1.2 Fossil Methane

Being the simplest hydrocarbon, methane is also used heavily for combustion processes and is considered a fossil fuel. Methane along with other light alkanes is found in the headspace of oil pockets deep beneath the surface or in shale rock formations. It is piped up to the surface, and then transported to a processing plant before being delivered to customers. The mixture of methane, ethane and propane found in oil wells is known as natural gas. Natural gas that reaches end users varies in composition in different regions but is generally over 90% methane.⁴⁷

End users of natural gas are both industrial and residential. Industrially, it is used to produce electricity as an alternative to coal. In residential settings, natural gas is used for heating, both for the whole house and for cooking. Recently, there has been a surge in the use of natural gas to fuel automobiles and buses. Natural gas is currently being touted as a bridge fuel towards renewable energy sources. Many are excited about the growth of its use due to the efficiency with which it burns. Compared to coal, when burned, natural gas releases over 100 pounds less CO₂ per million British Thermal Units of energy produced.⁴⁸ It has just recently surpassed coal as the dominant source for electricity generation in the United States.⁴⁹ Further, due to advances in fracking and shale gas recovery, it has become cheaper than ever to produce keeping its price low in spite of increased demand (Figure 1.5).⁵⁰ Supply of natural gas is plentiful with current estimates having peak production occur between the present day and 2050.⁵¹

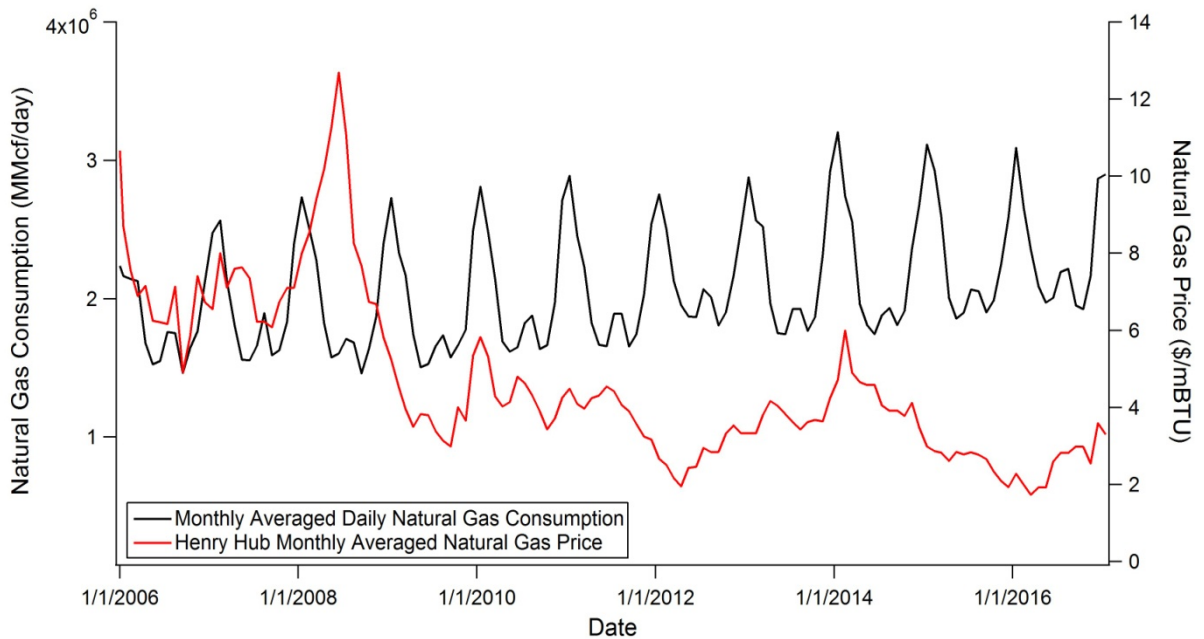


Figure 1.5 Price and consumption of natural gas in the United States since 2005. Due to advances in fracking and shale gas technology, natural gas prices have continued to drop despite increased demand. Data for plot taken from Energy Information Administration.⁴⁸

As we continue to transition away from coal and toward renewable sources of electricity generation, it is clear that natural gas will have a larger role in the energy sector. However, natural gas is not without its own issues. The biggest of these is the concern over leakage. Unlike gasoline, natural gas is gaseous and therefore much more prone to leakage from transmissions and distribution pipes.^{52,53} Leakage can occur at every step of the natural gas life cycle: in mining, processing and transmission. Specifics of leakage will be discussed in more detail in the following section.

A small amount of methane emissions can also be tied to combustion of larger hydrocarbons found in gasoline. Due to incomplete combustion in older or malfunctioning engines, methane can be released via the tailpipe of the car to the atmosphere. A 1994 tunnel study showed that methane made up the largest percentage of all the VOCs measured.⁵⁴ More

recent studies on vehicular emissions tend to not include methane, due to its low reactivity and therefore low ability to form smog.^{55,56} However, with the shift of focus to climate change, methane emissions from tailpipes should be studied more closely. It is undetermined how much methane is emitted from tailpipes given the advancements in engine technology in the modern fleet. The EPA estimates the 2015 tailpipe emission of methane to be 0.2 Tg, which is less than 1% of the U.S. total.²¹ While nearly negligible on a national or global scale, in an urban region such as Southern California, this is a source to consider.

1.2.2.1.3 Pyrogenic Methane

The last segment of anthropogenically emitted methane is from biomass burning. Wildfires are natural and are not directly linked to human activity; however, in many parts of the world, not only is wood, grass, or sometimes dung burned for heat and to cook with, but more importantly, in developing countries, large swaths of land are cleared by burning so as to be used for agriculture. It has been noted that over 80% of all biomass burning takes place in the tropics where development is still occurring and where rainforests are found.⁵⁷ Methane is emitted from biomass burning due to incomplete combustion from a lack of oxygen in the most intense parts of the fire.⁵⁸ In a top-down study, it was estimated that 10% of global anthropogenic methane stems from biomass burning.²⁷

1.2.2.2 Natural Methane Sources

It is worth mentioning that some of the methane released to the atmosphere stems from natural sources. As above, this can be broken down into three distinct source types. First, biogenic methane is released in the form of anaerobic respiration of methanogens. Methanogens are naturally occurring in swamps and wetlands. Wetlands make up the bulk of biogenic methane emissions, however there is large uncertainty in the exact emissions total.²⁷ Further, other

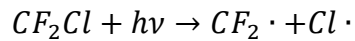
sources also emit methane through the symbiotic relationship with bacteria in their stomachs. Of these, termites are the biggest contributor, accounting for almost 2% of all methane emissions.²⁷ Thermogenic methane is released naturally in the form of seeps in various locations around the globe. These can include seeps from along fault lines or through mud volcanoes.^{59,60} Seeps have also been noted from beneath the ocean floor.⁶¹ These seeps usually occur over stretches of several miles, however microseepage from a small hot spot can play a role in regional emissions as well.⁶² Finally, natural occurring brush and wildfires should also be taken into account for their methane production.

1.2.3 Halocarbons

1.2.3.1 Chlorofluorocarbons

Another class of GHGs consists of a wide variety of halocarbons which are largely created by humans. These gases serve a variety of industrial purposes including being used as refrigerants, propellants, or solvents. The defining characteristic of these halocarbons is the high degree of substitution with either chlorine or fluorine. They generally contain three or less carbons so they are liquids or gases at room temperature, and are relatively unreactive. The first generation of these industrial gases was chlorofluorocarbons (CFCs). CFCs were first implemented industrially in the 1930s as less flammable refrigeration options. Previously, ammonia, propane and other dangerous gases were used as refrigeration gases because of their low cost and optimal heat of vaporization.⁶³ CFCs, most prominently CFC-11 and CFC-12, were widely accepted by industry over the next several decades due to their inertness and ease of handling, with production peaking in the 1970s at one million tons produced per year.⁶⁴ In 1974, Rowland and Molina published a landmark paper in which it discussed how UV-B and UV-C

radiation could cleave a carbon chlorine bond CFCs and begin the cycle of catalytically destroying ozone molecules in the stratosphere by the following reactions.⁶⁵



The destruction of the ozone layer would lead to more UV radiation reaching earth and increasing the risk of skin cancer for all humans. A short 13 years later, the Montreal Protocol was agreed to and now signed by over 200 countries of the world pledging to phase out CFC use to protect the ozone layer.¹ Since the rise of the issue of climate change, it has been determined that not only do CFCs have high ozone depletion potentials (ODPs), they are very potent greenhouse gases with GWPs on the order of thousands. Due to the Montreal Protocol's phase out plan immediate reductions in consumption occurred, and CFC use has been globally banned since 2010. In recent year global background levels have begun to decrease as shown in Figure 1.6.²⁶

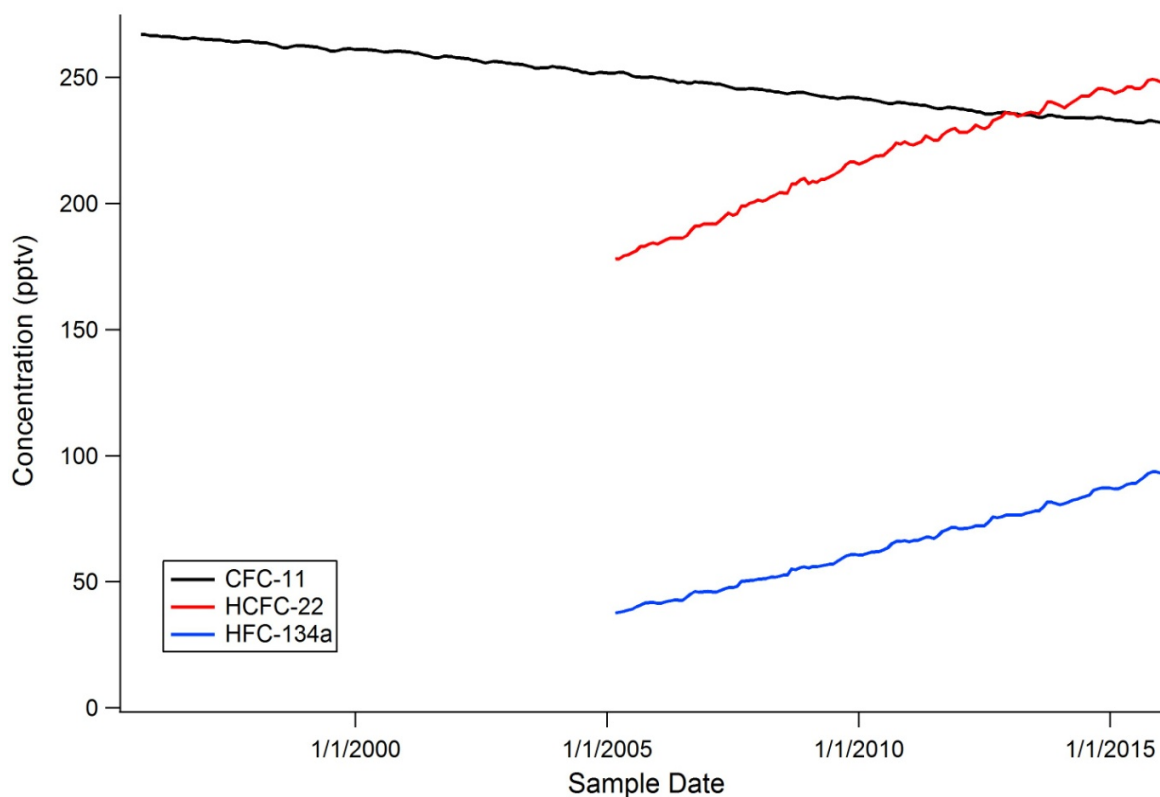


Figure 1.6 Monthly average atmospheric concentrations of various halocarbons as seen at Trinidad Head, CA. Plot was created with data from the AGAGE Network.⁵

1.2.3.2 Hydrochlorofluorocarbons

In the wake of the ban on CFC use, the halocarbon industry switched their manufacturing efforts to hydrochlorofluorocarbons (HCFCs). HCFCs highly resemble their parent CFCs but with the addition of a number of hydrogen atoms. The most widely used HCFC, HCFC-22, is simply CFC-12 with one chlorine atom replaced with a hydrogen atom.⁶⁶ This replacement allowed for the gases to have a tropospheric removal mechanism. The hydroxyl radical will scavenge the hydrogen atom and then cause a series of reactions eventually breaking down the molecule.¹ These HCFCs were widely brought into use as their ODPs were 10-100 times lower than CFCs. However, the presence of just a few hydrogen atoms surrounded by bulkier halogen

atoms meant that their atmospheric lifetimes are still on the order of years, and concentrations in the atmosphere will continue to build up (Figure 1.6). This meant that some could still reach the stratosphere and cause ozone depletion. They were viewed from the beginning as a bridge gas due to their ODPs and the original Montreal Protocol had in place a plan to begin to phase out HCFC use in 2013.⁶³ In 2007, the parties of the Montreal Protocol came together with the goal of strengthening the agreement in terms of limiting HCFC emissions. While total phaseout will not occur until 2040, the 2007 update capped use in developing countries at the rate in which they were consumed in 2009, starting in 2013. Montzka et al.⁶⁷ reported that in the years immediately following the update, emissions of HCFCs did not increase appreciably suggesting that the update made developing countries strongly scrutinize their use of these gases. Due to their high GWPs, many countries are moving forwards with plans to phase out HCFCs even sooner. The EPA under the Clean Air Act has set up an aggressive phase out schedule of HCFCs for the United States. By selling allowances for corporations to purchase allowing them to use the gases, and decreasing the number of allowances every year, they have a plan in place to cut HCFC usage by 99.5% by 2020. This is in addition to bans on production and importation of varying HCFCs staggered from between 2003 and 2015.⁶⁸

1.2.3.3 Hydrofluorocarbons

The third generation of synthetic refrigerants is hydrofluorocarbons (HFCs). HFCs have no ozone depletion potential due to their lack of chlorine. These gases have all of the qualities of HCFCs and CFCs, but have been approved for industrial use because they will not cause destruction of the ozone layer. However, these gases are GHGs such that monitoring their emission is incredibly important. Further, because their atmospheric lifetimes are shorter than previous generation refrigerants, they are seen as a great target for overall GHG reduction. Just

recently, HFCs have come under regulatory control. In 2016, the Kigali Amendment to the Montreal Protocol was signed which enacted a phase out schedule for HFCs starting for developed countries with a 10% reduction in 2019.⁶⁹ The U.S. has not made any further plans to regulate the use of HFCs, and so as of this writing their use is completely unregulated. Global background levels of HFCs continues to grow as is shown by the plot of HFC-134a over time (Figure 1.6)

1.2.3.4 Fourth Generation Refrigerants

The current task for halocarbon manufacturers is to find a stable refrigerant molecule that is not a significantly strong greenhouse gas. The answer to that challenge as yet has been to devise halocarbons that have the same properties but a very reactive aspect, such that if they should get emitted they would not last in the atmosphere long enough to have a climatic effect. Several fourth generation refrigerants are currently on the market and it does not appear that one has taken hold yet. One proposed idea is to return to using hydrocarbons like propane, or even carbon dioxide. Another alternative is to develop a molecule that can be broken down in the atmosphere. One such group for refrigeration is hydrofluoroolefins (HFOs). HFOs resemble the older generation molecules but with a carbon-carbon double bond. This makes them much more reactive in the atmosphere and will easily fall apart before doing climatic damage.⁷⁰ However, they are not as effective as refrigerants and can be flammable. Others are suggesting returning to ammonia or propane, some of the original refrigeration compounds.⁷⁰

1.3 The Fossil Fuel Industry

1.3.1 Coal

The first fossil fuel that was widely used was coal. Coal is a mineable solid which was formed from ancient forests becoming covered in layers of water and soil. This carbon rich

material was compressed over millennia. Coal was used to power steam engines and later burned to create electricity. To this day, coal is still the dominant fossil fuel used for electricity generation, globally.⁷¹ However, in recent years it has come under fire due to negative health effects. When coal is burned to produce heat, chemicals found in coal get volatilized and released into the air. These contaminants, such as polycyclic aromatic hydrocarbons (PAHs), and heavy metals, are detrimental to human health when inhaled.⁷² A recent study in Europe has shown that the burning of coal for electricity generation leads to an extra 24.5 deaths per TWh of electricity generated.⁷³ Further, the mining of coal is hazardous to miners due to acute inhalation of large quantities of particulate matter.⁷⁴ Because of these public health concerns, along with the noted decrease in cost of natural gas, coal production in the United States has decreased steadily since 2008.⁷⁵

1.3.2 Oil

By the late 1800s, crude oil was regularly being mined from the ground and used as a fuel source. As a liquid, it was much easier to transport and pipelines were soon built. Crude oil is then refined and sold as a variety of fuels most importantly for transportation with 64% of all crude oil used in that sector.⁷¹ Gasoline, one such fuel, burns more efficiently than coal and produces more energy per unit volume than coal making it preferable for mobile sources. Americans are using more gasoline than ever before burning 9.3 million barrels per day to fuel their cars and trucks.⁷⁶ Many have begun to worry around the world about the remaining oil reserves. They are concerned about what will happen to the price of oil once production begins to decline after peak oil. Predictions abound about when as a world we will reach peak oil production ranging from having hit it in 2006, to an optimistic view that we will not hit peak oil for hundreds of years.^{77,78} The variety of predictions is due to an inability to accurately assess

what reserves are still left. However, most predictions suggest that this peak will occur within the next twenty years. This concern is yet another reason why natural gas use and infrastructure continues to grow.

1.3.3 Natural Gas

The sources and rise of natural gas were discussed previously. It is important to understand the process of mining, refining, and delivering it to end users.

1.3.3.1 Sources of Leakage in Production and Transmission

As it concerns methane emissions, the process of taking natural gas from the ground to a customer's home contains several different steps where leakage could occur. This leakage begins in the exploratory phase where a potential well may be drilled into to confirm its composition. Once the gas deposit is reached by the drill, some amount of natural gas can escape to the atmosphere. After a well is drilled hydraulic fracturing (fracking) occurs. Hydraulic fracturing is the process of stimulating an oil or natural gas well by blowing a mixture of water and chemicals, known as brine, into the drilled well at high pressures. This works to open up the vein more and allow for the hydrocarbons to flow out more easily. During the flowback step of the fracturing process, the brine that was flown into the well is pumped back out and often times natural gas is brought up with it. This natural gas is often not collected and allowed to escape to the atmosphere.⁷⁹

Once the well has been fractured, extraction of the gaseous hydrocarbons can begin. The natural gas pumped up from the well is considered "wet gas" meaning that it contains a substantial amount of higher hydrocarbons and other gases that must be separated prior to transmission. Wet gas will contain water, H₂S, and CO₂ which all must be removed to improve the burning efficiency of the gas. Further, C₂-C₅ hydrocarbons are also removed for use in other

fuel mixtures. This separation is sometimes done at the well head or at centralized processing facilities. In this refining step, methane leaks may come from leaky pipes or vents on liquids storage tanks after most of the natural gas is removed from the hydrocarbon liquids. A review of studies on natural gas processing reports an average loss of 0.2% of methane produced is lost to emissions during the refining process.⁷⁹

Most natural gas lost to the atmosphere before being utilized by an end user is lost in the transmission stage. The gas is pumped from the shale regions where it is drilled and refined to population centers across the U.S. in large high pressure pipelines. These pipelines require intermittent compressor stations to keep the pressure and flow high. Once in the desired region, the gas is handed off to local distribution companies, which then control its passage through lower pressure pipelines and eventually through individual meters. National estimates for methane lost in transmission vary significantly from less than 0.05 to 4% of total deliveries.⁷⁹ The losses at this step are due to the aging pipeline infrastructure that is not prepared to handle current demand. As demand continues to grow, the infrastructure is not being built to meet it, and the current infrastructure acts as a cap on total deliveries.⁸⁰ A recent report by the United States Department of Energy argues that regional pipelines need to be expanded as opposed to large transcontinental ones due to the many shale regions throughout the United States.⁸¹ The infrastructure was designed before shale innovations and so to fully take advantage of it, an investment in new pipelines is necessary. In older cities, cast iron pipes were used for natural gas transmissions and delivery. These cast iron pipes have been tied to increased leakage.⁸² Since the 1950s, transmission pipes have switched to steel and distribution pipes are plastic which have lower incidence and intensity of leaks.⁸³ Detecting these leaks effectively has become an important area of research with several real time on-road based studies having taken place.^{47,82-84}

It is clear that even determining a loss rate for each part of this process is currently still a topic for debate, and so coming up with a national natural gas leak rate is even more of a challenge. The literature has proposed a method of estimation based on the EPA's inventory of GHG emissions and data from the US Energy Information Administration.⁵³ The EPA reports that 6.5 million metric tons of methane was emitted in 2015 from the natural gas system from production to transmission.²¹ This is combined with reported total US production of natural gas of 28.7 trillion cubic feet at STP.⁵⁰ Assuming a density of methane of 0.0447 lbs ft⁻³ and a well head composition of 85% of natural gas being methane, this yields an estimated leak rate of 1.3% for the entire natural gas system. However, there is doubt that the actual leak rate is that low. The EPA estimate for leakage from the natural gas system is based off of total throughput and leakage rates from a 1993 study. It has been argued that a lot about the natural gas industry has changed since the early 1990s and the EPA's estimation methods are no longer valid.⁸⁵ One meta-analysis of previous emissions estimates shows that the leak rate of the whole system is most likely between 1.9-2.6%, larger than what the EPA reports.⁷⁹ They discuss that the challenges associated with making these estimates are based on separating out the different sources of methane from each other, especially in cities with many different emissions sources.

Methane leakage is also not limited to the natural gas industry. In oil mining and production, natural gas is often seen as a byproduct and not worth the effort of capturing. Most often this natural gas is flashed (burned) at the well head before liquid extraction begins. However, in some cases, natural gas is simply vented to the atmosphere. One study estimated that the oil and gas industry in Weld County, Colorado alone emitted 53.1 Gg per year of methane from wellhead venting.⁸⁶

If natural gas is going to become the fuel of the near future, it must ideally have a smaller carbon footprint than coal and gasoline. As mentioned previously, the energy per carbon ratio favors natural gas over other fossil fuels, however, the issue of leakage discussed herein complicates the matter due to methane being a more potent GHG. A few studies have attempted to calculate the environmental utility of switching to natural gas in light of the leakage issue. Of course, results vary widely due to the varying estimates for overall leak rates that are available. Studies are in agreement that switching electricity generation from coal to natural gas would have immediate climate benefits by reducing coal related GHG emissions. However, due to the leakage issue with natural gas, switching over vehicular fleets from gasoline or LPG would not have as dramatic an effect on climate. In fact, it would take upwards of 50 years to start to show a net benefit to the climate because of how much natural gas would be lost to the atmosphere in the process.^{52,87} Another study showed that the abundance of natural gas actually hurts the push towards renewable energy sources. Beyond 2020, GHG emissions decrease begin to slow as the low price of natural gas make it so economically favorable that solar and nuclear power plants are not built.⁸⁸ This summarizes the current state of fossil energy and greenhouse gas emissions as they stand as of this thesis. This serves as a backdrop for the study that is reported here, which focuses on these GHG emissions in the Los Angeles megacity as a representative urban case study.

1.4 The South Coast Air Basin

1.4.1 Geographical and Meteorological Background

In this dissertation, the issues of greenhouse gas emissions will be studied on a regional level, within the South Coast Air Basin (SoCAB) of California. The SoCAB is home to the greater Los Angeles, CA area including Los Angeles, Orange, and parts of Riverside and San

Bernardino counties. The SoCAB is geographically defined by the Southern California coastline on the southwest, the San Gabriel Mountains to the north and the San Jacinto and the Peninsular Mountain ranges to the east (Figure 1.7). The region is home to over 17 million people, accounting for 44% of the total state's population in only 3% of the state's total area.

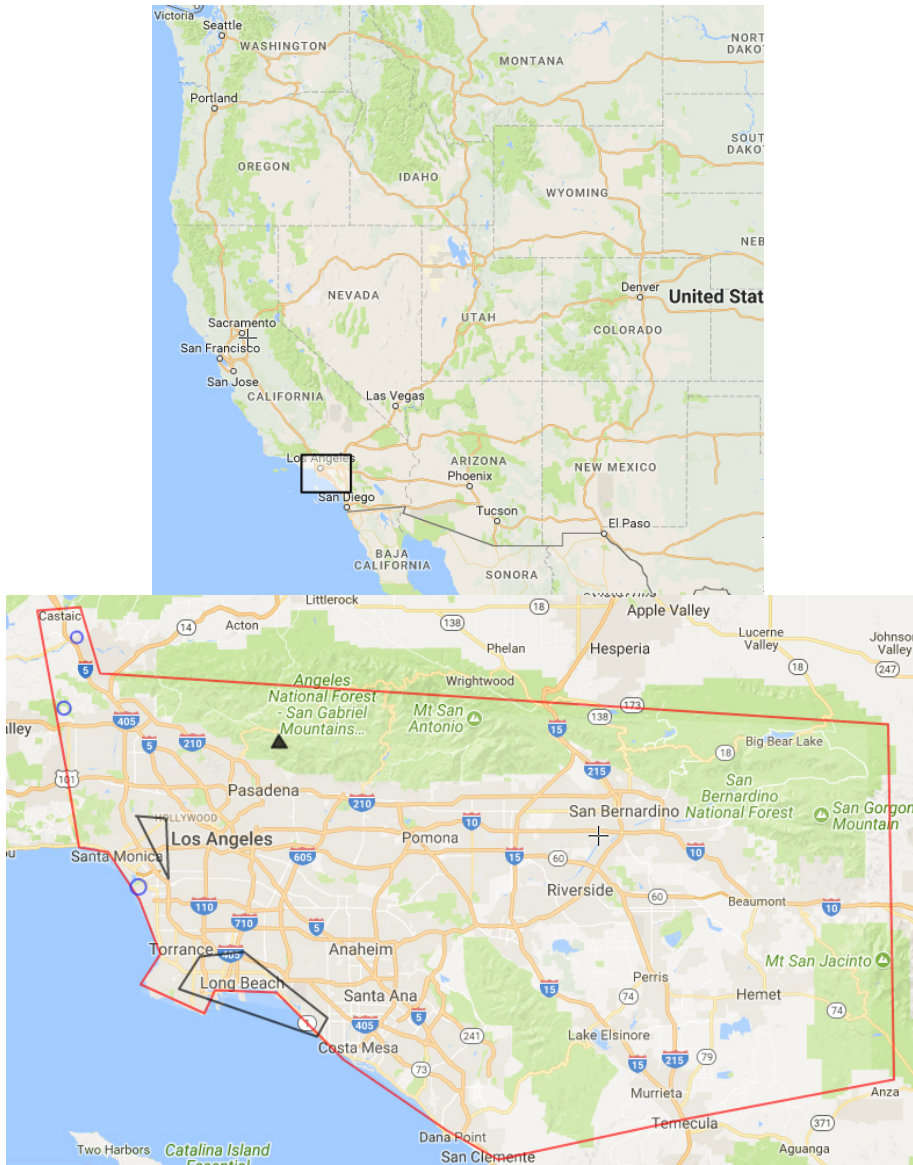


Figure 1.7. Map of the western United States with the Southern California region outlined. In the lower map, the South Coast Air Basin is outlined in red. Outlined in black are the active oil fields in the SoCAB. The blue circles represent SoCalGas natural gas storage wells. The black triangle represents Mt. Wilson, where the air sampling study took place.

The SoCAB has a Mediterranean climate with cool and wet winters and warm and dry summers. Rain is typical for the region in January through March with Los Angeles averaging 14.8 inches of rain each year.⁸⁹ May and June have the potential to be unseasonably cool due to the local weather phenomenon known as June Gloom. June Gloom occurs when a particularly thick marine layer flows into the region overnight. It can take into the early afternoon hours for the sun to burn off the cloud layer. The predominant winds in the region are from off the coast from the south and west. These ocean breezes act to keep the temperatures in the region relatively mild. Clean air masses will blow into the region and then be pushed towards the low mountains that act as barriers, trapping the lower air parcels. Occasionally during the fall and winter months an area of high pressure can form over the desert to the east of the SoCAB. This high pressure system pushes hot dry winds down onto the SoCAB known to locals as Santa Ana Winds.^{90,91}

1.4.2 History of Air Quality and Emissions in the SoCAB

Since the 1950s, smog has been noted in the greater Los Angeles area on the hottest and sunniest days. This smog is the combination of particulate matter and ozone in the troposphere after the emission of volatile organic compounds (VOCs) and primary aerosol from industry and tailpipes.¹ These VOCs can react with NO_x in the presence of sunlight to eventually form tropospheric ozone. Ozone in the troposphere is a strong oxidant that can lead to more particle formation.⁹² Further, it has a detrimental effect on human health; ozone is a toxic gas that even in quantities on the parts per billion level begins to eat away at the lining of the lungs causing pulmonary problems such as decreased lung function and the potential for infection. It is estimated that a 10 ppb increase in ozone in a city increases the mortality rate by 0.52%.⁹³ To

protect city dwellers now and into the future, it is important to study sources of these VOCs and how they contribute to tropospheric ozone formation.

Air quality and emissions in the SoCAB have been well studied over the past several decades.⁹⁴ This academic study has translated to policy on both the state and federal level that has seen significant improvements in overall air quality. In 1967, the California Air Resources Board (CARB) was formed by state legislation and was tasked with trying to control emissions and smog formation across the state. By 1970, they had instituted the first automobile emissions standard in the nation which limited the amount of VOCs and NO_x an engine could emit.⁹⁵ In the 1980s, attention turned to toxic air contaminants, species that while short lived were determined to be hazardous to human health. These are emitted from fossil fuel combustion as well as stationary sources such as dry cleaners and agriculture. The Toxic Air Contamination and Control Act was passed in 1983 which gave CARB further power to being to regulate the emission of these gases.⁹⁵ Continued evaluation and updating of these regulations has made California a leader in air quality despite the state's population density. In fact, many of the provisions written into the federal Clean Air Act were based on successes in California.⁹⁵ Examples of the quantitative improvements seen in California include a reduction in ozone non-attainment days. These are days in which monitoring stations detect 8 hour average ozone concentrations above the state recommended level for health effects. In 1986, downtown Los Angeles experienced 89 such days. Thirty years later in 2016, that same station reported only four non-attainment days. Areas located in the eastern portions of the basin, still face ozone issues more regularly, but have also seen the frequency of such events decrease.⁹⁶ Studies of total VOC concentration have shown a decrease of two orders of magnitude since the 1960s,

averaging a 7.5% reduction per year.⁹⁴ Shorter term reductions (or lack thereof) will be discussed in this dissertation.

1.4.3 Recent Greenhouse Gas Emissions Regulations and Studies

Since the early 1990s, greenhouse gas emissions have become important to monitor and control in the state and the SoCAB.^{97,98} The earliest model prediction of effects of climate change on Los Angeles was published in 2004, and showed how devastating continued unregulated emissions would be to the climate.⁹⁹ Just two years later, the California Legislature passed and Governor Schwarznegger signed into law AB 32 known as the Global Warming Solutions Act. This act was the first of its kind in setting tangible GHG emissions goals for the state starting with a reduction to 1990 GHG emissions levels by 2020 (431 million metric tons of CO₂ equivalents). AB 32 gave CARB power to create a scoping plan and regulations to achieve this goal. The plan is multifaceted including specific measures and protocols for different sectors. A statewide cap and trade program was instituted for the industry sector. For energy, a goal of one third of all electricity coming from renewable sources by 2020 was set. Due to their lower emissions levels, high GWP gases including methane and halocarbons have their own section of the scoping plan.¹⁰⁰

In the SoCAB, most greenhouse gas emissions stem from anthropogenic urban sources. Agriculture has been decreasing in the region as more of the farming in the state shifts north to the Central Valley, with the four counties that make up the SoCAB ranking 13th, 24th, 32nd, and 36th of all California counties in terms of agricultural production.¹⁰¹ The continued urbanization of the SoCAB minimizes GHG emissions from agricultural sources such as livestock. Recent studies have sought to quantitate GHG emissions from the SoCAB with the goal of apportionment of the sources.^{102–105} The most academically studied of these gases is methane.

In a mixed emission source environment such as the SoCAB, there are two widely used methods to determine an estimate of total emissions: top-down and bottom-up. In top-down estimates, ambient mixing ratios are measured from a site downwind of the region and a total estimate for the entire basin can be calculated. This method says nothing about where the emissions are coming from and is often limited by short monitoring time scales.¹⁰⁶ The bottom-up estimate looks at each individual emissions sector and tries to sum up total emissions in a region. This method relies on reporting to regulatory bodies as well as field sampling at individual locations. This data can often be incomplete and reported emissions are often underestimated.¹⁰⁷ While both methods are flawed, together they can be used to better understand the emissions in an air basin and what still needs to be done.

Previous studies have attempted to quantify and sort through the several potential methane and sources in the SoCAB using these two techniques. Wunch et al.¹⁰² calculated top-down estimates for both methane and CO₂ based on a 2007-2008 sampling period in Pasadena, CA. They found that CARB's bottom-up inventory for statewide emissions only summed to half of the total emissions calculated therein. Wennberg et al.¹⁰³ assembled a bottom-up inventory of methane and ethane emissions for biogenic (anaerobic) sectors as well as petroleum refining and pipeline natural gas in 2010. Their inventory was only able to account for half of the total methane emissions and less than 20% of the ethane seen in top-down measurements. Peischl et al.¹⁰⁸ built on the previous bottom-up methane inventory and used C₂-C₅ alkanes as tracers to further apportion the emissions. They proposed seven major emissions sources for the SoCAB including five sources of methane: pipeline natural gas, bacterial breakdown, local natural gas processing and seepage, vehicular sources and industrial solvent and coating use. The bacterial breakdown source of methane contains both agricultural and landfill sources of methane as they

were not able to determine a distinct tracer to separate the two. Clearly, there is still work to be done to accurately determine the sources of methane to the region and how much they contribute to overall emissions.

For halocarbon emissions, because of a lack of tracers and fewer actual source types, bottom-up inventories are not often compiled. Three top-down studies have been published in the last 15 years on halocarbon emissions in the SoCAB.¹⁰⁹⁻¹¹¹ Two of these studies were based on airborne missions over a short time period, and potentially suffer from a lack of representativeness.^{109,110} The third tracks mixing ratios over summer and fall 2005, but is missing many of the second and third generation compounds. Further, the mission was completed before any regulations went into place on HCFC or HFC emissions.¹¹¹ It is important that these emissions estimates be updated to ensure that regulations are working to limit GHG emissions.

1.4.4 Oil and Natural Gas in the SoCAB

The SoCAB is an interesting air shed to study in light of the recent focus on emissions from natural gas and oil production. Consumption of natural gas and oil is high, but production in the region is relatively low. California as a whole produces 6% of the United States' total crude oil averaging 508,000 barrels per day.¹¹² Of the state's total, roughly 14% comes from the greater SoCAB region (Los Angeles, Orange, Riverside and San Bernardino counties).¹¹³ There are two currently active oil fields in the region, both in Los Angeles county: the Beverly Hills Oil Field just northwest of downtown Los Angeles and the Long Beach Oil Field in the area known as the South Bay (Figure 1.7). Despite not being rich in recoverable oil, California is a leader in the refining of oil ranking third in the United States in total refining capacity. Over half of the state's twenty one refineries are located in the SoCAB. These are clustered in the City of Long Beach, which is home to the Port of Los Angeles.¹¹⁴ Freighter ships from around the world bring

crude oil to the port; it is then offloaded and quickly sent to the refineries nearby. California has the largest annual consumption of gasoline of any state.¹¹⁵ This demand is then combined with the strict blending regulations as put forth by CARB to decrease air pollution and the formation of ozone. Some of these rules include the addition of 10% ethanol and the exclusion of higher volatility compounds in summer months.¹¹⁶ These blend regulations are stricter than any other state, and as such California needs refineries locally to meet this demand for cleaner fuel.

In terms of natural gas, California relies heavily upon it for electricity production, making up 60% of its portfolio.¹¹⁵ The California Department of Conservation has reported that only 6% of the natural gas used in the greater Southern California region was produced in the state. Only 10% of all the natural gas produced in the state was from the SoCAB.¹¹³ This production deficit leads to a dependence on natural gas from other regions being pumped into the SoCAB. SoCalGas maintains over 100,000 miles of pipes beneath the SoCAB to serve customers in the region.¹¹⁷ Further, they also maintain several underground storage sites in the SoCAB. These wells are used to meet demand in the winter months and store excess gas when prices are low. The locations of these wells are shown in Figure 1.7. The Environmental Defense Fund has undertaken a survey of the pipelines used by the Southern California Gas Company (SoCalGas) to service the greater Los Angeles area. The report states that 16% of SoCalGas' pipes are made of a corroded or leak prone material and more than a third are more than 50 years old.¹¹⁸ However, SoCalGas has stated on several occasions that they have removed all cast iron pipes from use and have begun the process of removing unprotected steel pipes as well.^{119,120} It is expected that with Los Angeles being a newer city compared to many on the East Coast that natural gas leaks from transmission and distribution pipelines are fewer and lead to less overall emissions. The nature of GHG emissions and the sources of methane in particular in the SoCAB

will be analyzed in this dissertation.

1.5 References

- (1) Finlayson-Pitts, B.; Pitts, J. *Chemistry of the Upper and Lower Atmosphere*; Academic Press, 2000.
- (2) Ramanathan, V.; Callis, L.; Cess, R.; Hansen, J.; Isaksen, I.; Kuhn, W.; Lacis, A.; Luther, F.; Mahlman, J.; Reck, R.; et al. Climate-chemical interactions and effects of changing atmospheric trace gases. *Rev. Geophys.* **1987**, *25* (7), 1441–1482.
- (3) American Chemical Society. What are the properties of a greenhouse gas? <https://www.acs.org/content/acs/en/climatescience/greenhousegases/properties.html> (accessed Nov 10, 2017).
- (4) National Center for Atmospheric Research. Air Composition https://www.eo.ucar.edu/basics/wx_1_b_1.html (accessed Nov 11, 2017).
- (5) MacFarling Meure, C.; Etheridge, D.; Trudinger, C.; Steele, P.; Langenfelds, R.; van Ommen, T.; Smith, A.; Elkins, J. Law Dome CO₂, CH₄ and N₂O ice core records extended to 2000 years BP. *Geophys. Res. Lett.* **2006**, *33* (14), L14810.
- (6) Hansen, J.; Ruedy, R.; Sato, M.; Lo, K. Global Surface Temperature Change. *Rev. Geophys.* **2010**, *48* (4), RG4004.
- (7) Cal Adapt. *Annual Averages Climate Tool*; University of California at Berkeley's Geospatial Innovation Facility, 2017.
- (8) National Oceanic and Atmospheric Administration. U.S. Climate Extremes Index (CEI) <https://www.ncdc.noaa.gov/extremes/cei/> (accessed Aug 3, 2017).
- (9) Cal Adapt. *Extreme Heat Climate Tool*; University of California at Berkeley's Geospatial Innovation Facility, 2017.
- (10) Bindoff, N.; Stott, P.; AchutaRao, K. M.; Allen, M. R.; Gillett, N.; Gutzler, D.; Hansingo, K.; Hegerl, G.; Hu, Y.; Jain, S.; et al. *Detection and Attribution of Climate Change: from Global to Regional. In: Climate Change 2013: The Physical Science Basis. Contribution of Working Group I to the Fifth Assessment Report of the Intergovernmental Panel on Climate Change*; Intergovernmental Panel on Climate Change, 2013.
- (11) Mann, M. E.; Rahmstorf, S.; Steinman, B. A.; Tingley, M.; Miller, S. K. The Likelihood of Recent Record Warmth. *Sci. Rep.* **2016**, *6*, 19831.
- (12) Meinshausen, M.; Smith, S. J.; Calvin, K.; Daniel, J. S.; Kainuma, M. L.; Lamarque, J.; Matsumoto, K.; Montzka, S. A.; Raper, S. C.; Riahi, K.; et al. The RCP greenhouse gas concentrations and their extensions from 1765 to 2300. *Clim. Change Dordr.* **2011**, *109* (1–2), 213–241.
- (13) Thomson, A. M.; Calvin, K. V.; Smith, S. J.; Kyle, G. P.; Volke, A.; Patel, P.; Delgadoarias, S.; Bond-lamberty, B.; Wise, M. A.; Clarke, L. E.; et al. RCP4.5: a pathway for stabilization of radiative forcing by 2100. *Clim. Change Dordr.* **2011**, *109* (1–2), 77–94.
- (14) United Nations. *Paris Agreement on Climate Change*; 2016.
- (15) Heinmiller, B. T. The Politics of “Cap and Trade” Policies. *Nat. Resour. J.* **2007**, *47* (2), 445–467.
- (16) NIST Mass Spec Data Center. Infrared Spectra. In *NIST Chemistry WebBook, NIST Standard Reference Database*; Linstrom, P. J., Mallard, W. G., Eds.; National Institute of Standards and Technology, 2017; Vol. 69.

- (17) Makino, A.; Mae, T. Photosynthesis and plant growth at elevated levels of CO₂. *Plant Cell Physiol.* **1999**, *40* (10), 999–1006.
- (18) Orr, J. C.; Fabry, V. J.; Aumont, O.; Bopp, L.; Doney, S. C.; Feely, R. A.; Gnanadesikan, A.; Gruber, N.; Ishida, A.; Joos, F.; et al. Anthropogenic ocean acidification over the twenty-first century and its impact on calcifying organisms. *Nature* **2005**, *437* (7059), 681–686.
- (19) Archer, D.; Eby, M.; Brovkin, V.; Ridgwell, A.; Cao, L.; Mikolajewicz, U.; Caldeira, K.; Matsumoto, K.; Munhoven, G.; Montenegro, A.; et al. Atmospheric Lifetime of Fossil Fuel Carbon Dioxide. *Annu. Rev. Earth Planet. Sci.* **2009**, *37* (1), 117–134.
- (20) EDGARv4.3.2. *CO₂ time series 1990-2015 per region/country*; European Commission, Joint Research Centre (JRC)/PBL Netherlands Environmental Assessment Agency, 2016.
- (21) Environmental Protection Agency. *Inventory of U.S. Greenhouse Gas Emissions and Sinks: 1990-2015*; Environmental Protection Agency, 2017.
- (22) Stevens, J. P. *549 U.S.* 497.
- (23) Kenneth A. Roberts. *Clean Air Act*; 1963; Vol. 88–206.
- (24) Myhre, G.; Shindell, D.; Breon, F.-M.; Collins, W.; Fuglestedt, J.; Huang, J.; Koch, D.; Lamarque, J.-F.; Lee, D.; Mendoza, B.; et al. *Anthropogenic and Natural Radiative Forcing. In: Climate Change 2013: The Physical Science Basis. Contribution of Working Group I to the Fifth Assessment Report of the Intergovernmental Panel on Climate Change*; Cambridge University: United Kingdom, 2013.
- (25) Sheahan, T. Methane: The Irrelevant Greenhouse Gas. *Watts Up With That?*, 2014.
- (26) Prinn, R. G.; Weiss, R. F.; Krummel, P. B.; O’Doherty, S.; Fraser, P. J.; Muhle, J.; Reimann, S.; Vollmer, M. K.; Simmonds, P. G.; Maione, M.; et al. *The ALE / GAGE AGAGE Network*; Carbon Dioxide Information Analysis Center (CDIAC), Oak Ridge National Laboratory, U.S. Department of Energy (DOE), 2016.
- (27) Kirschke, S.; Bousquet, P.; Ciais, P.; Saunio, M.; Canadell, J. G.; Dlugokencky, E. J.; Bergamaschi, P.; Bergmann, D.; Blake, D. R.; Bruhwiler, L.; et al. Three decades of global methane sources and sinks. *Nat. Geosci.* **2013**, *6* (10), 813–823.
- (28) Simpson, I. J.; Chen, T.-Y.; Blake, D. R.; Rowland, F. S. Implications of the recent fluctuations in the growth rate of tropospheric methane. *Geophys. Res. Lett.* **2002**, *29* (10), 117–1.
- (29) Rigby, M.; Montzka, S. A.; Prinn, R. G.; White, J. W. C.; Young, D.; O’Doherty, S.; Lunt, M. F.; Ganesan, A. L.; Manning, A. J.; Simmonds, P. G.; et al. Role of atmospheric oxidation in recent methane growth. *Proc. Natl. Acad. Sci.* **2017**, *114* (21), 5373–5377.
- (30) Hausmann, P.; Sussmann, R.; Smale, D. Contribution of oil and natural gas production to renewed increase in atmospheric methane (2007–2014): top–down estimate from ethane and methane column observations. *Atmos Chem Phys* **2016**, *16* (5), 3227–3244.
- (31) Saunio, M.; Bousquet, P.; Poulter, B.; Peregón, A.; Ciais, P.; Canadell, J. G.; Dlugokencky, E. J.; Etiope, G.; Bastviken, D.; Houweling, S.; et al. The global methane budget 2000–2012. *Earth Syst. Sci. Data* **2016**, *8* (2), 697–751.
- (32) Mitsumori, M.; Sun, W. Control of rumen microbial fermentation for mitigating methane emissions from the rumen. *Asian-Australas. J. Anim. Sci.* **2008**, *21* (1), 144–154.
- (33) Le Mer, J.; Roger, P. Production, oxidation, emission and consumption of methane by soils: A review. *Eur. J. Soil Biol.* **2001**, *37* (1), 25–50.

- (34) Smith, P.; Martino, D.; Cai, Z.; Gwary, D.; Janzen, H.; Kumar, P.; McCarl, B.; Ogle, S.; O'Mara, F.; Rice, C.; et al. Greenhouse gas mitigation in agriculture. *Philos. Trans. R. Soc. B-Biol. Sci.* **2008**, *363* (1492), 789–813.
- (35) Fraser, A.; Palmer, P. I.; Feng, L.; Boesch, H.; Cogan, A.; Parker, R.; Dlugokencky, E. J.; Fraser, P. J.; Krummel, P. B.; Langenfelds, R. L.; et al. Estimating regional methane surface fluxes: the relative importance of surface and GOSAT mole fraction measurements. *Atmos Chem Phys* **2013**, *13* (11), 5697–5713.
- (36) van Groenigen, K. J.; van Kessel, C.; Hungate, B. A. Increased greenhouse-gas intensity of rice production under future atmospheric conditions. *Nat. Clim. Change* **2013**, *3* (3), 288–291.
- (37) Wilson, J. O.; Crill, P. M.; Bartlett, K. B.; Sebacher, D. I.; Harriss, R. C.; Sass, R. L. Seasonal Variation of Methane Emissions from a Temperate Swamp. *Biogeochemistry* **1989**, *8* (1), 55–71.
- (38) Morrison, I. M. Carbohydrate chemistry and rumen digestion. *Proc. Nutr. Soc.* **1979**, *38* (3), 269–274.
- (39) Kleiber, M.; Cole, H. H.; Mead, S. W. Bloat in Cattle and Composition of Rumen Gases. *J. Dairy Sci.* **1943**, *26* (10), 929–933.
- (40) USDA ERS - Statistics & Information <https://www.ers.usda.gov/topics/animal-products/cattle-beef/statistics-information.aspx> (accessed Jul 24, 2017).
- (41) Schmit, T. M.; Kaiser, H. M. Forecasting fluid milk and cheese demands for the next decade. *J. Dairy Sci.* **2006**, *89* (12), 4924–4936.
- (42) Beauchemin, K. A.; Kreuzer, M.; O'Mara, F.; McAllister, T. A. Nutritional management for enteric methane abatement: a review. *Aust. J. Exp. Agric.* **2008**, *48* (2), 21–27.
- (43) Eckard, R. J.; Grainger, C.; de Klein, C. A. M. Options for the abatement of methane and nitrous oxide from ruminant production: A review. *Livest. Sci.* **2010**, *130* (1), 47–56.
- (44) Scheutz, C.; Kjeldsen, P.; Bogner, J. E.; De Visscher, A.; Gebert, J.; Hilger, H. A.; Huber-Humer, M.; Spokas, K. Microbial methane oxidation processes and technologies for mitigation of landfill gas emissions. *Waste Manag. Res.* **2009**, *27* (5), 409–455.
- (45) van Haarlem, R. P.; Desjardins, R. L.; Gao, Z.; Flesch, T. K.; Li, X. Methane and ammonia emissions from a beef feedlot in western Canada for a twelve-day period in the fall. *Can. J. Anim. Sci.* **2008**, *88* (4), 641–649.
- (46) Safley, L. M.; Westerman, P. W. Biogas production from anaerobic lagoons. *Biol. Wastes* **1988**, *23* (3), 181–193.
- (47) Townsend-Small, A.; Marrero, J. E.; Lyon, D. R.; Simpson, I. J.; Meinardi, S.; Blake, D. R. Integrating Source Apportionment Tracers into a Bottom-up Inventory of Methane Emissions in the Barnett Shale Hydraulic Fracturing Region. *Environ. Sci. Technol.* **2015**, *49* (13), 8175–8182.
- (48) U.S. Energy Information Administration. How much carbon dioxide is produced when different fuels are burned? <https://www.eia.gov/tools/faqs/faq.php?id=73&t=11> (accessed Aug 4, 2017).
- (49) U.S. Energy Information Administration. Net generation for all sectors, monthly <https://www.eia.gov/electricity/data/browser/> (accessed Aug 4, 2017).
- (50) U.S. Energy Information Administration. *Natural Gas Withdrawal and Production*; U.S. EIA, 2017.
- (51) Mohr, S. H.; Evans, G. M. Long term forecasting of natural gas production. *Energy Policy* **2011**, *39* (9), 5550–5560.

- (52) Alvarez, R. A.; Pacala, S. W.; Winebrake, J. J.; Chameides, W. L.; Hamburg, S. P. Greater focus needed on methane leakage from natural gas infrastructure. *Proc. Natl. Acad. Sci.* **2012**, *109* (17), 6435–6440.
- (53) Hausfather, Z.; Muller, R. *New EPA Report Reveals Significantly Lower Methane Leakage from Natural Gas*; Berkeley Earth, 2013.
- (54) Kirchstetter, T. W.; Singer, B. C.; Harley, R. A.; Kendall, G. R.; Chan, W. Impact of Oxygenated Gasoline Use on California Light-Duty Vehicle Emissions. *Environ. Sci. Technol.* **1996**, *30* (2), 661–670.
- (55) Gentner, D. R.; Harley, R. A.; Miller, A. M.; Goldstein, A. H. Diurnal and Seasonal Variability of Gasoline-Related Volatile Organic Compound Emissions in Riverside, California. *Environ. Sci. Technol.* **2009**, *43* (12), 4247–4252.
- (56) Pang, Y.; Fuentes, M.; Rieger, P. Trends in selected ambient volatile organic compound (VOC) concentrations and a comparison to mobile source emission trends in California's South Coast Air Basin. *Atmos. Environ.* **2015**, *122*, 686–695.
- (57) Andreae, M. Biomass burning- Its history, use, and distribution and its impact on environmental quality and global climate. In *Global Biomass Burning: Atmospheric, Climatic and Biospheric Implications*; Levine, J. S., Ed.; MIT Press, 1991; pp 3–21.
- (58) Delmas, R. An overview of present knowledge on methane emission from biomass burning. *Fertil. Res.* **1994**, *37* (3), 181–190.
- (59) Etiope, G.; Klusman, R. W. Geologic emissions of methane to the atmosphere. *Chemosphere* **2002**, *49* (8), 777–789.
- (60) Etiope, G.; Caracausi, A.; Favara, R.; Italiano, F.; Baciù, C. Methane emission from the mud volcanoes of Sicily (Italy). *Geophys. Res. Lett.* **2002**, *29* (8), 56–1.
- (61) Sauter, E. J.; Muyakshin, S. I.; Charlou, J. L.; Schluter, M.; Boetius, A.; Jerosch, K.; Damm, E.; Foucher, J. P.; Klages, M. Methane discharge from a deep-sea submarine mud volcano into the upper water column by gas hydrate-coated methane bubbles. *Earth Planet. Sci. Lett.* **2006**, *243* (3–4), 354–365.
- (62) Chang, K.; Baril, R.; Hull, M.; Pepe, N. T. M.; Nwachuku, I. B.; Doezema, L. A. Microseepage of C2–C5 alkanes over the Baldwin Hills in Los Angeles. *Atmos. Environ.* **2014**, *87*, 170–174.
- (63) Sarbu, I.; Valea, E. S. Past, present and future perspectives of refrigerants in air-conditioning, refrigeration and heat pump applications. *WSEAS Trans. Heat Mass Transf.* **2014**, *9*, 27–38.
- (64) American Chemical Society Historical Landmarks. Chlorofluorocarbons and Ozone Depletion
<https://www.acs.org/content/acs/en/education/whatischemistry/landmarks/cfcs-ozone.html> (accessed Jul 27, 2017).
- (65) Molina, M. J.; Rowland, F. S. Stratospheric sink for chlorofluoromethanes: chlorine atom-catalysed destruction of ozone. *Nature* **1974**, *249* (5460), 810–812.
- (66) Graziosi, F.; Arduini, J.; Furlani, F.; Giostra, U.; Kuijpers, L. J. M.; Montzka, S. A.; Miller, B. R.; O'Doherty, S. J.; Stohl, A.; Bonasoni, P.; et al. European emissions of HCFC-22 based on eleven years of high frequency atmospheric measurements and a Bayesian inversion method. *Atmos. Environ.* **2015**, *112*, 196–207.
- (67) Montzka, S. A.; McFarland, M.; Andersen, S. O.; Miller, B. R.; Fahey, D. W.; Hall, B. D.; Hu, L.; Siso, C.; Elkins, J. W. Recent Trends in Global Emissions of

- Hydrochlorofluorocarbons and Hydrofluorocarbons: Reflecting on the 2007 Adjustments to the Montreal Protocol. *J. Phys. Chem. A* **2015**, *119* (19), 4439–4449.
- (68) US EPA. Phaseout of Class II Ozone-Depleting Substances <https://www.epa.gov/ods-phaseout/phaseout-class-ii-ozone-depleting-substances> (accessed Jun 7, 2017).
- (69) United Nations Environment Program. *Kigali Amendment to the Montreal Protocol*; 2016.
- (70) Yang, Z.; Wu, X. Retrofits and options for the alternatives to HCFC-22. *Energy* **2013**, *59*, 1–21.
- (71) Birol, F. *Key World Energy Statistics*; International Energy Agency, 2016.
- (72) Wang, Y.; Xu, Y.; Chen, Y.; Tian, C.; Feng, Y.; Chen, T.; Li, J.; Zhang, G. Influence of different types of coals and stoves on the emissions of parent and oxygenated PAHs from residential coal combustion in China. *Environ. Pollut.* **2016**, *212* (Supplement C), 1–8.
- (73) Markandya, A.; Wilkinson, P. Energy and Health 2: Electricity Generation and Health. *The Lancet* **2007**, *370*, 979–990.
- (74) Stephens, C.; Ahern, M. *Worker and Community Health Impacts Related to Mining Operations Internationally: A Rapid Review of the Literature*; London School of Hygiene and Tropical Medicine, 2001.
- (75) U.S. Energy Information Administration. *Aggregate coal mine production*; U.S. Department of Energy, 2016.
- (76) U.S. Energy Information Administration. How much gasoline does the United States consume? - FAQ <https://www.eia.gov/tools/faqs/faq.php?id=23&t=10> (accessed Aug 10, 2017).
- (77) Inman, M. The World has Passed Peak Oil, says Top Economist <http://newswatch.nationalgeographic.org/2011/05/05/the-world-has-passed-peak-oil-says-top-economist/> (accessed Aug 10, 2017).
- (78) Mouawad, J. Oil Innovations Pump New Life Into Old Wells. *The New York Times*. March 5, 2007.
- (79) Balcombe, P.; Anderson, K.; Speirs, J.; Brandon, N.; Hawkes, A. The Natural Gas Supply Chain: The Importance of Methane and Carbon Dioxide Emissions. *ACS Sustain. Chem. Eng.* **2017**, *5* (1), 3–20.
- (80) ISO New England. Fuel Security for Natural Gas-Fired Generators <https://www.iso-ne.com/about/regional-electricity-outlook/grid-in-transition-opportunities-and-challenges/natural-gas-infrastructure-constraints> (accessed Aug 10, 2017).
- (81) U.S. Department of Energy. *Natural Gas Infrastructure Implications of Increased Demand from the Electric Power Sector*; 2015.
- (82) Phillips, N. G.; Ackley, R.; Crosson, E. R.; Down, A.; Hutyra, L. R.; Brondfield, M.; Karr, J. D.; Zhao, K.; Jackson, R. B. Mapping urban pipeline leaks: Methane leaks across Boston. *Environ. Pollut.* **2013**, *173*, 1–4.
- (83) von Fischer, J. C.; Cooley, D.; Chamberlain, S.; Gaylord, A.; Griebenow, C. J.; Hamburg, S. P.; Salo, J.; Schumacher, R.; Theobald, D.; Ham, J. Rapid, Vehicle-Based Identification of Location and Magnitude of Urban Natural Gas Pipeline Leaks. *Environ. Sci. Technol.* **2017**, *51* (7), 4091–4099.
- (84) Hopkins, F. M.; Kort, E. A.; Bush, S. E.; Ehleringer, J. R.; Lai, C.-T.; Blake, D. R.; Randerson, J. T. Spatial patterns and source attribution of urban methane in the Los Angeles Basin. *J. Geophys. Res. Atmospheres* **2016**, 2015JD024429.

- (85) Lamb, B. K.; Edburg, S. L.; Ferrara, T. W.; Howard, T.; Harrison, M. R.; Kolb, C. E.; Townsend-Small, A.; Dyck, W.; Possolo, A.; Whetstone, J. R. Direct Measurements Show Decreasing Methane Emissions from Natural Gas Local Distribution Systems in the United States. *Environ. Sci. Technol.* **2015**, *49* (8), 5161–5169.
- (86) Pétron, G.; Frost, G.; Miller, B. R.; Hirsch, A. I.; Montzka, S. A.; Karion, A.; Trainer, M.; Sweeney, C.; Andrews, A. E.; Miller, L.; et al. Hydrocarbon emissions characterization in the Colorado Front Range: A pilot study. *J. Geophys. Res. Atmospheres* **2012**, *117* (D4), D04304.
- (87) Brandt, A. R.; Heath, G. A.; Kort, E. A.; O’Sullivan, F.; Pétron, G.; Jordaan, S. M.; Tans, P.; Wilcox, J.; Gopstein, A. M.; Arent, D.; et al. Methane leaks from North American natural gas systems. *Science* **2014**, *343* (6172), 733–735.
- (88) Energy Modeling Forum. *Changing the Game?: Emissions and Market Implications of New Natural Gas Supplies*; 26; Stanford University.
- (89) Total Seasonal Rainfall 1877-Present for Downtown Los Angeles, California <http://www.laalmanac.com/weather/we13.php> (accessed Nov 15, 2017).
- (90) Western Regional Climate Center. Predominant Wind Directions. Desert Research Institute.
- (91) Western Regional Climate Center. CLIMATE OF CALIFORNIA <https://wrcc.dri.edu/narratives/CALIFORNIA.htm> (accessed Nov 15, 2017).
- (92) Haagen-Smit, A. J. Chemistry and Physiology of Los Angeles Smog. *Ind. Eng. Chem.* **1952**, *44* (6), 1342–1346.
- (93) Bell, M. L.; McDermott, A.; Zeger, S. L.; Samet, J. M.; Dominici, F. Ozone and Short-term Mortality in 95 US Urban Communities, 1987-2000. *JAMA* **2004**, *292* (19), 2372–2378.
- (94) Warneke, C.; de Gouw, J. A.; Holloway, J. S.; Peischl, J.; Ryerson, T. B.; Atlas, E.; Blake, D.; Trainer, M.; Parrish, D. D. Multiyear trends in volatile organic compounds in Los Angeles, California: Five decades of decreasing emissions: Trends in VOCs in Los Angeles. *J. Geophys. Res. Atmospheres* **2012**, *117* (D21).
- (95) California Air Resources Board. History of Air Resources Board. October 22, 2014.
- (96) California Air Resources Board. iADAM: Air Quality Data Statistics. 2017.
- (97) Turnbull, J. Use of Biomass in Electric-Power Generation - the California Experience. *Biomass Bioenergy* **1993**, *4* (2), 75–84.
- (98) Dwyer, J. California Tradable Emissions Policy and Greenhouse Gas Control. *J. Energy Eng.-Asce* **1992**, *118* (2), 59–76.
- (99) Hayhoe, K.; Cayan, D.; Field, C. B.; Frumhoff, P. C.; Maurer, E. P.; Miller, N. L.; Moser, S. C.; Schneider, S. H.; Cahill, K. N.; Cleland, E. E.; et al. Emissions pathways, climate change, and impacts on California. *Proc. Natl. Acad. Sci. U. S. A.* **2004**, *101* (34), 12422–12427.
- (100) California Air Resources Board. First Update to the Climate Change Scoping Plan. California Environmental Protection Agency May 22, 2014.
- (101) Ross, K. *California Agricultural Statistics Review, 2015-2016*; California Department of Food and Agriculture, 2016.
- (102) Wunch, D.; Wennberg, P. O.; Toon, G. C.; Keppel-Aleks, G.; Yavin, Y. G. Emissions of greenhouse gases from a North American megacity. *Geophys. Res. Lett.* **2009**, *36* (15), L15810.

- (103) Wennberg, P. O.; Mui, W.; Wunch, D.; Kort, E. A.; Blake, D. R.; Atlas, E. L.; Santoni, G. W.; Wofsy, S. C.; Diskin, G. S.; Jeong, S.; et al. On the Sources of Methane to the Los Angeles Atmosphere. *Environ. Sci. Technol.* **2012**, *46* (17), 9282–9289.
- (104) Brown, S. G.; Frankel, A.; Hafner, H. R. Source apportionment of VOCs in the Los Angeles area using positive matrix factorization. *Atmos. Environ.* **2007**, *41* (2), 227–237.
- (105) Hsu, Y.-K.; VanCuren, T.; Park, S.; Jakober, C.; Herner, J.; FitzGibbon, M.; Blake, D. R.; Parrish, D. D. Methane emissions inventory verification in southern California. *Atmos. Environ.* **2010**, *44* (1), 1–7.
- (106) Lyon, D. R.; Zavala-Araiza, D.; Alvarez, R. A.; Harriss, R.; Palacios, V.; Lan, X.; Talbot, R.; Lavoie, T.; Shepson, P.; Yacovitch, T. I.; et al. Constructing a Spatially Resolved Methane Emission Inventory for the Barnett Shale Region. *Environ. Sci. Technol.* **2015**, *49* (13), 8147–8157.
- (107) Allen, D. T. Methane emissions from natural gas production and use: reconciling bottom-up and top-down measurements. *Curr. Opin. Chem. Eng.* **2014**, *5*, 78–83.
- (108) Peischl, J.; Ryerson, T. B.; Brioude, J.; Aikin, K. C.; Andrews, A. E.; Atlas, E.; Blake, D.; Daube, B. C.; de Gouw, J. A.; Dlugokencky, E.; et al. Quantifying sources of methane using light alkanes in the Los Angeles basin, California: SOURCES OF METHANE IN L.A. *J. Geophys. Res. Atmospheres* **2013**, *118* (10), 4974–4990.
- (109) Barletta, B.; Carreras-Sospedra, M.; Cohan, A.; Nissenson, P.; Dabdub, D.; Meinardi, S.; Atlas, E.; Lueb, R.; Holloway, J. S.; Ryerson, T. B.; et al. Emission estimates of HCFCs and HFCs in California from the 2010 CalNex study. *J. Geophys. Res. Atmospheres* **2013**, *118* (4), 2019–2030.
- (110) Barletta, B.; Nissenson, P.; Meinardi, S.; Dabdub, D.; Sherwood Rowland, F.; VanCuren, R. A.; Pederson, J.; Diskin, G. S.; Blake, D. R. HFC-152a and HFC-134a emission estimates and characterization of CFCs, CFC replacements, and other halogenated solvents measured during the 2008 ARCTAS campaign (CARB phase) over the South Coast Air Basin of California. *Atmos Chem Phys* **2011**, *11* (6), 2655–2669.
- (111) Gentner, D. R.; Miller, A. M.; Goldstein, A. H. Seasonal Variability in Anthropogenic Halocarbon Emissions. *Environ. Sci. Technol.* **2010**, *44* (14), 5377–5382.
- (112) U.S. Energy Information Administration. Crude Oil Production https://www.eia.gov/dnav/pet/pet_crd_crpdn_adc_mbbldpd_a.htm (accessed Aug 9, 2017).
- (113) Division of Oil, Gas, & Geothermal Resources. *Well Count and Production of Oil, Gas, and Water by County- 2015*; California Department of Conservation, 2016.
- (114) California Energy Commission. *Oil Refinery Locations in California*, 2016.
- (115) U.S. Energy Information Administration. *State Energy Data System*; U.S. Department of Energy, 2016.
- (116) Frank, M. What Is Winter-Blend Gasoline, Anyway? <http://www.popularmechanics.com/cars/news/auto-blog/summer-blend-vs-winter-blend-gasoline-whats-the-difference-13747431> (accessed Aug 9, 2017).
- (117) Southern California Gas Company. Pipeline Basics. December 2013.
- (118) Environmental Defense Fund. Los Angeles Area: Snapshot of natural gas leaks <https://www.edf.org/climate/methanemaps/city-snapshots/los-angeles-area> (accessed Apr 10, 2017).
- (119) SoCalGas. Methane Emissions Map FAQ <https://www.socalgas.com/stay-safe/methane-emissions/methane-emissions-map-faq> (accessed Aug 10, 2017).

- (120) SoCalGas. SoCalGas Efforts to Reduce Its Methane Emissions
<https://www.socalgas.com/stay-safe/methane-emissions/SoCalGas-efforts-to-reduce-methane-emissions> (accessed Aug 10, 2017).

CHAPTER 2: Methods

2.1 Sampling Site

Mt. Wilson, which sits in the San Gabriel Mountains behind Sierra Madre, CA, peaks at 5,700 ft above sea level bounding the South Coast Air Basin to the north. The geography of the region allows for integrated air sampling of the SoCAB at the site as the region is bounded on three sides by low mountain ranges and the Pacific Ocean. The predominant wind patterns in the region are from off the coast heading northeast right to the base of Mt. Wilson. During the daytime, the tropospheric boundary layer rises due to heating and air from the SoCAB reaches the mountains. As evening approaches, the temperature drops and the upslope cools trapping the air in a much lower boundary layer.¹ This change in boundary layer height allows for sampling at Mt. Wilson during the daytime to be representative of the polluted troposphere in Los Angeles and at night be part of the lower free troposphere with only global background levels of VOCs present. For these reasons, several different studies have used Mt. Wilson as a sampling site to gather a better understanding of the atmospheric chemistry of the SoCAB.^{2,3,4}

2.2 Project Description

The bulk of the dissertation work is based around a two year monitoring project funded by the California Air Resources Board. Our laboratory was funded to collect whole air samples representative of the South Coast Air Basin and study emissions from the region. The original goals of the project were the detection and quantitation of CFCs, HCFCs, and HFCs. I was put in charge of carrying out the collection, laboratory analysis, and quantitation of all VOCs in all samples and then given the entire data set with which to analyze various aspects of emissions from the Los Angeles megacity.

Each month, starting in June of 2014 and ending in May of 2016, 32 whole air samples were collected at the California Laboratory for Atmospheric Remote Sensing site at Mt. Wilson

(34° 13' 15.28", -118° 3' 25.79"). The site is on the front face of Mt. Wilson and looks out over the SoCAB (Figure 2.1). At the site, quarter inch stainless steel tubing was run from where the canisters were housed to a tree on the slope facing into the wind.

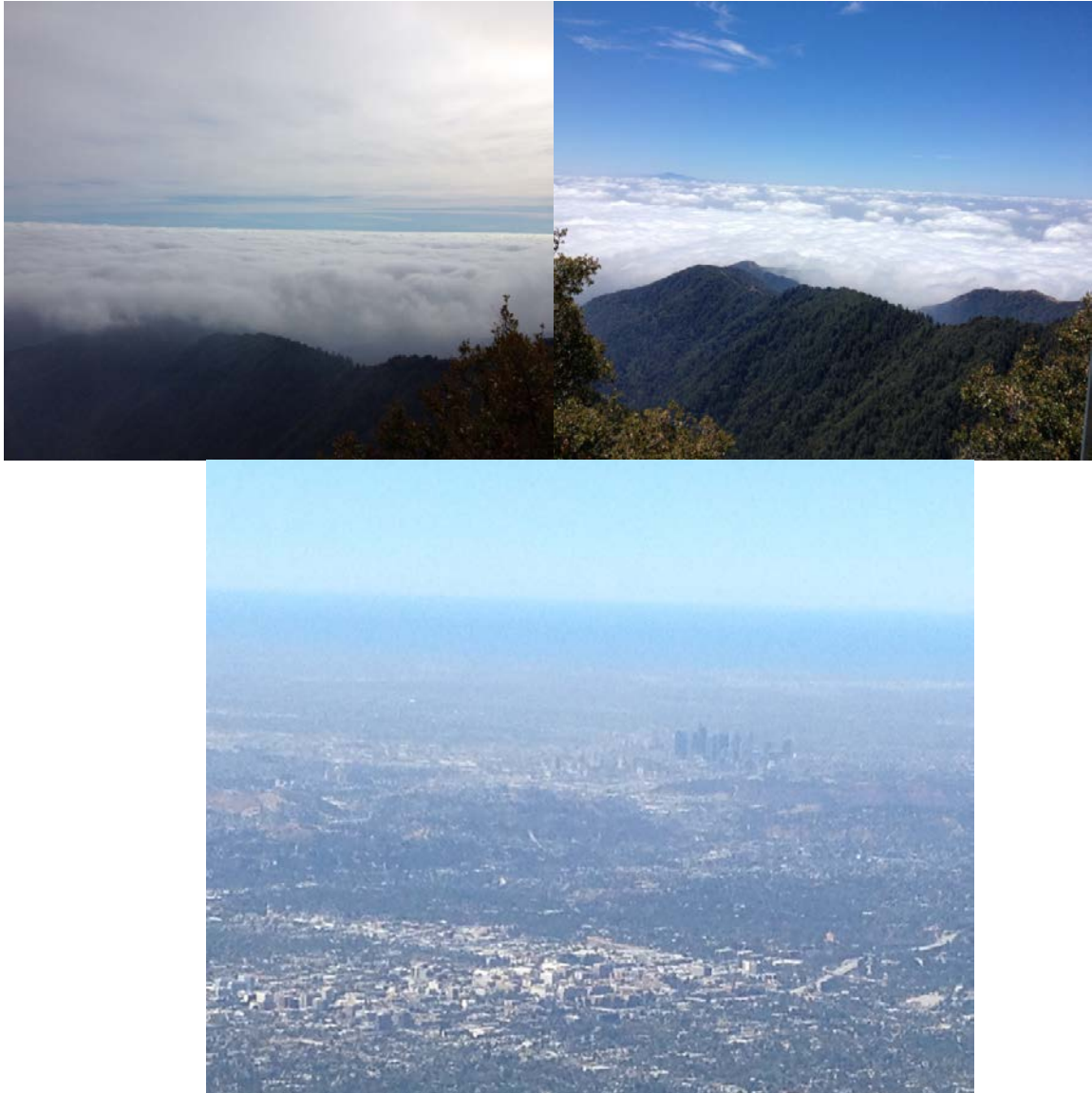


Figure 2.1. The greater South Coast Air Basin as seen from the Mt. Wilson sampling site at various times of day and the year. The top left image shows the extent to which the marine layer can infiltrate the region. The top right image shows the marine layer breaking up later that same day, and the bottom image shows a summer afternoon in which one can see to the coast.

Samples were collected in evacuated 1.9 L stainless steel canisters that were sealed with Swagelok Nupro metal bellows valves. These canisters were pretreated by baking them overnight at 150 °C to form an oxidized coating inside the canister. This coating minimizes potential wall losses of less volatile compounds. Prior to each use, the canisters were flushed with high purity helium and then evacuated to ~0.01 torr before being transported to the sampling site. Once at the Mt. Wilson site, they were connected to one eighth inch stainless steel sampling lines via a Swagelok “T union”. The third end of the “T union” was plugged with a brass Swagelok stopper. The sampling lines were connected to an Atmospheric Technology Model 8001 Automated Canister Sampler, that was connected via brass fittings to the sampling line mentioned above (Figure 2.2). This “auto-sampler” is capable of collecting integrated air samples at times specified by the user, without a technician being present.

Here, one hour integrated air samples were collected, filling each canister to roughly 30 psia. For this study, the sampling week was defined as starting on the third Thursday of each month. Four samples were collected each day of that ensuing week at 11:00, 13:00, 15:00, and 17:00. These times were chosen to achieve a broad picture of emissions in the SoCAB during daytime hours when Mt. Wilson is within the boundary layer. The four remaining cans each month were used to sample at midnight to check for any local emissions and determine background VOC levels at that latitude. When setting up the canisters at the site, a dual bellows pump was used to pump and flush each of the 32 sampling lines. The lines were pressurized to 30 psi and then the valve next to the gauge was opened allowing the lines to return to ambient pressure. This was done three times to ensure that the lines were clean of any debris or stale air. Once the lines were flushed, the “T-union” was replugged and the canister valves were opened to allow them to be filled.

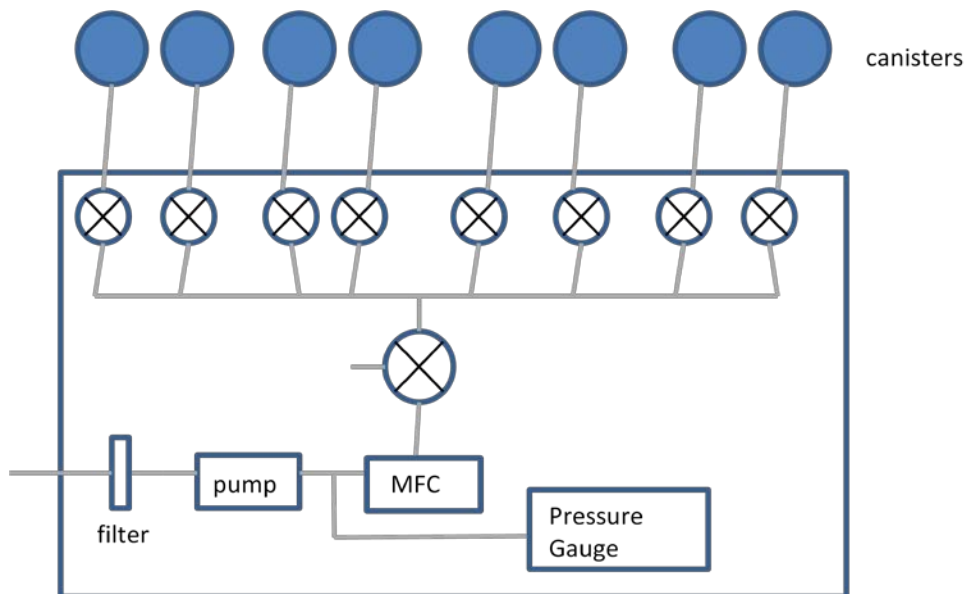


Figure 2.2. Schematic of the autosampler setup that was used at the Mt. Wilson site. Shown are 8 of the 32 canisters and lines. Each line has its own pneumatic valve that allows for the filling of one canister at a time.

The 24 months of sampling theoretically yielded a total of 768 different air samples; however, certain mechanical and experimental issues limited that number slightly. For the first 14 months of sampling, a mechanical problem with two of the ports caused the canisters attached to these ports to not fill at all. This issue was addressed by returning the “autosampler” to ATEC for service. Further, there were a few instances where the O-ring in the “T-union” was faulty and not properly fixed resulting in a slow leak into the canister before sampling began. These leaks were detected by the “auto-sampler”, and when the time came to fill it, the noted pressure was above the threshold for an empty canister. This pressure difference caused the “autosampler” to immediately stop filling the canister and wait for the next sampling time to begin. Finally, in April of 2016, an unexpected power outage occurred at the Mt. Wilson site during the sampling week. When power was restored, the “auto-sampler” had reset and lost the programming

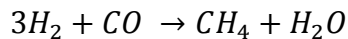
schedule. This resulted in only six samples being collected during that month. Due to these issues, a total of 587 samples over two years were actually collected.

2.3 Gas Chromatography Analysis

The filled canisters were returned to the laboratory in Irvine for analysis. Three separate gas chromatography (GC) systems were used for the quantitative analysis of over 70 VOCs. On each system, a working standard is analyzed at the start and end of every day and after every eight sample injections. The first system has been specifically designed for methane detection. Briefly, an HP 5890 GC is equipped with a packed 80/100 mesh spherocarb molecular sieve column which is attached to a flame ionization detector (FID). A portion of the air sample is flown into the evacuated manifold until the pressure reaches 400 torr. The sample is then injected into the column. The resulting chromatogram is printed on a Spectra-Physics ChromJet Integrator. This method has an accuracy of $\pm 1\%$ and a precision of ± 3 ppb.

The second system is capable of measuring carbon monoxide and carbon dioxide. This system pairs two GCs working in parallel (a schematic is shown in Figure 2.3). An aliquot of the air sample is flowed into the evacuated manifold and sample loops to a final pressure of 500 torr. Samples are injected into the two columns via two manual switching valves. The first system detects CO_2 via an HP 5890 GC and a packed 80/100 mesh spherocarb molecular sieve column connected to a thermal conductivity detector with an accuracy of $\pm 1\%$ and a precision of ± 1 ppm. The second detects CO via an FID after conversion to methane. For CO detection, the sample of air from the injection loop is passed through an HP 5890 GC housing a molecular sieve 5A column. For the first three and a half minutes the resolved air is vented to the room. After that point, a switching valve activates passing the flow into a catalysis chamber. The

chamber contains a Chromosorb G plate covered with a 2% nickel coating. Hydrogen gas is flown in to convert the CO to methane via the reaction:



This method of conversion is 100% efficient at temperatures between 360°C and 385°C and so the catalysis chamber is kept at 360°C.^{5,6} The eluent is then flown through to the FID for analysis. This analysis has a limit of detection of 5 ppb, accuracy of $\pm 7\%$ and precision of $\pm 3\%$.⁵ After a run is completed, the automatic switching valve returns to the load position, and then a manual valve is switched that allows for the flow of helium back into the column. This “backflushing” step pushes any CO₂ stuck in the column back out, so as to not interfere with the CO separation in the next analysis. The helium is allowed to flush out the column for two minutes before the flow is shut off and the next sample can be loaded. This technique allows for the system to be run for an entire day without CO₂ affecting the baseline of the chromatogram.

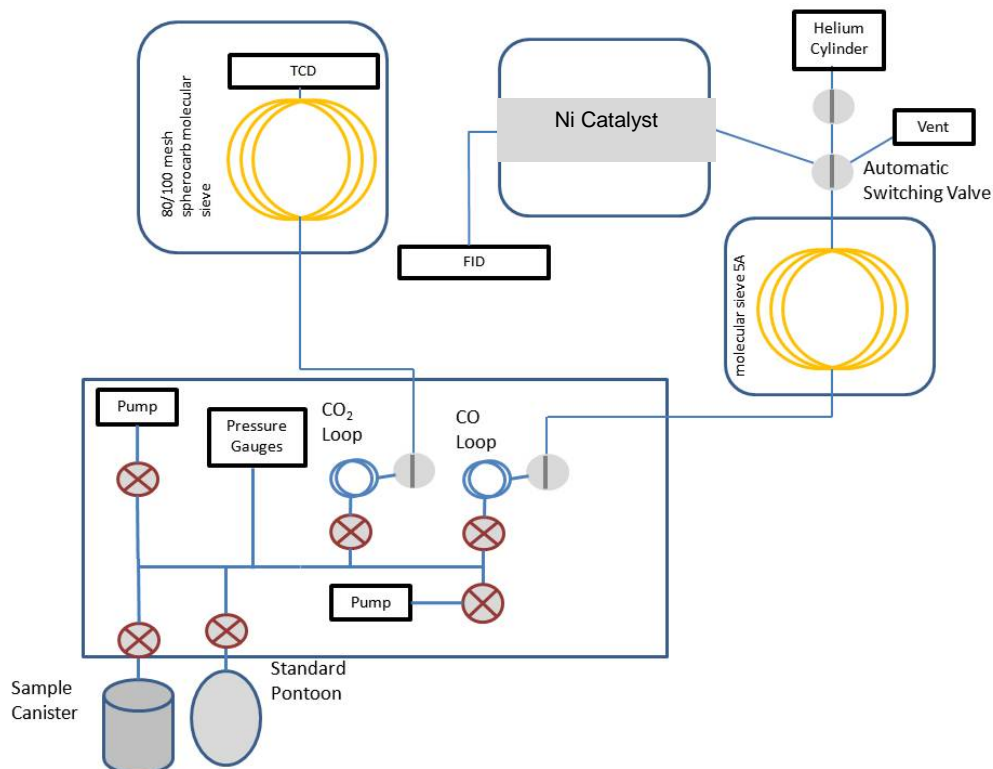


Figure 2.3 Schematic of the parallel gas chromatography system used to analyze carbon monoxide and carbon dioxide. To detect CO via FID, the CO must first be catalytically converted to methane.

When not in use, the oven temperature on the CO system is set to 150°C to ensure any remaining CO₂ is removed. A complete run of the CO/CO₂ system takes approximately 10 minutes.

Finally, all other VOCs are detected via a trio of GCs working in parallel. Whole air samples are connected to the evacuated manifold which is shown in Figure 2.4. Of note in the design of this system and manifold, is the inclusion of two vacuum pumps and a valve that separates the two. Having dual pumps attached to the manifold isolating one side of the manifold from the other allows for the preparation of one sample while the previous is being run and therefore speeding up the analysis time. After the manifold is helium flushed for a minute and then evacuated, the sample canister is attached and the valve to the pump is closed. Any excess air is pumped off such that 0.05 moles of gas is within the manifold and canister. Next, the valve that separates the left half of the manifold from the right is opened and the air begins to flow through a 5 mL loop which is filled with glass beads. The flow is kept constant using a Brooks Instruments mass flow controller set to 500 mL min⁻¹. During the “trapping” process, this loop is submerged in liquid nitrogen, which allows for the condensation of the VOCs of interest aided by the glass beads that increase the surface area for condensation to occur. Exactly 900 torr of the sample is passed through the loop before the valve is closed isolating the two halves of the manifold again. After pumping on the loop for one minute to remove oxygen, the loop is further isolated by moving the switching valve to the bypass mode which forms a closed loop. Finally, just prior to injection, the preconcentrated sample is revitalized by replacing the liquid nitrogen on the loop with near boiling water. The switching valve is switched to inject, and a toggle button is pressed to signal the GCs to start the heating sequence. The sample is injected into the system where it passes through a splitter box that sends a predetermined portion of the air to each individual column. This split is determined by the interior diameter of each column and the

amount of air necessary for a clean peak. After injection, the manifold is evacuated before starting the loading and “trapping” process again. This cycle takes 21 minutes per sample.

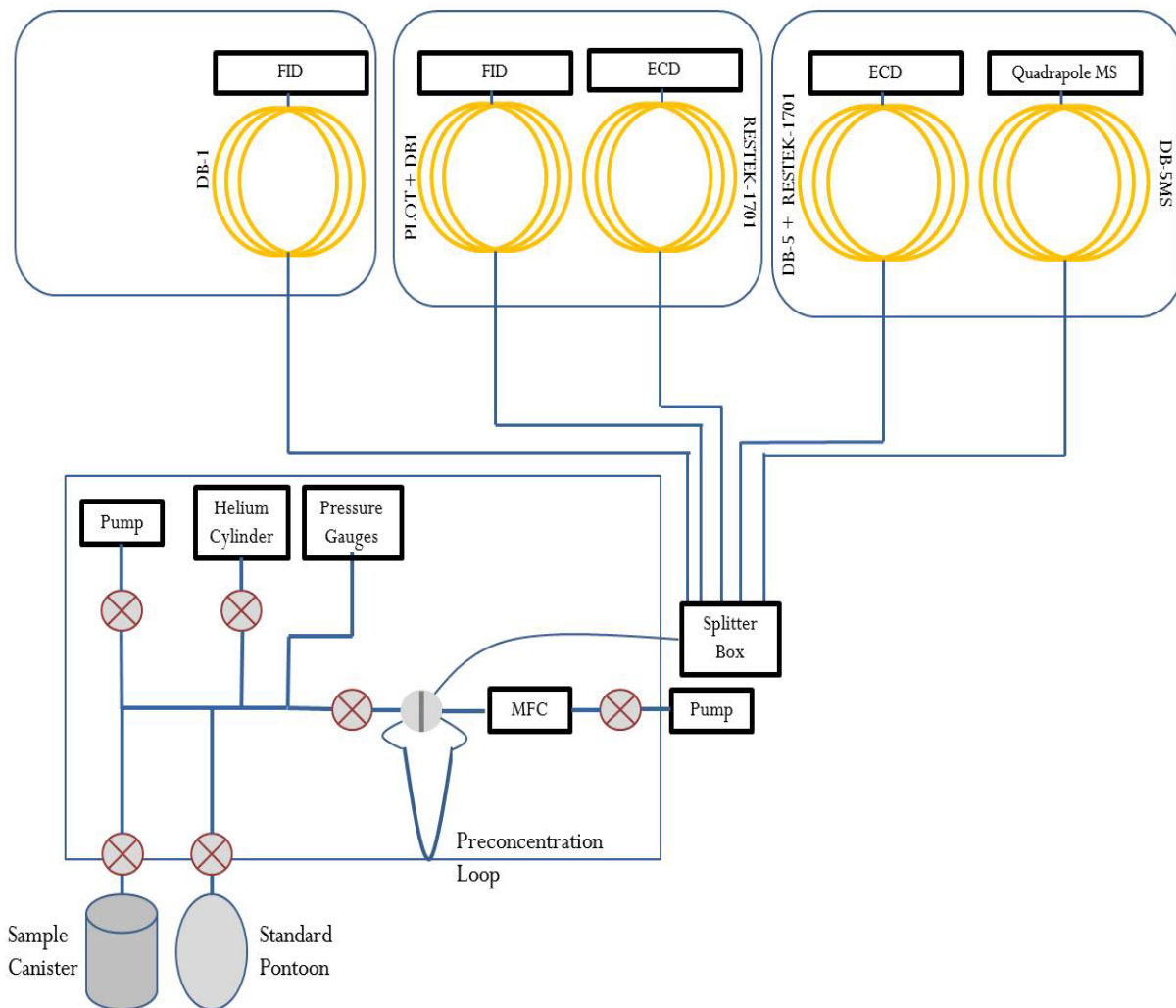


Figure 2.4 Schematic of the parallel 5 column gas chromatography system used to analyze VOCs.

There are 5 columns in this system inside three HP 6890 GCs (as seen in Figure 2.4), each of which is connected to a different detector as follows: a DB-1 column attached to an FID, PLOT+DB1 attached to an FID, RESTEK-1701 attached to an electron capture detector (ECD), DB5+RESTEK-1701 attached to an ECD, and DB-5 MS attached to a HP 5970 quadrupole mass

spectrometer. This multicolumn system allows for the precise separation and detection of over 70 VOCs including hydrocarbons, chlorofluorocarbons and their replacements, alkyl nitrates and oxygenated species down to single part per trillion detection limits. Accuracy of hydrocarbon concentrations reported here is $\pm 5\%$ and ranges from $\pm 5-20\%$ for halocarbons. Limits of detection, precision and accuracy of compounds analyzed in this text are shown in Table 2.1 Further specific details of the analytical system including oven temperature ramping schemes and flow rates can be found in Colman et al.⁷

Table 2.1 Statistical overview of the hydrocarbons and halocarbons used in analysis herein as measured by gas chromatography

Compound	Formula	LOD	Accuracy	% Precision
Carbon monoxide	CO	5 ppb	7%	3%
Carbon dioxide	CO ₂	<1 ppm	1 ppm	1%
Methane	CH ₄	<1 ppm	3 ppb	1%
Ethane	C ₂ H ₆	3 ppt	5%	1%
Ethene	C ₂ H ₄	3 ppt	5%	2%
Ethyne	C ₂ H ₂	3 ppt	5%	1%
Propene	C ₃ H ₆	3 ppt	5%	5%
Propane	C ₃ H ₈	3 ppt	5%	3%
i-Butane	C ₄ H ₁₀	3 ppt	5%	4%
n-butane	C ₄ H ₁₀	3 ppt	5%	1%
i-pentane	C ₅ H ₁₂	3 ppt	5%	1%
n-pentane	C ₅ H ₁₂	3 ppt	5%	6%
Isoprene	C ₅ H ₈	3 ppt	5%	3%
n-hexane	C ₆ H ₁₄	3 ppt	5%	6%
2-methylpentane	C ₆ H ₁₄	3 ppt	5%	2%
3-methylpentane	C ₆ H ₁₄	3 ppt	5%	6%
n-heptane	C ₇ H ₁₆	3 ppt	5%	9%
Benzene	C ₆ H ₆	3 ppt	5%	7%
Ethylbenzene	C ₈ H ₁₀	3 ppt	5%	5%
m/p-xylenes	C ₈ H ₁₀	3 ppt	5%	4%
o-xylene	C ₈ H ₁₀	3 ppt	5%	6%
1,2,4-trimethylbenzene	C ₉ H ₁₂	3 ppt	5%	9%
Halocarbons				
CFC-12	CCl ₂ F	10 ppt	3%	1%
CFC-11	CCl ₂ F ₂	10 ppt	3%	1%
CFC-113	CCl ₂ FCF ₂	5 ppt	3%	1%
HFC-134a	CH ₂ FCF ₃	1 ppt	10%	1%
HFC-152a	CHF ₂ CH ₃	1 ppt	5%	3%
HCFC-22	CHF ₂ Cl	2 ppt	5%	2%
HCFC-141b	CH ₃ CCl ₂ F	0.5 ppt	10%	2%
HCFC-142b	CH ₃ CClF ₂	0.5 ppt	10%	2%
Chloroform	CHCl ₃	0.1 ppt	10%	3%
Methylchloroform	CH ₃ CCl ₃	0.1 ppt	5%	1%
Dichloromethane	CH ₂ Cl ₂	1 ppt	10%	1%
perchloroethylene	C ₂ Cl ₄	0.01 ppt	10%	1%

Samples were analyzed within three months of collection. The laboratory has previously shown that most of the gases we detect are stable in the canister over this time period. Some alkenes and aromatics such as ethene and benzene do experience a growth in concentration on the order of 0.1 ppt day⁻¹, which is negligible in comparison to the 1-5% precision in each measurement.⁸

2.4 Creation and Use of Working Standards

Concentrations of VOCs in air samples were determined via the peak areas and their relationship to a known working standard containing all analytes. This working standard is run at the start of every analysis, after eight subsequent runs, and at the end of every analysis. Standards are made in house. This process begins by first collecting clean air at the University of California Crooked Creek Research Station in the White Mountains that form the California-Nevada border. The station sits at 3100 m above sea level and is removed from any urban center. This site serves as a remote sampling location that contains only background levels of the long lived VOCs. Clean air is collected at this site as needed by the lab, roughly every three years. Briefly, a custom made setup is brought to the site that allows for the filling of 43.8 L gas cylinders to 2000 psi of pressure. Steel tubing is run from the top of a 10m pole at the site to a dual bellows pump in one of the research buildings. The pump is then connected to a gas cylinder that is submerged in liquid nitrogen. The valve assembly is kept warm in a bath of hot water to prevent the inlet from freezing shut during filling. The cylinder fills for roughly two hours and, once pressurized, it is removed from the liquid nitrogen and allowed to come to room temperature. The cylinder is then inverted over night to allow for any water to collect in the valve. The water is then removed by quickly opening the valve until only dry air is released.

Working standards are made by transferring some of the White Mountain air into a 34 L pontoon. The pontoon is then doped with a small volume of known secondary standard mixtures purchased from Scott Specialty Gases (Philadelphia, PA). These standards have undergone rigorous intercomparisons, and most compounds are NIST traceable.^{9,10}

After laboratory analysis, the baseline of each analyte peak in each chromatogram is hand modified for quality control purposes using Chromeleon (version 6.40) for the ECD and FID

channels and Chemstation (version 2.0) for the mass spectral data. Concentrations of analytes in air samples (C_s) are calculated in relation to the average peak area of standards run that day (PA_s) via:

$$C_U = PA_U \times \left(\frac{C_s}{PA_s} \right)$$

Where PA_U is the peak area of the analyte in the air sample and C_s is the known concentration of analyte in the working standard. On rare occasion, more than 900 torr of pressure was passed through the preconcentration loop due to analyst error. The total pressure passed through the loop is noted and the final analyte concentrations for that sample are scaled appropriately.

2.5 Detection and Quantitation of new HFCs

As part of the service contract with CARB, the detection and quantitation of six halocarbons previously not studied by our lab was explored. These halocarbons are among the second and third generation of refrigerants as noted in the introduction. These gases were HCFC-225ca&cb, HFC 4310mee, HFC-227ea, HFC-236fa, HFC-245fa, and HFC-365mfc. To test to see if our GC system could detect these species, bottles containing samples of these gases were opened in the lab briefly to allow for the head space to dissipate into the room. The manifold of the three GC system was then opened to the room and a sample of the room air was collected. The six new compounds were identified via the quadrupole MS with retention times listed in Table 2.2 and a sample chromatogram seen in Figure 2.5. Unfortunately, NIST standards of these compounds are not available, and so a different standardization process had to be used.

Table 2.2 Overview of HCFCs and HFCs detected for the first time on our analytical system and their presence in our working standard as well as in global background samples

Name	Formula	100 Year Global Warming Potential	Retention Time on DB-5MS (Min)	Amount in Working Standard (pptv)	July 2015 Trinidad Head, CA Background Mixing Ratio ¹¹ (pptv)
HCFC-225ca&cb	CF ₃ CF ₂ CHCl ₂ / CF ₂ ClCF ₂ CHClF	127/525	9.757	---	1.08
HFC-43-10mee	CF ₃ CF ₂ (CFH) ₂ CF ₃	1650	6.910	---	0.271
HFC-227ea	CF ₃ CFHCF ₃	3350	3.755	1.45	1.12
HFC-236fa	CF ₃ CH ₂ CF ₃	8060	4.478	---	0.147
HFC-245fa	CF ₃ CH ₂ CHF ₂	858	5.555	---	2.56
HFC-365mfc	CF ₃ CH ₂ CF ₂ CH ₃	804	7.162	1.45	---

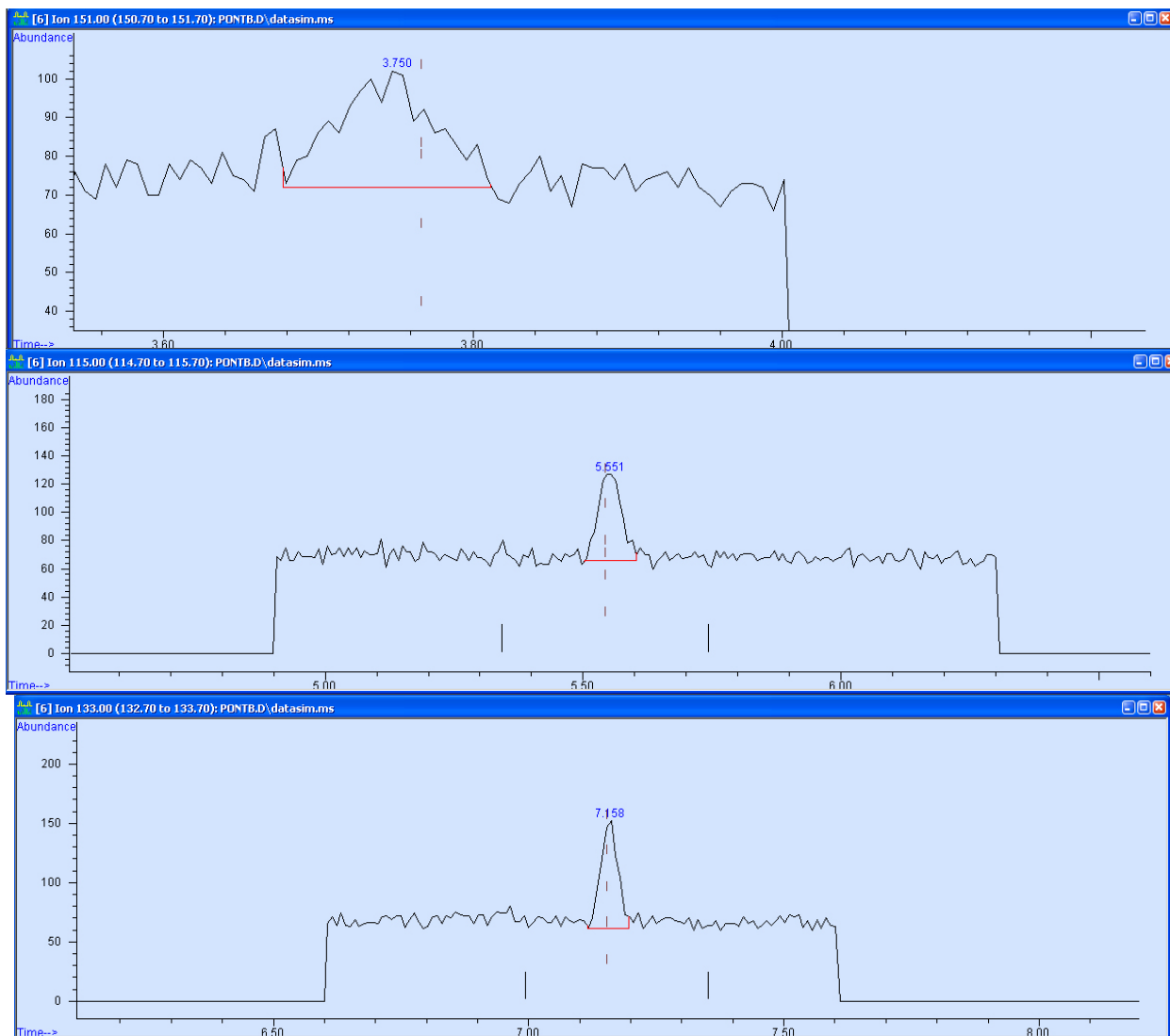


Figure 2.5 Single ion monitoring chromatograms from the DB-5 MS column of newly detected HFCs. In the top chromatogram is the peak representing HFC-227ea. In the middle chromatogram is the peak representing HFC-245fa. In the bottom chromatogram is the peak representing HFC-365mfc. The ions being monitored were m/z 151, m/z 115, and m/z 133 respectively.

Although not doped with these halocarbons, peaks were detected in the working standards used in this thesis for HCFC-225ca&cb, HFC-227ea, HFC-245fa, and HFC-365mfc. The peaks seen in the working standard are global background levels of these gases as seen when the clean air to make the standards was collected in the White Mountains in October 2014 as described above. Using this knowledge, it is possible to determine the mixing ratios in the

standard using data from the Advanced Global Atmospheric Gases Experiment (AGAGE) network. The AGAGE network is a group of remote research stations around the world that regularly sample the air in the region and analyze it for greenhouse gas mixing ratios. The data are freely available online for any researcher to use.¹¹ AGAGE maintains a station at Trinidad Head, CA (41° 3' 13.86" N , 124° 9' 3.564" W) which reports monthly averages of the mixing ratios of all of the exploratory gases herein except HCFC-225ca&cb. The monthly average for the gases seen by AGAGE can be used as the standard mixing ratio for the White Mountain standard. Unfortunately, data for HFC-245fa were not reported at Trinidad Head until after our standard was collected. Both HFC-227ea and HFC-365mfc can be detected and quantitated on our system at this time. Because the results are based off of another group's measurements, we report the absolute accuracy as $\pm 50\%$, but the precision as $\pm 10\%$. Quantitation of HFC-365mfc began in September 2014 and in August 2015 for HFC-227ea.

2.6 Autosampler Offgassing Test

On July 23, 2014, four samples were collected at the Mt. Wilson site while the autosampler was filling the hour long integrated sample that started at 11:00. These samples were collected next to the inlet, halfway between the inlet and the autosampler, next to the autosampler and inside the patio where the autosampler and cans were housed. These samples were collected to ensure that the autosampler was functioning properly and not off gassing any VOCs. Further, the samples served as a check for any local emissions at the sampling site. For all species included in Table 2.1, the percent difference between the average mixing ratio seen in the four hand collected samples and the sample collected via the autosampler was less than 100% with the exception of toluene. The four samples collected by hand had an average toluene concentration of 43 ± 10 ppt. The integrated sample, however, contained 614 ppt of toluene. This

is a 1300% difference and a very surprising result. Upon further investigation, it was determined that the pump in the autosampler used to pressurize canisters offgasses toluene. After this discovery, toluene was not quantified in the Mt. Wilson data set.

2.7 Precision Test

A series of seven canister samples were collected at the same time on March 16, 2016 at the Mt. Wilson sampling site. The canisters were connected via Swagelok “T-Unions” and steel tubing to a dual bellows pump. The pump was turned on and then the canisters were rapidly opened. Once the pressure reached 30 psi, the canisters were closed and returned to the lab. These canisters were analyzed on the systems discussed previously over the course of two days to determine the day to day precision of the analyses. The methane precision was found to be $\pm 0.152\%$ which is between 3 and 4 ppb for all samples collected at Mt. Wilson. For the CO/CO₂ system, the precision was found to be $\pm 0.176\%$ for CO₂ and 3% for CO. On the five column system, hydrocarbon precisions ranged from $\pm 1\%$ to $\pm 10\%$, and halocarbons and nitrates from $\pm 1\%$ to $\pm 10\%$ as shown in Table 2.1

2.8 Historical Data

As a way to put the data from this project in context of trends seen globally and in the SoCAB, data from previous sampling missions was also used. First, a similar intensive sampling study was undertaken from May 2007 through February 2008 at Mt. Wilson. Hourly samples were taken for 10 straight days during four seasonal campaigns. The specific methods and sampling dates are explained in Gorham et al.² Daytime air samples were said to have been collected between 11:00 and 17:00 yielding 244 air samples representative of the SoCAB.

Second, airborne whole air samples were collected in June of 2012 and 2013 aboard the NASA DC-8 aircraft above the Los Angeles area. Samples were collected as part of the Student

Airborne Research Project in which flight plans are devised to sample air coming into and flowing out of different regions of California.¹¹ Whole air sampling onboard the DC-8 is described in Simpson et al.¹² Several flight segments during each campaign are low passes over the SoCAB including approaches into different airports.

2.9 References

- (1) Finlayson-Pitts, B.; Pitts, J. *Chemistry of the Upper and Lower Atmosphere*; Academic Press, 2000.
- (2) Gorham, K. A.; Blake, N. J.; VanCuren, R. A.; Fuelberg, H. E.; Meinardi, S.; Blake, D. R. Seasonal and Diurnal Measurements of Carbon Monoxide and Nonmethane Hydrocarbons at Mt. Wilson, California: Indirect Evidence of Atomic Cl in the Los Angeles Basin. *Atmos. Environ.* **2010**, *44* (19), 2271–2279.
- (3) Wennberg, P. O.; Mui, W.; Wunch, D.; Kort, E. A.; Blake, D. R.; Atlas, E. L.; Santoni, G. W.; Wofsy, S. C.; Diskin, G. S.; Jeong, S.; et al. On the Sources of Methane to the Los Angeles Atmosphere. *Environ. Sci. Technol.* **2012**, *46* (17), 9282–9289.
- (4) Hsu, Y.-K.; VanCuren, T.; Park, S.; Jakober, C.; Herner, J.; FitzGibbon, M.; Blake, D. R.; Parrish, D. D. Methane Emissions Inventory Verification in Southern California. *Atmos. Environ.* **2010**, *44* (1), 1–7.
- (5) Lopez, J. del P. Seasonality and Global Growth Trends of Carbon Monoxide During 1995-2001, University of California, Irvine, 2002.
- (6) Thompson, B.; Wood, R. The Methanizer in the Model 3700 & Vista Series Gas Chromatograph. *Varian Instrum. Work* **1981**.
- (7) Colman, J. J.; Swanson, A. L.; Meinardi, S.; Sive, B. C.; Blake, D. R.; Rowland, F. S. Description of the Analysis of a Wide Range of Volatile Organic Compounds in Whole Air Samples Collected during PEM-Tropics A and B. *Anal. Chem.* **2001**, *73* (15), 3723–3731.
- (8) Sive, B. C. Atmospheric Nonmethane Hydrocarbons: Analytical Methods and Estimated Hydroxyl Radical Concentrations, University of California, Irvine, 1998.
- (9) Apel, E. C.; Calvert, J. G.; Gilpin, T. M.; Fehsenfeld, F. C.; Parrish, D. D.; Lonneman, W. A. The Nonmethane Hydrocarbon Intercomparison Experiment (NOMHICE): Task 3. *J. Geophys. Res. Atmospheres* **1999**, *104* (D21), 26069–26086.
- (10) Apel, E. C.; Calvert, J. G.; Gilpin, T. M.; Fehsenfeld, F.; Lonneman, W. A. Nonmethane Hydrocarbon Intercomparison Experiment (NOMHICE): Task 4, Ambient Air. *J. Geophys. Res. Atmospheres* **2003**, *108* (D9), 4300.
- (11) Student Airborne Research Program (SARP) | NSRC <https://airbornescience.nasa.gov/nsrc/sarp> (accessed Mar 3, 2017).
- (12) Simpson, I. J.; Blake, N. J.; Barletta, B.; Diskin, G. S.; Fuelberg, H. E.; Gorham, K.; Huey, L. G.; Meinardi, S.; Rowland, F. S.; Vay, S. A.; et al. Characterization of Trace Gases Measured over Alberta Oil Sands Mining Operations. *Atmospheric Chem. Phys.* **2010**, *10* (23), 11931–11954.

CHAPTER 3: Trends in SoCAB Hydrocarbon Mixing Ratios and Emissions

3.1 Data Overview

Daytime mixing ratio statistics for the full two years of sampling at Mt. Wilson for selected hydrocarbons are shown in Table 3.1 (n=539). For a quick comparison, the daytime average of all samples collected in the 2007 Mt. Wilson campaign is included as well (n=245). It is immediately apparent that, when compared to 2007, average daytime mixing ratios seen at the same Mt. Wilson site are lower for many of the hydrocarbons. However, this comparison is incomplete without factoring in the global background concentrations of the gases of interest. As noted in the introduction, several of the hydrocarbons to be studied have lifetimes on the scale of months to years, much longer than transport time across the SoCAB. Further, as described in Chapter 1 for methane, the global background mixing ratios of many gases have increased with time and so it is necessary to determine background values for both campaigns. The difference between the background value and a given sample mixing ratio is called the “enhancement” and is used commonly to better aid in describing emissions from a region instead of globally.¹⁻³ In order to determine a local background, it is first necessary to determine what samples should be included in this analysis based on meteorological conditions.

Table 3.1. Overview of mixing ratio results for selected hydrocarbon species from the daytime samples collected during the two year Mt. Wilson sampling project. Nd stands for not detected and means that at least one sample fell below our detection limits for that species. The 2007 daytime average mixing ratio is included for reference. IQR stands for interquartile range and is the difference between the mixing ratio at the 75th percentile and the 25th percentile.

Species	Minimum (pptv)	Maximum (pptv)	Median (pptv)	Average (pptv)	Standard Deviation	IQR	2007 Average (pptv)
Methane (ppmv)	1.798	2.362	1.925	1.932	0.057	0.060	1.881
Ethane	703	16471	2867	3110	1554	1547	2313
Ethene	59	8096	397	489	505	316	581
Ethyne	75	1993	491	542	293	328	792
Propane	216	9509	1197	1440	1006	931	1634
Propene	13	3432	87	132	213	67	101
i-butane	25	1774	204	247	190	182	331
n-butane	59	3701	396	501	417	376	572
i-Pentane	9	2052	236	297	229	255	618
n-Pentane	17	1251	146	179	140	128	240
Isoprene	13	8151	465	882	1135	840	799
2-methylpentane	nd	583	63	78	65	65	100
3-methylpentane	nd	370	50	59	45	48	89
n-hexane	nd	418	55	67	51	52	85
benzene	37	396	122	134	60	76	182
ethylbenzene	4	167	29	37	28	31	61
m/p-xylene	7	248	50	62	44	48	59
o-xylene	3	116	21	27	20	22	50
1,2,4-trimethylbenzene	nd	59	9	11	7	7	18

3.2 Wind Direction and Speed Data

Previous studies at Mt. Wilson have shown that most air masses reaching the peak are influenced by the SoCAB, as is determined by the meteorology and topography of the region discussed in Chapter 2. However, it cannot be assumed that each individual sample is influenced by the SoCAB in this manner. Therefore, meteorological data were used to check for air mass influence. Wind data were not available at the specific sampling site at Mt. Wilson; however, a

National Weather Service Station monitors meteorological conditions at Clear Creek, CA, which is less than 5 miles due west in the San Gabriel mountains (34.72° N, 118.15° W). Here, hourly wind speed and directional data were collected and used for this dissertation.⁴ A wind rose plot for the western San Gabriel Mountains at the beginning of sampling of each integrated air sample collected at Mt. Wilson is shown in Figure 3.1. The prevailing winds in the region come from the west through the southeast which is where the SoCAB lies. The largest fraction of all measurements was from the southeast and in the 4-6 mile per hour range. Indeed, the strongest winds seen at the site were seen when winds stemmed from the southeast. During 86% of the daytime samples (n=464), the wind was blowing from across the SoCAB defined as from the W through the ESE. Daytime samples during which the wind was calm or from the WNW through the E were removed prior to any further analysis. These removed samples were collected largely during Santa Ana wind conditions. This is shown in the seasonal wind rose plots in Figure 3.2. The non-dominant wind events occurred largely during the fall and winter, when Santa Ana wind conditions most often occur as discussed in Chapter 1. The most common of the non-SoCAB influenced wind directions was from the east (n=13) followed by the north by northwest.

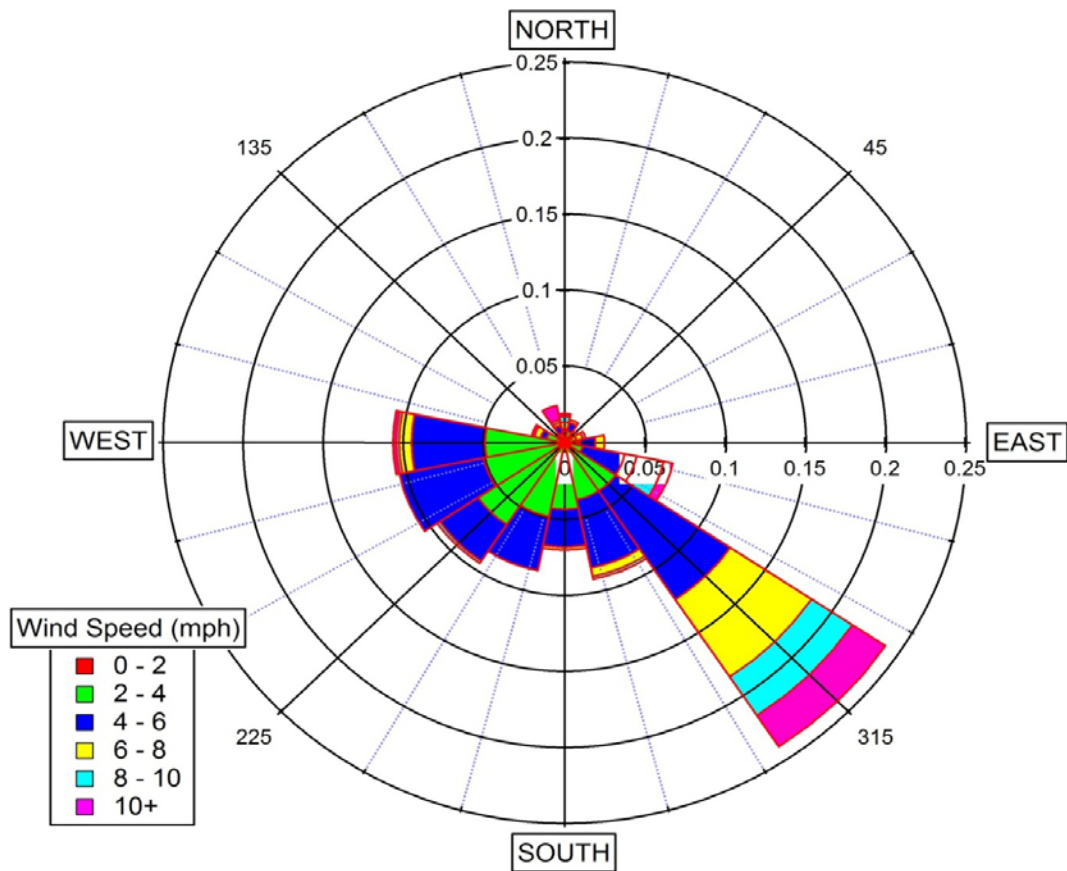


Figure 3.1. Wind rose plot of winds arriving at the Mount Wilson sampling site at the start of each daytime sample during the full two years of the study. The radial axis represents the fraction of the time the wind was blowing from a given direction, and the speed is color coded. Meteorological data was taken from the nearby Clear Creek weather station five miles east of Mt. Wilson.⁴

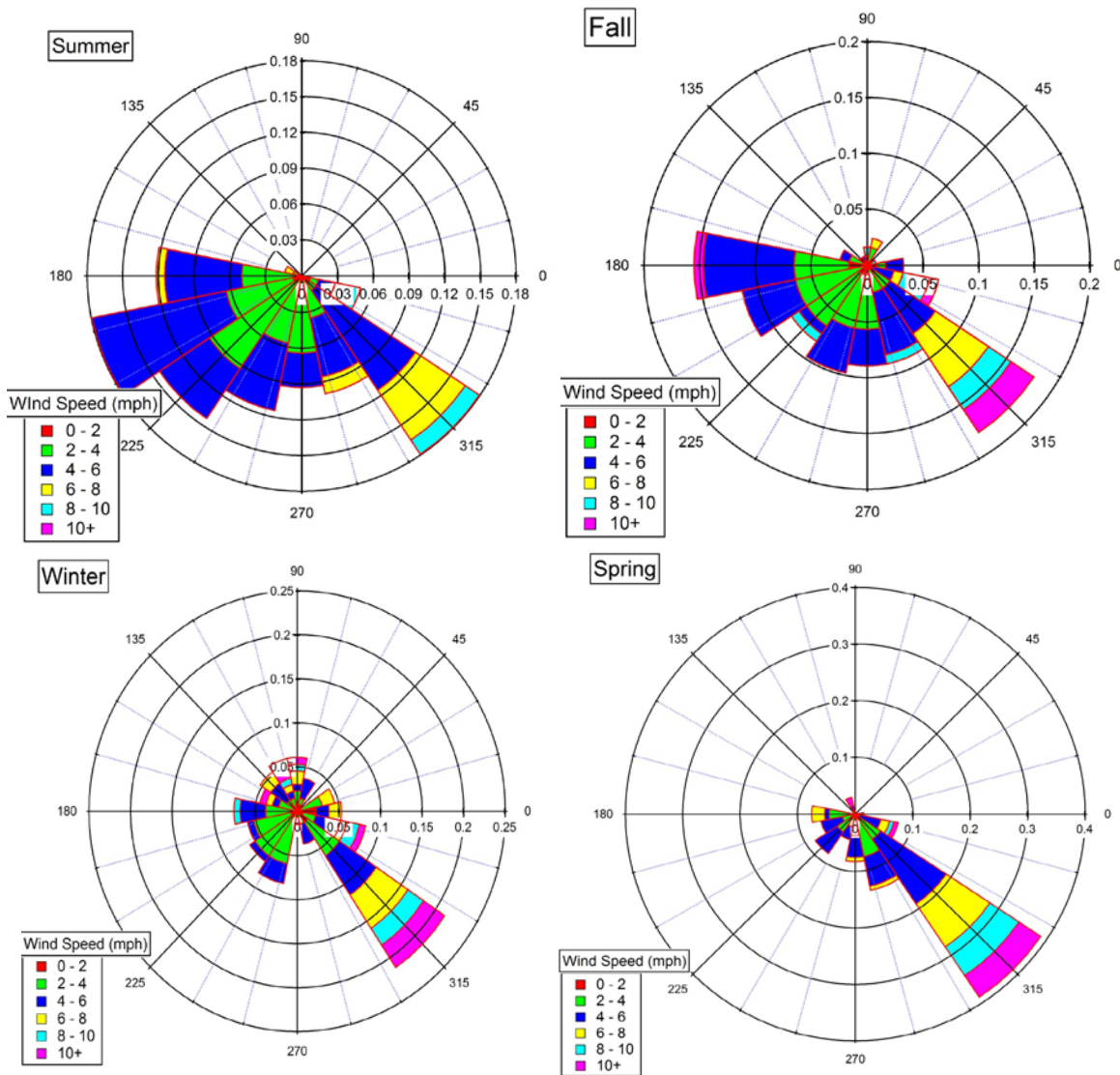


Figure 3.2. Wind rose plot of winds arriving at the Mount Wilson sampling site at the start of each daytime sample during the full two years of the study separated by season. The radial axis represents the fraction of the time the wind was blowing from a given direction, and the speed is color coded. Meteorological data was taken from the nearby Clear Creek weather station five miles east of Mt. Wilson.⁴

It is interesting to note the dominance of the SE wind direction in each season. This direction of the wind suggests that most air masses passed over more inland regions of the SoCAB before reaching the mountains. The dominance of the southeast wind is only challenged in the summer months when the direction is more variable and an equal share also comes from the southwest. These southwest on shore breezes are very common, especially during the summer months, and represent air masses that took a more direct route to the base of the mountains. Overall, the meteorological conditions that were sample are exciting to see as they suggest that results from this study are indicative of the full breadth of industries and sectors present in the region, making accurate source apportionment more likely.

To confirm that the wind measurements collected from the National Weather Service were representative of where the air mass for each sample last came from, a back trajectory model was utilized. HYSPLIT is a specific back trajectory model created for open use by the National Oceanic and Atmospheric Administration. Forward and back trajectories at any point in the world can be mapped over varying time periods.⁵ Since the SoCAB is a relatively small region, all HYSPLIT trajectories shown in this dissertation were capped at 24 hours back and feature four trajectories. The first back trajectory begins at the beginning of the given sampling hour. Three more trajectories begin at the same location two, four, and six hours before sampling. The starting point for these trajectories was the base of the San Gabriel Mountains directly in front of Mt. Wilson in Sierra Madre, CA with a starting height of 500m above ground level. A HYSPLIT back trajectory model was run for each day of sampling starting at 17:00 local time to confirm that the air that reached Mt. Wilson had passed through the SoCAB.⁵

Overall, HYSPLIT analysis confirmed that the wind direction data sufficiently determined whether an air mass was influenced by the SoCAB. A sample trajectory for each

season is shown below (Figure 3.3) as an example of the typical travel patterns of the air masses before they reached the base of the mountains and upwelling began. Most air masses began off the coast over the Pacific Ocean before being pushed onshore at varying angles across the SoCAB. It is very interesting to note the amount of time some air masses spend over the region as they swirl through different parts of the SoCAB. Indeed, in the winter example trajectory, the air masses were over land in the SoCAB for upwards of 10 hours. This time is compared to the summer example in which the wind was from the west and it took less than three hours to transport the air to the mountains. The variety of results seen in HYSPLIT analysis is encouraging as it suggests that air masses take different paths through the SoCAB. This allows for potential analysis of a variety of point sources and industries throughout the region. Further, the varying length of time air masses spend over the region allows for a wider picture of emissions, with some samples being much more photochemically aged than others.

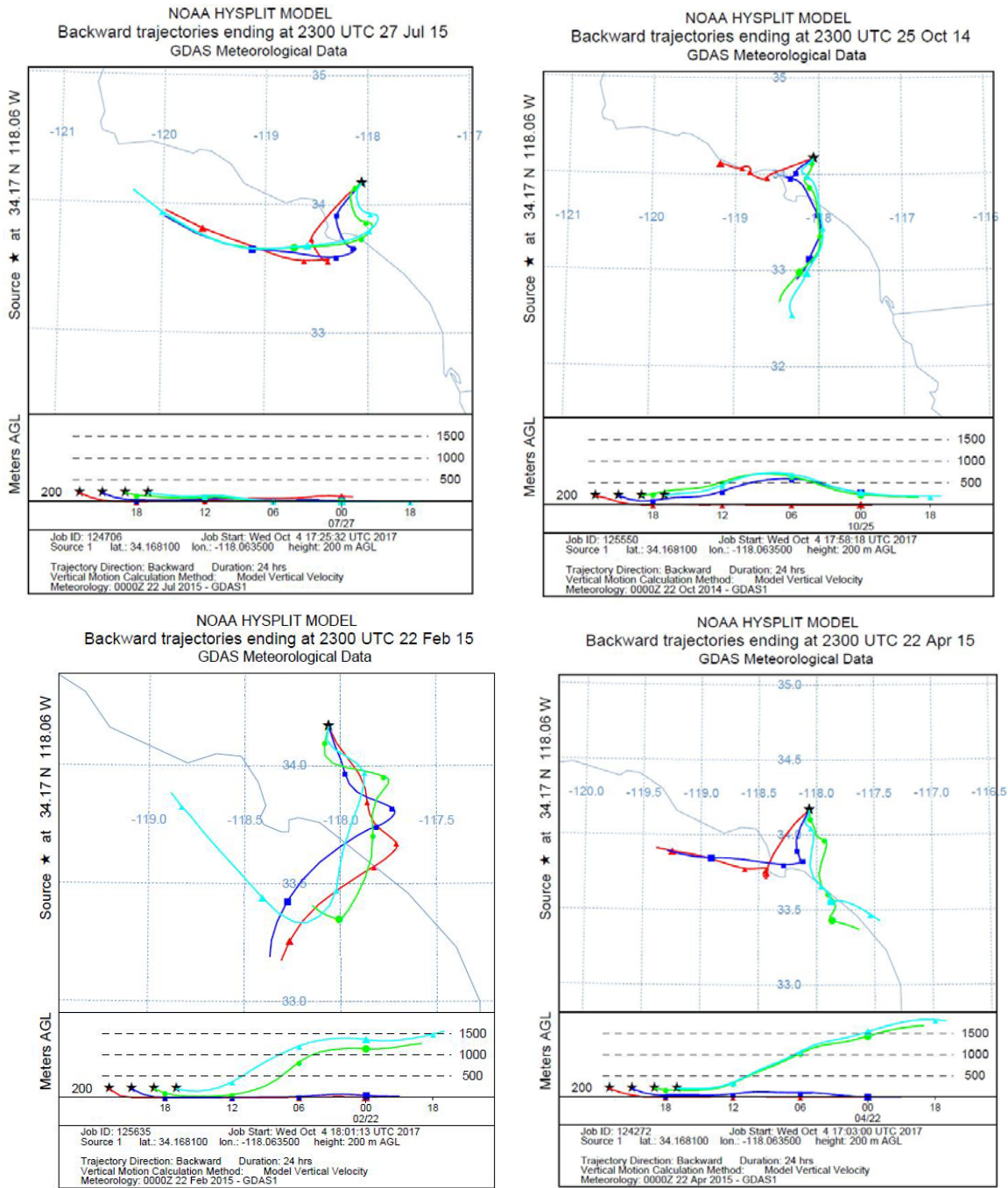


Figure 3.3. HYSPLIT back trajectories starting from the base of the San Gabriel Mountains in front of Mt. Wilson that are representative of the trajectories commonly found in each season. In a vast majority of cases, air masses passed through the SoCAB before reaching the mountains.

3.3 Enhancement Analysis

3.3.1 Selection of Background Values

With a trimmed data set of daytime air samples that are all representative of the SoCAB, analysis and determination of what background mixing ratios of various species are for the region is possible. Background mixing ratios are determined via analysis of samples collected from clean air masses which are found away from urban areas. These locations can include mountain tops or beaches where the air mass has come off of the ocean.^{6,7} Our research group conducts background air sampling through the UCI monitoring network around the Pacific Rim. Our group has sampled remote air dating back to the late 1970s to understand what trends are occurring in greenhouse gases over long periods of time. Samples are collected seasonally ranging in latitudes as far north as 71° to 47° S. This long term sampling has shown that there is strong variation in mixing ratios for certain gases by season and by latitude. Further, it has shown for several gases, background mixing ratios are increasing or decreasing over time.^{7,8} These trends in background values make determining the background to use for a given sample non-trivial.

Determining background values is a very important part of gaseous air analysis as the calculation is done prior to any other analysis method or type of evaluation and thus will always have an effect on the results. Due to this, it is a source of debate within the field, and many argue in favor of different types of background choices.⁹⁻¹¹ The first to be considered was the use of mixing ratios from the UCI sampling network. These background samples are useful in that the locations sampled at make the likelihood of polluted air masses small. Further, the spread of sampling allows for a fairly accurate prediction of mixing ratios at specific latitude (Mt. Wilson, in this case). However, there are problems with this choice that outweigh the perks. First is the

relatively small size of the data for the years in question (eight samples per location) in comparison to the hundreds collected at Mt. Wilson. Further, in several samples from the nearest remote sampling site at Jalama Beach, CA (34.51° N, 120.50° W), the wind direction was from onshore, meaning elevated concentrations of gases from the Los Angeles area were seen, and not global backgrounds from the Pacific Ocean. These issues made using this data set a poor choice.

Another option considered was using nighttime values collected from Mt. Wilson. Each month up to four midnight samples were collected at the Mt. Wilson site. Over the two years of sampling, 47 useable midnight samples were collected. These samples have the benefit of being at the exact same location as the daytime sampling and can be considered free of influence from the SoCAB due to the falling of the boundary layer and lack of venting overnight.¹² However, these samples were collected at over 1.7 km above sea level which creates a problem when measuring gases that have relatively short atmospheric lifetimes. The vertical mixing time in the atmosphere to such heights is longer than the lifetime of several gaseous species.¹³ Therefore, samples taken at altitude do not have the same mixing ratios as those taken at sea level for many species. Because the SoCAB air masses that reach Mt. Wilson are the result of upslope heating and venting, they resemble ground level air masses. Therefore, using background values collected at altitude for air masses resulting from sea level is not an adequate method of calculating enhancement.

The chosen method for determining backgrounds, using minimum values seen in daytime samples, does not have the same issues as above. It uses a large data set, and it allows for backgrounds to be of surface air masses. Due to the noted seasonality of background levels of several gases, background values were calculated seasonally. The average mixing ratio of the lowest 5% of influenced samples for each compound in a given season was used as the seasonal

background. This value was subtracted from each daytime Mt. Wilson sample to yield an enhancement value. Enhancement values were calculated via the same method for the 2007 Mt. Wilson data set. Because the background was based on daytime SoCAB influenced air masses, samples in which the methane mixing ratio was elevated less than 20 ppb (1%) over the nighttime minima were said to have not been enhanced and removed prior to any further calculation, similar to a study in the Barnett Shale.² Methane is the most emitted hydrocarbon to the atmosphere, and for the sample to not be enhanced more than 1% over background from an urban environment is surprising, suggesting that the air mass was not influenced by the SoCAB. This may have occurred due to a low boundary layer or thick marine layer on a particular day.

Confirming this method choice, background methane values in 2007 and between 2014 and 2016 in this data set are in agreement with remote background samples taken along the Pacific Rim as part of the UCI monitoring network.⁷ The eight seasonal averages from Mt. Wilson are all less than 4% than different than the average of those samples collected between 27° N and 36° N latitude at the remote sampling locations. Background tropospheric methane and ethane in the Northern Hemisphere has been increasing since the late 2000s as noted in UCI monitoring network samples.^{14,15} These trends are noted in the new Mt. Wilson data set and the one from 2007, where the local background samples show a distinct rise over the seven year period between missions with methane increasing on average 8.5 ± 1.9 ppb/yr (Figure 3.4). This comparison confirms that the local background averages calculated from the Mt. Wilson data set are representative of the larger long term trends in emissions occurring globally. However, this data also shows the importance of routine sampling for long term trends. Even with upwards of fifty samples in each season, there is still some variation in the background and seasonal patterns are not always followed.

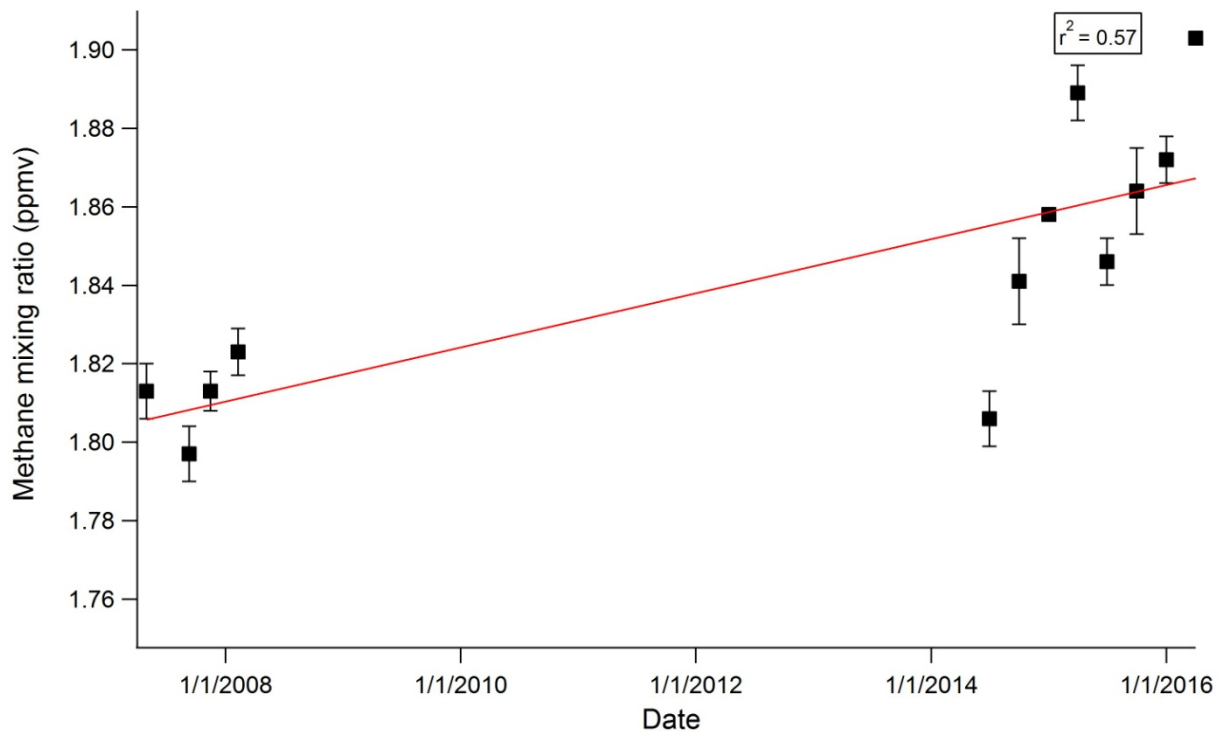


Figure 3.4 Seasonally averaged background methane mixing ratios taken from the two Mt. Wilson data sets. The background methane mixing ration rose 8.5 ± 1.9 ppb/yr over the span between the two studies.

3.3.2 Alkane Enhancement Results

The alkane enhancement values from the two Mt. Wilson data sets were compared, and the results are summarized in Table 3.2. The results show the change in local SoCAB alkane emissions over the eight year period between the studies. These species were chosen as they all have lifetimes such that enhancement calculations were necessary. Further, alkanes as discussed in the introduction have various anthropogenic sources and so will allow some insight into trends in point sources. The first noted result is that alkanes larger than ethane have seen decreases in their daytime average mixing ratios; however, methane and ethane have seen an average increase (or at least have held constant). This result begins to show the variety of sources at play in the

SoCAB. While most hydrocarbon species are being controlled and emissions have decreased, methane and ethane enhancements have gone up suggesting a source that is largely just the two species. This profile aligns quite well with natural gas and is suggestive of increased pipeline emissions in the region even after accounting for the increased background.^{16,17}

Table 3.2. Average daytime enhanced mixing ratios for alkanes as seen from the same sampling site at Mt. Wilson during two different sampling intensives. The previous study ran from April 2007-February 2008, sampling every hour for a week during each of the 4 seasons. The reported errors are the 1σ uncertainties in the mean.

Hydrocarbon	2007-08 Average Daytime Enhancement (ppt) ²⁴	2014-16 Average Daytime Enhancement (ppt)	Percent Change
Methane	74 ppb ± 3	78 ppb ± 3	+ 5 ± 5%
Ethane	1305 ± 77	1865 ± 68	+ 43± 8%
Ethyne	552 ± 34	383 ± 14	-31± 7%
Propane	1302 ± 82	1117 ± 49	- 14± 7%
i-butane	290 ± 20	204 ± 9	- 30± 8%
n-butane	501 ± 29	407 ± 20	- 19± 7%
i-pentane	556 ± 33	268 ± 11	-52 ± 7%
n-pentane	217 ± 13	153 ± 7	- 29± 7%
n-hexane	89 ± 5	56 ± 2	- 37± 6%
benzene	125 ± 7	78 ± 3	- 38± 6%

3.3.3 Enhancement Ratio Analysis

3.3.3.1 Ethane to Methane Ratio

To further study emissions from the SoCAB and potential sources, several ratios between VOC species can be determined. These ratios are between gases that are known as tracer species. These tracer species have specific profiles in a given emissions source type and have been used widely in the field.^{2,3,18,19} The first of these ratios is the ratio of ethane to methane. As is described in the introduction, methane emissions stem from a variety of sources, only some of which are anthropogenic in nature and linked to higher hydrocarbons. Therefore, this ratio is useful in determining to what extent various methane sources contribute in an air sample. The ethane to methane enhancement ratio is calculated by:

$$\frac{\Delta E}{\Delta M} = \frac{E_{sample} - E_{bkrd}}{M_{sample} - M_{bkrd}}$$

Where E and M are the mixing ratios of ethane and methane in a given sample. The seasonal averaged background ethane and methane mixing ratios are subtracted from these values. The $\Delta E/\Delta M$ ratio is often reported as a percentage, as methane mixing ratios are, generally, at least an order of magnitude larger than ethane mixing ratios. The ratio from a point source can range from near zero, as is the case for landfills, to over 10% from conventional oil wells.²⁰

The average ethane to methane enhancement ratio seen at Mt. Wilson changed over the course of the two year study. In the first year of sampling from June 2014 to May 2015, the average ratio was $2.21 \pm 0.13\%$; whereas from June 2015 to May 2016 it was $2.53 \pm 0.10\%$. When looking at the average enhancement during each year, this makes sense as methane enhancement values did not increase (77 ± 3 ppb to 80 ± 5 ppb in year two) while ethane mixing ratios did (1689 ± 73 ppt to 2094 ± 131 ppt in year two). To check the validity of these results and further put these percentages into context, comparisons to previous work can be made. First, during the 2007-2008 Mt. Wilson campaign, the average $\Delta E/\Delta M$ was $1.69 \pm 0.11\%$. Using the data from this sampling mission, the $\Delta E/\Delta M$ in the SoCAB and the Los Angeles megacity increased $0.84 \pm 0.15\%$ over the nine year period. This is a substantial result and suggests a change in emissions profiles or sources to the region. As further confirmation the 2007-2008 $\Delta E/\Delta M$ ratio was compared to the averages reported in Wennberg et al.⁹ for various campaigns from 2007-2010 in the SoCAB. The results therein range from 1.5% to 2.05% which are in good agreement with the $1.69 \pm 0.11\%$ discussed above.

The more recent results do agree with the non-point source derived $\Delta E/\Delta M$ values from Hopkins et al.²⁰ They conducted a mobile study of the SoCAB in June 2013 with real time methane and ethane analyzers determining ratios from different types of point sources. Most of

their driving time was between sites and so a bulk of their data was considered integrated air sampling like the sampling done at Mt. Wilson. Their $\Delta E/\Delta M$ ratios varied by day ranging from 1.4% to 3.1%.²⁰ This day to day variation is noted in our data set as well. There is a significant variance in $\Delta E/\Delta M$ values day to day indicating the variety of sources in the SoCAB (Figure 3.5). Here, we noticed significant variations in this ratio even between samples on the same day in some cases.

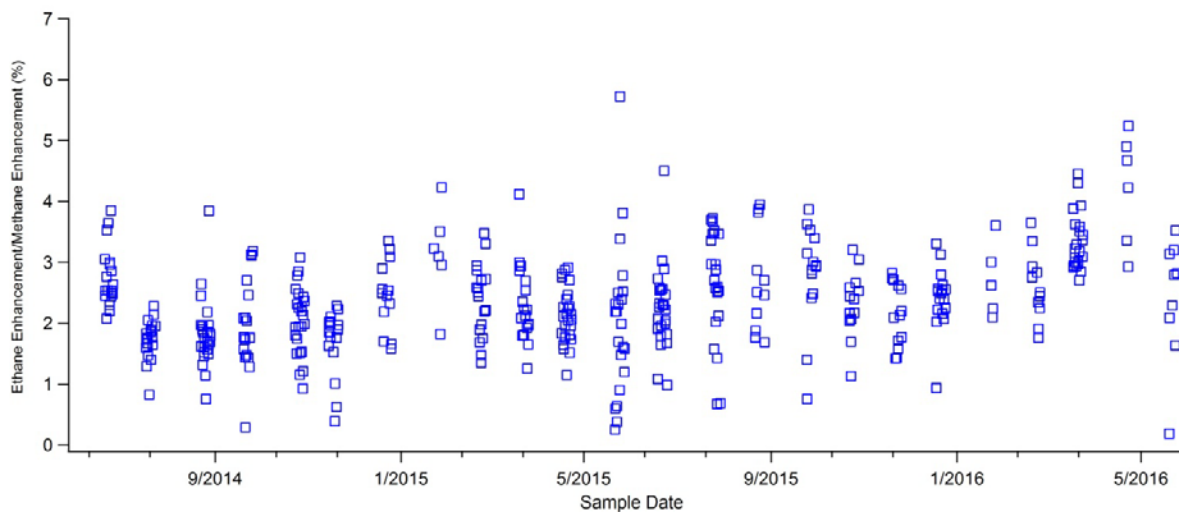


Figure 3.5. Ethane to methane enhancement ratios seen at Mt. Wilson over the two year sampling period. A slight overall increase is noted along with significant variation day to day. Average error in each ratio is $\pm 0.12\%$, due to error propagation.

To explain such daily variation, one of two situations, or even both are occurring. The first possible explanation is that the meteorological conditions shifted and the air masses that reached Mt. Wilson in two consecutive samples passed over different point sources. This explanation is valid and did occur to some extent. The spring HYSPLIT back trajectory shown in Figure 3.3 is an excellent example of this. The E/M of the four samples taken that day ranged from 1.74% to 2.15%. The highest E/M occurred in the 5:00 PM sample, which was of an air mass that passed over the South Bay region of the SoCAB where most of the petrochemical

processing in the region occurs.²¹ The emissions from these refineries and processing plants are “wetter”, containing more ethane.³ This profile makes the change seen in the $\Delta E/\Delta M$ at Mt. Wilson over the course of the day make sense.

The other possibility that would explain the variance in $\Delta E/\Delta M$, is that the E/M profiles of like, but individual, point sources are not identical or one point source had temporal changes in its profile. This point was argued in Hopkins et al.²⁰ where different oil fields within the SoCAB had $\Delta E/\Delta M$ ranging from 1-7%. It is confirmed here in many cases where HYSPLIT back trajectories did not change over the course of a day, and yet $\Delta E/\Delta M$ changed. As an example, the $\Delta E/\Delta M$ for the samples collected on May 26, 2015 ranged from 1.61-3.81%, while HYSPLIT analysis showed the same back trajectory of the air masses reaching Mt. Wilson over the course of the day (Figure 3.6). These results show that there are different reasons why an $\Delta E/\Delta M$ might change over time; however, the second scenario in which the source profile changes needs to be studied more directly. Here, that task was undertaken with direct sampling of pipeline natural gas as described in the next chapter. This course of study and the $\Delta E/\Delta M$ results presented here are worth noting because of their use in bottom-up emissions inventories and source profiles. In the past, natural gas composition and the composition of other ethane emitters had been taken to be static over the course of a year or more.^{9,22} This data set begins to show that this is certainly not the case. It would be difficult to include daily variations of $\Delta E/\Delta M$ into bottom-up inventories, but certainly, the assumptions regarding a source profile leading to a bottom-up estimate need to be fully noted in future studies.

NOAA HYSPLIT MODEL
 Backward trajectories ending at 2300 UTC 26 May 15
 GDAS Meteorological Data

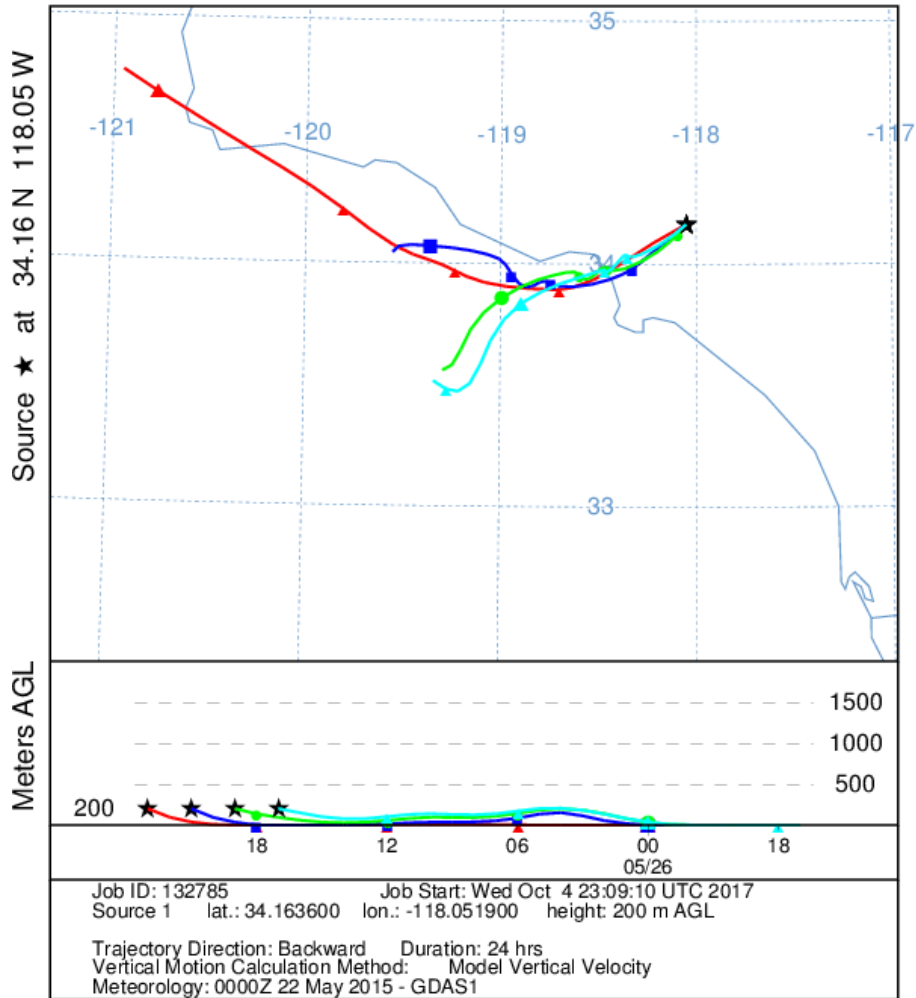


Figure 3.6. HYSPLIT back trajectory analysis for May 26, 2015 in which the four samples collected at Mt. Wilson varied substantially in ethane to methane enhancement ratios despite showing the same trajectory to the site.

3.3.3.2 Propane to Ethyne

Another useful VOC ratio in air mass characterization is the ratio of propane to ethyne. Ethyne is an excellent tracer of fossil fuel combustion used in vehicles and for power generation.¹⁹ It is formed as a result of incomplete combustion in an engine and emitted from the tailpipe.²³ It has no other significant sources to the atmosphere and so it can be compared to other VOC emissions to determine the importance of combustion emissions to a region.^{24,25} Strong correlation between a species and ethyne suggest that the dominant source of that species is vehicular emissions. Of interest here is how well propane correlates to ethyne. Propane emissions are tied to the use of liquefied petroleum gas (LPG) and combustion of fossil fuels. Further, propane is emitted from oil and gas producing regions in the same manner as methane described in the introduction.¹⁹ If oil wells and refining have strong influence on a region, correlation between propane and ethyne will be minimized and the ratio will increase. The average enhancement ratio of propane to ethyne seen in the 2014-2016 Mt. Wilson sampling campaign was 3.27 ± 0.30 , and the linear fit had a correlation coefficient of 0.79. Unlike the $\Delta E/\Delta M$, the enhancement ratio of propane to ethyne did not change within the two year sampling period. In the 2007-2008 Mt. Wilson campaign, the enhancement ratio was 2.70 ± 0.15 , and the linear fit had a correlation coefficient of 0.86. These ratios are in agreement with those found in previous studies of Los Angeles and other major cities.^{24,25} In pure vehicular exhaust the ratio is significantly below unity as ethyne emissions dominate over propane. In oil and gas drilling regions, ratios above 90 have been seen as propane emissions come from well heads and not tail pipes. Here, a ratio an order of magnitude below oil producing regions and two orders above those seen in exhaust, suggest dominance of vehicular emissions but with some influence of natural gas and gasoline production.¹⁹ This result is expected given the size of the Southern

California vehicular fleet. However, it is noted that the ratio has increased between the two sampling projects. Average daytime ethyne mixing ratios are down $31 \pm 7\%$ from 2007. It is possible that the current vehicular fleet is burning fuel more efficiently than previous fleets. A study of SoCAB vehicles ranging from 1995 to 2003 showed a 95% decrease in ethyne emissions per mile between the two fleets.²⁶ This result suggests that advances in technology and an increase in hybrid and fully electric vehicles on the road have decreased vehicular ethyne emissions and therefore increased the ratio of propane to ethyne seen in the SoCAB. This result also further suggests a greater importance of natural gas and oil production emissions in the region than in previous years, as engine technology continues to improve.

3.3.3.3 *i*-pentane to *n*-pentane

A final ratio that is often used to determine the extent to which oil and gas emissions affect an air mass is the ratio of *i*-pentane to *n*-pentane (iC_5/nC_5). It has been suggested that an iC_5/nC_5 of less than unity is typical of oil and gas drilling and refining.²⁷ The ratio of *i*-pentane to *n*-pentane seen in gasoline liquids and vapors has been noted to be between two and four.¹⁹ Due to the difference in composition of gas and oil in a given shale, the ratio may vary by location but is expected to remain relatively low if influenced by oil and gas. Over the two years of sampling at Mt. Wilson, the average daytime iC_5/nC_5 was 1.88 ± 0.04 . This result suggests that oil and natural gas production is not the dominant emission source. This result is to be expected given the dominance of automobile combustion emissions in the region.^{28,29} Only 31 samples over the two year study have a ratio of one or lower. However, surprisingly, the average pentane ratio for this study is much lower than any previous study in the region. During the 2010 CalNex study, emissions in Pasadena were monitored over the course of May and June yielding an iC_5/nC_5 ratio of 2.41 ± 0.02 .¹⁹ Further, during the previous study at Mt. Wilson in 2007 the average daytime

iC_5/nC_5 was 2.60 ± 0.02 . This decrease over the last several years is worth noting as alkane mixing ratios are lower across the board from the 2007 intensive, as is highlighted in Table 3.2. However, it can be seen that emissions are not decreasing at the same rate. *i*-pentane emissions have been cut more dramatically than *n*-pentane. If the emission of pentanes were completely colocated, this difference would not be noted. This change suggests that there is an emission source with a much lower *i*-pentane to *n*-pentane ratio which hasn't been controlled as well over the last eight years, potentially an oil and gas production source. Figure 3.7 further confirms that a variety of sources contribute to pentane emissions in the SoCAB. This ratio is useful in further suggesting the importance of natural gas emissions in the region.

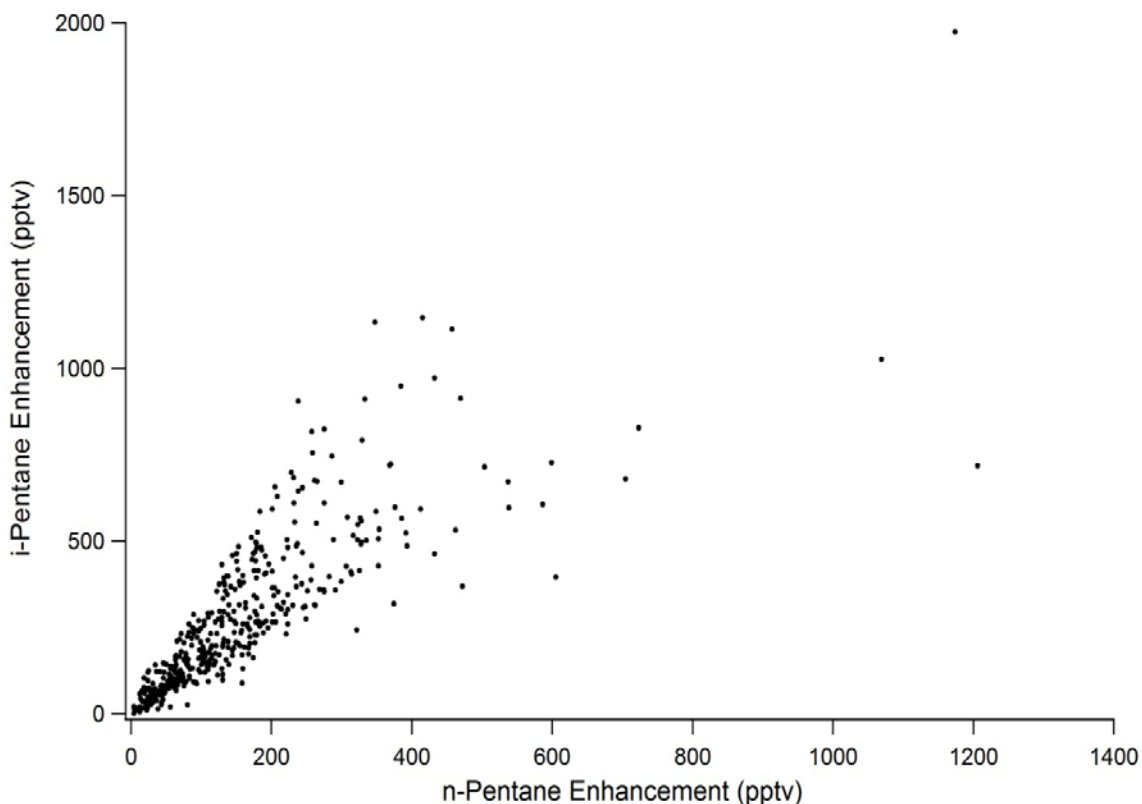
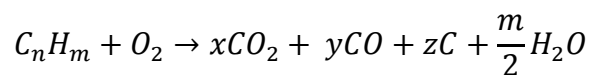


Figure 3.7. Correlation plot of isopentane and n-pentane enhancements in SoCAB influenced samples seen at Mt. Wilson. There appear to be a variety of sources of pentanes to the region.

3.4 Seasonal Variation

3.4.1 Carbon monoxide

Another well-established method to help characterize an air shed and an urban region's emissions is to study how mixing ratios change as a function of time. Carbon monoxide has been used for decades as a tracer of anthropogenic emissions.^{1,30,31} It is formed during the burning of fossil fuels as a result of incomplete combustion. When an engine is not operating as designed, excess fuel might be entering, or air flow might be restricted such that upon combustion of a hydrocarbon, the ratio of oxygen to fuel is off producing carbon monoxide instead of carbon dioxide. This combustion is described by the reaction:



Where the sum of y and z is much smaller than x. This lack of oxygen produces both CO and elemental carbon, which is emitted from the tailpipe in particulate form. Later in this dissertation, CO will be used as a reference compound for anthropogenic emissions to help aid in calculating emissions estimates.

Seasonally averaged CO emissions from the 2014-2016 Mt. Wilson sampling campaign are shown in Table 3.3. It is immediately clear that CO emissions spike in the summer months. Summer values are significantly higher than the rest of the year as shown by a one tailed ANOVA ($p < 0.05$). Statistical analysis further shows that there is no difference between the CO enhancements in any of the other seasons. This trend has been noted in the literature for other regions of the country but not for the SoCAB.³² Barnes et al.³² proposed that this summertime increase is due to the production of CO from photochemical processes in the atmosphere. Due to the increased sunlight and temperature, more oxidation of VOCs occurs creating excess CO. However, a modeling study that compared the SoCAB to the East Coast of the United States

suggests that photochemical CO production accounts for only 1% of the CO emitted from the region. Further, due to the meteorology of the region, photochemical CO production peaks in the most eastern portions of the region in the area surrounding Riverside, CA.³³ Even with longer and hotter days, this photochemical production is not enough to account for the 37% increase in average daytime CO mixing ratio between the three other seasons and summer seen in the first year. This result is significant to note due to CO's use in emissions inventory calculations. Many studies sample a region for only a small window of time and extrapolate the results to the entire year.^{1,30,34} This practice may not be advisable due to the summer increase in CO emissions. If sampling does not include summer and one other season, the data cannot be used to extrapolate to the whole year without significant caveats being placed on the resulting inventories.

Table 3.3. Average daytime enhanced mixing ratios for carbon monoxide across the eight seasons of sampling at Mt. Wilsons. The reported errors are the 1σ uncertainties in the mean.

Year	Average Daytime CO Enhancement-Summer (ppbv)	Average Daytime CO Enhancement-Fall (ppbv)	Average Daytime CO Enhancement-Winter (ppbv)	Average Daytime CO Enhancement-Spring (ppbv)	Average of Non-summer Seasons (ppbv)	Percent increase during summer
June 2014 - May 2015	112 ± 7.3	72 ± 7.3	68 ± 9.5	74 ± 5.6	71 ± 13	37 ± 14
June 2015 - May 2016	109 ± 9.9	71 ± 9.6	76 ± 8.2	59 ± 6.1	68 ± 14	38 ± 16

3.4.2 Other Species

While seasonal trends have been noted in remote and background air samples for longer lived species, trends in mixing ratios in the SoCAB did not follow these same patterns. Instead, mixing ratios of most hydrocarbon species were found to be the same throughout the course of the year in the Mt. Wilson study, largely due to the temperate climate and large percentage of sunny days. For a few species however, average mixing ratios increased in the summer as

compared to the rest of the year, like the trend described above for CO. This trend is strongest for ethyne, propane, i-pentane and benzene (Table 3.4). This pattern does not occur globally, and is fairly localized to the SoCAB due to the temperate climate. Literature on seasonality of alkanes is focused on urban centers at more northern latitudes. In these cities, hydrocarbon mixing ratios tend to peak in the winter due to a significant decrease in the hydroxyl radical and therefore an increased atmospheric lifetime.^{35,36} Industrial areas show little if any seasonality in emissions.³⁷ For ethyne, propane, isopentane and benzene, the causes of the summer spike could be several. One possible cause is that due to the increased temperatures, evaporation of volatile species occurs more readily. This is especially important for gasoline emissions which contains benzene and several other aromatic compounds.²⁹ The importance of such evaporative emissions in the SoCAB will be further explored using positive matrix factorization in the next chapter. Another possibility is that the summertime peaking could be a result of meteorological conditions and a change in wind direction. As shown in Figure 3.3, the predominant wind direction in the summer is split between the southwest and the southeast. Air masses coming from the southwest have passed over downtown Los Angeles and the western portions of the SoCAB which is heavily trafficked by automobiles. The increased ethyne emissions could be linked to having passed over more freeways.³⁸

Table 3.4. Average daytime enhanced mixing ratios for species which showed summer values significantly higher than the rest of the year. The reported errors are the 1 σ uncertainties in the mean.

Species	Average Daytime Enhancement-Summer (pptv)	Average Daytime Enhancement-Fall (pptv)	Average Daytime Enhancement-Winter (pptv)	Average Daytime Enhancement-Spring (pptv)	Average of other seasons (pptv)	Percent increase during summer
Ethyne	469 \pm 28	372 \pm 28	362 \pm 30	338 \pm 24	345 \pm 16	26 \pm 7%
Propane	1481 \pm 115	1304 \pm 90	1018 \pm 88	901 \pm 70	959 \pm 47	35 \pm 9%
i-Pentane	373 \pm 24	283 \pm 21	253 \pm 23	187 \pm 13	223 \pm 11	40 \pm 7%
Isoprene	2218 \pm 130	1157 \pm 41	314 \pm 30	518 \pm 31	459 \pm 20	80 \pm 8%
Benzene	104 \pm 6	89 \pm 5	65 \pm 6	63 \pm 5	67 \pm 3	36 \pm 6%

Finally, isoprene was the only species studied that showed true four season variation, with mixing ratios peaking in summer, and decreasing to a minimum in winter (Table 3.4 and Figure 3.8). This trend has been well studied and is a direct result of changes in sunlight hours.^{35,38,39} Isoprene is produced as a byproduct of photosynthesis in plants and is emitted to the atmosphere. Isoprene has no known anthropogenic sources, and as the sampling at Mt. Wilson took place in a forest environment, the summer levels upwards of a ppb are reasonable.

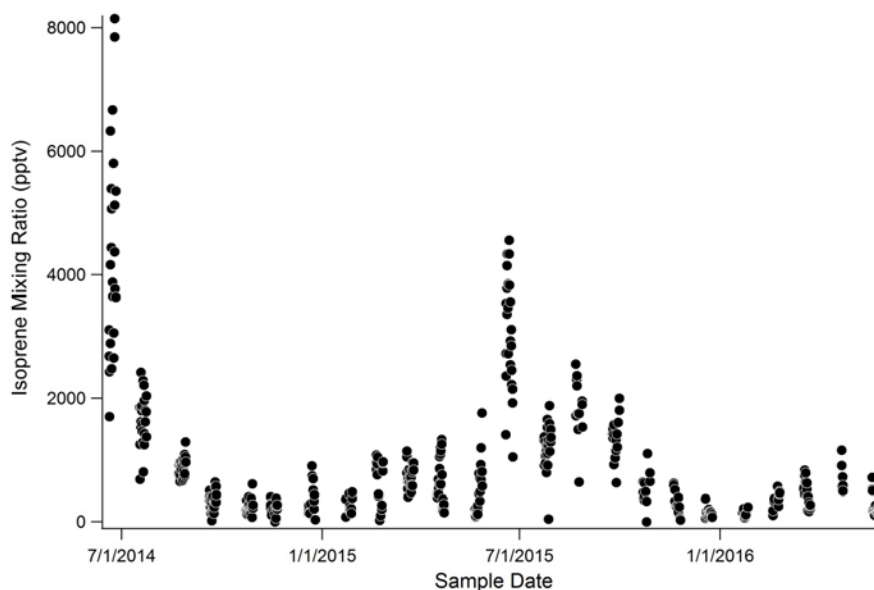


Figure 3.8. Seasonality of isoprene mixing ratios as seen at Mt. Wilson, CA over the full two years of sampling. Due to the increased temperatures and more intense daylight, isoprene emissions spike in the summer months.

3.5 Conclusions

With such a large data set, it is best to start analysis with large overarching trends before digging too deeply into smaller anomalies. Meteorological data showed that the samples collected at Mt. Wilson between 2014 and 2016 were largely representative of the SoCAB. By collecting these samples each month, various wind patterns were sampled. This allowed for the analysis of air masses that had passed over different portions of the region. Further, seasonal and other temporal trends show the importance of long term sampling studies. Short but intensive sampling missions do not give a full picture of the air masses in a given region.

The analysis in this chapter has shown the variety of emissions sources that are present in the SoCAB. While the mixing ratios of many hydrocarbon species were lower than they were in 2007, not all followed this trend. Ethane and methane mixing ratios have increased since 2007 even after accounting for an increase in global background levels. Several ratios were used to help characterize air masses that have passed over the SoCAB. These ratios agree well with previous work in the region and that of other urban measurement sites in that the incomplete combustion of fossil fuel and other vehicular sources dominates the alkane emissions in the region. However, the *i*-pentane to *n*-pentane ratio was significantly lower than had been previously noted for the region, suggesting that vehicular emissions sources are being more well controlled than those related to the processing and distribution of oil and natural gas. Further, the ethane to methane ratio rose over the past several years suggesting a change in composition of natural gas that has been previously assumed to be constant. Evidence from tracer species and ratios presented here suggests that natural gas is playing a more important role as a source of alkane emissions (especially methane) in the SoCAB. To better understand natural gas and other emissions sources in the region, a new statistical technique will be used to attempt apportionment

of the alkanes listed here and other hydrocarbon species in the next chapter.

3.6 References

- (1) Barletta, B.; Carreras-Sospedra, M.; Cohan, A.; Nissenson, P.; Dabdub, D.; Meinardi, S.; Atlas, E.; Lueb, R.; Holloway, J. S.; Ryerson, T. B.; et al. Emission estimates of HCFCs and HFCs in California from the 2010 CalNex study. *J. Geophys. Res. Atmospheres* **2013**, *118* (4), 2019–2030.
- (2) Marrero, J. E.; Townsend-Small, A.; Lyon, D. R.; Tsai, T. R.; Meinardi, S.; Blake, D. R. Estimating Emissions of Toxic Hydrocarbons from Natural Gas Production Sites in the Barnett Shale Region of Northern Texas. *Environ. Sci. Technol.* **2016**.
- (3) Pétron, G.; Karion, A.; Sweeney, C.; Miller, B. R.; Montzka, S. A.; Frost, G. J.; Trainer, M.; Tans, P.; Andrews, A.; Kofler, J.; et al. A new look at methane and nonmethane hydrocarbon emissions from oil and natural gas operations in the Colorado Denver-Julesburg Basin: Hydrocarbon emissions in oil & gas basin. *J. Geophys. Res. Atmospheres* **2014**, *119* (11), 6836–6852.
- (4) National Weather Service Forecast Office. *Hourly Observations Historical Data*; NOAA.
- (5) Stein, A. F.; Draxler, R. R.; Rolph, G. D.; Stunder, B. J. B.; Cohen, M. D.; Ngan, F. NOAA's HYSPLIT Atmospheric Transport and Dispersion Modeling System. *Bull. Am. Meteorol. Soc.* **2015**, *96* (12), 2059–2077.
- (6) Prinn, R. G.; Weiss, R. F.; Krummel, P. B.; O'Doherty, S.; Fraser, P. J.; Muhle, J.; Reimann, S.; Vollmer, M. K.; Simmonds, P. G.; Maione, M.; et al. *The ALE / GAGE AGAGE Network*; Carbon Dioxide Information Analysis Center (CDIAC), Oak Ridge National Laboratory, U.S. Department of Energy (DOE), 2016.
- (7) Simpson, I. J.; Chen, T.-Y.; Blake, D. R.; Rowland, F. S. Implications of the recent fluctuations in the growth rate of tropospheric methane. *Geophys. Res. Lett.* **2002**, *29* (10), 117–1.
- (8) Blake, D. R.; Rowland, F. S. World-wide increase in tropospheric methane, 1978–1983. *J. Atmospheric Chem.* **1986**, *4* (1), 43–62.
- (9) Wennberg, P. O.; Mui, W.; Wunch, D.; Kort, E. A.; Blake, D. R.; Atlas, E. L.; Santoni, G. W.; Wofsy, S. C.; Diskin, G. S.; Jeong, S.; et al. On the Sources of Methane to the Los Angeles Atmosphere. *Environ. Sci. Technol.* **2012**, *46* (17), 9282–9289.
- (10) Wunch, D.; Toon, G. C.; Hedelius, J. K.; Vizenor, N.; Roehl, C. M.; Saad, K. M.; Blavier, J.-F. L.; Blake, D. R.; Wennberg, P. O. Quantifying the loss of processed natural gas within California's South Coast Air Basin using long-term measurements of ethane and methane. *Atmos Chem Phys* **2016**, *16* (22), 14091–14105.
- (11) Simpson, I. J.; Blake, N. J.; Barletta, B.; Diskin, G. S.; Fuelberg, H. E.; Gorham, K.; Huey, L. G.; Meinardi, S.; Rowland, F. S.; Vay, S. A.; et al. Characterization of trace gases measured over Alberta oil sands mining operations. *Atmospheric Chem. Phys.* **2010**, *10* (23), 11931–11954.
- (12) Finlayson-Pitts, B.; Pitts, J. *Chemistry of the Upper and Lower Atmosphere*; Academic Press, 2000.
- (13) Jacob, D. J. *Introduction to Atmospheric Chemistry*; Princeton University Press, 1999.
- (14) Helmig, D.; Rossabi, S.; Hueber, J.; Tans, P.; Montzka, S. A.; Masarie, K.; Thoning, K.; Plass-Duelmer, C.; Claude, A.; Carpenter, L. J.; et al. Reversal of global atmospheric

- ethane and propane trends largely due to US oil and natural gas production. *Nat. Geosci.* **2016**, 9 (7), 490–495.
- (15) Nisbet, E. G.; Dlugokencky, E. J.; Manning, M. R.; Lowry, D.; Fisher, R. E.; France, J. L.; Michel, S. E.; Miller, J. B.; White, J. W. C.; Vaughn, B.; et al. Rising atmospheric methane: 2007–2014 growth and isotopic shift. *Glob. Biogeochem. Cycles* **2016**, 30 (9).
- (16) Townsend-Small, A.; Botner, E. C.; Jimenez, K. L.; Schroeder, J. R.; Blake, N. J.; Meinardi, S.; Blake, D. R.; Sive, B. C.; Bon, D.; Crawford, J. H.; et al. Using stable isotopes of hydrogen to quantify biogenic and thermogenic atmospheric methane sources: A case study from the Colorado Front Range. *Geophys. Res. Lett.* **2016**, 43 (21).
- (17) Buzcu, B.; Fraser, M. P. Source identification and apportionment of volatile organic compounds in Houston, TX. *Atmos. Environ.* **2006**, 40 (13), 2385–2400.
- (18) Lamb, B. K.; Edburg, S. L.; Ferrara, T. W.; Howard, T.; Harrison, M. R.; Kolb, C. E.; Townsend-Small, A.; Dyck, W.; Possolo, A.; Whetstone, J. R. Direct Measurements Show Decreasing Methane Emissions from Natural Gas Local Distribution Systems in the United States. *Environ. Sci. Technol.* **2015**, 49 (8), 5161–5169.
- (19) Gilman, J. B.; Lerner, B. M.; Kuster, W. C.; de Gouw, J. A. Source Signature of Volatile Organic Compounds from Oil and Natural Gas Operations in Northeastern Colorado. *Environ. Sci. Technol.* **2013**.
- (20) Hopkins, F. M.; Kort, E. A.; Bush, S. E.; Ehleringer, J. R.; Lai, C.-T.; Blake, D. R.; Randerson, J. T. Spatial patterns and source attribution of urban methane in the Los Angeles Basin. *J. Geophys. Res. Atmospheres* **2016**.
- (21) California Energy Commission. Oil Refinery Locations in California, 2016.
- (22) Hsu, Y.-K.; VanCuren, T.; Park, S.; Jakober, C.; Herner, J.; FitzGibbon, M.; Blake, D. R.; Parrish, D. D. Methane emissions inventory verification in southern California. *Atmos. Environ.* **2010**, 44 (1), 1–7.
- (23) Whitby, R. A.; Altwicker, E. R. Acetylene in the atmosphere: Sources, representative ambient concentrations and ratios to other hydrocarbons. *Atmospheric Environ.* **1977**, 12 (6), 1289–1296.
- (24) Baker, A. K.; Beyersdorf, A. J.; Doezema, L. A.; Katzenstein, A.; Meinardi, S.; Simpson, I. J.; Blake, D. R.; Sherwood Rowland, F. Measurements of nonmethane hydrocarbons in 28 United States cities. *Atmos. Environ.* **2008**, 42 (1), 170–182.
- (25) Warneke, C.; McKeen, S. A.; de Gouw, J. A.; Goldan, P. D.; Kuster, W. C.; Holloway, J. S.; Williams, E. J.; Lerner, B. M.; Parrish, D. D.; Trainer, M.; et al. Determination of urban volatile organic compound emission ratios and comparison with an emissions database. *J. Geophys. Res. Atmospheres* **2007**, 112.
- (26) Pang, Y.; Fuentes, M.; Rieger, P. Trends in the emissions of Volatile Organic Compounds (VOCs) from light-duty gasoline vehicles tested on chassis dynamometers in Southern California. *Atmos. Environ.* **2014**, 83, 127–135.
- (27) Swarthout, R. F.; Russo, R. S.; Zhou, Y.; Miller, B. M.; Mitchell, B.; Horsman, E.; Lipsky, E.; McCabe, D. C.; Baum, E.; Sive, B. C. Impact of Marcellus Shale Natural Gas Development in Southwest Pennsylvania on Volatile Organic Compound Emissions and Regional Air Quality. *Environ. Sci. Technol.* **2015**, 49 (5), 3175–3184.
- (28) Gentner, D. R.; Harley, R. A.; Miller, A. M.; Goldstein, A. H. Diurnal and Seasonal Variability of Gasoline-Related Volatile Organic Compound Emissions in Riverside, California. *Environ. Sci. Technol.* **2009**, 43 (12), 4247–4252.

- (29) Pang, Y.; Fuentes, M.; Rieger, P. Trends in selected ambient volatile organic compound (VOC) concentrations and a comparison to mobile source emission trends in California's South Coast Air Basin. *Atmos. Environ.* **2015**, *122*, 686–695.
- (30) Gorham, K. A.; Blake, N. J.; VanCuren, R. A.; Fuelberg, H. E.; Meinardi, S.; Blake, D. R. Seasonal and diurnal measurements of carbon monoxide and nonmethane hydrocarbons at Mt. Wilson, California: Indirect evidence of atomic Cl in the Los Angeles basin. *Atmos. Environ.* **2010**, *44* (19), 2271–2279.
- (31) Lopez, J. del P. Seasonality and Global Growth Trends of Carbon Monoxide During 1995-2001, University of California, Irvine, 2002.
- (32) Barnes, D. H.; Wofsy, S. C.; Fehla, B. P.; Gottlieb, E. W.; Elkins, J. W.; Dutton, G. S.; Montzka, S. A. Urban/industrial pollution for the New York City–Washington, D. C., corridor, 1996–1998: 2. A study of the efficacy of the Montreal Protocol and other regulatory measures. *J. Geophys. Res. Atmospheres* **2003**, *108* (D6), 4186.
- (33) Griffin, R. J.; Chen, J.; Carmody, K.; Vutukuru, S.; Dabdub, D. Contribution of gas phase oxidation of volatile organic compounds to atmospheric carbon monoxide levels in two areas of the United States. *J. Geophys. Res. Atmospheres* **2007**, *112* (D10), D10S17.
- (34) Gentner, D. R.; Miller, A. M.; Goldstein, A. H. Seasonal Variability in Anthropogenic Halocarbon Emissions. *Environ. Sci. Technol.* **2010**, *44* (14), 5377–5382.
- (35) Gong, Q.; Demerjian, K. L. Measurement and analysis of C2-C10 hydrocarbons at Whiteface Mountain, New York. *J. Geophys. Res. Atmospheres* **1997**, *102* (D23), 28059–28069.
- (36) Lee, B. H.; Munger, J. W.; Wofsy, S. C.; Goldstein, A. H. Anthropogenic emissions of nonmethane hydrocarbons in the northeastern United States: Measured seasonal variations from 1992–1996 and 1999–2001. *J. Geophys. Res. Atmospheres* **2006**, *111*.
- (37) Cheng, L.; Fu, L.; Angle, R. P.; Sandhu, H. S. Seasonal variations of volatile organic compounds in Edmonton, Alberta. *Atmos. Environ.* **1997**, *31* (2), 239–246.
- (38) Li, L.; Wang, X. Seasonal and Diurnal Variations of Atmospheric Non-Methane Hydrocarbons in Guangzhou, China. *Int. J. Environ. Res. Public Health* **2012**, *9* (5), 1859–1873.
- (39) Kesselmeier, J.; Staudt, M. Biogenic Volatile Organic Compounds (VOC): An Overview on Emission, Physiology and Ecology. *J. Atmospheric Chem.* **1999**, *33* (1), 23–88.

CHAPTER 4: Using Positive Matrix Factorization for Source Apportionment

4.1 Positive Matrix Factorization Background and Theory

As discussed in Chapter 1, several methods have been used to attempt to apportion methane and other VOCs to sources in the Los Angeles area. Here, Positive Matrix Factorization (PMF), will be used to study the SoCAB, and its utility will be analyzed. PMF is a mathematical technique that solves the chemical mass balance problem by breaking down the data matrix into two matrices that represent factor profiles and their contributions to individual samples. The analyst inputs the number of desired factors and the matrix of measured data. Possible solutions are fitted to the number of factors, and the solutions are then ranked by how well they fit the original data set.¹ This mathematical method has found use in the atmospheric chemistry community due to its ability to separate out sources in a measurement of mixed origins.²⁻⁴ The inputted matrix is the series of measurements that were collected, and the factors that PMF outputs are sources that contribute to the total mass of the VOCs measured. This method is intriguing to atmospheric scientists as it does not require any knowledge or inputs of the potential sources.

Chemical Mass Balance (CMB) is a similar method that PMF results often get compared to. Chemical Mass Balance is a receptor model that fits known source profiles to the resultant matrix. For VOC analysis, CMB requires speciated profiles of different emissions sources. It then fits the minimized set of contributions to those speciated profiles. This method has been used frequently in the past,⁵⁻⁸ although several issues with it have been brought up. First, the profiles used are sources of contention. Profiles of traffic emissions, or gasoline vapors are not consistent across states, regions, or even seasons.^{9,10} Further, as engine technology has advanced the emissions profile of mobile sources have changed and will continue to change such that one

profile cannot possibly accurately represent the variety of automobiles on the road.¹¹ As will be discussed in the next chapter, this variation is also the case for natural gas. Second, CMB requires that you choose these profiles before running the analysis. For a large air basin in an urban environment, this is difficult to do. It is hard to know whether or not a sector does contribute to the overall total, unless extensive studies of the region have been conducted. These are a few reasons as to why apportionment modelers have been switching to PMF or other methods as of late.^{4,12,13}

PMF analysis is described in detail in Paatero and Tapper (1994).¹ In brief, a series of solutions are found to the matrix X containing a series of concentrations of various VOCs, m , noted at, n , different times by breaking down the matrix into two matrices G and F which describe the mass contribution of each factor and the profile of that factor, respectively. This result is then summed over all time points and any residual (e) is noted. This process is summarized by the equation:

$$X_{ij} = \sum_{k=1}^p G_{ik}F_{kj} + e_{ij}$$

where p is the number of factors suggested by the user, with i ranging from 1 to m and j ranging from 1 to n . Here G and F are constrained such that there can be no negative masses or contributions. The solution to this problem is done by least squares analysis trying to minimize Q such that:

$$Q_{actual} = \sum_i^m \sum_j^n \frac{e_{ij}^2}{\sigma_{ij}^2}$$

where σ is the variance in any given data point. In a perfect solution, the residuals are equal to the variances in each data point making the fraction equal unity and Q_{actual} would be equal to the minimum theoretical Q. Q_{theo} can be defined further as:

$$Q_{theo} = (X) - ((p \times R) + (p \times S))$$

where X is the total number of individual points in the matrix, and R and S are the number of elements in column matrices G and F. The Q_{actual}/Q_{theo} ratio is an often used statistic to show how likely it is that a true global solution has been reached. A Q_{actual}/Q_{theo} greater than 100 suggests that the result is not a global minimum and the data set should be reevaluated for outliers or more factors should be considered.² It is possible that multiple solutions could yield a similar Q value and so it is important for the user to inspect the solution for feasibility. Using previous work that has been done in the SoCAB, any output solution set from PMF can be checked to ensure the profiles in the minimized solution are realistic and possible. Using PMF also requires the analysis of results across a varying number of factors inputted. These caveats to effective use of PMF will be discussed herein.

This type of analysis has been performed on numerous urban VOC data sets from major urban centers from around the globe including Houston, Texas and Beijing, China.^{4,12,14} It can be used as an exploratory tool or as a confirmation of other apportionment methods. Here, PMF will be to apportion methane and ethane emissions in the basin, using the two year Mt. Wilson data set. This technique was used here to attempt to apportion methane emissions to better understand its sources in the region and test the viability of the technique on the region.

4.2 Positive Matrix Factorization Analysis

4.2.1 Data Filtering

As discussed in Chapter 3, not all samples collected were representative of the SoCAB. 86% of the daytime samples collected during two years at Mt. Wilson were during normal wind events. Samples collected during times when the wind was not blowing from across the SoCAB were removed prior to further PMF analysis. Enhancement values were used as described in

Chapter 3 due to the goal of apportionment of SoCAB emissions sources and using the whole mixing ratio seen would introduce the issue of oceanic and long range transport sources into the problem. After these filters were applied, 452 samples were used for PMF analysis.

4.2.2 Positive Matrix Factorization Inputs

EPA PMF 5.0 software was used in robust mode to analyze the 2014-2016 Mt. Wilson filtered daytime data set. A subset of the hydrocarbons that were measured in our laboratory analysis was selected to improve PMF outputs as it has been noted that PMF analysis can struggle with missing values.² Therefore, hydrocarbons that had mixing ratios above the minimum detection limit (MDL) in at least 80% of all samples were selected to minimize the effect of missing data on the analysis.¹⁵ PMF analysis requires the inputting of two matrices, the first being the matrix with the measurements from Mt. Wilson. The second is a matrix with the same dimensions as the first but containing the uncertainty of each given measurement. PMF does not allow for the inputting of zeros or blanks, and therefore estimates must be made for missing data. As suggested by literature, values below the MDL were estimated as 0.01 pptv and the uncertainty set as 3 pptv (the MDL for hydrocarbons on our analytical system).^{15,16} These values were chosen so as to minimize the effect of below detection limit values on the results of the analysis. The uncertainty in these values is 3000% larger than the estimated measurement, thereby signaling to the algorithm that this value is not to be trusted. Absolute uncertainties in all hydrocarbons were calculated via the precision test described in Chapter 2 with results shown in Table 2.1. To ensure the global minimum solution was reached for each set of inputs, the PMF algorithm was run 100 times with a random seed start.

At the end of the run of the algorithm, the Q_{actual} value for the lowest converging result was noted and the factors determined were studied. Output results were checked to see how well

the modeled mixing ratio correlated with the experimental concentration. Species for which the r^2 was below 0.8 for such a plot were heavily scrutinized, and if the residuals were non-gaussian across several factor numbers, the species was downweighted to weakly correlating. This change in species strength triples the uncertainty inputted into the algorithm, which has the effect of limiting the effect of a species with one or two outlier mixing ratios from having large impacts on the resulting factors.

For analyses with at least one converging run, displacement and bootstrap error analysis were further run. These two error analysis algorithms are useful to help the user decide if the results of a runs should be trusted. Displacement analysis shows how much rotational ambiguity exists. Rotational ambiguity in PMF is defined as alternate G and F matrix pairs that could yield the same Q. Significant rotational ambiguity in a result suggests that a global minimum has not been found and the number of factors should be reconsidered. Displacement analysis is achieved by adjusting each individual mixing ratio value up and down such that a change in Q is achieved. This new matrix is analyzed via PMF to study the effects on the output factors. If a result had displacement analysis that showed significant swapping of factors, this result was considered to be suspect as there is not much to differentiate one factor from one or many others. Bootstrap error analysis is useful in determining weaknesses in the data set and random errors. This analysis is done by randomly selecting a subset of the data to reanalyze and comparing the factors produced with the main result. The output can be studied to see if there was a certain factor that was reassigned or unmapped suggesting significant variation or noise in some subset of the data. For reporting factor profiles, plots are shown with the fraction of the species total assigned to a given factor with the displacement analysis upper and lower bounds as error bars.

4.3 Analysis of Number of Factors

The full two year data set was used to study the effect of changing the number of factors. The resulting output with the lowest Q value for each number of factors is plotted in Figure 4.1. The Q value is expected to decrease as the number of factors increase as observed.¹ However, these solutions must be checked to determine if the result is reasonable. Here, with the Mt. Wilson data set it was determined that after a point, adding additional factors only served to yield a factor that contained only one VOC species. It was determined that for the SoCAB, it is reasonable to expect up to 10 different sources, and so for all analysis herein between 4 and 10 factor solutions were considered.

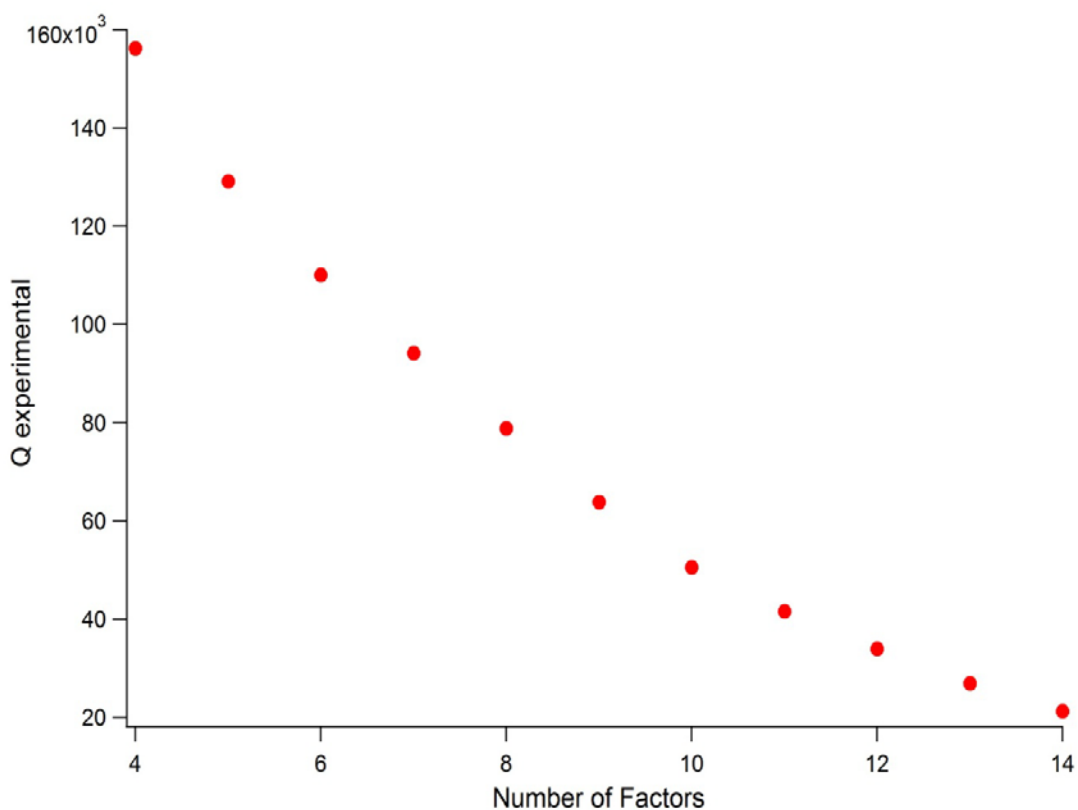


Figure 4.1. Relationship between the experimental Q value and the number of factors selected for a PMF analysis of the full two year Mt. Wilson data set

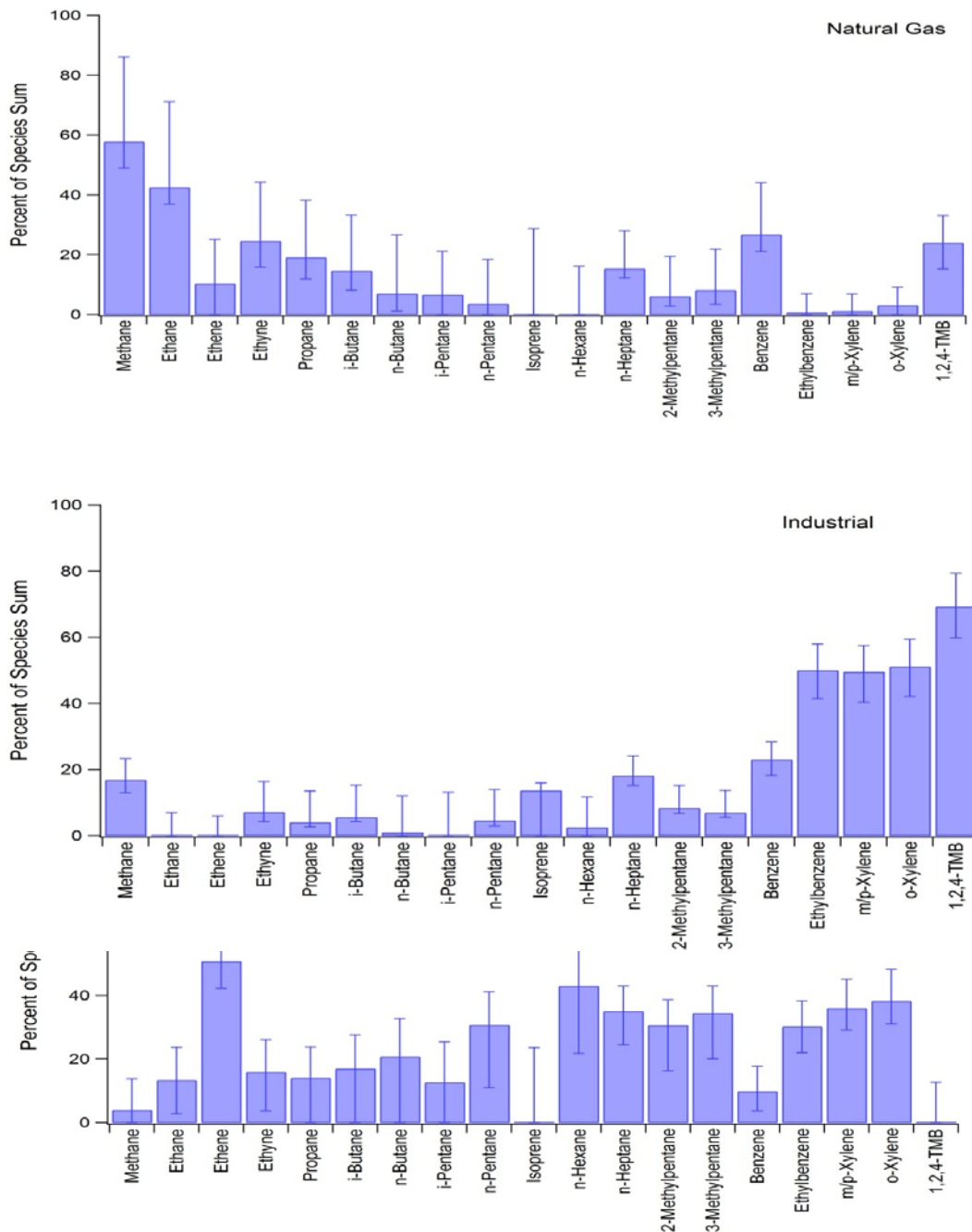
4.3 Results from Seasonal Analysis

4.3.1 Summer

To explore the potential for seasonal and transient sources to affect total emissions in the SoCAB, PMF analysis was undertaken for each of the four seasons using the Mt. Wilson data set, filtered as above. Determination of sources from factors for the optimal result from PMF analysis for each season was done using a variety of techniques. First, profiles were compared to known profiles in the EPA's SPECIATE 4.5 database. This database is a repository for profiles of known emissions point sources for NMHCs and was last updated in 2016.¹⁷ These profiles include various vehicular sources and emissions from various industries. Second, key ratios that are used in atmospheric apportionment such as those discussed in Chapter 3 were used to confirm sources. Another useful tool for source determination is the normalized factor contributions data that is an output of the PMF software. This data set contains each sample and each factor's contribution to the mixture of gases seen in it. The contribution of an individual factor is normalized to one across all samples. This data allows for an analysis of temporal variability in a factor. If a source has a greater variability in contributions than another, the first source can be said to be more transient in nature in the sample region. Finally, more recent literature profiles of sources along with reported results of PMF used on other cities and regions were referenced for further confirmation. Certain source profiles will be highlighted in the subsequent subsections for each season. A full example of how sources were determined from factors will be shown in Section 4.4.

For summer, (June-August), 137 daytime samples from both 2014 and 2015 were included. A six factor analysis with propene excluded, (Q=27182) was selected as the most reasonable result with a maximum change in Q of -0.16 from displacement analysis, and no

factor having more than 20% mismapping in bootstrap analysis. The source profiles of this result are shown in Figure 4.2. The six factors resolved were biogenic, natural gas, vehicular emissions, gasoline liquids, industrial processes, and oil and gas production. A five factor result was also considered; however, it merged most of the gasoline source with natural gas and assigned an unusually large amount of ethyne and ethene to this large source. When a seventh factor was introduced, 1,2,4-trimethylbenzene is given its own factor, which is highly unlikely.



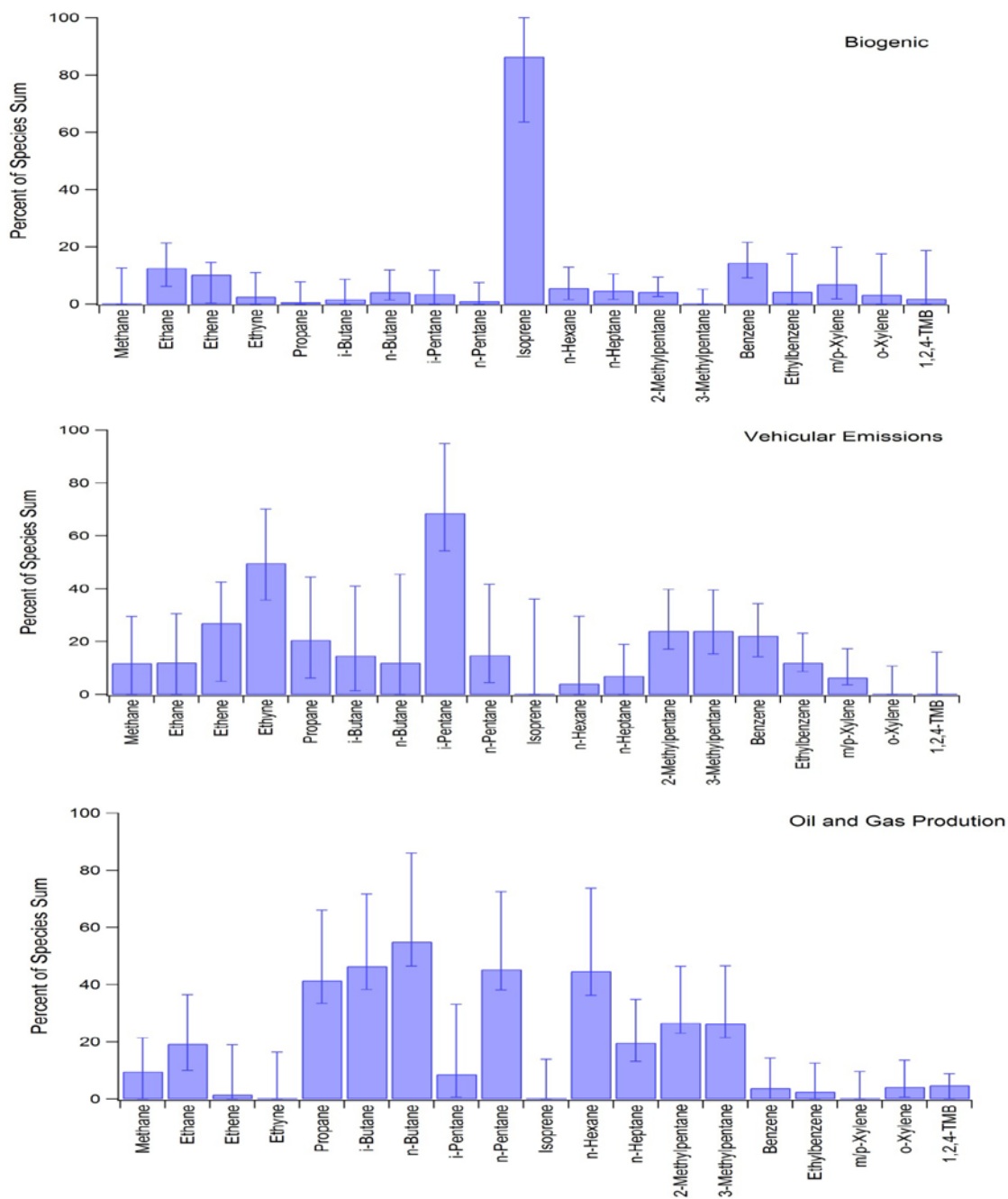


Figure 4.2 Profiles of the six factors resolved from positive matrix factorization of the summer SoCAB influenced samples.

Of note in the factor profiles, are the two more transient sources, gasoline liquids and oil and gas production. These two sources contribute a large portion of the total of most of the heavier alkanes while only contributing 14% of the methane and less than a third of the ethane. These two factors are more transient in nature, meaning that they contribute heavily to some sampling times but very little to others. This varying nature can be seen by studying the contribution profiles for each factor. PMF reports for each sample the normalized average contribution by each factor. Contributions are normalized such that the average contribution of a factor across all samples is unity. The time resolved profiles of the oil and gas factor and evaporative emissions factors are shown in Figure 4.3 along with the natural gas factor for comparison. The two factors contribute most heavily in August of 2014 and July of 2015 as compared to the other four summer months. When compared to the natural gas factor, their relative contributions to any one sample vary much more widely with standard deviations of 1.47 for production and 1.07 for liquids as compared to 0.75 for natural gas. This makes sense as natural gas emissions are thought to be widespread across the basin and constant in nature.¹⁸ Oil and gas refineries are located in a small section of the SoCAB and have flare and venting events that are not announced publicly.¹⁹ Further, gasoline evaporation occurs more readily when the ambient temperature is higher resulting in day to day variation.¹⁰ These factors lead to the expected result seen here, emissions associated with oil and natural gas production and gasoline evaporation are temporally varied in intensity.

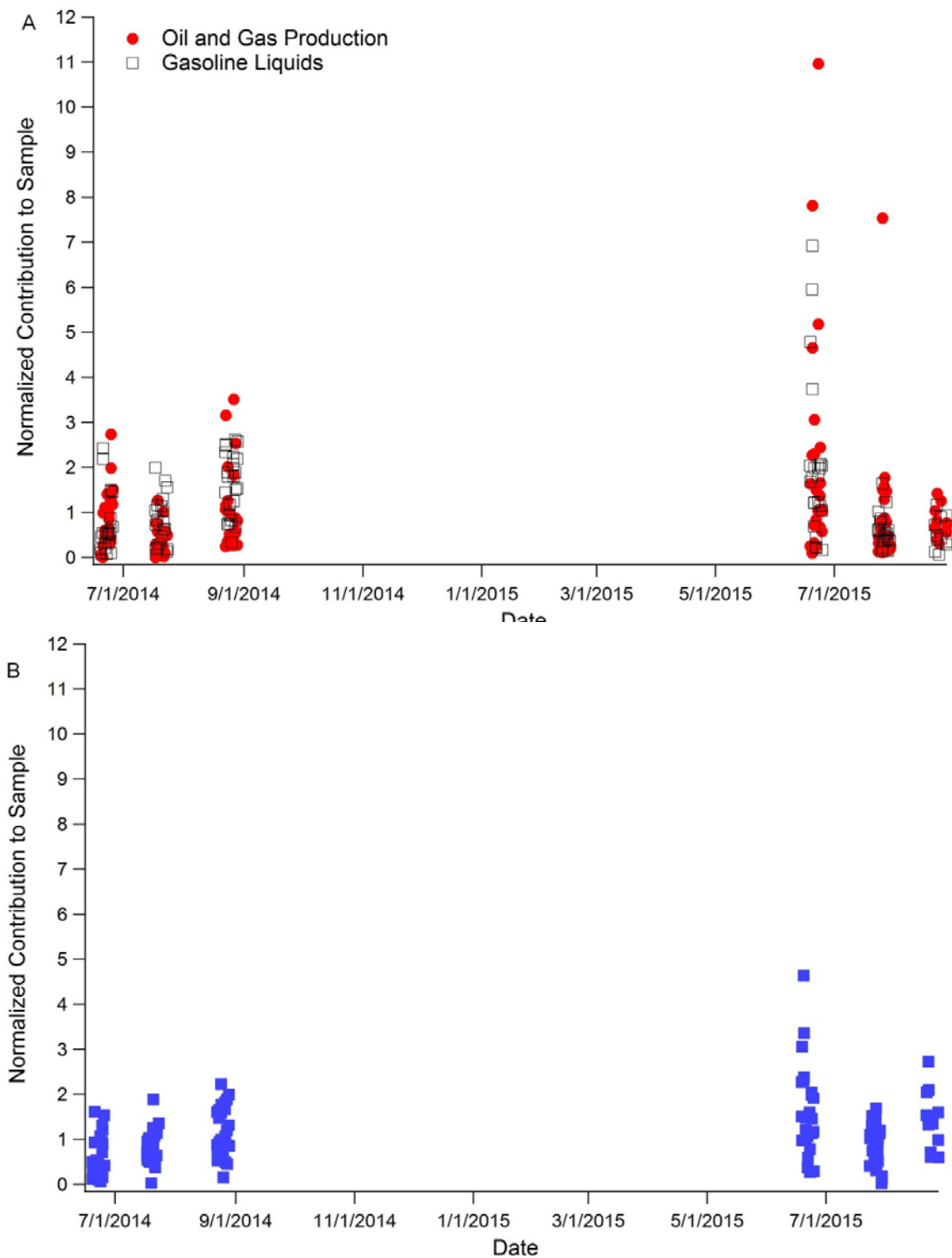
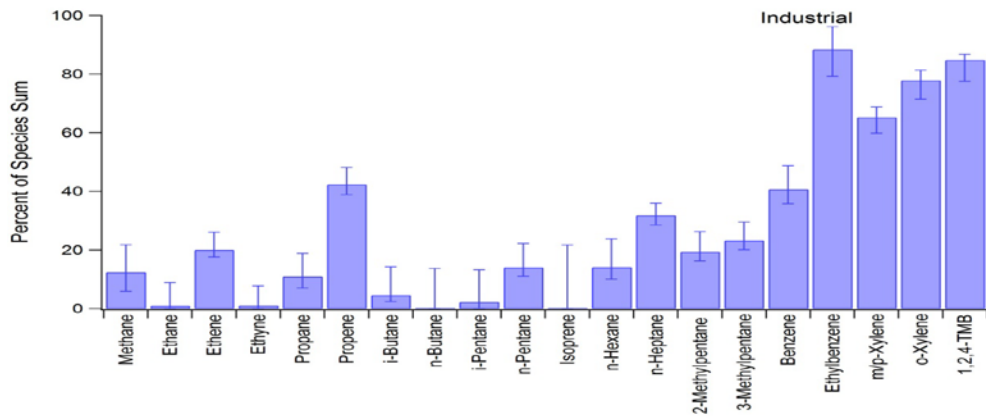
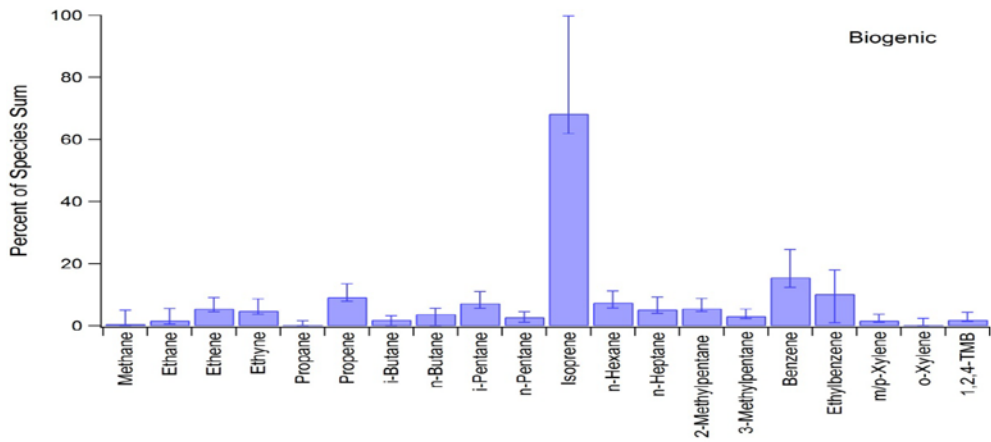
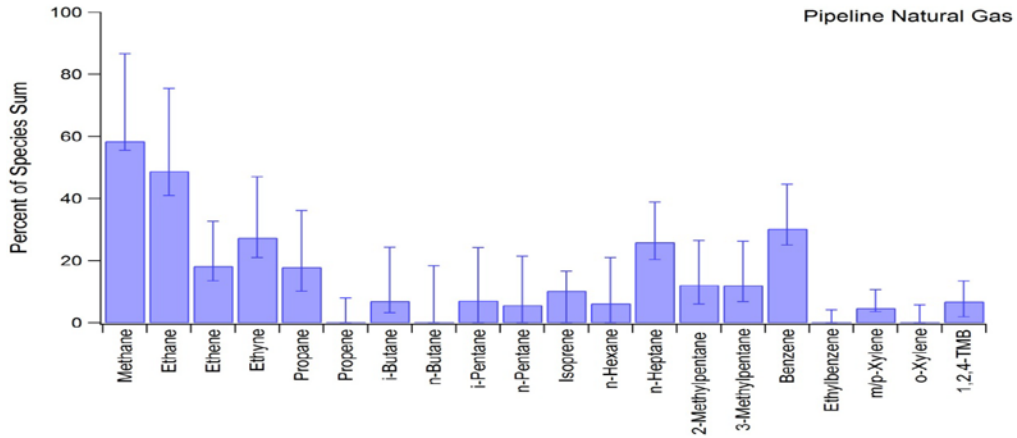


Figure 4.3 A) Normalized contributions of oil and gas production and gasoline liquids factors to the samples collected at Mt. Wilson in summer 2014 and summer 2015. B) Normalized contributions of the natural gas factor during the same time period. Contributions from a factor are normalized such that the average is unity.

4.3.2 Fall

For Fall (September-November), 107 samples from both 2014 and 2015 were included. A five factor analysis with propene weakly correlating ($Q=15595$) was selected as the most reasonable result with a dQ_{\max} of -0.71 for displacement analysis, and only one factor with any swaps in mapping in bootstrap analysis. The source profiles of this result are shown in Figure 4.4. The five factors resolved were biogenic, natural gas, vehicular emissions, industrial solvent use, and oil and gas production. When a sixth factor was introduced, an unexpected source of *n*-butane arose. This butane is included in the oil and gas production factor in the five factor result.



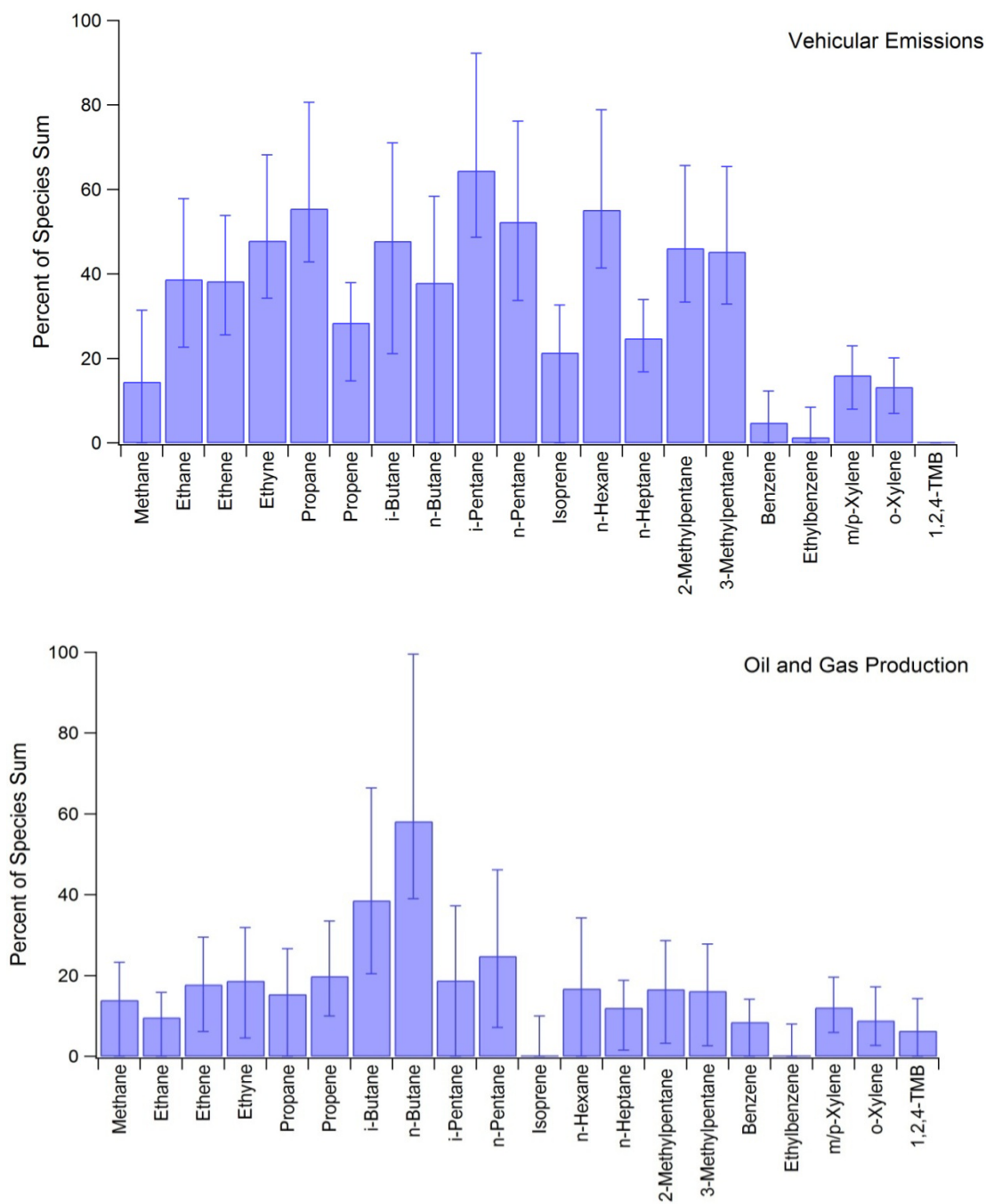
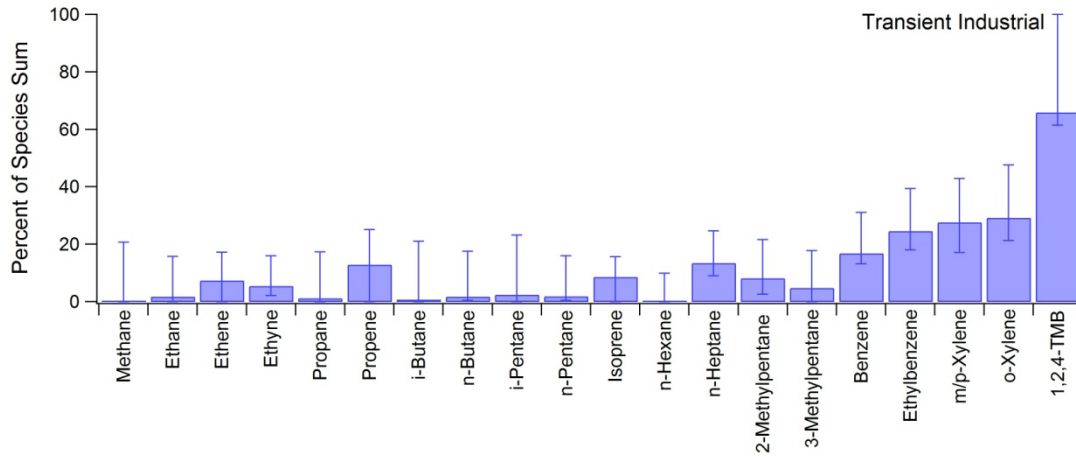
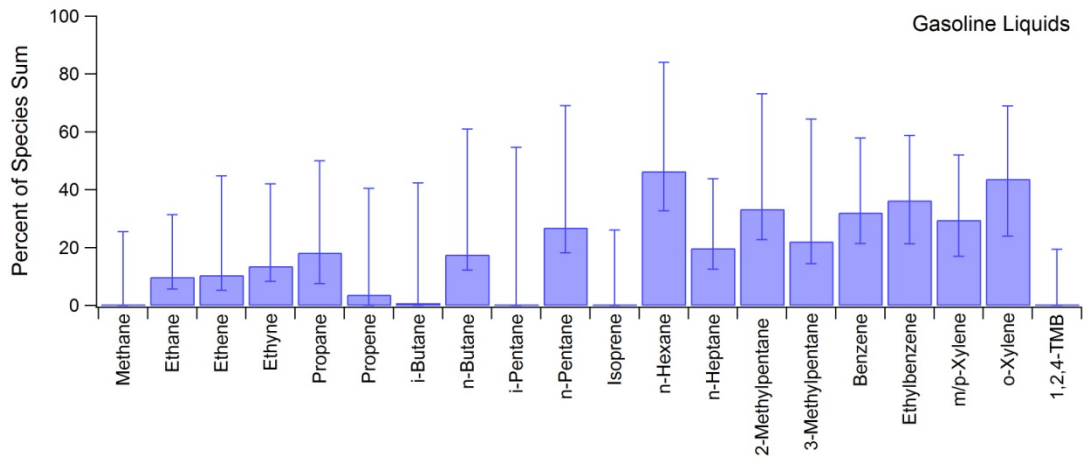
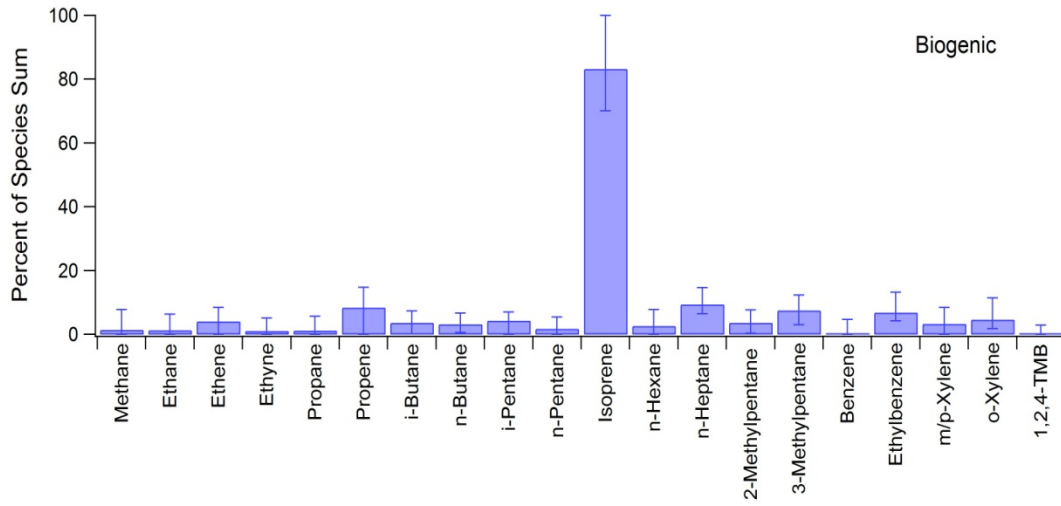


Figure 4.4 Profiles of the five factors resolved from positive matrix factorization of the fall SoCAB influenced samples.

It is interesting that a different number of factors were resolved in this analysis versus the summer. Whereas, in the summer analysis, adding a sixth factor allowed for the separation of vehicular sources, here, the sixth factor separated out the more transient oil and gas source and created a factor profile that is largely dominated by *n*-butane. This result is not completely unexpected as four samples (from November 2014 and November 2015) fall in the top 5% of all samples for *n*-butane mixing ratios. It is unclear as if this increase in *n*-butane in November is coincidental or aligns with some event in the SoCAB. The wind direction at the time of the four samples varies, as does the HYSPLIT analysis as to where the air mass had come from. This result is likely a remnant of coincidence and PMF analysis picked it up as a trend. This result does show one of the potential issues with PMF. An analyst needs to be careful in interpreting outputs from the algorithm. Just because one data set was best described by a given number of factors does not mean that another will behave the same way.⁴ It is expected that gasoline evaporation still took place during the Fall months, however the evaporation was not occurring strongly enough for PMF analysis to detect it as separate from the vehicular source.

4.3.3 Winter

For winter (December-February), 83 samples from both 2014-2015 and 2015-2016 were included. A six factor analysis with all species strongly correlated ($Q=17555$) was selected as the most reasonable result with a dQ_{\max} of -0.22 for displacement analysis, and only one factor with any swaps in mapping in bootstrap analysis. The source profiles of this result are shown in Figure 4.5 The six factors resolved were biogenic, natural gas, vehicular emissions, gasoline liquids, oil and gas production, and a transient industrial source.



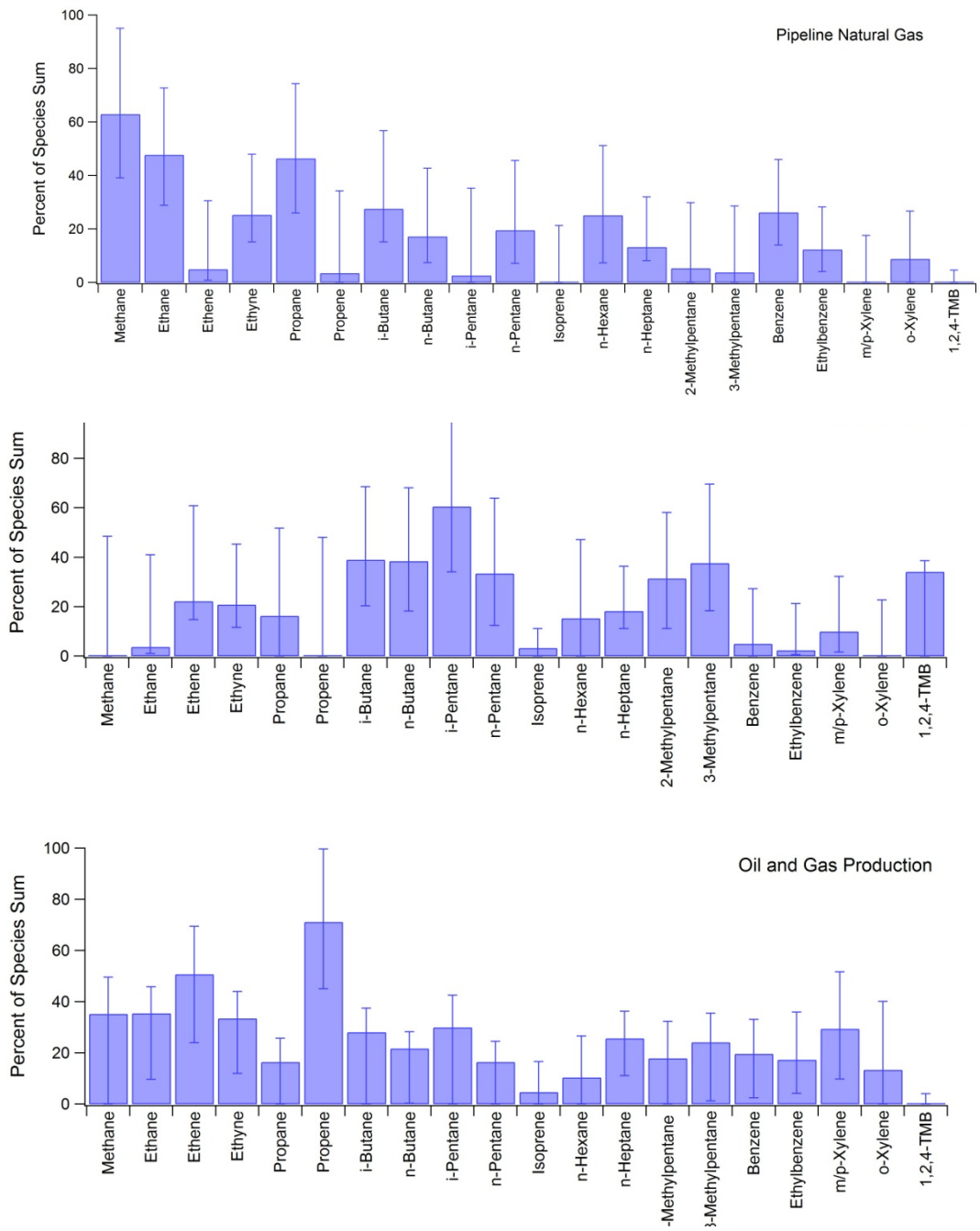


Figure 4.5 Profiles of the six factors resolved from positive matrix factorization of the winter SoCAB influenced samples.

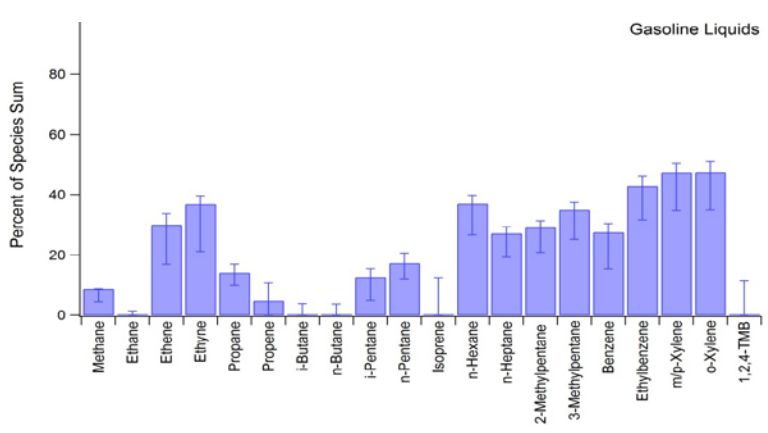
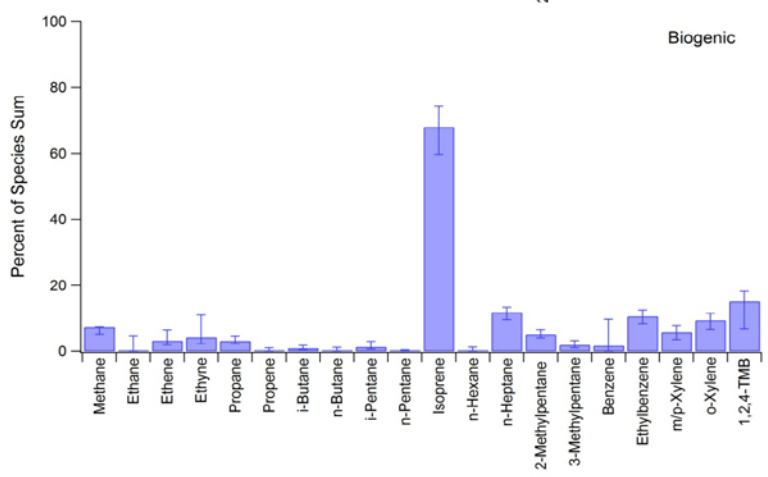
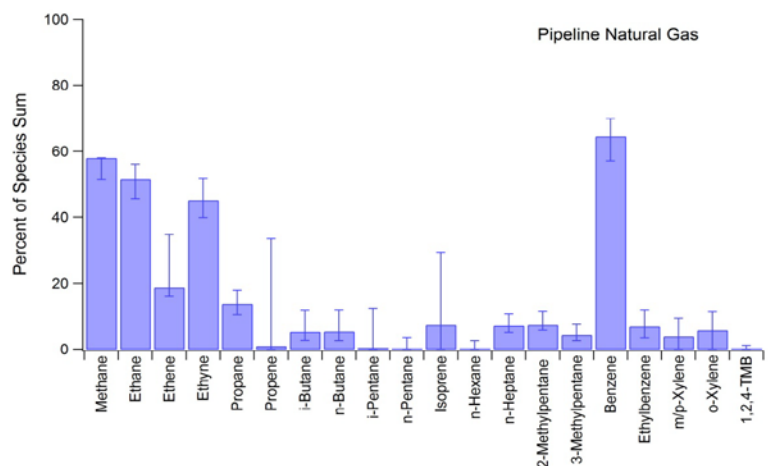
This season had the fewest useable samples for PMF due to a high incidence of Santa Ana Wind events, along with sampling issues. The size of this data set had a significant impact on the PMF analysis. Several outcomes studied had rotational ambiguity. This ambiguity was caused by the influence of a few samples in determining a factor. With a smaller number of samples, the importance of an individual sample increases and the chance for ambiguity and errors. Even when rotational ambiguity is minimal, the importance of one sample on a smaller data set can also be seen. The sixth factor resolved in the winter data set is a transient source that has a normalized contribution of almost nine in a particular sample on January 26, 2016. Factors that are the result of one sample are due to too many factors being selected.¹⁶ However, when five factors are analyzed, the same result occurs with the 1/26/2016 sample having its own factor. This further result causes the analyst to consider the sample in greater detail. The sample had the highest mixing ratio of *o*-xylene, *m/p*-xylene, 1,2,4-trimethylbenzene, and benzene seen in the entire month of January 2016 and in the top 3% for all winter samples for these gases. The two samples that have larger mixing ratios in winter for these species also showed large enhancements for all other hydrocarbons. The sample from January 26th does not have such strong enhancements for smaller hydrocarbons which is unexpected if this is a vehicular emissions source, but furthers the result produced by PMF that this sample does not fit in with any other.

This result furthers the utility of PMF analysis as it gives the analyst another tool to find interesting data points that may have otherwise been lost in a large data set. HYSPLIT analysis shows the air mass having come into the region from the high desert to the northeast before swirling around the SoCAB and reaching Mt. Wilson from the SSW. This is not a particularly unusual trajectory as per the wind rose in Figure 3.3, which furthers the evidence for some sort

of transient emissions source. Upon removing this sample and rerunning the PMF analysis, only four factors could be resolved. This includes a biogenic factor, a natural factor, and two alkane factors that look very similar. Again, this shows the necessity of large data set for successful PMF analysis.

4.3.4 Spring

For spring (March-June), 125 samples from both 2015 and 2016 were included. A six factor analysis with all species strongly correlating ($Q=27851$) was selected as the most reasonable result with a dQ_{\max} of -7.96 for displacement analysis, and only one factor with more than 10 swaps out of 100 bootstrap runs. The source profiles of this result are shown in Figure 4.6. The six factors resolved were biogenic, natural gas, vehicular emissions, industrial, oil and gas production, and gasoline liquids. When a seventh factor was introduced, the natural gas factor becomes a significant source of higher alkanes and an unexplainable benzene factor was noted.



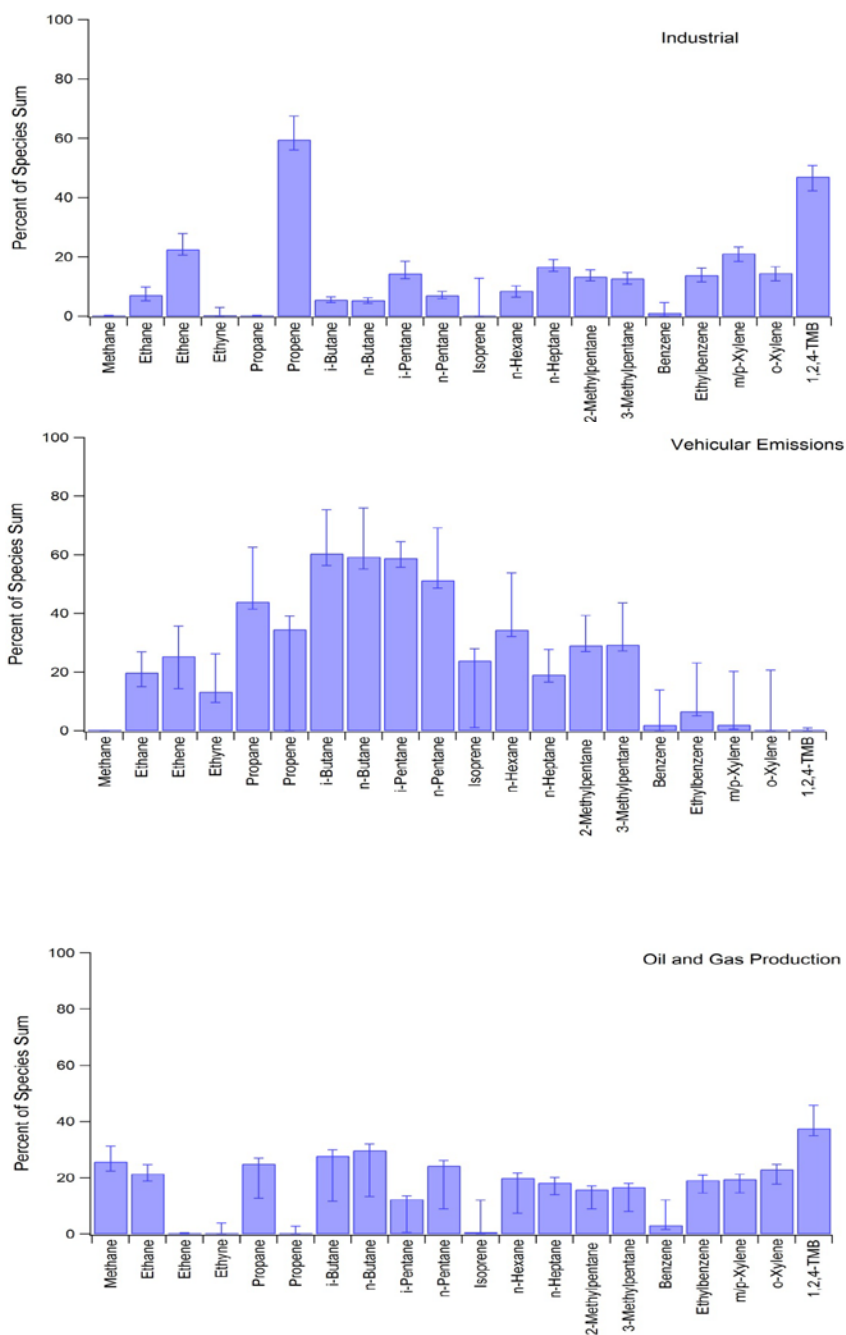


Figure 4.6 Profiles of the six factors resolved from positive matrix factorization of the spring SoCAB influenced samples including the transient industrial source.

It is interesting to compare the factor profiles found in spring samples with those found in the summer samples. The defining characteristics of each emissions source remain constant, and in fact the profiles look very similar across seasons showing the usefulness of PMF for apportionment. Further of note in the analysis of spring samples, it is apparent that the samples from May 2016, the last month of sampling, show less VOC enhancement than those of any other month sampled. The contributions of gasoline liquids and oil and natural gas production, sources, that have been shown to be more transient in nature, show larger contributions in spring 2015 than spring 2016 and especially in spring 2015 versus May 2016 (Table 4.1) Indeed, even the natural gas factor which is generally consistent across months, shows a significant drop in May 2016 with an average contribution of 0.19 ± 0.29 compared to an average contribution of 1.21 ± 0.32 across the five other months. This is potentially a result of significantly deeper than normal marine layers that kept emissions trapped beneath the level of Mt. Wilson.

Table 4.1 Averaged normalized contributions of emissions sources as determined via PMF analysis for the spring season by month shown with standard deviation

	March 2015	April 2015	May 2015	March 2016	April 2016	May 2016
Oil and Gas Production	1.29 ± 0.54	1.80 ± 1.13	1.13 ± 0.60	0.59 ± 0.52	0.20 ± 0.40	0.30 ± 0.45
Gasoline Liquids	1.34 ± 1.07	1.78 ± 1.26	0.81 ± 0.61	0.61 ± 0.52	1.03 ± 0.67	0.39 ± 0.27
Pipeline Natural Gas	1.19 ± 0.68	1.47 ± 0.91	0.38 ± 0.36	1.79 ± 0.94	1.22 ± 0.59	0.19 ± 0.29

The emissions sources determined via seasonal PMF analysis are in line with previous apportionment of sources in urban atmospheres.^{4,5} Given the dominance of personal vehicles for transportation in the region, it is no surprise that a majority of the non-methane VOC mass is associated with the incomplete combustion of fossil fuels. In regions where oil drilling is more prevalent, emissions associated with the processing and refining of crude oil into useable

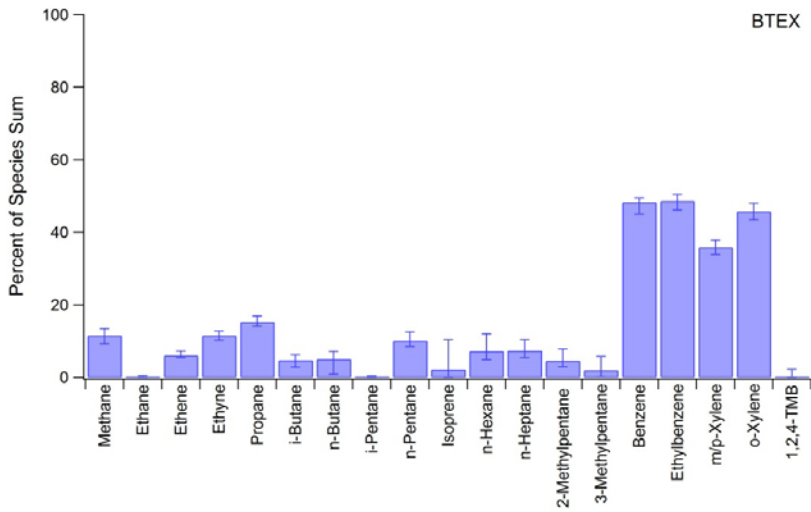
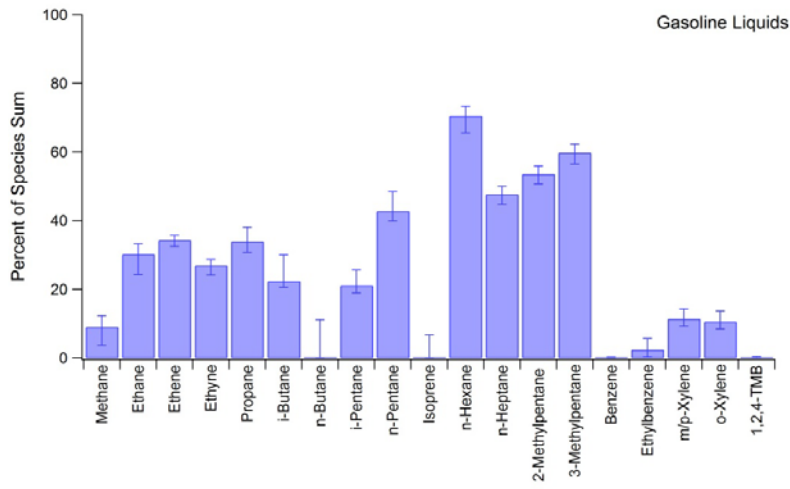
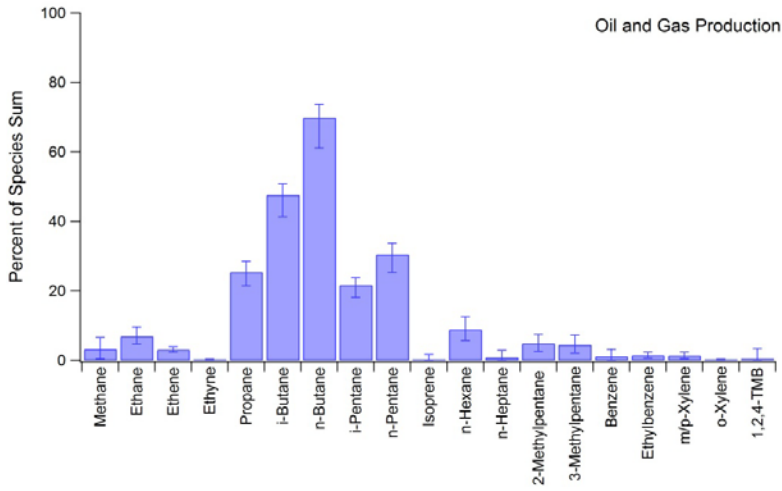
products has a much stronger contribution to overall emissions.²⁰⁻²² In the analysis thus far, an oil and gas production factor has been season in every season, but is not a constant day to day source, and the total mass of VOC does not approach that of the vehicular sources identified.

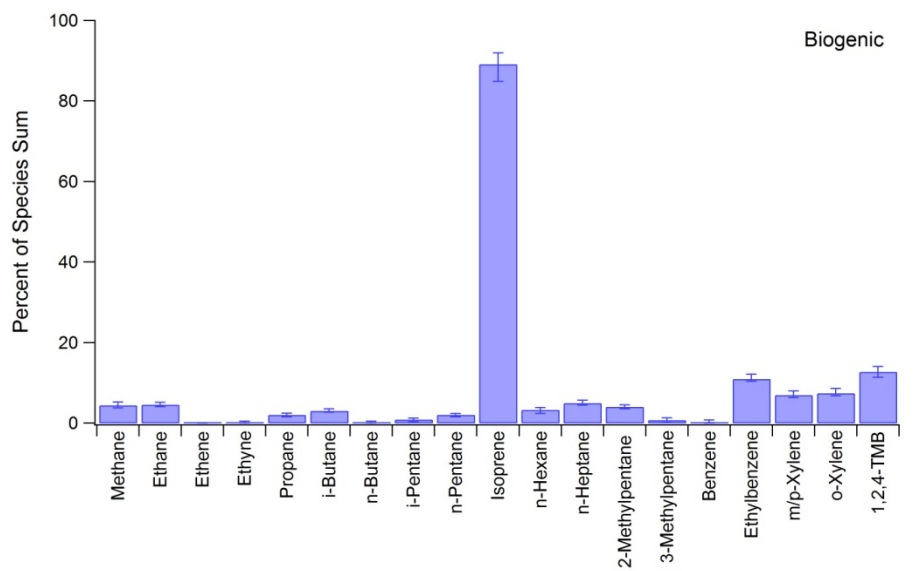
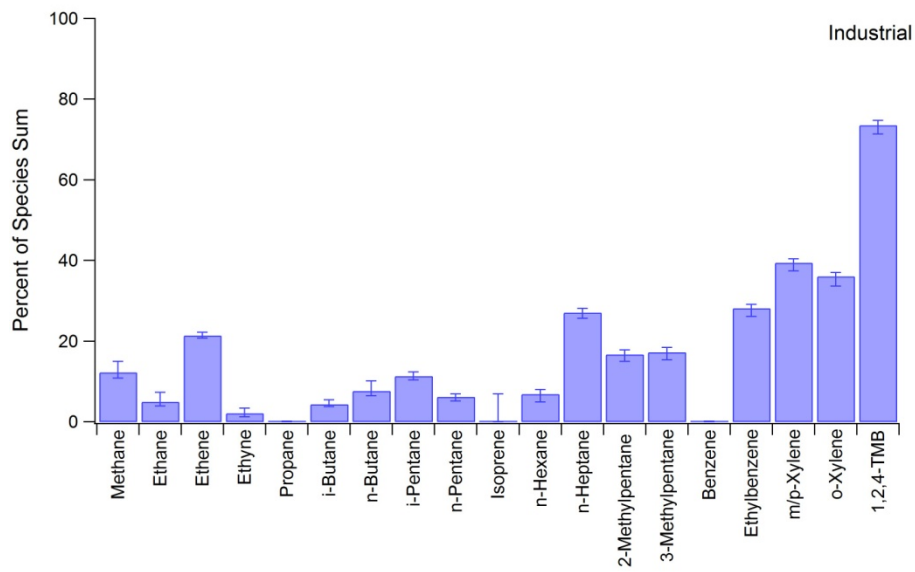
In terms of attempting to accurately apportion methane emissions, the seasonal analysis resulted in some intriguing findings. An average of 59% (49-82% using displacement upper and lower bounds) of excess methane seen in each season stems from natural gas. As evidenced in the previous chapter, natural gas plays a large role in total emissions to the region, and PMF was able to apportion a majority of total methane to it in each individual season analyzed. The next largest fraction of methane comes from oil and gas production as is seen in each season. While not appearing in every season and within the error of this method is the methane associated industrial sources. This does not seem reasonable as there are no SPECIATE profiles that show methane associated with the use of solvents.¹⁷ Further, most PMF studies opt to not include methane in their profiles.^{3,4,23} This choice is most likely due to the long atmospheric lifetime of methane, and therefore it having a positive correlation with most other gases. Further, the remaining methane sources (dairies, landfills and other biogenic sources) do not emit larger tracer hydrocarbons and so the profiles are just methane.¹⁷ A biogenic methane factor was not separated when analyzing each season. This may be due to the small samples size. PMF studies generally have data sets with the number of samples on the scale of hundreds.^{4,12} Therefore, it was imperative to utilize the entirety of the Mt. Wilson dataset as one to best understand the dominant sources of emissions to the region.

4.4 Results from Full Two Year Mt. Wilson Data Set

4.4.1 Source Identification and Analysis

A seven factor analysis using seventeen hydrocarbon species over the entire observed period of which ethene was determined to be weakly correlating and propene was excluded ($Q=87158$) was selected as the most meaningful result. Rotational analysis of the seven factor run yielded no decrease in the Q , and so the base run was used. Displacement error analysis showed a very small ($<1\%$) dQ indicating a strong solution. Bootstrap error analysis showed less than 20% mismatching for any of the factors indicative of a global minimum. The sources associated with the seven factors were determined to be vehicular emissions, evaporative emissions, BTEX, oil and natural gas refining and production, biogenic, industrial, and pipeline natural gas. The factor profiles are seen in Figure 4.7.





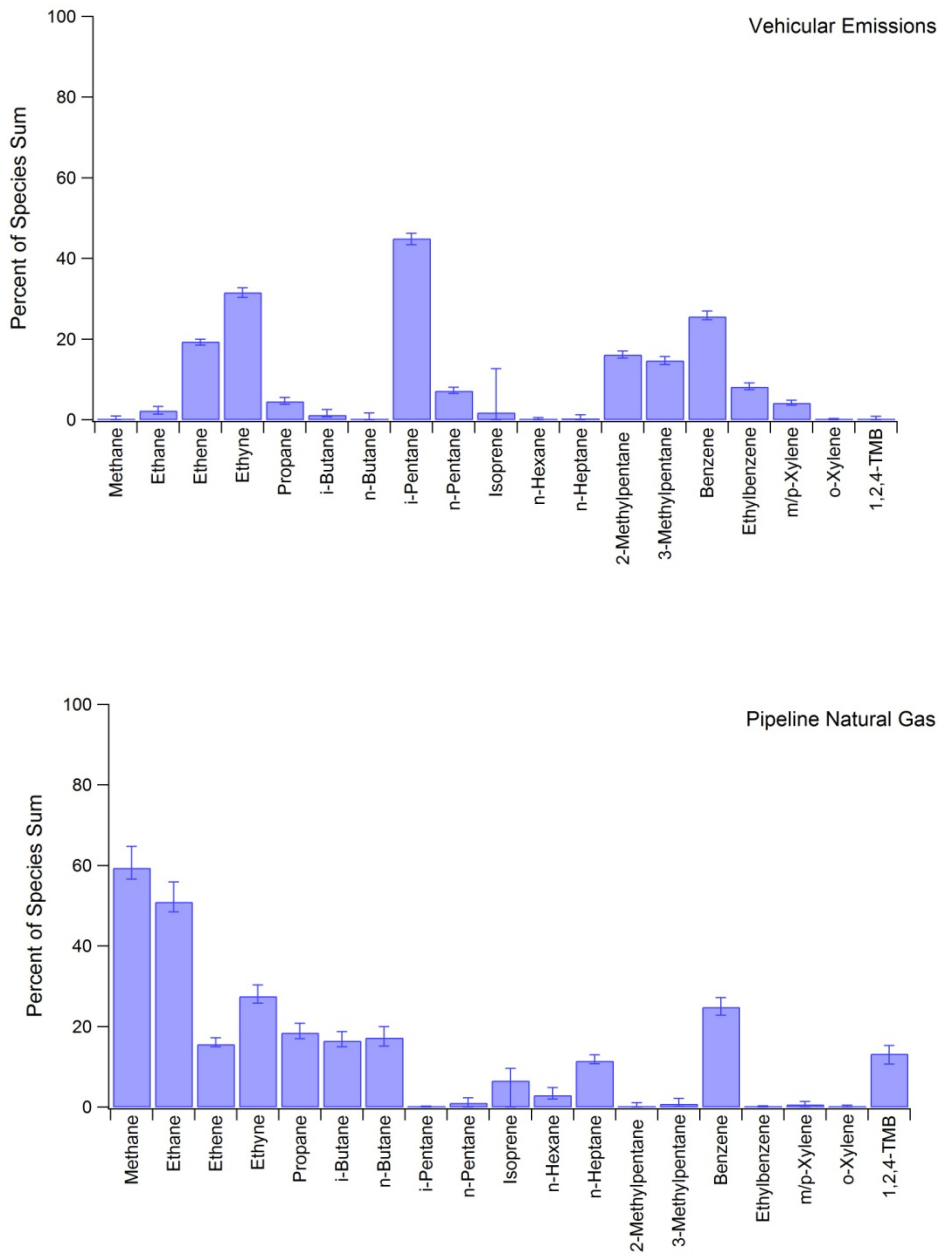


Figure 4.7. Profiles of the seven factors resolved from positive matrix factorization of the SoCAB influenced samples for the two full years of sampling

An analysis with both ethene and propene being labeled as strongly correlated was also considered, however, produced some atypical results to be discussed later (Section 4.4.8). An eight factor solution was also considered; however, the algorithm began to assign single species such as benzene or the alkenes their own factors. Further, eight factor results consistently had large numbers of mismatched factors in bootstrap analysis, indicative of the wrong number of chosen factors. No solution was capable of accurately predicting the mixing ratios of n-heptane or 1,2,4-trimethylbenzene ($r^2 < 0.8$). However, these correlations were weakened by the inclusion of one data point each in which the mixing ratios were extremely large. The effect of outliers on the ability of PMF to resolve results will be discussed later as well. To fully show the role of the analyst and the robustness of the PMF results, the process of identifying the source of each factor will be discussed here. Generally, as the number of factors chosen rose beyond four, factor profiles remained similar with one profile generally splitting into two.

4.4.2 Biogenic Emissions Factor

The most striking and consistent of the eight source profiles determined here is the biogenic factor. The biogenic emission factor was determined by the presence of isoprene. This factor alone contributed to 89% (85-91%) of all the isoprene seen in the study. Furthermore, the factor identified as being biogenic in origin only contributed to at most 12% of the total of any other species. This isoprene only factor is seen in analyses with as few as four factors showing how weakly correlated isoprene emissions are with other species. Further evidence for this factor identification comes from the annual cycling trend in contributions from this factor. Biogenic factor contributions peak in June of both years and slowly decrease over the course of the Fall reaching a minimum in the winter months of December and January. The summer daytime average mixing ratio seen at Mt. Wilson was 2218 ± 1527 ppt as compared to the winter average

of 314 ± 273 ppt. Plotting the normalized contributions of this factor versus the isoprene mixing ratio seen at that time further confirms this assignment (Figure 4.8). As noted in the literature, isoprene emissions tend to increase in the summer months when the number of sunlight hours is at a maximum and ambient temperatures are warmest allowing for the most photosynthesis.^{24,25} The result is consistent across many different factor numbers and along with seasonal agreement. It shows the utility of PMF and that it can be used for further source attribution.

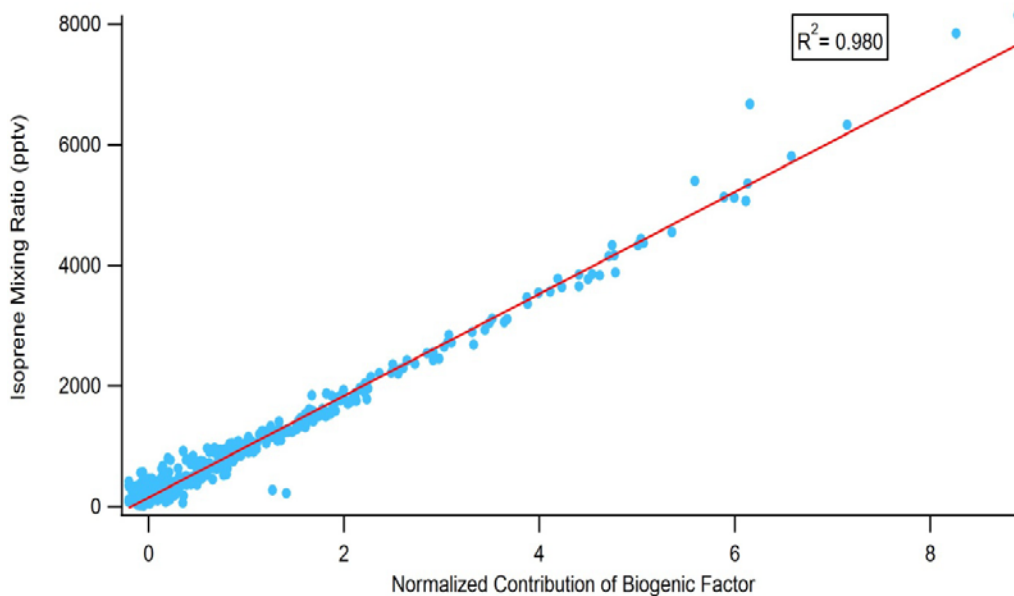


Figure 4.8. Relationship between the normalized contribution of the biogenic factor from PMF analysis and the mixing ratio of isoprene in a given sample. The positive correlation confirms the factor as biogenic in nature.

4.4.3 Vehicular Emissions Factors

The seven factor PMF result was able to distinguish two distinct vehicular emissions sources: gasoline liquids, and tailpipe emissions. Further, a BTEX factor was resolved that was not previously resolved in seasonal analysis. In runs with fewer factors, these sources were often lumped into one factor with most of the total mass of the higher alkanes; however, they have very distinct profiles that although colocated, are worth noting individually.

Tailpipe emissions are typified by the prevalence of ethyne as a result of incomplete combustion.¹⁴ The source often further contains many of the C₃-C₆ alkanes that are typically found in gasoline.²⁶ Here, a factor that contains 31% (30-33%) of the noted ethyne along with 45% (43-46%) of the *i*-pentane is determined to be tailpipe emissions. The *i*-pentane to *n*-pentane ratio discussed in the previous chapter can be further used to confirm this source. The factor has an *i*C₅/*n*C₅ ratio over 10 further suggesting a tailpipe emissions source. The tailpipe and gasoline liquids factors combine to contribute less than 10% of the methane and 33% of the ethane seen in the SoCAB. This result is in line with previous studies into the region where methane and ethane emissions are more prominently stemming from natural gas.^{27,28}

As has been seen in other apportionment studies, it is possible to delineate gasoline headspace and vapors from gasoline liquids.^{23,29} The composition of gasoline is often separated out into higher volatility compounds such as pentanes and butanes and the lower volatility compounds including the BTEX (benzene, toluene, ethylbenzene, and xylenes) compounds.¹⁰ These two factors are seen here in this analysis where over 40% of the C₆ and C₇ alkanes are present in the BTEX factor and contribute less than 15% to the liquids factor. The liquids factor contains several straight chain and branched alkanes typically found in gasoline.²⁶ Further, as seen in Table 4.2, the contributions of the factor peak in the warmer summer months when

evaporation is more likely to occur. The BTEX and gasoline liquids factors also show the highest correlation between any two factors ($R^2 = 0.59$) showing that these are sources that have some degree of collocation.

Table 4.2 Averaged normalized contributions of emissions sources as determined via PMF analysis for the full Mt. Wilson data set by season shown with standard deviation

	Oil and Gas Production	Biogenic	Gasoline Liquids	Vehicular Emissions	BTEX	Industry	Pipeline Natural Gas
Summer 2014	0.91 ± 0.81	2.53 ± 1.99	1.05 ± 0.82	1.85 ± 1.48	1.51 ± 0.94	1.11 ± 0.96	0.84 ± 0.57
Fall 2014	0.67 ± 0.85	0.18 ± 0.14	0.93 ± 0.86	0.58 ± 0.69	1.43 ± 0.97	1.73 ± 1.05	0.94 ± 0.87
Winter 2014-2015	1.04 ± 1.10	0.35 ± 0.33	0.82 ± 0.88	0.51 ± 0.60	0.82 ± 0.71	0.77 ± 0.58	1.03 ± 0.74
Spring 2015	0.78 ± 0.76	0.60 ± 0.38	1.23 ± 0.93	0.52 ± 0.49	1.13 ± 0.97	1.09 ± 0.55	0.80 ± 0.55
Summer 2015	1.57 ± 2.25	2.23 ± 1.19	1.54 ± 1.63	1.08 ± 1.15	1.23 ± 1.36	0.52 ± 0.53	1.23 ± 0.79
Fall 2015	0.74 ± 1.03	0.75 ± 0.62	0.68 ± 0.94	1.34 ± 1.29	0.34 ± 0.39	0.77 ± 0.81	1.20 ± 1.42
Winter 2015-2016	1.81 ± 1.37	0.09 ± 0.17	0.68 ± 0.65	1.10 ± 0.91	0.39 ± 0.40	0.97 ± 0.73	1.56 ± 0.94
Spring 2016	0.74 ± 0.85	0.36 ± 0.24	0.72 ± 0.63	0.96 ± 0.86	0.41 ± 0.42	0.77 ± 0.40	0.71 ± 0.69

The BTEX factor cannot be assumed to be completely due to evaporation of processed gasoline. BTEX emissions factors are also suggestive of petrochemical production and refining.⁴ Here, when comparing the oil and gas production source resolved in each season with the 2 year full data set profile, it can be seen that in each season a larger fraction of the BTEX species are associated with the production factor. Some of the BTEX components of the production source may have been separated out into the BTEX source.

4.4.4 Industrial Solvent Use

As discussed in the seasonal analysis, an industrial solvent use factor was resolved in the full two year data set. This factor was resolved with slightly differing profiles in each season. As expected, the factor resolved from the full data set appears as an averaged version of the seasons. It accounts for 74% (71-75%) of the 1,2,4-trimethylbenzene and roughly a third of all of the C₈-C₉ aromatic compounds in the study. This sort of speciation has been reported many times in the literature and is considered an industrial solvent factor.^{8,23} This factor contributes the least total mass to emissions seen in the SoCAB. However, these species have larger rate constants with the hydroxyl radical than the small alkanes discussed thus far, meaning they have greater importance in terms of producing tropospheric ozone and forming secondary organic aerosol.³⁰ It is important, therefore, that this result be taken into account when creating inventories of solvent sources, as not all of the emissions are associated with gasoline. These compounds are used for cleaning, degreasing and other industrial processes as well.²³

4.4.5 Light Alkanes Factor: Oil and Gas Production Source

A fifth factor resolved was made up of predominantly light alkanes C₃-C₅. This factor contained only minimal ethylene (2-4%) and very little in the way of heavier aromatic compounds that are often tied to gasoline and combustion. Further, the factor contained a greater portion of the *n*-pentane (25-34%) than the isopentane (18-24%) typical of an oil and natural gas production source.²⁰ While most natural gas and petroleum is imported to the region, there are still active wells throughout the region which produced 26.8 millions of barrels of oil in 2015,³¹ and leakage from well pads and refining sites has been well documented.^{21,32} This profile is very similar to that found in the EPA's SPECIATE Database for refinery emissions including the presence of minimal ethene.¹⁷ Further, as in the seasonal profiles, the contributions vary

significantly day to day and peak in the summer of 2015 as seen in Table 4.2. The contributions agree well with those from the oil and gas production factor found in the summer analysis (Figure 4.2) further confirming the source of this factor.

The fact that only 3% (0.4-7%) of the methane is associated with oil and gas production is a surprising result when compared to the seasonal analysis where at least 10% was apportioned to refining in each season. As mentioned above, the BTEX factor did not get resolved in any individual season and was split between the gasoline liquids and oil and gas production factors. It is hypothesized that some of the 11% of methane apportioned to the BTEX factor is actually due to oil and gas refining as well, as in Peischl et al.²⁷

4.4.6 Natural Gas Factor

The factor determined to be pipeline natural gas had the largest contribution to both methane and ethane. Further, it contributed only minimally to any heavier species other than propane, and showed minimal fluctuations in its influence over the course of the year as seen in Table 4.2. From the PMF analysis, 59% (57-65%) of the excess methane and 51% (48-56%) of the excess ethane seen in the basin is associated with the emission of pipeline natural gas. This agrees well with the results of the seasonal analysis where over half of the methane was associated with natural gas in each season. It makes sense that there is less variance in the contributions by this factor day to day, as leaks are occurring at a constant rate and are slow to form, such that the emission of natural gas is a relative constant in the region.

The 59% (57-65%) of excess methane associated with natural gas, agrees with the results from the analysis of the trends in E/M ratio ($72 \pm 16\%$) in Chapter 4 as the ranges overlap. The PMF result further agrees with the result presented in Wunch et al.³³ of $58 \pm 13\%$ of excess methane seen in the SoCAB stemming from natural gas leakage. The agreement of these three

analyses from two different data sets is encouraging. First, the results validate the PMF results presented here. At some point, the amount of ethane in natural gas will stop increasing and so the comparison of slopes won't be useful in apportioning methane to natural gas. Therefore, PMF may be able to step in and allow for continued apportionment. Second, in terms of the SoCAB, the field is honing in on an accurate estimate of the leakage of natural gas, which will make for comparisons to bottom-up estimates easier and allow for more detailed analysis.

4.4.7 Bacterial Methane

Like in the seasonal analysis a bulk of the methane is apportioned to pipeline natural gas and oil and gas production sources as has been seen in other apportionment studies.^{27,28,33} The remaining third is spread across three other factors: biogenic, gasoline liquids, and industry. As in the seasonal analysis, the 12% (11-15%) of methane associated with industry is improperly assigned. The only other expected methane source that has not yet been separated out by PMF is methane associated with bacterial breakdown sources. These "biogenic" sources do not have a strong hydrocarbon tracer that can be used to help apportionment. It was anticipated that this methane would be separated out into its own factor, like as happened with isoprene. Despite not correlating at all with methane ($r^2 = 0.0002$), the biogenic isoprene factor in the full two year data set is associated with 4-5% of the excess methane seen in the region. There is evidence that methane is released by trees after being produced by methanogens near tree roots.^{34,35} This small fraction of methane associated with isoprene may be a result of sampling taking place in a forest and truly be biogenic methane. However, it is not possible to determine the fraction of methane associated with bacterial breakdown sources via this combination of data set and technique. It is hypothesized that the 12% (11-15%) of methane associated with industrial solvent use is likely the bacterial breakdown methane and is improperly assigned via the

algorithm. In the future, oxygenated species should be monitored as well, as ethanol has been noted to be a tracer of dairies.³⁶

Comparing some of the PMF results found here to Peischl et al.,²⁷ the last bottom-up inventory available for the SoCAB, suggests a potential shift in emissions from the SoCAB towards being even more dominated by anthropogenic and thermogenic sources. With data from 2010, they estimated that $47 \pm 16\%$ of the excess methane seen in the basin stems from natural gas leakage and $44 \pm 15\%$ from biogenic sources including landfills and dairies.²⁷ Their biogenic factor is larger than the result seen here. Peischl et al.²⁷ suggested that previous estimates calculated from Mt. Wilson underestimate biogenic emissions due to the biased sampling of the western SoCAB. The eastern portions of the SoCAB include the largest biogenic sources to the region including landfills and dairy farms. However, the wind rose plots seen in Chapter 3 show that the most common wind event seen in the San Gabriel Mountains is wind from the southeast. Air parcels reaching Mt. Wilson from the southeast would have passed over the regions two largest landfills: Brea Olinda and Puente Hills. Further this southeastern breeze would pass over the Norco and Chino areas where dairies are found within the SoCAB. Peischl's analysis is based on wind data from Pasadena, CA, at the base of the San Gabriel Mountains from May and June of 2010.²⁷ While in the summer, the winds predominantly come from the west and southwest, in the spring and Fall southeastern winds dominate. Therefore, it is unlikely that the difference between the apportionment results from Mt. Wilson presented here and bottom-up inventories of the region is due to sampling bias. A possible cause of the difference in the biogenic factor is the potential for biogenic emissions to have decreased since 2010. Biogenic methane inventories are often partially based on cattle populations as a mass of methane emitted per head of cattle can be easily determined.³⁷ By 2012, the number of cattle in San Bernardino and Riverside counties had

dropped from 295,000 to 227,000 per the USDA.^{38,39} It is possible that the number of active dairies in the region has continued to decline and decrease the role of biogenic methane to the region. This furthers the importance of this work, as most previous studies of the region were campaign based and lasted for only a few months.

4.4.8 Issues with Ethene and Propene

A strength of PMF is its ability to be used as a preliminary screen to detect for outlier and atypical air masses. This technique has been utilized here and is worth mentioning in more detail. In the results discussed above, the two alkenes, ethene and propene, were often set as weakly correlating or removed from analysis all together. This decision was often made because a resulting factor would be made up of nearly entirely propene and or ethene. These results make very little logical sense, and led to a closer look at the profiles. The ethene and propene profiles were based on a very high normalized contribution from a few samples. Indeed, for ethene, there are three samples in which the mixing ratio is more than eight standard deviations above the mean. The mixing ratios of selected hydrocarbons for these three samples are shown in Table 4.3. Interestingly, the other species in these samples do not show unusually strong enhancements. In only one of the three high ethene samples is there a large propene mixing ratio as well. Per the SPECIATE database and other characterization literature, ethene and propene are widely used as tracers for petrochemical production including the production of plastics.^{4,17} California is not a major player in plastics production accounting for only 2% of total plastics shipments in 2012.⁴⁰ However, the emissions profiles suggested by the literature fit for these few samples. Ethene and propene are greatly enhanced but not other hydrocarbon species. From the PMF analysis, this profile does not fit any other samples, and thus gives rise to the factor with a profile defined by four samples.

Table 4.3 Samples influenced by petrochemical production in the SoCAB and the mixing ratios of select hydrocarbons in the samples

Sample Date and Time	Ethane (pptv)	Ethene (pptv)	Propane (pptv)	Propene (pptv)	<i>i</i> -butane (pptv)	<i>n</i> -butane (pptv)	<i>i</i> -pentane (pptv)	<i>n</i> -pentane (pptv)	Benzene (pptv)
5:00 PM 8/27/2014	4035	4085	2806	3432	432	850	309	358	156
5:00 PM 8/22/2014	2474	8096	2051	729	323	637	385	411	211
5:00 PM 6/20/2014	2936	5534	1382	336	270	475	549	222	193
2 year average and standard deviation	3110 ± 1550	489 ± 542	1440 ± 1006	124 ± 197	247 ± 190	501 ± 416	297 ± 229	179 ± 140	134 ± 60

Ethene is also a product of incomplete combustion and can be useful in determining a vehicular emission source, so it was decided to down weight ethene when possible, so as to still have it to help in apportionment.⁴ The goal of this analysis was to determine the major emissions sources in the region, and so having a very transient factor was counterproductive. However, the very occasional emission from a local petrochemical facility is noted going forward. This is not a source of emissions discussed in the literature for the SoCAB but has been seen readily in the Houston, Texas region.⁴

4.5 Discussion of PMF Utility in the SoCAB

The source profiles determined via PMF analysis for the SoCAB are in line with the results of other recent studies in the region. Peischl et al.²⁷ used seven factors to try and apportion light alkane emissions via linear analysis. These sources are nearly identical to the ones found above: pipeline natural gas, biogenic, local natural gas, liquefied petroleum gas (LPG), evaporated gasoline, vehicular sources and other. Their analysis only went to the C₅ alkanes and as such they did not resolve a BTEX or industry factor for these heavier hydrocarbons. The choice to separate LPG out as its own leakage source apart from the oil and gas industry does differ with what was found here. In no analysis was propane ever pulled out as its own factor. This inability to separate LPG makes sense as LPG production occurs at the same location as gasoline refining.⁴¹ Peischl and colleagues estimate that one third of all propane emissions come from the use of LPG with half still coming from wetter oil and gas production sources.²⁷ The result here differs with that analysis due to the lack of an LPG source. 25% (21-29%) of propane emissions stem from oil and gas production via PMF analysis and 34% (31-38%) stem from gasoline liquids. It is likely that the LPG source identified in Peischl et al.²⁷ is contained in this gasoline liquids source as LPG is used as a vehicular fuel source and would have the same patterns of use as gasoline vehicles. PMF derived source profiles for other large cities agree with those found here and vary in the fraction of emissions stemming from vehicular sources depending on the reliance on individual cars in the region.^{4,12,42}

Positive Matrix Factorization is a newer technique in comparison to CMB and is a burgeoning method of analysis for gaseous species in a mixed environment. As a young method, there is some pushback against its use in the literature. It has been argued that results from PMF are meaningless as rotational analysis results in different factor profiles.⁴³ Rotational analysis on

the PMF results presented here did not show such variability. This rotational ambiguity is a factor that should be studied when analyzing PMF results, but this issue does not apply to every data set that could be analyzed.

Here, the utility of PMF for apportionment of gaseous VOCs and methane in particular was studied. Using the Mt. Wilson data set, solutions were found that in comparison to other apportionment methods are plausible and make sense. The strengths of PMF include removing the need for preexisting source profiles, relatively short calculation time, and easy to use software. It can be recommended for use with any urban atmosphere data set with the caveat that it should not be used alone. It should be used in parallel with other apportionment techniques such as CMB, tracer species, isotope analysis or historical analysis. PMF necessitates that the analyst understand the science of emissions and atmospheric chemistry. It would be very easy for an analyst to blindly follow the resulting factors outputted by the program without stopping to question if these profiles really exist. Further, PMF requires a fairly large data set to be useful. This drawback is seen here with the large errors associated with certain factors in the seasonal analysis. Having this many data points requires a great deal of time and laboratory analysis and may not fit every desire for apportionment. As discussed above, even if the data set is sufficiently large, outlier points can have a strong effect on the result and caution must be used when considering such results. It was also noted that PMF struggled with separating out biogenic methane emissions from every other factor. PMF is a useful tool to confirm other apportionment techniques or as a primary exploration tool into an air mass that is new to the literature. It is recommended by the author as a valuable addition to apportionment problems with an understanding of its limitations and drawbacks.

4.6 References

- (1) Paatero, P.; Tapper, U. Positive matrix factorization: A non-negative factor model with optimal utilization of error estimates of data values. *Environmetrics* **1994**, *5* (2), 111–126.
- (2) Brown, S. G.; Eberly, S.; Paatero, P.; Norris, G. A. Methods for estimating uncertainty in PMF solutions: Examples with ambient air and water quality data and guidance on reporting PMF results. *Sci. Total Environ.* **2015**, *518–519*, 626–635.
- (3) Yuan, B.; Shao, M.; de Gouw, J.; Parrish, D. D.; Lu, S.; Wang, M.; Zeng, L.; Zhang, Q.; Song, Y.; Zhang, J.; et al. Volatile organic compounds (VOCs) in urban air: How chemistry affects the interpretation of positive matrix factorization (PMF) analysis. *J. Geophys. Res. Atmospheres* **2012**, *117* (D24), D24302.
- (4) Buzcu, B.; Fraser, M. P. Source identification and apportionment of volatile organic compounds in Houston, TX. *Atmos. Environ.* **2006**, *40* (13), 2385–2400.
- (5) Fujita, E. M.; Watson, J. G.; Chow, J. C.; Magliano, K. L. Receptor model and emissions inventory source apportionments of nonmethane organic gases in California's San Joaquin valley and San Francisco bay area. *Atmos. Environ.* **1995**, *29* (21), 3019–3035.
- (6) Fujita, E. M.; lu, Z.; Sagebiel, J. C.; Robinson, N. F.; Watson, J. *VOC source apportionment for the Coastal Oxidant Assessment for Southeast Texas*; 1995.
- (7) Scheff, P. A.; Wadden, R. A. Receptor modeling of volatile organic compounds. 1. Emission inventory and validation. *Environ. Sci. Technol.* **1993**, *27* (4), 617–625.
- (8) Watson, J. G.; Chow, J. C.; Fujita, E. M. Review of volatile organic compound source apportionment by chemical mass balance. *Atmos. Environ.* **2001**, *35* (9), 1567–1584.
- (9) Anair, D.; Mahmassani, A. *State of Charge: Electric Vehicles' Global Warming Emissions and Fuel-Cost Savings across the United States*; Union of Concerned Scientists, 2012.
- (10) Gentner, D. R.; Harley, R. A.; Miller, A. M.; Goldstein, A. H. Diurnal and Seasonal Variability of Gasoline-Related Volatile Organic Compound Emissions in Riverside, California. *Environ. Sci. Technol.* **2009**, *43* (12), 4247–4252.
- (11) Pang, Y.; Fuentes, M.; Rieger, P. Trends in the emissions of Volatile Organic Compounds (VOCs) from light-duty gasoline vehicles tested on chassis dynamometers in Southern California. *Atmos. Environ.* **2014**, *83*, 127–135.
- (12) Song, Y.; Shao, M.; Liu, Y.; Lu, S.; Kuster, W.; Goldan, P.; Xie, S. Source Apportionment of Ambient Volatile Organic Compounds in Beijing. *Environ. Sci. Technol.* **2007**, *41* (12), 4348–4353.
- (13) Townsend-Small, A.; Marrero, J. E.; Lyon, D. R.; Simpson, I. J.; Meinardi, S.; Blake, D. R. Integrating Source Apportionment Tracers into a Bottom-up Inventory of Methane Emissions in the Barnett Shale Hydraulic Fracturing Region. *Environ. Sci. Technol.* **2015**, *49* (13), 8175–8182.
- (14) Huang, Y.; Ling, Z. H.; Lee, S. C.; Ho, S. S. H.; Cao, J. J.; Blake, D. R.; Cheng, Y.; Lai, S. C.; Ho, K. F.; Gao, Y.; et al. Characterization of volatile organic compounds at a roadside environment in Hong Kong: An investigation of influences after air pollution control strategies. *Atmos. Environ.* **2015**, *122*, 809–818.
- (15) Bari, M. A.; Kindzierski, W. B.; Wheeler, A. J.; Héroux, M.-È.; Wallace, L. A. Source apportionment of indoor and outdoor volatile organic compounds at homes in Edmonton, Canada. *Build. Environ.* **2015**, *90*, 114–124.

- (16) Norris, Gary A.; Duvall, R.; Brown, S. EPA Positive Matrix Factorization (PMF) 5.0 Fundamentals and User Guide. U.S. Environmental Protection Agency 2014.
- (17) Hsu, Y.; Divita, F.; Dorn, J. *SPECIATE Version 4.5 Database Development Documentation*; Environmental Protection Agency, 2016.
- (18) Phillips, N. G.; Ackley, R.; Crosson, E. R.; Down, A.; Hutyra, L. R.; Brondfield, M.; Karr, J. D.; Zhao, K.; Jackson, R. B. Mapping urban pipeline leaks: Methane leaks across Boston. *Environ. Pollut.* **2013**, *173*, 1–4.
- (19) Pétron, G.; Frost, G.; Miller, B. R.; Hirsch, A. I.; Montzka, S. A.; Karion, A.; Trainer, M.; Sweeney, C.; Andrews, A. E.; Miller, L.; et al. Hydrocarbon emissions characterization in the Colorado Front Range: A pilot study. *J. Geophys. Res. Atmospheres* **2012**, *117* (D4), D04304.
- (20) Gilman, J. B.; Lerner, B. M.; Kuster, W. C.; de Gouw, J. A. Source Signature of Volatile Organic Compounds from Oil and Natural Gas Operations in Northeastern Colorado. *Environ. Sci. Technol.* **2013**, *47* (3), 1297–1305.
- (21) Marrero, J. E.; Townsend-Small, A.; Lyon, D. R.; Tsai, T. R.; Meinardi, S.; Blake, D. R. Estimating Emissions of Toxic Hydrocarbons from Natural Gas Production Sites in the Barnett Shale Region of Northern Texas. *Environ. Sci. Technol.* **2016**.
- (22) Pétron, G.; Karion, A.; Sweeney, C.; Miller, B. R.; Montzka, S. A.; Frost, G. J.; Trainer, M.; Tans, P.; Andrews, A.; Kofler, J.; et al. A new look at methane and nonmethane hydrocarbon emissions from oil and natural gas operations in the Colorado Denver-Julesburg Basin: Hydrocarbon emissions in oil & gas basin. *J. Geophys. Res. Atmospheres* **2014**, *119* (11), 6836–6852.
- (23) Brown, S. G.; Frankel, A.; Hafner, H. R. Source apportionment of VOCs in the Los Angeles area using positive matrix factorization. *Atmos. Environ.* **2007**, *41* (2), 227–237.
- (24) Kesselmeier, J.; Staudt, M. Biogenic Volatile Organic Compounds (VOC): An Overview on Emission, Physiology and Ecology. *J. Atmospheric Chem.* **1999**, *33* (1), 23–88.
- (25) Jobson, B. T.; Wu, Z.; Niki, H.; Barrie, L. A. Seasonal trends of isoprene, C2–C5 alkanes, and acetylene at a remote boreal site in Canada. *J. Geophys. Res. Atmospheres* **1994**, *99* (D1), 1589–1599.
- (26) Pang, Y.; Fuentes, M.; Rieger, P. Trends in selected ambient volatile organic compound (VOC) concentrations and a comparison to mobile source emission trends in California’s South Coast Air Basin. *Atmos. Environ.* **2015**, *122*, 686–695.
- (27) Peischl, J.; Ryerson, T. B.; Brioude, J.; Aikin, K. C.; Andrews, A. E.; Atlas, E.; Blake, D.; Daube, B. C.; de Gouw, J. A.; Dlugokencky, E.; et al. Quantifying sources of methane using light alkanes in the Los Angeles basin, California: Sources of Methane in L.A.. *J. Geophys. Res. Atmospheres* **2013**, *118* (10), 4974–4990.
- (28) Wennberg, P. O.; Mui, W.; Wunch, D.; Kort, E. A.; Blake, D. R.; Atlas, E. L.; Santoni, G. W.; Wofsy, S. C.; Diskin, G. S.; Jeong, S.; et al. On the Sources of Methane to the Los Angeles Atmosphere. *Environ. Sci. Technol.* **2012**, *46* (17), 9282–9289.
- (29) Mugica, V.; Watson, J.; Vega, E.; Reyes, E.; Ruiz, M. E.; Chow, J. Receptor Model Source Apportionment of Nonmethane Hydrocarbons in Mexico City. *Sci. World J.* **2002**, *2*, 844–860.
- (30) Finlayson-Pitts, B.; Pitts, J. *Chemistry of the Upper and Lower Atmosphere*; Academic Press, 2000.
- (31) Harris Jr., K. 2015 Report of California oil and gas production statistics. Division of Oil Gas and Geothermal Resources April 2016.

- (32) Swarthout, R. F.; Russo, R. S.; Zhou, Y.; Miller, B. M.; Mitchell, B.; Horsman, E.; Lipsky, E.; McCabe, D. C.; Baum, E.; Sive, B. C. Impact of Marcellus Shale Natural Gas Development in Southwest Pennsylvania on Volatile Organic Compound Emissions and Regional Air Quality. *Environ. Sci. Technol.* **2015**, *49* (5), 3175–3184.
- (33) Wunch, D.; Toon, G. C.; Hedelius, J.; Vizenor, N.; Roehl, C. M.; Saad, K. M.; Blavier, J.-F. L.; Blake, D. R.; Wennberg, P. O. Quantifying the Loss of Processed Natural Gas Within California’s South Coast Air Basin Using Long-term Measurements of Ethane and Methane. *Atmospheric Chem. Phys. Discuss.* **2016**, 1–20.
- (34) Rice, A. L.; Butenhoff, C. L.; Shearer, M. J.; Teama, D.; Rosenstiel, T. N.; Khalil, M. A. K. Emissions of anaerobically produced methane by trees. *Geophys. Res. Lett.* **2010**, *37* (3), L03807.
- (35) Keppler, F.; Hamilton, J. T. G.; Braß, M.; Röckmann, T. Methane emissions from terrestrial plants under aerobic conditions. *Nature* **2006**, *439* (7073), 187.
- (36) Allen, D. T. Methane emissions from natural gas production and use: reconciling bottom-up and top-down measurements. *Curr. Opin. Chem. Eng.* **2014**, *5*, 78–83.
- (37) Garnsworthy, P. C.; Craigon, J.; Hernandez-Medrano, J. H.; Saunders, N. On-farm methane measurements during milking correlate with total methane production by individual dairy cows. *J. Dairy Sci.* **2012**, *95* (6), 3166–3180.
- (38) U.S. Department of Agriculture. *Ag Census 2012 San Bernardino County Report*; 2012.
- (39) U.S. Department of Agriculture. *Ag Census 2012 Riverside County Report*; 2012.
- (40) American Chemistry Council. *Plastic Resins in the United States*; 2013.
- (41) Liang, B.; Balasubramanian, S.; Wang, B.; Yang, A.; Kennedy, D.; Le, V.; Legaspi, J.; Southern, J. LPG characterization and production quantification for oil and gas reservoirs. *J. Nat. Gas Sci. Eng.* **2010**, *2* (5), 244–252.
- (42) Baudic, A.; Gros, V.; Sauvage, S.; Locoge, N.; Sanchez, O.; Sarda-Estève, R.; Kalogridis, C.; Petit, J.-E.; Bonnaire, N.; Baisnée, D.; et al. Seasonal variability and source apportionment of volatile organic compounds (VOCs) in the Paris megacity (France). *Atmos Chem Phys* **2016**, *16* (18), 11961–11989.
- (43) Bon, D. M.; Ulbrich, I. M.; de Gouw, J. A.; Warneke, C.; Kuster, W. C.; Alexander, M. L.; Baker, A.; Beyersdorf, A. J.; Blake, D.; Fall, R.; et al. Measurements of volatile organic compounds at a suburban ground site (T1) in Mexico City during the MILAGRO 2006 campaign: measurement comparison, emission ratios, and source attribution. *Atmos Chem Phys* **2011**, *11* (6), 2399–2421.

CHAPTER 5: Further Natural Gas Analysis

5.1 Natural Gas Composition Testing

5.1.1 Collection and Gas Chromatography Analysis

As discussed in Chapter 3, the leakage of natural gas is important to the total GHG budget of the SoCAB, and the industrialized world. To that end, an important piece of information to have is the composition of natural gas especially within the SoCAB. It has been noted that the composition of natural gas can vary from region to region based on the shale it was mined from.¹ Depending on how “wet” the shale is, the percentage of ethane, propane, and even higher alkanes in natural gas can vary. While several studies have looked into characterizing emissions from shale regions where mining and refining occur, very little literature exists on the composition of gas that reaches the consumer’s home or office.¹⁻³ To better understand the composition of pipeline natural gas and how it contributes to total methane emissions, especially in the SoCAB region which is not an active shale, it was deemed necessary to collect and analyze natural gas samples.

Starting in November 2014 and running through August 2015, a sample of pipeline natural gas was collected each month during the Mt. Wilson sampling week in a laboratory on the California Institute of Technology campus in Pasadena, CA. In September and October of 2015, samples were collected in a laboratory on the University of California, Irvine campus. Teflon tubing was connected to the natural gas outlet inside a fume hood. The gas valve was then opened and allowed to flow through the tubing for several seconds to purge any air in the line. The tubing was then connected to the port on a canister and the valve was opened to collect the sample. Due to the nature of these samples, it was necessary to dilute them before gas chromatography analysis. The sampling canister was connected to the CO/CO₂ manifold as

described in Chapter 2. The valves to the two loops were closed and the canister was opened. A small volume of gas flowed into the manifold. The gas sample canister was removed from the manifold and an evacuated canister was added in its place. The evacuated canister was opened to the manifold and the natural gas flowed into the canister. Excess natural gas was pumped off such that the resulting gas pressure in the canister was 2 torr. Nitrogen gas was added to the system. The final pressure in the canister was 1000 torr creating a 1:500 natural gas dilution. The diluted samples were analyzed on the NMHC system described in Chapter 2. Because of the high concentration of hydrocarbons, no preconcentration was necessary. One half torr of pressure from the diluted sample was added the manifold shown in Figure 2.4. The sample was injected into the system as described previously. The manifold was helium flushed and a sample of clean air collected at Crooked Creek Research Station was injected after each gas sample to further allow for the purge of concentrated gas. The DB-1 column chromatogram was used for the compositional analysis. A sample chromatogram with hydrocarbon peaks labelled is shown in Figure 5.1. To determine the composition of the sampled gas, the peak areas for each straight chain alkane were calculated. The areas were then divided by the number of carbons in the molecule and then percentages relative to methane were calculated.

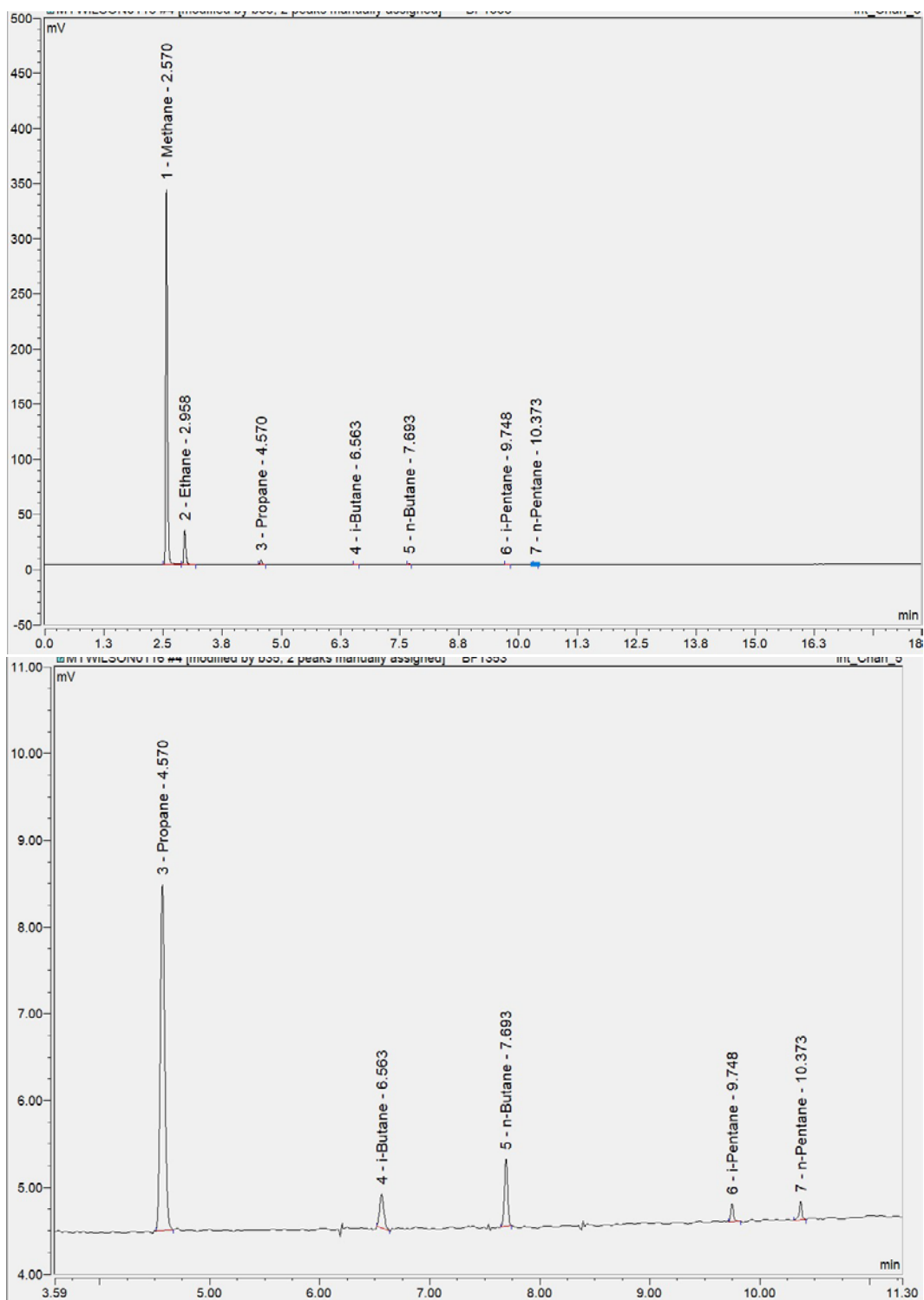


Figure 5.1 Top: Chromatogram of a natural gas sample run on the Db-1 column of the NMHC system described in Chapter 2. Bottom: A portion of the above chromatogram zoomed in 50x. All retention times are in minutes.

5.1.2 Results

The composition of the 15 natural gas samples collected is shown for species up to the butanes in Table 5.1. The ethane percentage results were first reported in Wunch et al.⁴ Species larger than the butanes were not included as they were not seen in every sample and are considered trace. The average E/M found in SoCAB natural gas samples was $3.73 \pm 0.21\%$ with the ratio in individual samples ranging from 2.26% to 5.04%. Propane averaged $0.312 \pm 0.027\%$ of the total composition and the butanes accounted for less than a tenth of a percent. It is very clear that there is significant variation in the composition of natural gas delivered to the SoCAB. Over the 12 months of sampling, the lowest ethane to methane ratio seen was in April of 2015 ($2.37 \pm 0.03\%$) and the highest ($5.17 \pm 0.03\%$) seen in late July. No temporal trends can be gleaned from this data set, as the variation in the amount of ethane changed over a full percentage in the course of a month. After analyzing the first several samples and seeing the variation, it was decided to test the natural gas twice a month to see how quickly the composition could change. Between July 1 and July 16, 2015 the amount of ethane in the delivered gas changed from $3.53 \pm 0.03\%$ to 4.98 ± 0.05 . This variance was not expected and suggests that natural gas composition changes daily. A search of the literature shows that this topic has not been discussed before.

Table 5.1. Composition of natural gas collected once a month in canisters from the SoCAB.

Date	Ethane (%)	Propane (%)	Butanes (%)	Isobutane/n-butane
11/17/2014	3.15 ± 0.03	0.236 ± 0.007	0.059 ± 0.001	0.768 ± 0.038
12/19/2014	3.99 ± 0.04	0.221 ± 0.007	0.047 ± 0.001	0.809 ± 0.040
1/21/2015	3.48 ± 0.04	0.356 ± 0.011	0.105 ± 0.002	0.739 ± 0.037
2/25/2015	3.41 ± 0.03	0.301 ± 0.009	0.080 ± 0.001	0.740 ± 0.037
3/20/2015	4.81 ± 0.05	0.505 ± 0.015	0.114 ± 0.002	0.677 ± 0.034
4/17/2015	2.26 ± 0.02	0.206 ± 0.006	0.086 ± 0.001	0.474 ± 0.024
5/12/2015	2.93 ± 0.03	0.195 ± 0.006	0.072 ± 0.001	0.386 ± 0.019
5/29/2015	2.91 ± 0.03	0.162 ± 0.005	0.031 ± 0.001	1.021 ± 0.051
6/15/2015	4.22 ± 0.04	0.371 ± 0.011	0.082 ± 0.002	0.767 ± 0.038
7/1/2015	3.53 ± 0.03	0.304 ± 0.009	0.056 ± 0.001	0.958 ± 0.048
7/16/2015	4.98 ± 0.05	0.441 ± 0.013	0.080 ± 0.001	0.740 ± 0.037
8/5/2015	5.04 ± 0.05	0.473 ± 0.014	0.128 ± 0.002	0.287 ± 0.014
8/25/2015	4.14 ± 0.04	0.360 ± 0.011	0.090 ± 0.001	0.332 ± 0.017
9/23/2015	3.65 ± 0.04	0.276 ± 0.008	0.045 ± 0.001	0.570 ± 0.029
10/26/2015	3.50 ± 0.04	0.269 ± 0.008	0.045 ± 0.001	0.811 ± 0.041
Average	3.73 ± 0.21	0.312 ± 0.027	0.075 ± 0.007	0.672 ± 0.056

5.1.3 Discussion

The natural gas composition results presented here can be compared to previous measurements to better understand whether the variation should have been expected or not. Due to the variations in natural gas composition regionally, the only comparisons that can be made are within the SoCAB. Wunch et al.⁴ includes the E/M seen in these samples along with previous

sampling conducted at the California Institute of Technology. The work shows that during a particular sampling intensive in 2013, there is greater than 1% change in the E/M over the course of just a few weeks. This agrees with the results here which show a substantial variation in composition between samples. They also show a general increasing trend in the amount of ethane in natural gas between 2013 and the end of 2015. This change is due to ethane rejection within the oil and gas industry.⁴ Due to the boom in production in shale gas, the market became flooded with ethane which is commonly removed from natural gas to use in petrochemical production.⁵ The process of separating out ethane became economically unfavorable, and so ethane was left in natural gas and sold to gas companies instead. This created the steady rise in ethane in natural gas seen by Wunch et al.⁴ During the year of natural gas sampling shown here, it appears that the ethane concentration in natural gas has levelled off. The petrochemical industry projects that demand for ethane will rise over the next several years as more plants begin production of chemicals.⁶ This demand will almost certainly lead to less ethane rejection and a decreasing trend of the amount of ethane left in natural gas.

It is also worth noting that ethane rejection tends to correlate with an increased concentration of larger alkanes in natural gas as well. As seen in Figure 5.2, there is a strong correlation between the percentage of propane in the collected natural gas samples and the percentage of ethane ($m = 0.11$ $r^2 = 0.77$). This result does make sense as if it is not economically favorable to natural gas producers to remove ethane, it is doubtful that it would be worthwhile to remove the propane. Ethane rejection in natural gas matters not only for the ability to track and estimate methane emissions more easily, but it also contributes in its own right to tropospheric ozone formation. In a polluted urban region, reaction of a hydrocarbon with the hydroxyl radical can be the start of a chain of reactions that eventually lead to ozone formation.⁷ While ethane is

not highly reactive in the atmosphere when compared to alkenes and aromatic compounds, it has a rate constant 38 times larger than that of methane with the hydroxyl radical.⁸ Further, assuming complete hydrocarbon break down to carbon dioxide, ethane can produce 1.75 as much ozone on a molecular basis then can methane.⁹ Currently, the composition of natural gas is around 4% ethane compared to the 2% seen in 2012. By doubling the concentration of ethane in natural gas and not making any repairs to try and limit pipeline losses, the natural gas industry is responsible for three and a half times more ozone forming potential than before ethane rejection began.

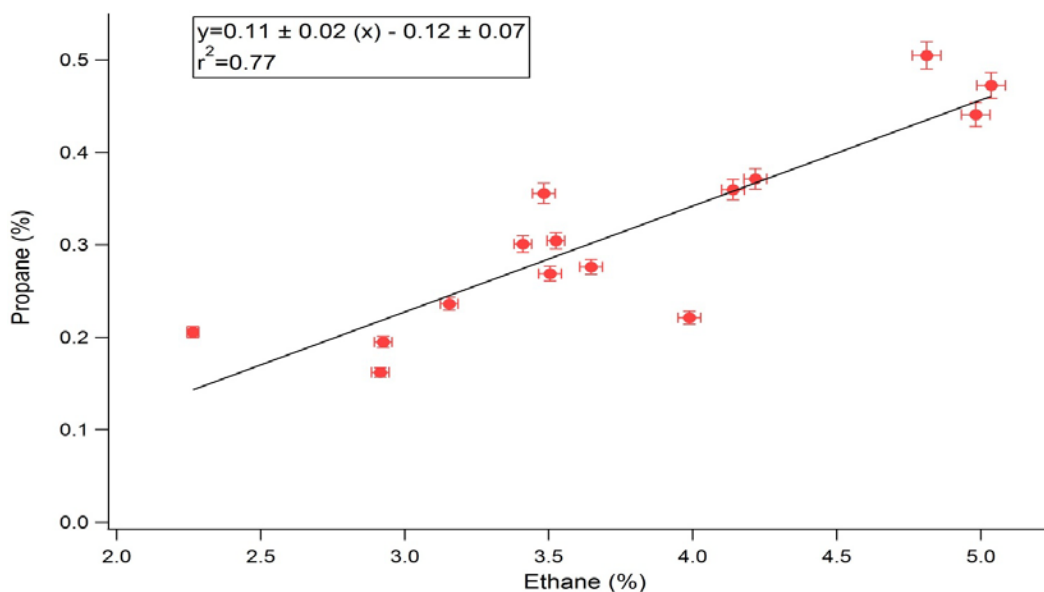


Figure 5.2 Correlation between the percentage of propane and ethane in natural gas samples collected in the SoCAB.

Only two other data sets were found which report the natural gas composition in the region. Both of these were reported, in some manner, by the Southern California Gas Company (SoCalGas), the supplier of natural gas to all of the SoCAB. First, Wennberg et al.¹⁰ report E/M values for three discrete sampling periods between 2007 and 2010. These values were given to

the authors by a contact at SoCalGas. They have no knowledge of where these samples were taken in the greater Los Angeles area nor how many samples make up the average for a given sampling site. The most recent data included was from April-June 2010 and the average E/M was 1.65 ± 0.25 .¹⁰ Between 2007 and 2010, the E/M varied less than 0.4% and the greatest variation between two different pipelines is 0.83%. Comparing the composition values in Wennberg et al.¹⁰ with the more recent data presented here, it is clear that there is more ethane in natural gas supplied to the region than previously. It is noted elsewhere that the ethane rejection and increase in ethane in SoCAB natural gas did not begin until 2012.⁴ This 2010 value can be viewed as a minimum ethane concentration and may be composition that is reached in the near future if the industry projections for ethane demand are correct.

The second data set was reported directly by SoCalGas. They have released the composition of natural gas that is being withdrawn from their storage facility in Playa del Rey, California, represented by the blue circle just south of Santa Monica in Figure 1.6.¹¹ Their reports show compositional data for each month dating back to 2012. Their reported data from the Playa del Rey well are shown in Figure 5.3 along with the samples collected here at CalTech. There is a distinct lack of correlation between these two data sets ($r^2 = 0.092$). The collected gas samples show much more substantial variation month to month than do the Playa del Rey samples. Both do show that over the year period of sampling, there was a continued increase in the percent of ethane in natural gas. Further, averaging the E/M seen in the Playa del Rey samples over the year of sampling yields a value of $3.83 \pm 0.2\%$. While there might be a lack of correlation month to month, the collected samples do agree with the reported values from SoCalGas over a year's time. The latest data available from SoCalGas from March 2017

show that a local maximum in E/M has been reached in August 2016, and might be starting to decrease.¹¹

There are a few potential reasons for the discrepancy between the samples taken at CalTech and the SoCalGas reports. Most likely, the SoCalGas reports show a monthly average of what was being withdrawn from the well. Since both data sets do show the trend of increasing ethane over time, it is highly possible that the SoCalGas data are the result of many repeated measurements. It is also possible that the Playa del Rey well does not service all of the SoCAB. The Playa del Rey well is 20 miles from the CalTech campus, and it is possible that the campus is served by a different pipeline. Indeed, day to day, SoCalGas withdraws gas from wells and uses varied pipelines to meet demand.¹² For the rest of this chapter, the Playa del Rey data set will be used to further analyze natural gas emissions.

As mentioned in Chapter 3, the variability in the composition of natural gas has a definite impact in the creation of bottom-up inventories. In the thermodynamics and energy production fields, this variation in natural gas composition is not concerning as the change in the heating capability is negligible (less than 3% difference in Btus between wettest and driest Playa del Rey samples).^{11,13} However, from an environmental engineering and climate science view, this is a very significant result. The variation in composition is surprising given past literature attempting bottom-up inventories. Previously, it had been assumed that the composition of natural gas did not vary much at all. Indeed both Wennberg et al.¹⁰ and Peischl et al.¹⁴ use a constant ethane to methane ratio in their bottom up inventories. While changing the gas composition even monthly would be difficult for these bottom-up inventories, based off the data presented here, it is important to note going forward, what the natural gas composition used in any bottom-up inventory is and acknowledge the fluctuation as a source of error.

5.2 Quantifying Natural Gas Emissions in the SoCAB

As was shown in Chapter 3, the ethane to methane ratio in SoCAB influenced air masses has increased since the previous Mt. Wilson campaign in 2007. Indeed as seen in Figure 3.6, there appears to be an increasing trend within the two years of sampling during the most recent campaign. With the knowledge that there has been an increase in the ethane in natural gas, the two noted trends can be combined to determine to what extent natural gas leakage contributes to total methane emissions.^{4,11} First, monthly average E/M ratios for each month during the 2014-2016 sampling campaign were calculated with the exception of April 2016, when the unexpected power outage only allowed for the collection of six samples.

Because the noted ethane rejection began in 2012, and the Mt. Wilson data set began in 2014 other potential data sets were considered for inclusion to fully understand basin wide E/M. Airborne whole air samples were collected in June of 2012 and 2013 aboard the NASA DC-8 aircraft above the Los Angeles area.¹⁵ The data set from this project was trimmed to include samples taken within the SoCAB boundary layer (below 1000 m AGL) yielding 38 samples in 2012 and 64 in 2013. Enhancement values from both of these data sets were calculated as above and then averaged to give one data point per year. No other SoCAB data sets were available to continue to fill in the years 2012 and 2013.

To conduct the analysis, the 2014-2016 E/M monthly averages were plotted as a function of time along with the airborne flight data dating back to 2012. SoCalGas reported natural gas composition from the Playa del Rey Storage Facility was plotted over the same time period (Figure 5.4). The slope of the fitted linear regression shows that the E/M seen in the SoCAB between June of 2012 and May 2016 was increasing at a rate of $0.41 \pm 0.09\%$ per year ($r^2=0.48$). The E/M in natural gas show that the percentage of ethane was increasing by $0.58 \pm 0.04\%$ per

year ($r^2=0.87$). As noted in Chapter 3, methane emissions in the SoCAB remained relatively constant over the course of the 2014-2016 Mt. Wilson campaign. Further, data presented in Wunch et al.⁴ shows that total methane emissions in the SoCAB have remained relatively constant since 2007. The fact that methane enhancement values have not increased makes it more likely that the increase in the E/M in the SoCAB is directly related to the increase in E/M in pipeline natural gas. As a further check, the SoCAB monthly average E/M and the Playa del Rey natural gas E/M have a slight positive correlation ($r^2=0.36$). Therefore, as in Wunch et al.⁴ the ratio of the two slopes over time can be taken to be the fraction of methane coming from natural gas leakage in the basin. Via this analysis, $72 \pm 16\%$ of all excess methane seen in the basin can be attributed to leakage of pipeline natural gas over the period between June 2012 and May 2016. Wunch et al.⁴ reported $58\% \pm 13\%$ of all excess methane coming from natural gas over the similar period of spring 2012 through the end of 2015. These two ranges do overlap suggesting good agreement. The confidence interval is larger for our result due to a smaller data set with more scatter. This result overlaps with the results from the full two year PMF analysis reported in the previous chapter of 59% (57-65%) between 2014 and 2016. Each seasonal analysis resolved a pipeline natural gas factor that accounted for between one half and two thirds of all the methane emitted in the SoCAB. It is exciting to have two different apportionment techniques agree with each other and with the previous work in Wunch et al.⁴

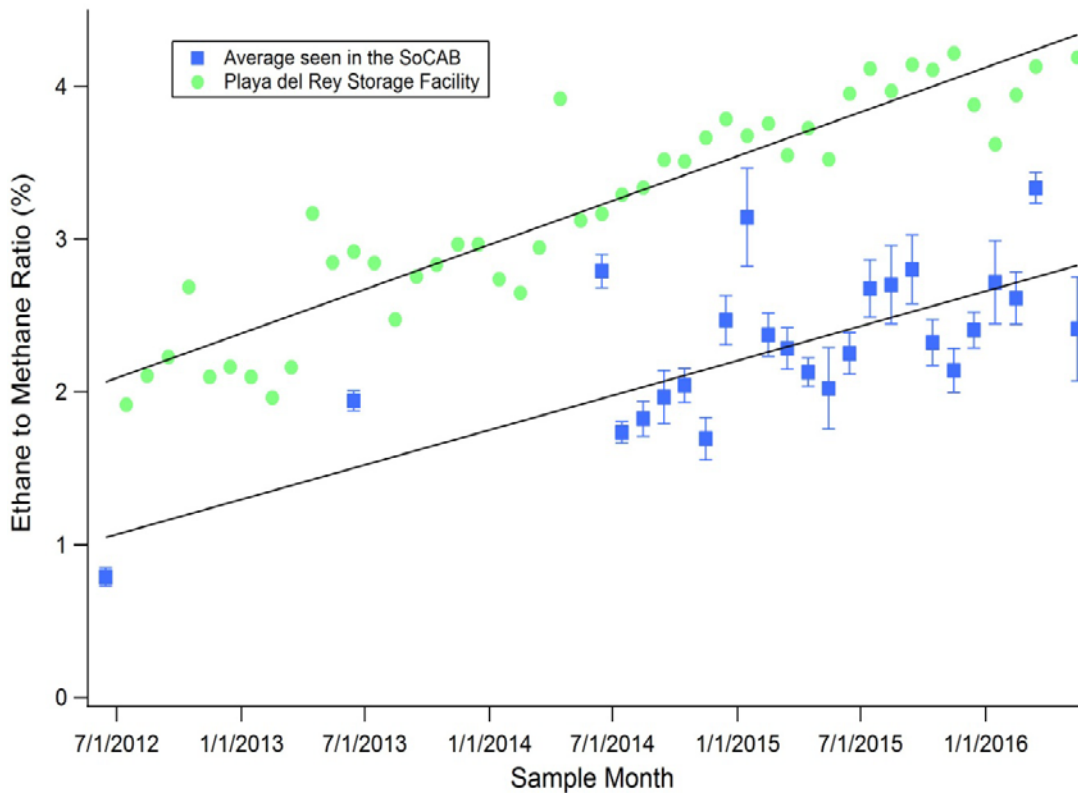


Figure 5.4. Trends seen in ethane to methane ratios in the South Coast Air Basin and in natural gas supplied to the region.

Comparing these results to bottom-up estimates, however, yields a different outlook on the question of apportionment of methane emissions. As discussed in the introduction, bottom-up inventories of the SoCAB over the past decade have been unable to sum to total emissions seen in top-down studies.¹⁰ Further, within the confines of their inventories the apportionment of methane is different than the results presented herein. Wennberg et al.¹⁰ built an inventory based on reported values and estimates of different sectors. While only able to account for less than half of the total methane emitted in the SoCAB in 2008, only 10% of that was assigned to pipeline natural gas. This fraction is based on a reported total of gas lost by SoCalGas from a personal contact at the company who reported a loss of 22 Gg of methane each year which is 0.1% of their total deliveries. A Leakage Abatement Report that was released by SoCalGas in 2014 reports an estimated loss of 0.13% of deliveries of pipeline natural gas as either fugitive or

planned emissions (1593.57 million cubic feet).¹⁶ If industry standard operating conditions are followed and a molar mass of 17 g/mol for natural gas, SoCalGas emitted 32 Gg of natural gas into the SoCAB in 2014. SoCalGas is therefore reporting that they lost roughly 10 Gg more natural gas in 2014 than they did in 2008 with only a small increase in reported losses as the fraction of total deliveries. If SoCalGas reports are to be believed then there must be an unaccounted for source of natural gas in the SoCAB.

5.3 Natural Gas Leakage Studies

5.3.1 UCI Indoor Sampling Study

5.3.1.1 Background

One possible unaccounted for source of natural gas is leakage from the customer side of the meter. As first hypothesized in Wennberg et al.¹⁰, it is possible that there is widespread loss of natural gas between the meter outside each home or business and when it is ultimately burned for heat or fuel in hot water heaters, stoves or turbines. The potential for this leakage is significant as it would not be leakage that SoCalGas would account for in their own reporting as they delivered the gas. What happens to the gas beyond that is no longer an issue for them. Wennberg et al.¹⁰ go on to argue that in an average house there are over 100 pipe fittings which could be sources of leaks. Further, given the age of much of the housing in the SoCAB, older appliances and steel pipes have a higher likelihood of leakage. The low pressure flow of gas into individual homes would make it such that a small leak would be well below the olfactory limit of detection of the odorant placed into natural gas. If this sort of leakage was happening broadly over the SoCAB, it would have the potential to substantially close the gap between bottom-up and top-down studies. Given the importance of natural gas emissions seen in the Mt. Wilson studies and the clear natural gas factor in each PMF analysis, it was decided that testing this

hypothesis was the next necessary step in the study of SoCAB methane emissions.

5.3.1.2 Methods and Site Description

A pilot study was conducted in conjunction with Dr. Jack Brouwer's group in the engineering department here at UC, Irvine. This study sought to detect leakage of natural gas from inside buildings on campus, after the meter. Samples were collected between March 28th and April 13th 2016. Ambient whole air samples were collected using the canisters described in Chapter 2. Evacuated canisters were slowly opened to introduce room air and then sealed and returned to the laboratory. Air samples were collected at various sites around the UCI campus including known natural gas users like the central plant and dining commons. Other lab building sites that have natural gas hookups but might not be actively being used were also sampled at. The full list of these sites is shown in Table 5.2. At each of these locations, a sample was collected both inside the building and outside and upwind of the building. This outdoor sampling was done to allow for a local background to be determined as Irvine does sit within the SoCAB and other urban methane sources are likely. The samples were analyzed for the full suite of hydrocarbons as described in Chapter 2. Enhancements in both methane and ethane were calculated relative to the concentrations found in the outdoor sample.

5.3.1.3 Results and Discussion

Methane enhancements and the E/M ratio for each indoor sample are listed in Table 5.2. The E/M ratio is reported here to confirm the influence of natural gas on the samples. All of the samples with methane enhancements have an E/M ratio in a reasonable range for what could be expected in natural gas. The Playa del Rey Storage Facility reports show a natural gas E/M of 4.13% and 4.21% for March and April 2016 respectively. It is interesting to note that all but two of the indoor air samples have an E/M below that seen in the Playa del Rey data. Considering

that the UC, Irvine campus is 39 miles from the Playa del Rey storage facility, it seems possible that a different SoCalGas pipeline is servicing the campus and surrounding area or that the Playa del Rey storage facility was not used heavily during that month to supply customers. However, the average E/M of $2.48 \pm 0.18\%$ is in agreement with the average seen at Mt. Wilson as well as other months of Playa del Rey Storage Facility data. Considering that this E/M is based on enhancements over already enhanced urban samples, and that there are no other known sources of methane inside a building, these results are likely due to the leakage of unburned natural gas.

Table 5.2. Results from the UCI pilot study on indoor natural gas leakage. Errors shown are based on precision of individual measurements and error propagation.

Site	Sample Date	Indoor Methane Enhancement (ppb \pm 4 ppb)	Ethane to methane enhancement ratio (%)
Engineering Laboratory Facility room 101	3/28/2016	104	$2.25 \pm .03$
Engineering Laboratory Facility room 113	3/28/2016	49	$3.04 \pm .05$
Engineering Laboratory Facility room 213	3/28/2016	45	$2.43 \pm .04$
Engineering Laboratory Facility 2 nd floor Hallway	3/28/2016	557	$1.52 \pm .02$
Engineering Laboratory Facility Compressor	3/28/2016	430	$3.13 \pm .05$
Newport Beach, CA Apartment	3/30/2016	853	$2.59 \pm .04$
Pippin Dining Commons	4/1/2016	259	$3.18 \pm .05$
Pippin Dining Kitchen	4/1/2016	276	$2.01 \pm .03$
Phoenix Grill	4/1/2016	1281	$3.21 \pm .05$
Palo Verde Graduate Apartment Meter	4/4/2016	1225	$3.64 \pm .05$
Palo Verde Graduate Apartment Inside	4/4/2016	36	$2.23 \pm .03$
Central Plant Turbine	4/13/2016	2012	$4.81 \pm .07$
Central Plant Compressor	4/13/2016	-3	n.a.
Middle Earth Dormitory Hallway	4/13/2016	-2	n.a.
Middle Earth Dormitory Boiler Room	4/13/2016	79	$5.36 \pm .08$
Average	---	237 ± 62	2.48 ± 0.18

With the exception of the dormitory hallway and the central plant compressor station, all of the samples collected indoors or near a natural gas meter showed enhancements in methane and ethane over local background suggesting natural gas leakage. This result seems to confirm, at least on a small scale, the hypothesis put forth in Wennberg et al.¹⁰ that widespread, post-meter natural gas leakage is occurring within the SoCAB. Analyzing the results a little more closely, it was noted that the second highest indoor enhancement was found at the Phoenix Grill restaurant complex where methane was enhanced a full ppm over the outside background. The Phoenix Grill offers several different food options inside one large cafeteria and features exposed kitchens. Considering that the central plant turbine only had an enhancement of 2 ppm, the Phoenix Grill result seems surprisingly high. The Pippin Dining Hall which serves one of the two dormitory communities on campus also showed a significant enhancement in methane. Average flows to a residence are between 0 and 4 m² hr⁻¹.¹⁷ This is in comparison to power plants that have flows into their combustion chambers 3 orders of magnitude larger. The fact that UCI's power plant and Phoenix Grill were on the same order of magnitude of methane emissions illustrates the importance of this study. These results show that the emission of methane from both post meter pipe leakage and incomplete combustion at the burner head is a serious issue. A great deal of regulation effort is put in to gas producing and distribution companies as well as those that generate electricity.¹⁸ However, the same amount of monitoring and effort does not go into post-meter use. Because the leakage is occurring after the metering point, it has not been in the interest of gas companies to monitor these leaks.

There is very little in the literature about end user leakage of natural gas. One study found enhanced radon levels in kitchens due to the presence of natural gas, suggesting that it may be leaking in small quantities.¹⁹ The results presented herein should be seen as a pilot study that

confirms a larger issue. One of the reasons that bottom-up and top-down inventories do not agree on methane emissions is in part due to the fact that natural gas leakage after the meter is not accounted for. Future studies should seek to determine to what extent this issue noted at UC, Irvine extends throughout the SoCAB. The goal would be to come up with a method with which to quantify the rate of these emissions. This estimate could be achieved by conducting a larger sampling campaign to get a large enough sample size of homes to determine what percentage of end users have such a leak. Then, real time monitoring of a known leaking home or business could be undertaken to attempt to calculate how much methane is leaking per hour per square foot. These two results could go a long way to being able to accurately determine how much methane is currently unaccounted for in bottom-up estimates of the SoCAB. The positive results seen here are encouraging that accurate inventories that agree with top-down estimates are possible in an urban region sooner rather than later.

5.3.2 SoCalGas Leakage Map Study

5.3.2.1 Background of Pipeline Leaks in Cities

SoCalGas reported that they intend to fix all known non-hazardous pipeline leaks by the end of 2018 which will reduce their methane emissions by 16%.²⁰ This report suggests that they believe that a bulk of the methane emitted as natural gas was from controlled or known releases or vents. It is impossible to know when and or where these intentional releases of natural gas will occur thus making it difficult to study. However, studying smaller unintentional leaks has been done in several cities. Partnering with Google, researchers have attached a real time methane detector to a vehicle sent to photograph neighborhoods for Google Street View.²¹ Their results show that natural gas leaks are occurring sporadically throughout both older and newer cities as is shown by elevated methane readings. Cities that were developed in the early 20th century have

steel or cast iron pipes that are more susceptible to corrosion and therefore leakage.²¹ Indeed a separate study in Boston, MA showed that natural gas leaks were strongly associated with older neighborhoods with cast iron pipes.²² These types of studies are useful in further closing the gap between top-down and bottom-up studies as well as reducing total methane emissions. Very recently, the team partnering with Google Street View has mapped four Los Angeles communities with their methane analyzer and has found that a natural gas leak exists every four to six miles of roadway driven in these SoCAB cities.²³ These results were published online very recently, and so it has not been possible for our lab to validate their mapped results yet. They reported that 16% of all natural gas pipes in the Los Angeles area are either steel or cast iron and 38% of all pipes are over 50 years old. These numbers are much lower than in some east coast cities, but considering the rate of leaks they detected, it is a concerning amount and a source of methane that should be monitored.²³ However, this vehicular study was somewhat flawed in that it only has a methane analyzer on board. It was unable to determine if the methane is from natural gas or some other source. Therefore, until real-time ethane analyzers become more common place, whole air sampling for leak detection is still important.

5.3.2.2 SoCalGas Leak Map and Study Details

In cooperation with Mothers Out Front, a grass roots campaign to combat climate change, a study was conducted to find and attempt to quantify pipeline natural gas leaks within Orange County. SoCalGas publishes a website with a built-in map tool showing the locations of natural gas leaks throughout the SoCAB. There are two types of leaks marked: ones that are confirmed non-hazardous leaks that are scheduled to be repaired and those that are sites that are being monitored due to a high methane reading.²⁴ The map is readily available to customers and searches can be done by zip code.²⁵ A sample of the map is shown in Figure 5.5 that depicts the

Whole air samples were collected at seven sites marked on the SoCalGas website between April 26 and May 2, 2017. Five of the sites were in Laguna Beach, CA and two in Tustin, CA including the location in Figure 5.5 on La Limonar Road. Four sites were designated for repair, and three were being monitored. Both an upwind and downwind sample were collected at each site to determine a local enhancement. The list of sites sampled at is shown in Table 5.3 Of note, as of October 17, 2017, only three of the seven sites remain on the SoCalGas map, only one of which is still designated for repair.

Table 5.3. Results from the pilot study into locations marked by SoCalGas as being potential or known points of natural gas leakage in the SoCAB

Sample Site	Type of Site as Reported by SoCalGas	Methane Enhancement (ppbv \pm 4 ppbv)
Pacific Coast Highway between Ocean and Forest Avenues Laguna Beach, CA	Marked for Repair	0
3 rd and Mermaid Streets Laguna Beach, CA	Marked for Repair	11
Cliff Drive and Myrtle Street Laguna Beach, CA	Marked for Repair	102
Browncroft Road Laguna Beach, CA	Monitoring	12
Pacific Coast Highway and 5 th Avenue Laguna Beach, CA	Marked for Repair	2
La Limonar Road between Bimini Drive and Arroyo Avenue Tustin, CA	Monitoring	0
Arroyo Avenue between Foothill Boulevard and La Limonar Road Tustin, CA	Monitoring	0

5.3.2.3 Results and Discussion

Methane enhancements from downwind at each site as compared to upwind values are shown in Table 5.3. Only one of the seven locations samples showed more than a 100 ppb enhancement in methane. These enhancements are all much lower than those seen in the indoor UCI study and most are within our analytical margins of error. This result was somewhat surprising as SoCalGas has marked these sites as being known sources of natural gas leakage. It is possible that these sites were fixed prior to sampling and that the website is slightly outdated. However, the fact that the map has changed since sampling occurred suggests that the map is readily used by SoCalGas. The one positive result suggestive of a natural gas leak at the corner of Cliff and Myrtle Streets in Laguna Beach has been taken off the map as having been repaired. The result further suggests that sites that are marked as being monitored may be noted as such due to one high reading from a transient air mass. As mentioned previously, there are other urban sources of methane and so one spike in methane cannot really be used to detect a gas leak. Both sites along the Pacific Coast Highway sit directly above a large distribution pipeline that operates at over 200 psi and serves the entirety of south Orange County.²⁶ It was surprising that no enhancements were found at these sites despite the volume of gas just beneath the roadway. Due to these results, it cannot be recommended to use the SoCalGas website as an accurate map of locations of natural gas leaks within the SoCAB. Despite the cost, the vehicular studies with real time methane and ethane analyzers are necessary if we are to continue to note the locations of known leaks and put pressure on SoCalGas to fix them.

5.4 Aliso Canyon Natural Gas Leak

On October 23, 2015, SoCalGas reported a leak stemming from one of their wells in their Aliso Canyon natural gas storage facility which sits just 29 miles WNW of Mt. Wilson and 25 miles NW of Downtown Los Angeles in Porter Ranch, CA.^{4,27} It was estimated by Conley et al²⁷ that over the nearly four months that the well leaked before it was capped on February 11, 2016, the well released 97,100 tonnes of methane to the atmosphere. This event was the largest single release of greenhouse gases on record, emitting more than 0.5% of the entire state of California's methane emissions for the previous year.

The Aliso Canyon site is situated in the San Fernando Valley in the northwestern corner of Los Angeles County and the SoCAB. Due to the predominantly coastal winds in the region and the geography of the San Fernando Valley, air masses that pass over Porter Ranch and the Aliso Canyon site (34.31 N 118.55 W) usually pass through the Soledad Pass to the northeast before continuing on into the high desert. It is only in rare instances where the wind in the San Fernando Valley is blowing from the northwest that air from that corner of the SoCAB reaches the Mt. Wilson sampling site. Such air masses that reach Mt. Wilson were defined in Chapter 3 as not having been influenced by the greater SoCAB. However, these select samples do allow us a chance to analyze the Aliso Canyon Blowout. During the three sampling periods while the leak was occurring, only twice were samples collected where the prevailing wind was from the west and the air had been affected by the Aliso Canyon blowout. These two samples were collected at 5 P.M. on October 24th and November 19 at 3 P.M. These samples have the largest mixing ratios of methane and ethane of any samples collected during the two year Mt. Wilson study. However, this is an atypical wind pattern for the region and so to further explore the

effects of the blowout on the SoCAB during the four months that it leaked, other methods needed to be used.

5.4.1 Determination of Porter Ranch Influenced Samples

Due to the scale of this leak, it was important to find another method to test for the influence of the Aliso Canyon blowout on the Mt. Wilson samples despite the winds at the time of sampling not suggesting it to be an issue. Both methane and ethane were plotted against carbon monoxide seen in all of the daytime samples collected. To help determine the influence of the Aliso Canyon leak, a 95% confidence ellipse was added to each plot (Figure 5.6). These plots show the strong correlation between hydrocarbons and carbon monoxide emissions seen at Mt. Wilson. These correlations will be used in the next chapter to help calculate top-down emissions estimates. Although methane, ethane, and carbon monoxide are not often emitted from the same sources, the air masses that reach Mt. Wilson are well mixed and show influence from many different point sources in the basin.²⁸ Seen in these plots, there are a few samples in which the ethane or methane mixing ratio fell outside and above its respective ellipse. These data points are atypical given SoCAB conditions and may show the influence of other regions or one-off emissions events. Of the 8 such data points for ethane, 5 were collected between October 2015 and January 2016. Four of these five samples are noted to have abnormally high methane mixing ratios (> 2 ppm) as seen in Figure 5.5. Two of the four were those that were found via analysis of wind direction. HYSPLIT was used to confirm that the air masses had at some point passed over the Porter Ranch area. A HYSPLIT back trajectory from the base of Mt. Wilson during the October 28th 3PM sample is shown in Figure 5.7. Despite the wind direction at the top of the sampling hour being from the southeast, winds earlier in the day were from the west and later were from the northwest. Due to upslope venting these air masses that had passed over the Aliso

Canyon site reached Mt. Wilson giving the sample an abnormally high methane and ethane to carbon monoxide ratio. A fifth sample, which was taken on October 25, 2015, was also explored for influence by the blow out, however, HYSPLIT back trajectories show that the air mass came from the east as part of a Santa Ana Wind event and was thus an anomaly for different reasons.

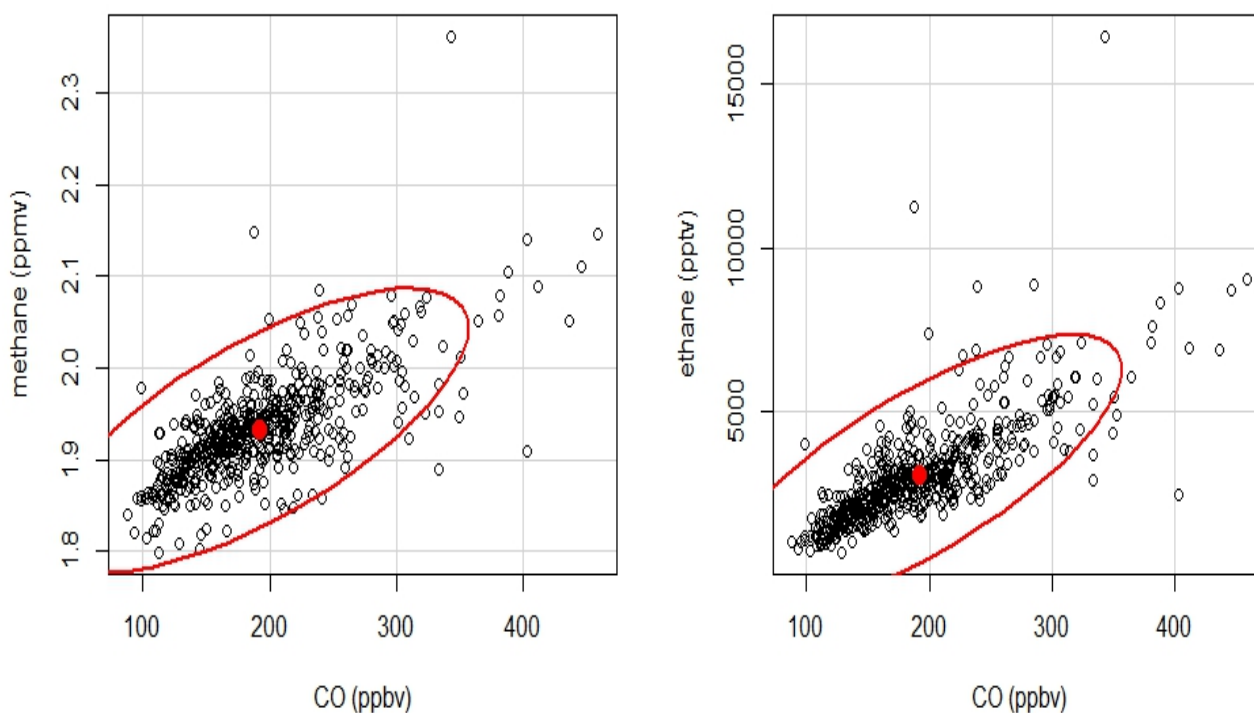


Figure 5.6 Correlation plots of methane and ethane mixing ratios versus carbon monoxide mixing ratios seen in daytime samples during the Mt. Wilson sampling period plotted with 95% confidence ellipses and median in red.

NOAA HYSPLIT MODEL
 Backward trajectories ending at 2200 UTC 28 Oct 15
 GDAS Meteorological Data

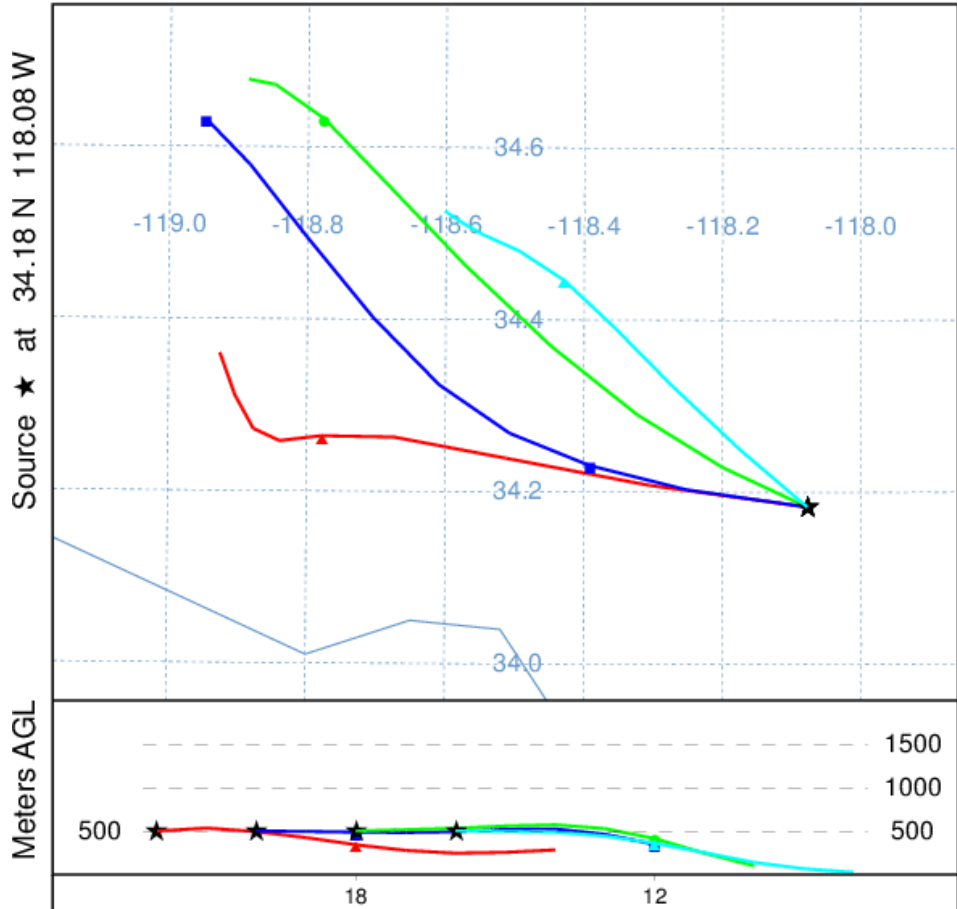


Figure 5.7 HYSPLIT back trajectory from the base of Mt. Wilson showing that the air mass had passed over the Aliso Canyon blowout at 34.31 N 118.55 W.

Table 5.4. Mixing ratios of selected alkanes and meteorological conditions for the four samples determined to have been influenced by the Aliso Canyon natural gas leak. The error in a given mixing ratio is based off of the stated precision in Table 2.1. The error associated with the averages is the standard error of the mean.

Sample Date and Time	Wind Direction and Speed (mph)	Methane (ppmv)	Ethane (pptv)	Ethane to Methane Enhancement Ratio (%)	Propane (pptv)	i-Butane (pptv)	n-Butane (pptv)	i-Pentane (pptv)	n-Pentane (pptv)	n-hexane (ppt)	Benzene (ppt)
10/24/2015 5 P.M.	NNW, 4	2.147	11246	3.52	1412	210	355	378	154	43	89
10/28/2015 3 P.M.	ESE, 4	2.362	16471	3.05	3378	584	892	804	319	119	189
11/19/2015 3 P.M.	WNW, 2	2.084	8804	3.42	2015	575	1327	685	283	103	131
12/21/2015 11 A.M.	SE, 4	2.053	7421	3.13	1611	372	736	297	156	54	134
Average of Aliso Canyon Influenced Samples	----	2.16 ± 0.07	10985 ± 1992	3.28 ± 0.11	2104 ± 443	435 ± 89	827 ± 201	541 ± 121	228 ± 43	79 ± 19	136 ± 21
Average of all SoCAB but not Aliso Canyon Influenced Samples	----	1.93 ± 0.01	3170 ± 72	2.71 ± 0.20	1513 ± 49	256 ± 9	502 ± 20	316 ± 11	190 ± 7	72 ± 2	139 ± 3

5.4.2 Analysis of Influenced Samples

The relevant meteorological conditions and results for all four Aliso Canyon influenced samples are shown in Table 5.4. Of the four samples deemed to have been influenced by the Aliso Canyon blowout, only two of them show wind directions that would immediately suggest the influence as such. Winds can swirl through the region, as is witnessed by these samples, bringing already polluted air to the foothill regions where the mountains halt the air's progress and more photochemistry occurs.

These four Aliso Canyon influenced samples show unusually high mixing ratios for both methane and ethane. Indeed, the samples collected on October 24th and October 28th represent the highest mixing ratios seen over the entire study for methane and ethane, but not for any larger hydrocarbon. Further, carbon monoxide is not abnormally elevated in either sample suggesting that this is not just a particularly dirty sample representative of the SoCAB. As a confirmation of the source of the excess methane and ethane, the E/M enhancement for each of these four samples was calculated and yielded an average of $3.28 \pm 0.23\%$. This result can be compared to the average of 3.51 ± 0.12 in Conley et al.²⁷ and $4.28 \pm 0.07\%$ reported in Wunch et al.⁴ Conley et al.²⁷ made 10 flights above the Aliso Canyon site over the four months in which it was leaking. Wunch et al.⁴ base their value on ground based methane and ethane measurements in Pasadena. The Conley et al.²⁷ average fits within the range presented here from our four influenced data points. The results presented in Wunch et al.⁴ differ from those presented here significantly. This difference is more than likely due to a difference in the daytime backgrounds used.

During the blowout, there was a great deal of concern from residents of the area about benzene exposure.²⁹ Benzene is a known carcinogen and is a component of gasoline and other fossil fuel products. OSHA regulates the amount of benzene a worker can be exposed to during

an 8 hour day at 1 ppm.³⁰ Of the four samples found in the two year data set to have been influenced by this event, only one was in the top 25% of all benzene mixing ratios, and it was still over 200 ppt lower than the sample with the largest mixing ratio of benzene. There is regularly more benzene in the air in the Los Angeles area than in the samples influence by the well blowout. While, the human health effects of this leak were greatly over exaggerated, the effects to the earth cannot be stated enough.

5.5 Conclusions

Throughout this chapter it has been shown that natural gas in the SoCAB is a more complicated topic than had been previously thought. The composition of gas delivered to residences and businesses in the basin has day to day variation in the E/M that was previously assumed to be relatively stable. The composition is largely driven by ethane rejection by which producers of natural gas choose not to remove ethane and other larger hydrocarbons from the gas supply. Between 2012 and 2015, the E/M in gas supplied to the region gradually increased allowing for a different method of estimation of the fraction of methane from natural gas leakage. This composition data were used in conjunction with Mt. Wilson data to show that $72 \pm 16\%$ of the excess methane in the region is due to natural gas leakage.

To further understand the source of the difference between bottom-up and top-down estimates of methane emissions, a previously unaccounted for source of methane, post-meter leakage, was studied. This pilot study confirmed a previous hypothesis that natural gas is leaking at low levels widely across homes and businesses after the gas meter. This study should be followed up upon to try and determine an estimate of this type of leakage across the basin.

Finally, the Mt. Wilson data set was used to further explore the Aliso Canyon natural gas blowout that emitted thousands of tons of methane into the SoCAB air. Several samples were

found to have been influenced by the blowout leading to anomalous values of methane and ethane that had a natural gas signature.

5.6 References

- (1) Gilman, J. B.; Lerner, B. M.; Kuster, W. C.; de Gouw, J. A. Source Signature of Volatile Organic Compounds from Oil and Natural Gas Operations in Northeastern Colorado. *Environ. Sci. Technol.* **2013**, *47*(3), 1297–1305
- (2) Swarthout, R. F.; Russo, R. S.; Zhou, Y.; Miller, B. M.; Mitchell, B.; Horsman, E.; Lipsky, E.; McCabe, D. C.; Baum, E.; Sive, B. C. Impact of Marcellus Shale Natural Gas Development in Southwest Pennsylvania on Volatile Organic Compound Emissions and Regional Air Quality. *Environ. Sci. Technol.* **2015**, *49* (5), 3175–3184.
- (3) Pétron, G.; Karion, A.; Sweeney, C.; Miller, B. R.; Montzka, S. A.; Frost, G. J.; Trainer, M.; Tans, P.; Andrews, A.; Kofler, J.; et al. A new look at methane and nonmethane hydrocarbon emissions from oil and natural gas operations in the Colorado Denver-Julesburg Basin: Hydrocarbon emissions in oil & gas basin. *J. Geophys. Res. Atmospheres* **2014**, *119* (11), 6836–6852.
- (4) Wunch, D.; Toon, G. C.; Hedelius, J. K.; Vizenor, N.; Roehl, C. M.; Saad, K. M.; Blavier, J.-F. L.; Blake, D. R.; Wennberg, P. O. Quantifying the loss of processed natural gas within California’s South Coast Air Basin using long-term measurements of ethane and methane. *Atmos Chem Phys* **2016**, *16* (22), 14091–14105.
- (5) Sikorski, T.; Tertzakian, A. Ethane rejection <https://www.energyaspects.com/> (accessed Oct 12, 2017).
- (6) ICIS News. US ethane to double by ’19, squeezing margins - Cowen <https://www.icis.com/> (accessed Oct 12, 2017).
- (7) Finlayson-Pitts, B.; Pitts, J. *Chemistry of the Upper and Lower Atmosphere*; Academic Press, 2000.
- (8) Atkinson, R.; Baulch, D. L.; Cox, R. A.; Crowley, J. N.; Hampson Jr., R. F.; Hynes, R. G.; Jenkin, M. E.; Kerr, J. A.; Rossi, M. J.; Troe, J. *Summary of Evaluated Kinetic and Photochemical Data for Atmospheric Chemistry*; IUPAC Subcommittee on Gas Kinetic Data Evaluation for Atmospheric Chemistry, 2006.
- (9) Bufalini, J. J.; Walter, T. A.; Bufalini, M. M. Ozone formation potential of organic compounds. *Environ. Sci. Technol.* **1976**, *10* (9), 908–912.
- (10) Wennberg, P. O.; Mui, W.; Wunch, D.; Kort, E. A.; Blake, D. R.; Atlas, E. L.; Santoni, G. W.; Wofsy, S. C.; Diskin, G. S.; Jeong, S.; et al. On the Sources of Methane to the Los Angeles Atmosphere. *Environ. Sci. Technol.* **2012**, *46* (17), 9282–9289.
- (11) Southern California Gas Company. Playa del Rey Natural Gas Storage Operations <https://www.socalgas.com/stay-safe/pipeline-and-storage-safety/playa-del-rey-storage-operations> (accessed Apr 7, 2016).
- (12) Southern California Gas Company. Daily Operations SoCalGas Information Sharing Archive.
- (13) Kakaee, A.-H.; Paykani, A.; Ghajar, M. The influence of fuel composition on the combustion and emission characteristics of natural gas fueled engines. *Renew. Sustain. Energy Rev.* **2014**, *38* (Supplement C), 64–78.

- (14) Peischl, J.; Ryerson, T. B.; Brioude, J.; Aikin, K. C.; Andrews, A. E.; Atlas, E.; Blake, D.; Daube, B. C.; de Gouw, J. A.; Dlugokencky, E.; et al. Quantifying sources of methane using light alkanes in the Los Angeles basin, California: SOURCES OF METHANE IN L.A. *J. Geophys. Res. Atmospheres* **2013**, *118* (10), 4974–4990.
- (15) Student Airborne Research Program (SARP) | NSRC
<https://airbornescience.nasa.gov/nsrc/sarp> (accessed Mar 3, 2017).
- (16) Southern California Gas Company. *Southern California Gas Company Natural Gas Leakage Abatement Report*; 2015.
- (17) Farzaneh-Gord, M.; Parvizi, S.; Arabkoohsar, A.; Machado, L.; Koury, R. N. N. Potential use of capillary tube thermal mass flow meters to measure residential natural gas consumption. *J. Nat. Gas Sci. Eng.* **2015**, *22*, 540–550.
- (18) Young, S. *CARB Approves Rule for Monitoring and Repairing Methane Leaks from Oil and Gas Facilities*; California Air Resources Board, 2017.
- (19) Şen, G. Y.; İçhedef, M.; Saç, M. M.; Yener, G. Effect of natural gas usage on indoor radon levels. *J. Radioanal. Nucl. Chem.* **2013**, *295* (1), 277–282.
- (20) SoCalGas. SoCalGas Efforts to Reduce Its Methane Emissions
<https://www.socalgas.com/stay-safe/methane-emissions/SoCalGas-efforts-to-reduce-methane-emissions> (accessed Aug 10, 2017).
- (21) von Fischer, J. C.; Cooley, D.; Chamberlain, S.; Gaylord, A.; Griebenow, C. J.; Hamburg, S. P.; Salo, J.; Schumacher, R.; Theobald, D.; Ham, J. Rapid, Vehicle-Based Identification of Location and Magnitude of Urban Natural Gas Pipeline Leaks. *Environ. Sci. Technol.* **2017**, *51* (7), 4091–4099.
- (22) Phillips, N. G.; Ackley, R.; Crosson, E. R.; Down, A.; Hutyra, L. R.; Brondfield, M.; Karr, J. D.; Zhao, K.; Jackson, R. B. Mapping urban pipeline leaks: Methane leaks across Boston. *Environ. Pollut.* **2013**, *173*, 1–4.
- (23) Environmental Defense Fund. Los Angeles Area: Snapshot of natural gas leaks
<https://www.edf.org/climate/methanemaps/city-snapshots/los-angeles-area> (accessed Apr 10, 2017).
- (24) Southern California Gas Company. Methane Emissions Map
<https://www.socalgas.com/stay-safe/methane-emissions/methane-emissions-map> (accessed Oct 17, 2017).
- (25) SoCalGas. Methane Emissions Map FAQ <https://www.socalgas.com/stay-safe/methane-emissions/methane-emissions-map-faq> (accessed Aug 10, 2017).
- (26) Southern California Gas Company. Orange County Pipeline Map
<https://www.socalgas.com/stay-safe/pipeline-and-storage-safety/natural-gas-pipeline-map/orange> (accessed Oct 17, 2017).
- (27) Conley, S.; Franco, G.; Faloona, I.; Blake, D. R.; Peischl, J.; Ryerson, T. B. Methane emissions from the 2015 Aliso Canyon blowout in Los Angeles, CA. *Science* **2016**.
- (28) Hsu, Y.-K.; VanCuren, T.; Park, S.; Jakober, C.; Herner, J.; FitzGibbon, M.; Blake, D. R.; Parrish, D. D. Methane emissions inventory verification in southern California. *Atmos. Environ.* **2010**, *44* (1), 1–7.
- (29) Barboza, T. Benzene risk from Porter Ranch gas leak is the same as rest of region, study finds. *Los Angeles Times*. January 15, 2016.
- (30) Occupational Safety and Health Administration. Chemical Sampling Information | Benzene https://www.osha.gov/dts/chemicalsampling/data/CH_220100.html (accessed Aug 23, 2017).

CHAPTER 6: Top-down Emissions Estimates of Hydrocarbons in the SoCAB

6.1 Background and History of Emissions Estimates

With source apportionment of hydrocarbons in the SoCAB conducted, we can now turn our attention to determining the quantity of these hydrocarbons emitted. This estimation of total emissions is a non-trivial task and can be conducted through various means. Global emissions estimates are usually calculated via models that estimate global burdens based off of known inputs and knowledge of transport and chemistry.^{1,2} Bottom-up estimates can also be calculated based off of emissions from different sectors as calculated in other literature.³ Nationally, the EPA estimates the emission of several greenhouse gases via bottom-up inventories at the individual facility level.⁴ Finally, on a more regional level, emissions estimates are somewhat more constrained and inventories more accurate based on reporting.^{5,6} A state environmental agency can then sum individual business reports together and factor in other sources to create a fairly accurate bottom-up inventory.⁷

Most of these methods are based on reported inventories and fall under the bottom-up approach. When dealing with large regions or even the globe, bottom-up estimates are by and large the only feasible method. However, when considering a smaller region or a city, top-down estimates can become possible. Here, a series of top-down emissions estimates for hydrocarbons will be calculated for the SoCAB using the Mt. Wilson data set. These estimates can then be combined with the results of PMF analysis in Chapter 4 to build a by sector inventory of greenhouse gas and other VOC emissions. Top-down emissions estimates have been calculated in the past for the SoCAB for hydrocarbons, halocarbons, and others species.⁸⁻¹² However, as mentioned in previous chapters many of these estimates were calculated based on much smaller or less temporally diverse data sets. The Mt. Wilson data set with two years of daytime samples

will be an excellent source from which to calculate emissions estimates and then compare the results to previous literature values.

6.2 Calculating Emissions Estimates

6.2.1 Top-Down Estimate Calculations

Emissions inventories for hydrocarbons are not as well established as they are for CO and CO₂.⁸ Carbon monoxide is often used as a tracer for anthropogenic emissions as it is emitted during the incomplete combustion of fossil fuels and has a lifetime on the order of months.¹³ The long atmospheric lifetimes of methane and ethane allow for these species to become well mixed with CO in air parcels travelling across the SoCAB and eventually reaching Mt. Wilson. It has been noted in previous work that air masses reaching Mt. Wilson that have passed over the basin show strong correlations between methane and CO, suggestive of mixing.^{6,8} It has been established that for these long lived VOCs, the relationship to the emission of CO can be used as a scaling factor by which to determine an emissions estimate for the VOC.^{6,8,11} The validity of this method is based on three tenets. The first is that the emissions of CO are fully understood and the estimate is accurate. Second, the hydrocarbon and CO must be colocated. Finally, the species must have atmospheric lifetimes significantly greater than that of the transport time.⁹ Here, CO emissions estimates for the SoCAB will be taken from the California Air Resources Board's annual inventory which is based on years of ambient monitoring along with point source measurements.^{6,14} While this estimate is assumed to be accurate, there is no mention of error inherent in it and so as in other studies, it is assumed to be $\pm 20\%$.^{10,11} While methane and ethane have non-combustion related sources, the emission of larger alkanes and hydrocarbons stem from the leakage and burning of fossil fuel which is the dominant source of CO.¹⁵ For methane and ethane, the validity of the colocation assumption will be discussed later in this chapter.

Finally, as discussed previously, the transport time through the SoCAB is on the order of hours, much shorter than the lifetime of alkanes and CO.

Therefore, with these assumptions being valid, the CO inventory from CARB can be used in combination with the enhancement values calculated from the Mt. Wilson data set to calculate top-down emissions observed at Mt. Wilson. To do this, the slope of the enhancement plot (m), in mole/mole, is multiplied by CARB's emissions almanac data (E_{CO}) yielding an emissions estimate for the hydrocarbon (E_{HC}), measured in Gg per year, such that,

$$E_{HC} = m_{enhancement} \times E_{CO} \times \frac{M_{HC}}{M_{CO}}$$

where M_{HC} is the molar mass of the hydrocarbon and M_{CO} is the molar mass of CO.⁶ Due to the importance of the CO inventory in this type of calculation, it is necessary to study it in more detail and ensure validity.

6.2.2 CARB's CO Estimate

Since AB 32 was enacted in 2006, CARB has maintained inventories for greenhouse gases that are updated annually based on reporting submitted by individual entities.⁷ Prior to this focus on climate change, work at the agency was focused on monitoring and reduction of criteria pollutants that contributed to tropospheric ozone or more directly adversely affected human health.¹⁶ Ambient levels of criteria pollutants are federally regulated, and so monitoring of emissions is incredibly important at a state and regional level. CARB's emissions estimates for criteria pollutants are updated every few years as part of the California Almanac of Emissions and Air Quality.¹⁷ Since the inventories rely on a bottom-up tabulation of emissions, results can be scaled from the whole state down to a regional or county level. Further, since the inventories can and do change, when using inventory projections into the future, the choice of inventory and total emissions value needs to be carefully noted when conducting hydrocarbon emissions

estimations. This step is crucial as future studies will want to compare their results to previous work and knowing the value of CO emissions per day used allows for a more nuanced analysis.

Complicating this issue is the fact that previous inventories are still searchable and accessible on CARB's website: several CO inventories for the same year exist on different pages within CARB's framework. As an example, for the year 2015, for which samples of the SoCAB were collected by the author here and by Wunch et al.,¹¹ there now exist two different CO emissions estimates for the SoCAB. The older of the two estimates, published in 2009, is based off of a base year of 2008 and then projected in the future for years 2010, 2015, and 2020.¹⁸ The more recent estimate was released in 2013 based off of data from 2012 and then projects estimates all the way until 2035.¹⁴ To illustrate the differences, the SoCAB estimated CO emissions for each of these inventories for past and future years are shown in Figure 6.1. It is clear that CO emissions have decreased significantly over the past few decades reflecting the effect that policies enacted to clean up engines and fuels had on the SoCAB. In the more recent past, the two inventories agree that less dramatic reductions have occurred since the year 2000. However, the more recent 2013 inventory estimated a lower total emission rate for the year 2000 than the 2009 inventory by 842 tons per day. Out to the year 2020, the 2013 inventory has a 550 ton per day lower estimate (25% difference). This difference is large enough such that it should not be ignored, and the choice of inventories must be noted when doing this type of calculation going forward.

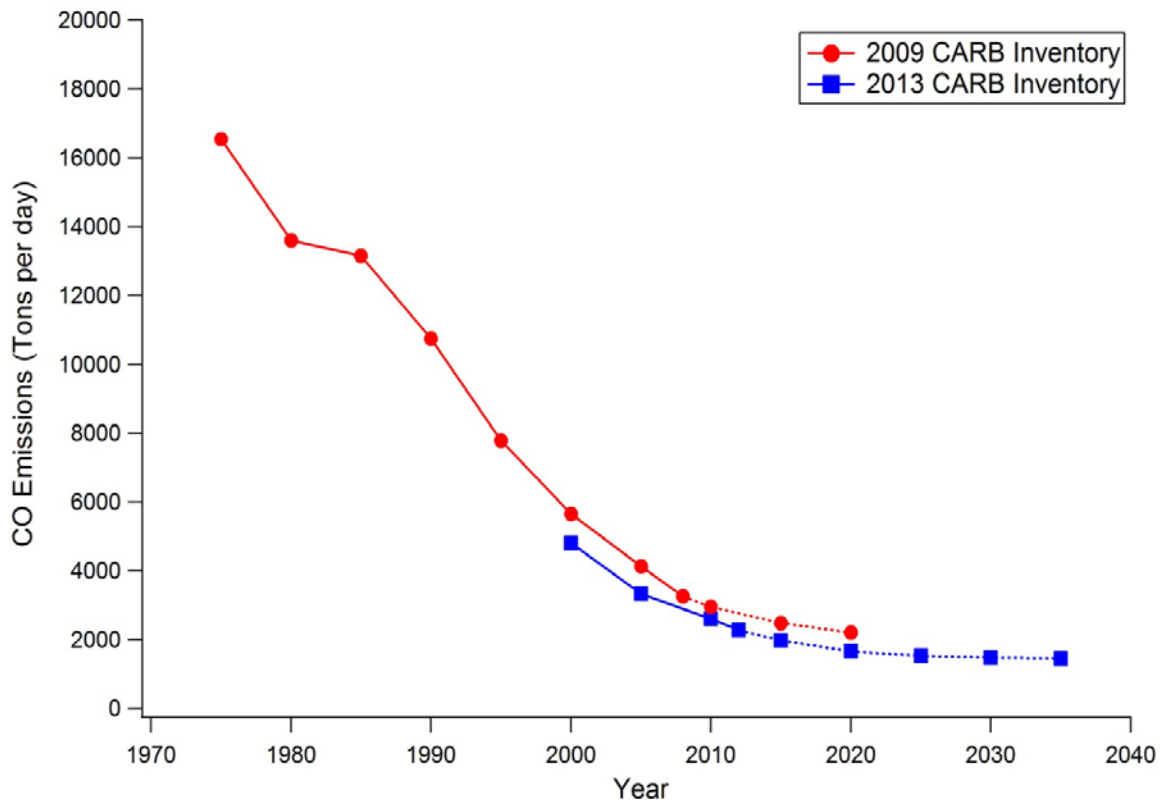


Figure 6.1 California Air Resources Board estimated inventories for CO emissions in the South Coast Air Basin based on base year 2008 and 2012.

To understand a little more fully what could cause this 25% decrease in total CO emissions between the two inventories, the full sector by sector breakdown was studied. For the year 2015 that was projected forward from the base year 2008 and 2012, the sector breakdowns are shown for each in Table 6.1. While all sectors saw changes from the previous 2009 inventory, the bulk of the reduction came from the changes made to the projections for mobile sources. On road and off road mobile sources together account for 94% of the total CO emissions found in the SoCAB, and so reduction in the inventories for these two sectors explain the overall reduction seen above. The updated 2013 inventory reduced CO emissions from passenger

vehicles, trucks, boats and airplanes. This reduction is likely the result of increased combustion efficiency that was under accounted for in 2009 projections.¹⁹ The authors find no reason to select an older estimate of emissions from the SoCAB and worked with the assumption that the 2013 almanac estimate is more accurate. Indeed for projecting forward to the year 2015, it seemed most logical to select the estimate with the most recent base year. Therefore, for the rest of this analysis, the 2013 emissions projections will be used for hydrocarbon emissions estimates. The 2015 estimated CO emissions total for the SoCAB is reported as 1969.9 tons per day in the 2013 almanac.

Table 6.1 California Air Resources Board estimated inventories for CO emissions in the South Coast Air Basin based on base year 2008 and 2012 by sector and how the estimate has changed.

	2009 CARB Almanac daily emissions estimate for CO in 2015 (tons/day)	2013 CARB Almanac daily emissions estimate for CO in 2015 (tons/day)	Difference from 2009 (%)	Fraction of total 2009 inventory from sector (%)
Fuel Combustion	35	49	29	1.4
Waste Disposal	1	1	2.5	0.047
Cleaning and Surface Coatings	0.08	1	562	0.0032
Petroleum Production and Marketing	9	5	-49	0.36
Industrial Processes	3	1	-54	0.11
Miscellaneous Processes	115	102	-12	4.7
On-Road Motor Vehicles	1306	1046	-20	53
Other Mobile Sources	1007	765	-24	41
Total	2476	1970	-20	100

6.3 Results and Discussion

6.3.1 Enhancement Plots and Correlations

Emissions estimates were calculated for several hydrocarbon species from the Mt. Wilson data set. Using the enhancements of both the hydrocarbon and CO as described in Chapter 3,

correlation plots were created to ensure that the two species correlate well of sources and determine the slope to be used in the emissions estimate. The slopes of each enhancement plot along with the coefficient of determination are shown in Table 6.2. Included as well is the percent of the species that was apportioned to tailpipe emissions in PMF along with the slopes from Gorham et al. (2010)⁸ that were from the 2007 Mt. Wilson sampling campaign.

Table 6.2 Enhancement slopes for hydrocarbons versus carbon monoxide ($\pm 1\sigma$ standard error) for the 2014-2016 Mt. Wilson data set along with the percentage of the species associated with tailpipe emissions

	Hydrocarbon Enhancement vs CO Enhancement Slope (pptv/ppbv)	Coefficient of Determination (R^2)	Percent of total species mass associated with tailpipe emissions in PMF	Hydrocarbon Enhancement vs CO Enhancement Slope (pptv/ppbv) from Gorham et al. ⁸	Coefficient of Determination (R^2) from Gorham et al. ⁸
Methane	693.3 ± 21.7	0.69	----	---	----
Ethane	18.1 ± 0.6	0.68	2.0	12.2 ± 0.4	0.79
Ethyne	4.3 ± 0.1	0.81	49.5	5.6 ± 0.1	0.90
Propane	13.7 ± 0.5	0.67	22.1	12.8 ± 0.3	0.81
<i>i</i> -Butane	2.4 ± 0.1	0.57	17.1	2.8 ± 0.1	0.64
<i>n</i> -Butane	4.6 ± 0.2	0.47	13.4	4.2 ± 0.2	0.60
<i>i</i> -Pentane	2.8 ± 0.1	0.57	68.5	5.3 ± 0.1	0.83
<i>n</i> -Pentane	1.8 ± 0.1	0.62	18.8	2.1 ± 0.1	0.80
<i>n</i> -Hexane	0.69 ± 0.02	0.68	----	---	----
Benzene	0.84 ± 0.02	0.75	22.9	1.2 ± 0.0	0.89

Of note from this table and comparison is that the coefficients of determination are all lower than they were in the 2007 campaign despite following largely the same order of most to least correlated. The exception to this trend is isopentane which went from being the third most correlated species to the second least correlated. This is particularly intriguing considering the dominant source of isopentane to the region is tailpipe emissions which is where over 90% of CO stems from as well.¹⁴ Upon further inspection of the isopentane data, the sample with the highest mixing ratio of isopentane (2052 pptv) appears to be heavily affecting the correlation. Despite having the largest isopentane value, the CO mixing ratio is only within the top 10% of

samples. This sample was influenced by the more transient oil and gas production factor in PMF analysis, which makes sense given the poor correlation. However, removal of this data point only increases the coefficient of determination to 0.61, which still doesn't make much sense with the trend. Indeed, ethyne which is the most emitted hydrocarbon product of combustion correlates strongly with CO in both data sets.¹⁹ The decrease in correlation serves as further evidence of the idea that combustion sources have been much better controlled that was first argued for in Chapter 3. It is well established that vehicular emissions dominate total emissions in the region.^{12,20} As regulators and industry continue to make strides towards improving combustion engines and limiting hydrocarbon emissions from the tailpipe, total emissions associated with vehicles are shown to be declining.

Also of note from these correlations is that most of the slopes that were also reported in Gorham et al.⁸ have changed significantly since the study in 2007. Despite there being large decreases in the average daytime mixing ratios of species larger than ethane since 2007 (Table 3.2), the decreases in slope are not as significant. Some slopes are even larger than they were in 2007. The propane slope increased from 12.8 ± 0.3 pptv/ppbv to 13.7 ± 0.5 pptv/ppbv, and similar results are seen for *n*-butane. For these results to have occurred, despite the decrease in hydrocarbon mixing ratios, CO mixing ratios must have decreased much more rapidly. Between the 2007 study and the current one the daytime average CO mixing ratio decreased $26\% \pm 6\%$ which falls within the range of the hydrocarbon decreases seen in Chapter 3. These results are corroborated by the CARB daily CO emissions estimate from the SoCAB, which dropped 41% from 3322.4 tons per day in 2005 to 1969.9 tons per day in 2015. This decrease in inventory estimate is larger than every other hydrocarbon listed in Table 3.2 except for isopentane which

did see its enhancement slope decrease. These results show that CO and hydrocarbon emissions within the SoCAB are not decreasing at the same rate.

Finally, before calculating emissions estimates for the hydrocarbons, it is important to note that despite not being colocated with the source of CO, methane and ethane do correlate well with carbon monoxide. This result suggests that within the SoCAB, mixing of air masses occurs and by the time they reach Mt. Wilson, methane, ethane and CO correlate. Plots of the correlations between the two hydrocarbons and CO are shown in Figure 6.2. Shown also are the plots prior to enhancement calculations showing a less strong but still positive correlation. There is less difference between the enhanced and non-enhanced ethane plots as compared to the methane plots. This may be a result of the strong seasonality of background methane. Regardless, the correlations are strong enough such that methane and ethane emissions estimates can be calculated from this data set.

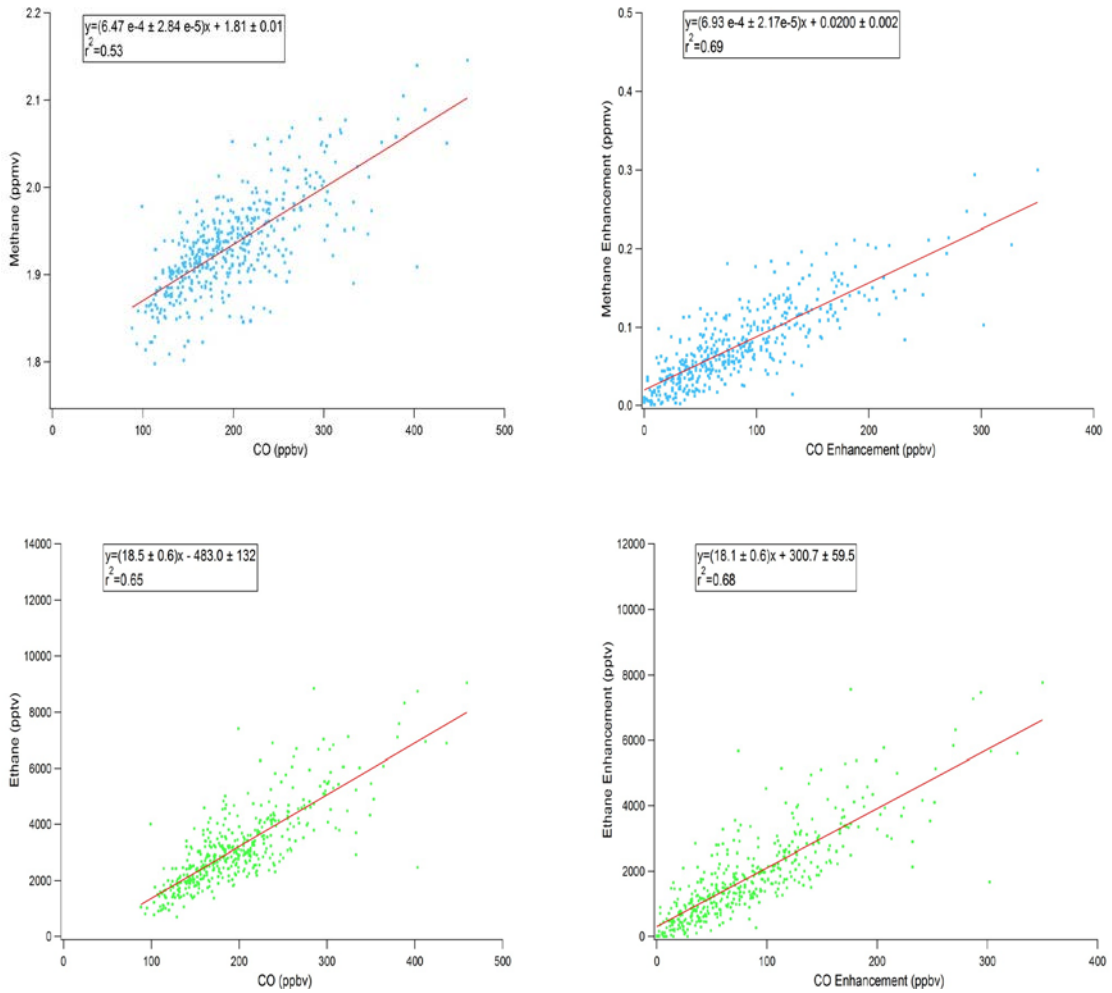


Figure 6.2 Correlation and enhancement plots of methane and ethane versus CO seen at the Mt. Wilson sampling site. Errors in the slope and y-intercept are 95% confidence intervals.

6.3.2 Hydrocarbon Emissions Estimates

Using the CARB almanac value of estimated CO emissions in the SoCAB for 2015 of 1969.9 tons per day, annual emissions estimates for the hydrocarbons presented in Table 6.2 were calculated. These results along with estimates from previous studies of the region as found in the literature are shown in Table 6.3 with results having units of Gg per year. The results from this current study can be said to be the average annual emissions for the period of the study, June 2014 through May 2016. This analysis works under the assumption that the 2015 CO estimate can be extrapolated to the last half of 2014 and the first half of 2016. In this data set, no significant difference in enhancements was seen when separating out 2014 from 2015 or 2016 that cannot be attributed to the increase in CO in summer as described in Chapter 3. The error associated with these estimates comes from the standard error of the enhancement slope and the assumed 20% error in the CARB CO inventory.

Table 6.3. Hydrocarbon emissions rates for the period of June 2014 through May 2016 for the SoCAB as reported in Gg per year. Also included are literature estimates for previous studies of the region. Note that the CO estimate used in the current study is from an updated inventory as compared to the older studies.

	Methane	Ethane	Ethyne	Propane	i-Butane	n-Butane	i-Pentane	n-Pentane	Hexane	Benzene
Current Study	243 ± 49	13 ± 3	2.6 ± 0.5	14 ± 3	3.2 ± 0.6	6.2 ± 1.3	4.7 ± 1.0	3.1 ± 0.6	1.4 ± 0.3	1.5 ± 0.3
Wunch et al. ¹¹ 2014-2015 data	413 ± 86	23 ± 3	-----	-----	-----	-----	-----	-----	-----	-----
Peischl et al. ¹² 2010 data	411 ± 37	11.4 ± 1.6	-----	19.8 ± 2.7	5.1 ± 0.7	8.3 ± 1.2	14.1 ± 1.8	6.5 ± 0.9	-----	-----
Wennberg et al. ⁵ 2010 data	440 ± 100	12.9	-----	-----	-----	-----	-----	-----	-----	-----
Gorham et al. ⁸ 2007 data	-----	17 ± 3	5.6 ± 0.1	26 ± 5	7.7 ± 1.5	11 ± 2.2	18 ± 4	6.9 ± 1.4	-----	4.4 ± 0.9

Overall, total hydrocarbon emissions rates are lower in this study than in previous studies of the region. This is to be expected given that the average daytime mixing ratio for the species larger than ethane are lower than in 2007 and the estimated CO emissions decreased as well. All of the gases remain on the same order of magnitude as in Gorham et al.⁸ with reductions in emissions rate ranging from 23% for ethane to 74% for isopentane. Results from Peischl et al.¹² with data from 2010, show that reductions have been gradual as the emissions rates presented there are between those from 2007 and the current study. The emission rates for several species deserve specific discussion and comparison to other studies.

6.3.2.1 Comparing Methane and Ethane Emissions Estimates

In this study, the emission rate of methane in the SoCAB was calculated as 243 ± 49 Gg per year. As a potent greenhouse gas, methane emission rates have been well studied.^{1,3,21} Even limiting the discussion to the SoCAB, three different studies have calculated an emissions estimate for methane in the past seven years.^{5,11,12} The result calculated here is significantly lower than these three previous estimates for the SoCAB including the estimate presented in Wunch et al.¹¹ which covers the period 2007-2015. The authors there argue that SoCAB enhancements in methane have remained constant over that period and so an averaged emissions rate estimate can be computed for that time.¹¹ The enhancement results presented in Chapter 3 agree with this assessment showing minimal change in SoCAB enhanced mixing ratios since 2007. The largest reason for the 40% difference between the estimate here and in Wunch et al.¹¹ is this the choice of CO emission rate. Wunch et al.¹¹ used the 2009 almanac data for their estimates of methane emissions. As shown above in Table 6.1, the newer estimate is 20% lower than that in the 2009 almanac. This is an extremely significant change and it is unclear why the authors chose to use the older data. If the older CO estimate was used for our study, the result

reported would be 305 ± 62 Gg per year, which would still be 20% lower than the Wunch et al. value, but the error ranges would overlap.¹¹ Considering the significant change to the CARB estimate, it is likely that the 20% error assumed in the estimate is too small a confidence interval, and when used in the future, a more careful error approximation should be undertaken.

A very similar analysis was done for ethane emissions. Average ethane mixing ratios were noted to be increasing within the two year study and more prominently since the 2007 study. Despite this, the ethane emission rate for the SoCAB of 13 ± 3 was lower than the estimates in Wunch et al.¹¹ and Gorham et al.⁸ Our estimate agreed well with that presented in Wennberg et al.⁵ and Peischl et al.¹² which used a 2010 data set. This result does not make sense as an increase in average mixing ratios should be due to an increase in the emission rate. The discrepancy, again, relates back to the change in the CARB CO estimate, and if the older estimate was used, better agreement would be found.

Another source of difference in the estimates presented here as compared to the literature is in the definition of background values. In Wunch et al.¹¹, only data points collected in the afternoon were used and the morning time value at the same solar zenith angle was used as a background to subtract off. It is possible that by having mixing ratios that start much earlier in the day than the earliest Mt. Wilson sample at 11:00, the background methane value was actually lower than presented here. This would have the effect of making the enhancement values larger and, therefore, the slope of the methane versus CO plot would be higher, creating a slightly larger estimate.

6.3.2.2 Hexane Emissions Estimate

The hexane emission rate in the SoCAB during the study period was 1.4 ± 0.3 Gg yr⁻¹. To the author's knowledge, this is the first estimate of hexane emissions in the SoCAB. Hexane

emission rates have been calculated for oil producing shale regions.²²⁻²⁴ As discussed previously, the SoCAB does not sit above a dominant oil shale and so emissions from well pads and drilling are minimal. In PMF analysis, over 60% of the hexane in the SoCAB was associated with the evaporation of gasoline with a smaller fraction associated with oil and gas refining. In the Barnett Shale region of Texas and Oklahoma, hexane emission rates were reported as being between 5.6 and 9.3 Gg per year.²² In the Uintah Basin of Utah, a similar emission rate of 5.4 Gg per year was found.²³ Considering that the dominant source of hexane to the region is not well pad leakage, the 1.4 Gg per year estimate presented here makes sense. In a non-shale, urban region, hexane emission rates were found to be roughly five times lower than those found in shale regions. It is expected that in an urban area with lower average temperatures such as Boston or New York, this emission rate will decrease due to less gasoline evaporation.

6.4 Combining PMF and Emissions Estimates for Inventory Creation

The ethane and methane estimated emissions rates can be combined with the PMF results presented in Chapter 4 to create an inventory of emissions by source. Using PMF, all seven resultant sources contributed to total methane or ethane emissions in the SoCAB. The fraction of the total emissions is then multiplied by the top-down emissions estimate from above to yield an estimate for emissions from a given sector. This inventory is shown in Table 6.4.

Table 6.4 Methane and ethane emissions inventories based on positive matrix factorization results and total emissions estimates calculated using the CARB CO inventory for 2015. The ranges associated with each sector fraction are the results from displacement analysis ($dQ_{\max} = 4$).

Source	Methane Factor Percentage from PMF	Methane Emissions Estimate from Source (Gg/year)	Ethane Factor Percentage from PMF	Ethane Emissions Estimate from Source (Gg/year)
Pipeline Natural Gas	59% (57-65%)	143 (111- 190)	51% (48-56%)	6.6 (4.8-8.9)
Oil and Natural Gas Production	3% (0-7%)	7 (0-20)	7% (5-9%)	0.9 (0.5-1.4)
Vehicular Emissions & Gasoline Evaporation	9% (4%-20%)	22 (7-58)	32% (25-56%)	4.2 (2.5-9.0)
BTEX	12% (9-13%)	29 (18-38)	---	---
Biogenic	5% (4-6%)	12 (8-18)	5% (4-5%)	0.7 (0.4-0.8)
Industrial	12% (11-15%)	29 (21-44)	5% (4-7%)	0.7 (0.4-1.12)
Total	100%	243 ± 49	100%	13 ± 3

This inventory was then compared with the most recent bottom-up inventory from the region presented in Peischl et al.¹² Ethane emissions have increased since 2010 (a difference of 1.6 Gg per year between 2010 and 2015), although the difference is within the error of the calculations. Peischl et al.¹² estimated 52% of all ethane emissions coming from pipeline natural gas which is in good agreement with the 51% (48-56%) reported here. Natural gas leakage continued to be the dominant source of ethane to the region suggesting that the control of pipeline natural gas leaks has not changed in the last several years. We report that only 7% (5-9%) of the excess ethane is coming from production of natural gas and oil which is lower than the nearly 40% in Peischl’s inventory.¹² This difference is made up by the 32% (25-56%) of ethane associated with vehicular and gasoline emissions. Ethane emissions from vehicular sources have increased significantly since 2010 via PMF. This is the only difference between the two ethane inventories suggesting that the slight increase in total ethane emissions would be due to vehicular sources. A study of a Northern California tunnel showed that tailpipe emissions of

ethane increased relative to benzene emissions between 1999 and 2005.²⁵ This agrees with the result here showing that ethane emissions from vehicular sources are increasing as fleet technology changes and improves.

Like ethane, total *n*-butane emissions have not changed significantly since 2010. Further, the fraction associated with each source has not changed with 69% (61-73%) associated with oil and gas production and refining as determined in this study. In 2010, $69 \pm 17\%$ of the *n*-butane was associated with the oil and gas industry.¹² This result seems likely as no new rules on VOC emissions have been implemented since 2010. Local air quality management rules require refineries to estimate total annual emissions of summed VOCs from planned and unexpected flaring events. While rules have been implemented regarding best practices so as to minimize total emissions, no hard caps exist on these gases.²⁶ Several studies have recently shown that total VOC emissions from refineries are higher than reported estimates from the individual sites.^{27,28} These discrepancies should be further studied to understand if this is a result of poor estimation guidelines or underreporting. If continued decreases in tropospheric ozone are sought, emissions from this sector must be more fully understood and regulated.

6.5 References

- (1) Bousquet, P.; Ciais, P.; Miller, J. B.; Dlugokencky, E. J.; Hauglustaine, D. A.; Prigent, C.; Van der Werf, G. R.; Peylin, P.; Brunke, E.-G.; Carouge, C.; et al. Contribution of anthropogenic and natural sources to atmospheric methane variability. *Nature* **2006**, *443* (7110), 439–443.
- (2) Fung, I.; John, J.; Lerner, J.; Matthews, E.; Prather, M.; Steele, L. P.; Fraser, P. J. Three-dimensional model synthesis of the global methane cycle. *J. Geophys. Res. Atmospheres* **1991**, *96* (D7), 13033–13065.
- (3) Kirschke, S.; Bousquet, P.; Ciais, P.; Saunio, M.; Canadell, J. G.; Dlugokencky, E. J.; Bergamaschi, P.; Bergmann, D.; Blake, D. R.; Bruhwiler, L.; et al. Three decades of global methane sources and sinks. *Nat. Geosci.* **2013**, *6* (10), 813–823.
- (4) Environmental Protection Agency. *Inventory of U.S. Greenhouse Gas Emissions and Sinks: 1990-2015*; Environmental Protection Agency, 2017.
- (5) Wennberg, P. O.; Mui, W.; Wunch, D.; Kort, E. A.; Blake, D. R.; Atlas, E. L.; Santoni, G. W.; Wofsy, S. C.; Diskin, G. S.; Jeong, S.; et al. On the Sources of Methane to the Los Angeles Atmosphere. *Environ. Sci. Technol.* **2012**, *46* (17), 9282–9289.

- (6) Hsu, Y.-K.; VanCuren, T.; Park, S.; Jakober, C.; Herner, J.; FitzGibbon, M.; Blake, D. R.; Parrish, D. D. Methane emissions inventory verification in southern California. *Atmos. Environ.* **2010**, *44* (1), 1–7.
- (7) California Air Resources Board. California Greenhouse Gas Emission Inventory: 2000–2014. California Environmental Protection Agency June 2016.
- (8) Gorham, K. A.; Blake, N. J.; VanCuren, R. A.; Fuelberg, H. E.; Meinardi, S.; Blake, D. R. Seasonal and diurnal measurements of carbon monoxide and nonmethane hydrocarbons at Mt. Wilson, California: Indirect evidence of atomic Cl in the Los Angeles basin. *Atmos. Environ.* **2010**, *44* (19), 2271–2279.
- (9) Barletta, B.; Nissenson, P.; Meinardi, S.; Dabdub, D.; Sherwood Rowland, F.; VanCuren, R. A.; Pederson, J.; Diskin, G. S.; Blake, D. R. HFC-152a and HFC-134a emission estimates and characterization of CFCs, CFC replacements, and other halogenated solvents measured during the 2008 ARCTAS campaign (CARB phase) over the South Coast Air Basin of California. *Atmos Chem Phys* **2011**, *11* (6), 2655–2669.
- (10) Barletta, B.; Carreras-Sospedra, M.; Cohan, A.; Nissenson, P.; Dabdub, D.; Meinardi, S.; Atlas, E.; Lueb, R.; Holloway, J. S.; Ryerson, T. B.; et al. Emission estimates of HCFCs and HFCs in California from the 2010 CalNex study. *J. Geophys. Res. Atmospheres* **2013**, *118* (4), 2019–2030.
- (11) Wunch, D.; Toon, G. C.; Hedelius, J. K.; Vizenor, N.; Roehl, C. M.; Saad, K. M.; Blavier, J.-F. L.; Blake, D. R.; Wennberg, P. O. Quantifying the loss of processed natural gas within California’s South Coast Air Basin using long-term measurements of ethane and methane. *Atmos Chem Phys* **2016**, *16* (22), 14091–14105.
- (12) Peischl, J.; Ryerson, T. B.; Brioude, J.; Aikin, K. C.; Andrews, A. E.; Atlas, E.; Blake, D.; Daube, B. C.; de Gouw, J. A.; Dlugokencky, E.; et al. Quantifying sources of methane using light alkanes in the Los Angeles basin, California: SOURCES OF METHANE IN L.A. *J. Geophys. Res. Atmospheres* **2013**, *118* (10), 4974–4990.
- (13) Newman, S.; Jeong, S.; Fischer, M. L.; Xu, X.; Haman, C. L.; Lefer, B.; Alvarez, S.; Rappenglueck, B.; Kort, E. A.; Andrews, A. E.; et al. Diurnal tracking of anthropogenic CO₂ emissions in the Los Angeles basin megacity during spring 2010. *Atmos Chem Phys* **2013**, *13* (8), 4359–4372.
- (14) California Air Resources Board. 2013 Almanac of Emissions - Emissions Calculator. 2013.
- (15) Gentner, D. R.; Harley, R. A.; Miller, A. M.; Goldstein, A. H. Diurnal and Seasonal Variability of Gasoline-Related Volatile Organic Compound Emissions in Riverside, California. *Environ. Sci. Technol.* **2009**, *43* (12), 4247–4252.
- (16) California Air Resources Board. History of Air Resources Board. October 22, 2014.
- (17) Cox, P.; Delao, A.; Komorniczak, A. *The California Almanac of Emissions and Air Quality - 2013 Edition*; California Air Resources Board, 2014.
- (18) California Air Resources Board. 2008 Almanac of Emissions- Emissions Calculator. 2009.
- (19) Pang, Y.; Fuentes, M.; Rieger, P. Trends in the emissions of Volatile Organic Compounds (VOCs) from light-duty gasoline vehicles tested on chassis dynamometers in Southern California. *Atmos. Environ.* **2014**, *83*, 127–135.
- (20) Brown, S. G.; Frankel, A.; Hafner, H. R. Source apportionment of VOCs in the Los Angeles area using positive matrix factorization. *Atmos. Environ.* **2007**, *41* (2), 227–237.

- (21) Simpson, I. J.; Chen, T.-Y.; Blake, D. R.; Rowland, F. S. Implications of the recent fluctuations in the growth rate of tropospheric methane. *Geophys. Res. Lett.* **2002**, *29* (10), 117–1.
- (22) Marrero, J. E.; Townsend-Small, A.; Lyon, D. R.; Tsai, T. R.; Meinardi, S.; Blake, D. R. Estimating Emissions of Toxic Hydrocarbons from Natural Gas Production Sites in the Barnett Shale Region of Northern Texas. *Environ. Sci. Technol.* **2016**.
- (23) Helmig, D.; Thompson, C. R.; Evans, J.; Boylan, P.; Hueber, J.; Park, J.-H. Highly Elevated Atmospheric Levels of Volatile Organic Compounds in the Uintah Basin, Utah. *Environ. Sci. Technol.* **2014**, *48* (9), 4707–4715.
- (24) Gilman, J. B.; Lerner, B. M.; Kuster, W. C.; de Gouw, J. A. Source Signature of Volatile Organic Compounds from Oil and Natural Gas Operations in Northeastern Colorado. *Environ. Sci. Technol.* **2013**, *47*(3), 1297-1305.
- (25) Pang, Y.; Fuentes, M.; Rieger, P. Trends in selected ambient volatile organic compound (VOC) concentrations and a comparison to mobile source emission trends in California's South Coast Air Basin. *Atmos. Environ.* **2015**, *122*, 686–695.
- (26) Air Quality Management District. *Control of Emissions from Refinery Flares*; 1998; Vol. 1118.
- (27) Ryerson, T. B.; Trainer, M.; Angevine, W. M.; Brock, C. A.; Dissly, R. W.; Fehsenfeld, F. C.; Frost, G. J.; Goldan, P. D.; Holloway, J. S.; Hübler, G.; et al. Effect of petrochemical industrial emissions of reactive alkenes and NO_x on tropospheric ozone formation in Houston, Texas. *J. Geophys. Res. Atmospheres* **2003**, *108* (D8), 4249.
- (28) Chambers, A. K.; Strosher, M.; Wootton, T.; Moncrieff, J.; McCready, P. Direct Measurement of Fugitive Emissions of Hydrocarbons from a Refinery. *J. Air Waste Manag. Assoc.* **2008**, *58* (8), 1047–1056.

CHAPTER 7: Emissions Estimates and Analysis of Refrigerant Halocarbons

7.1 Statistical Analysis and Calculation of Emissions Estimates

For the HCFCs discussed here, precision in any individual measurement is 2% and absolute accuracy is 5% for HCFC-22 and 10% for HCFC-141b and HCFC-142b as discussed in Chapter 2. For a sample to be truly enhanced in a given HCFC, the enhancement value must be greater than the 2σ precision inherent in the background average calculated as in Chapter 3. Compounds were said to have been emitted from the SoCAB in this study if more than 75% of the samples were enhanced in a given compound.

To calculate an annual emissions estimate for each of the HCFCs, CO is used as a tracer for anthropogenic emissions as it is emitted during the incomplete combustion of fossil fuels and has a lifetime on the order of months.¹ The long atmospheric lifetimes of HCFCs allow for these species to become well mixed with CO in air parcels travelling across the SoCAB.^{2,3} It has been established that for these long lived VOCs, the relationship to the emission of CO can be used as a scaling factor by which to get an emissions estimate for the VOC.²⁻⁵ The same calculation method that is presented in 6.2 is used here to calculate emissions estimates for both the 2014-2016 data set as well as the 2007 data set. There is no CARB CO emissions inventory for the year 2007. Instead the average from the 2006 and 2008 inventory is used to estimate 2007 CO emissions, yielding an estimate of 3389 tons day⁻¹ from the SoCAB.^{3,6} An error in these estimates is not given, but is assumed to be 20%.

7.2. Results

A statistical overview of the results obtained from the two sampling campaigns including the mean enhancements seen for each gas, is shown in Table 7.1. The overview suggests the continued emission of HFCs and some HCFCs, defined as having more than 75% of the samples

being enhanced at 2σ . For, HCFC-142b, the average enhancement has decreased dramatically and only 65% of samples were enhanced over 2σ suggesting that emissions may have stopped. For HFC-227ea and HFC-365mfc, detection and quantitation of these gases began during the current sampling campaign and 2007 data do not exist. The specific outcomes of the rules surrounding each gas will be discussed individually in the following sections.

Table 7.1 Summary of mixing ratios of first, second and third generation refrigerants seen in daytime samples collected at Mt. Wilson during the 2014-2016 campaign and the 2007 campaign (in parentheses).

Compound	Range (2007) ppt	Mean (2007) ppt	Mean Enhancement (2007) ppt	Percent of samples enhanced at 2σ (2007)	Percent of Samples enhanced 10% over background (2007)
CFC-12	513-564 (529-633)	531 ± 1 (559 ± 1)	16 ± 1 (21 ± 1)	67% (76%)	0% (3%)
CFC-11	225-276 (248-307)	238 ± 1 (263 ± 1)	10 ± 1 (10 ± 1)	77% (66%)	3% (6%)
CFC-113	72-83 (75-94)	75 ± 1 (81 ± 1)	2.3 ± 0.1 (2.4 ± 0.1)	65% (61%)	1% (2%)
HCFC-22	223-723 (195-1329)	351 ± 4 (374 ± 9)	91 ± 4 (133 ± 9)	94% (95%)	84% (96%)
HCFC-142b	23-41 (19-175)	26 ± 1 (34 ± 1)	2.02 ± 0.12 (12 ± 1)	65% (94%)	27% (88%)
HCFC-141b	23-96 (19-91)	33 ± 1 (28 ± 1)	7.8 ± 0.4 (7.0 ± 0.6)	91% (91%)	76% (80%)
HFC-134a	78-437 (45-435)	153 ± 3 (107 ± 4)	60.9 ± 2.477 (50 ± 3.5)	98% (97%)	91% (91%)
HFC-227ea	0.94-3.69	1.85 ± 0.04	0.69 ± 0.04	75%	---
HFC-365mfc	0.76-5.23	1.67 ± 0.02	0.50 ± 0.02	81%	---

Time series plots of mixing ratios for the three HCFCs for both Mt. Wilson campaigns are seen in Figures 7.1 through 7.4. The 2007 plots show samples collected each hour of the day for a nine day period, which illustrates the distinct diurnal pattern seen in samples collected at Mt. Wilson. Mixing ratios increase in daytime samples as the tropospheric boundary layer rises and Mt. Wilson is influenced by SoCAB air masses. At night, the boundary layer lowers to below the height of Mt. Wilson and samples collected are representative of the free troposphere.

For the 2007 Mt. Wilson data, it was determined that nighttime minima were not ever reached for HCFC-141b during the November sampling mission suggesting a local emissions sources considering the other gases show the normal diurnal cycle. Due to this unusual pattern, samples from November 2007 were removed prior to calculation of an emissions estimate for HCFC-141b. The plots from the campaign that began in 2014 show the seasonal patterns expected for HCFC mixing ratios (Figure 7.4). Daytime mixing ratios are often higher than the global background values as seen at Trinidad Head, CA.⁷ Mixing ratios peak in the summer when temperatures are highest in the SoCAB and mobile air conditioning units are most often used. Emissions slowly decrease reaching minima in the winter. This seasonal pattern has been noted previously for HCFC-22.⁸ The daily and seasonal mixing ratio patterns show the utility of the Mt. Wilson data sets; both global and local trends can be noted with long term monitoring at the site.

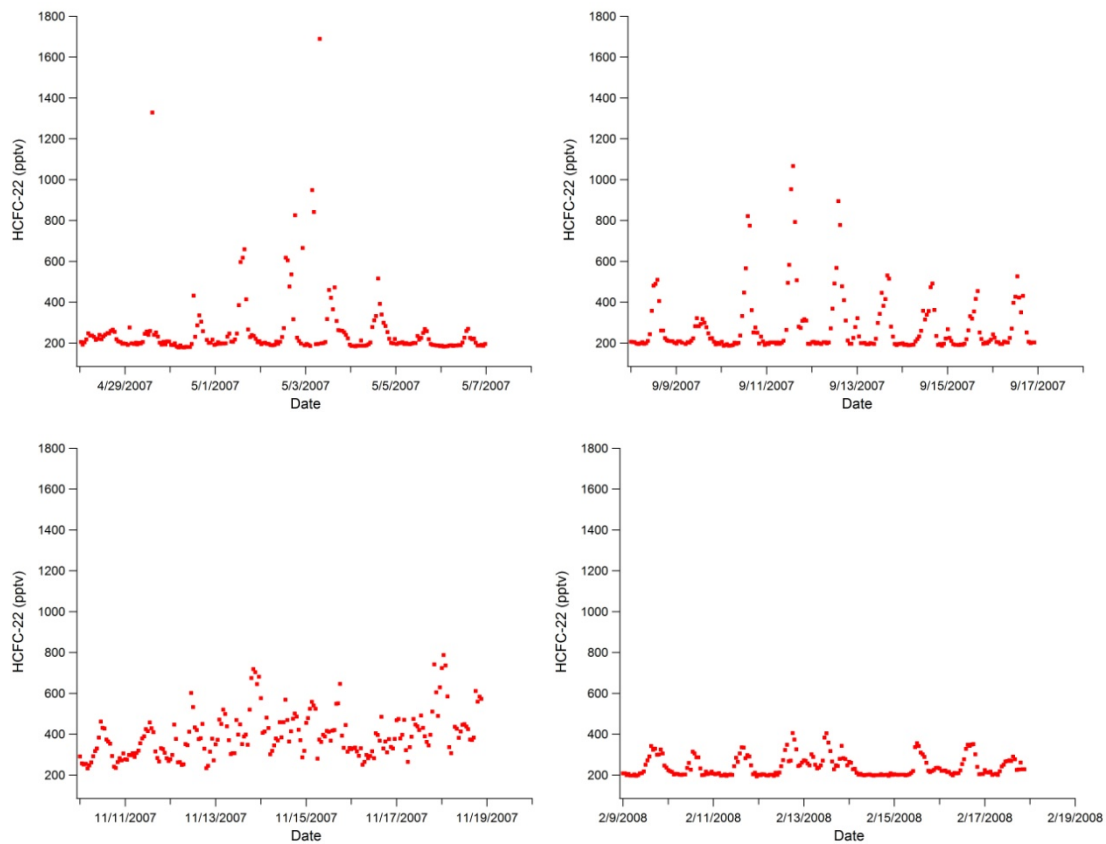


Figure 7.1. Temporal patterns of HCFC-22 mixing ratios as seen at Mt. Wilson during the 2007-2008 sampling campaign.

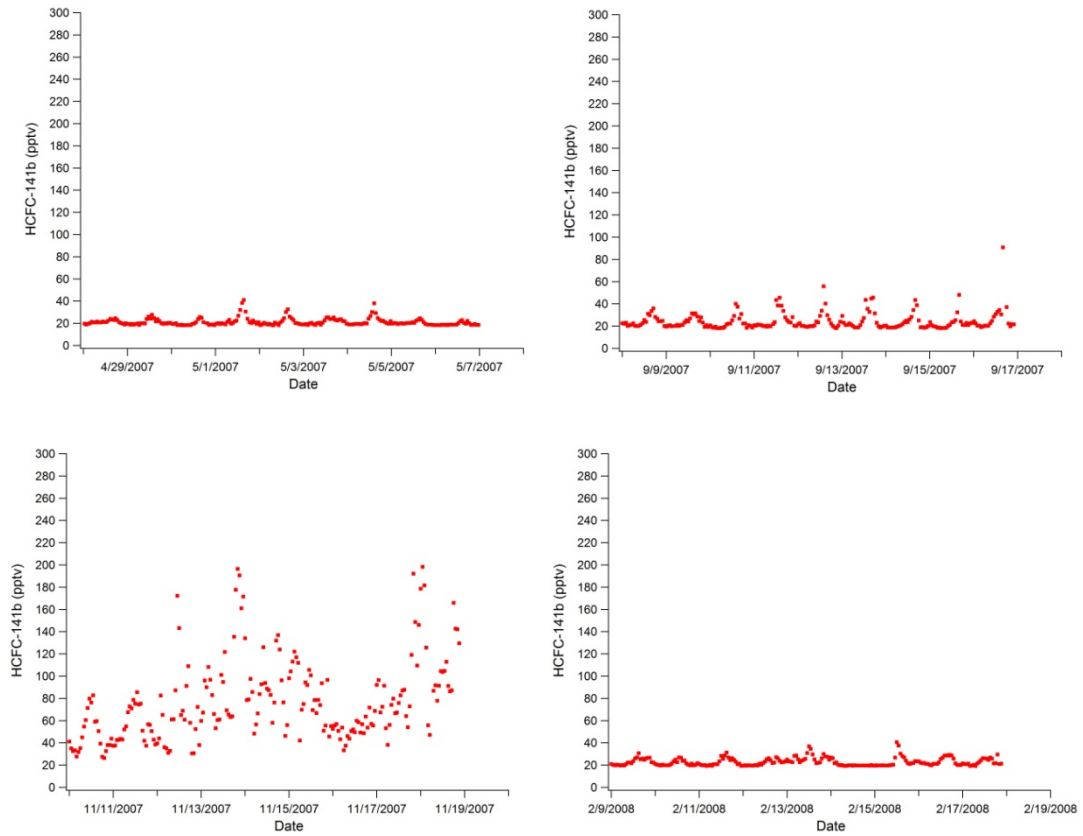


Figure 7.2 Temporal patterns of HCFC-141b mixing ratios as seen at Mt. Wilson during the 2007-2008 sampling campaign.

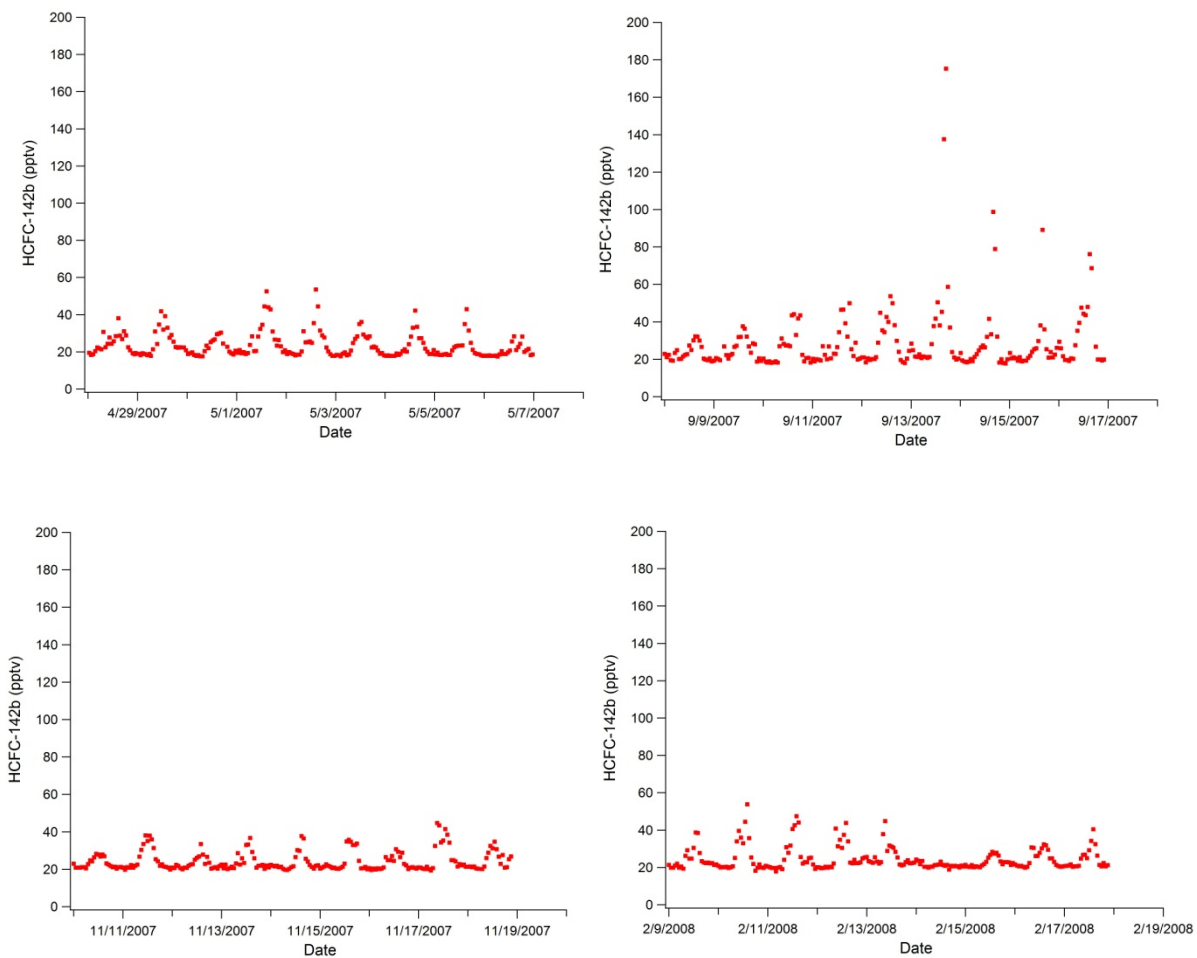


Figure 7.3 Temporal patterns of HCFC-142b mixing ratios as seen at Mt. Wilson during the 2007-2008 sampling campaign.

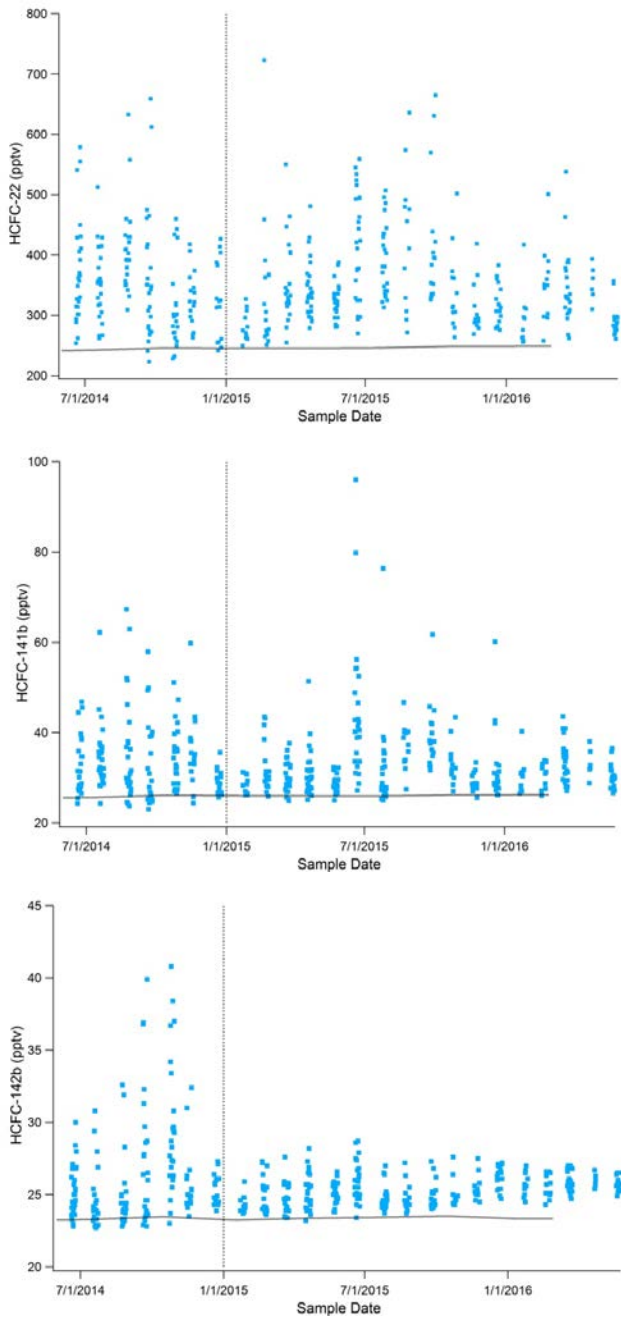


Figure 7.4 Temporal patterns in the mixing ratios of the three most emitted HCFCs as seen at Mt. Wilson during the 2014-2016 campaign. The vertical dotted line denotes the beginning of the lowered cap on HCFC consumption by the EPA, and the black horizontal line is the seasonal average seen at Trinidad Head, CA, part of the AGAGE Network.

7.2.1 Banned First Generation CFCs

The first generation of CFC refrigerants has been banned from use since the Montreal Protocol was enacted in 1989 with other countries banning the gases in the late 1970s. With the data sets available here, trends in atmospheric removal of the CFCs can be analyzed. Over the two years of data from Mt. Wilson, background F-12 concentrations have decreased by 5 ppt and F-11 concentrations by 6 ppt. When using the data set from 2007, background values have decreased 26 and 28 ppt for F-12 and F-11 respectively over the past eight years. Given that the atmospheric lifetimes of these species are on the scale of many decades, the rate of background decline is expected. Using the 75% cutoff for continued emission, it can be said that CFC-12 emissions have halted in the SoCAB, while CFC-11 emissions continue. This result is in agreement with a previous study of the region in 2005, where it was noted that CFC-11 emissions were occurring at a rate 0.24 Gg per year.⁹ This estimate is small in comparison to those of the replacement gases mentioned below, however it is still surprising given how long the ban has been in place. We are unable to calculate an updated emissions estimate for CFC-11 due to the low correlation between CFC-11 and carbon monoxide. It has been suggested previously that these continued emissions were stemming from landfills where old refrigeration units continue to leak out small amounts of CFC-11.⁹ The inability to calculate an emissions estimate using the known carbon monoxide inventory suggests that while there are continued F-11 emissions in the region, they are not collocated with carbon monoxide. This point gives a little more credence to the landfill emissions hypothesis. To test this, Gentner suggests studying the seasonality of emissions of CFCs. Due to higher temperatures and longer days, emissions from landfills increase in the summer months.⁹ The seasonality of CFC-11 emissions seen at Mt.

Wilson is shown in Figure 7.5. When comparing summer to autumn, as Gentner suggested, very little difference is seen in terms of enhancement ratios. The mean enhancement seen in summer samples (n=138) is 10 ± 1 ppt which is identical to the autumn ones (n= 107) of 10 ± 1 ppt. No seasonality is seen in either winter or spring as well. This result suggests that seasonality effects on landfill emissions as suggested by Gentner do not affect the emission of CFC-11. Finally, CFC-113 does not show any enhancement over background and therefore can be said to have

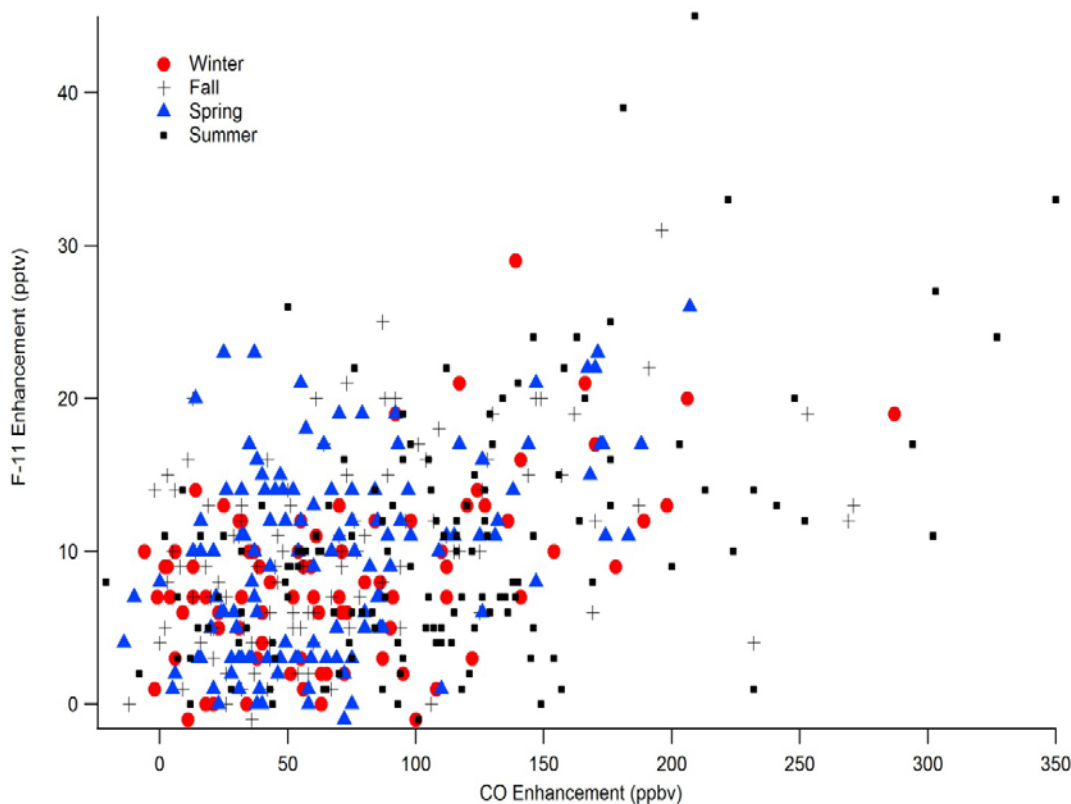


Figure 7.5 CFC-11 mixing ratio enhancements show no distinct seasonality in emissions when considering the two year Mt. Wilson data set presented here.

phased out successfully.

7.2.2 HCFC-22

HCFC-22 consumption is the largest of the three targeted HCFCs, and as such background levels are highest.¹⁰ Between spring (March-May) of 2007 and spring of 2016, the HCFC-22 background mixing ratio seen at Mt. Wilson was up 79 ppt (an 8.7 ppt yr⁻¹ increase) suggesting its continued use throughout the world. In terms of regulations, neither the 2007 amendment to the Montreal Protocol nor the EPA rules on HCFC consumption had been enacted making the 2007 data set is an excellent background from which to deduce if regulations have been working. In comparing the pre and post regulation campaigns, HCFC-22 mean enhancement values decreased 42 ± 12.5 ppt between 2007 and 2016. Further, calculating emissions estimates and comparing results with previous campaigns allows for a clear evaluation of how well these phase outs are working. Emissions estimates were calculated using the slopes of the correlation plots of HCFC-22 enhancement vs CO enhancement over background seen in Figure 7.6. The slope of the linear regression does not change when comparing enhancement plots to those of the measured mixing ratios, thus showing that seasonal backgrounds were calculated correctly. The R² values do increase when doing this analysis, suggesting the importance of background adjustments. The emissions estimates for the HCFCs studied here are summarized in Table 7.2. Annual HCFC-22 emissions decreased from 3.9 ± 0.8 Gg yr⁻¹ from 2007 to 1.9 ± 0.4 Gg yr⁻¹ in the SoCAB, which equates to a 53% reduction.

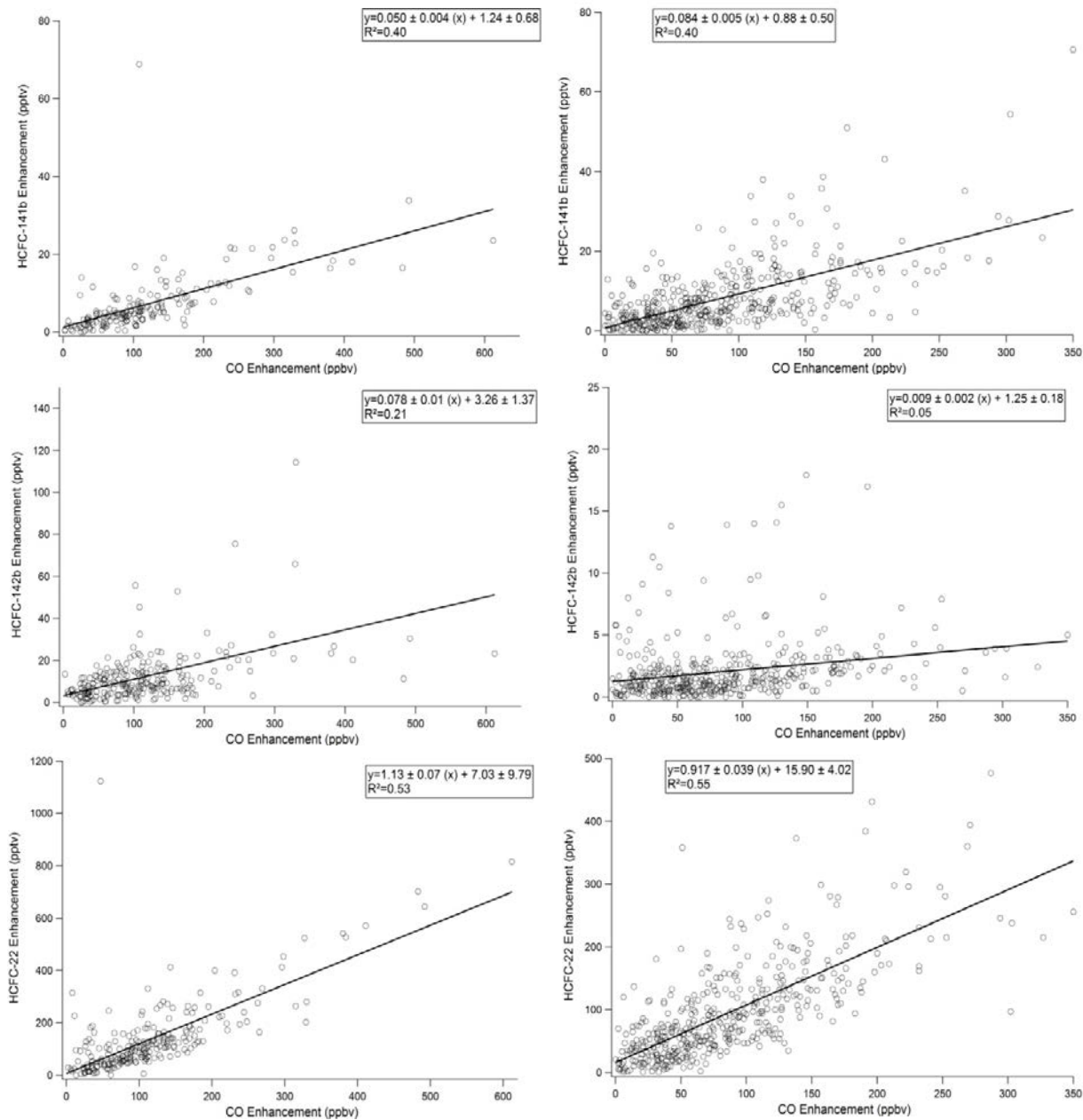


Figure 7.6 Enhancement plots of the three HCFCs studied here with carbon monoxide in both the 2007 (left) and 2014 (right) campaigns.

Table 7.2 Annual SoCAB emissions estimates for the three most emitted HCFCs and the major replacement, HFC-134a, during both Mt. Wilson sampling campaigns and Barletta et al. which was an airborne sampling mission over the SoCAB that took place in May 2010.

Study	HCFC-22 (Gg yr ⁻¹)	HCFC-142b (Gg yr ⁻¹)	HCFC-141b (Gg yr ⁻¹)	Total HCFC Emissions (Gg yr ⁻¹)	HFC-134a (Gg yr ⁻¹)
Mt. Wilson (2007-2008)	3.92 ± 0.82	0.32 ± 0.074	0.23 ± 0.05	4.47 ± 0.94	2.19 ± 0.44
Barletta et al ¹² (May 2010)	3.05 ± 0.70	0.06 ± 0.01	0.27 ± 0.07	3.38 ± 0.78	1.89 ± 0.43
Mt. Wilson (2014-2016)	1.85 ± 0.38	n.a.	0.23 ± 0.05	2.08 ± 0.43	1.77 ± 0.36

Saikawa et al.¹¹ modeled national HCFC-22 emissions using data dating back to 2005. They estimate that 65.80 ± 28.27 Gg yr⁻¹ of HCFC-22 was emitted in the continental United States in 2007. That estimate is further broken down by region with the western region contributing 19% of the total. This estimate can then be scaled down by population so as to calculate an estimate for the SoCAB. Using their estimate, the SoCAB would be responsible for 4.88 ± 1.94 Gg yr⁻¹ of HCFC-22 emissions in 2007. This result is higher than but agrees well with our regional emissions estimate of 3.92 ± 0.82 Gg yr⁻¹ suggesting the strength of the tracer gas estimation method, and furthering the conclusion that scaling national estimates by population overestimates emissions from the SoCAB.^{9,12}

Also included in Table 7.2 are results from a May 2010 airborne study of the SoCAB region by Barletta et al, which shows the immediate reduction in HCFC-22 emissions in light of the 2010 ban on importation and production.¹² Overall, the phase down appears to be working for HCFC-22 in the SoCAB as emissions have decreased since the start of regulations. However, continued decreases are not seen on a shorter term. The mean enhancement for June-December 2014 (108.6 ± 6.3 ppt) is nearly identical to that for the same 7 month stretch in 2015 (106.3 ± 7.7 ppt). CO emissions did not change significantly over that stretch either. This result is slightly

surprising as it was expected that further immediate reductions would be seen in light of the allowance reduction by the EPA that went into effect in January 1, 2015.¹³ The lack of a decrease suggests that while we might be on track to meet the goal of 100% reduction in consumption by 2030 of all HCFCs, it might be several years beyond that before local emissions become nonexistent. Air-conditioning and refrigeration units produced before regulations were instituted will be in service for years and decades to come, allowing for the opportunity for HCFCs to evaporate and be emitted into the troposphere. Indeed, after the appliance's lifetime ends, they will be transported to landfills where emissions of halocarbons has been noted.¹⁴

7.2.3 HCFC-141b

Background HCFC-141b mixing ratios between Spring 2007 and Spring 2016 are up $8.7 \text{ ppt} \pm 0.904$ ($0.97 \pm 0.10 \text{ ppt yr}^{-1}$). HCFC-141b was the first HCFC targeted for phase out due to its ozone depletion potential. The production and importation of HCFC-141b has been banned since 2003.¹³ Therefore, the 2007 Mt. Wilson campaign cannot be used as a baseline for SoCAB emissions, however it can still show the effectiveness of the rules put into place. The results suggest that there has been no reduction in HCFC-141b emissions since the 2007 campaign began. The mean daytime enhancement has increased slightly since 2007, equating to identical emissions estimates eight years apart. This result is surprising to the authors, as it was hypothesized that emissions reductions would happen gradually. However, this does not seem to be the case. Gentner et al.⁹ show that in November of 2005, HCFC-141b mixing ratios in Riverside, CA in the eastern portion of the SoCAB were regularly over 60 pptv.⁹ Here, there were only nine instances of the HCFC-141b mixing ratio being above 60 ppt in both data sets combined, suggesting that a significant reduction in consumption occurred between 2005 and 2007. A search of the literature did not yield any other urban HFC-141b measurements prior to

2005. The AGAGE network of remote monitoring stations does show that in the Northern Hemisphere, background levels of HCFC-141b leveled off for a two year stretch between 2004 and 2006 before continuing to rise.¹⁵ This pause in background mixing ratio increases might be a result of the 2003 ban on production and importation of HCFC-141b in the United States.

7.2.4 HCFC-142b

Background HCFC-142b mixing ratios between Spring 2007 and Spring 2016 are up $7.1 \text{ ppt} \pm 0.85$ ($0.788 \pm 0.0944 \text{ ppt yr}^{-1}$). In the 2007 campaign, it is clear that HCFC-142b was still being regularly emitted and therefore consumed. Daytime maxima are significantly higher than background values, and in seven instances, the noted mixing ratio was twice as large as the background. 88% of all daytime SoCAB samples were enhanced more than 10% above the background. Indeed, despite HCFC-142b being used primarily as a blowing agent, due to its wide use, there is still some correlation with CO allowing for an emissions estimate to be made. The 2007 estimate is five times larger than that seen in 2010 by Barletta et al.¹² suggesting that the initial ban on production and importation of HCFC-142b which went into effect on January 1, 2010 had an immediate effect on emissions.

The 2014-2016 campaign time series plot for HCFC-142b shows the most dramatic effect of the current phase out of HCFCs (Figure 7.4). It is very apparent that enhancements drop off dramatically after December 2014. While, HCFC-142b importation and production has been limited to servicing existing equipment since 2010, it is clear that the allowance holders turned away from using HCFC-142b after 2014. This may be due to the overall mandated decrease in consumption that began on January 1, 2015.¹³ The EPA phase down step mandated a 90% reduction in consumption and production of all HCFCs by 2015, stepping down from 75% reduction in 2010. In the seven months of 2014 that were sampled, local emissions were still

fairly minimal with an average daytime enhancement of only 3.3 ppt. However, some samples still showed significant enhancements indicating its use in the SoCAB (up to 18 ppt enhancement). The 32 most enhanced samples in the two year study are all from between June and December 2014 and only 7 of the top 10% of all daytime samples are from beyond December 2014. Due to the initial rule in 2010, emissions in 2014 were less widespread and did not correlate with CO which results in not being able to estimate emissions. In 2015, the mean enhancement was only 1.5 ppt over background with a range between the highest and lowest mixing ratio seen of 5.5 ppt. Further, no samples collected in 2015 or 2016 were enhanced over the 2σ error to be considered to be SoCAB emissions. Given these facts, we can say that as of 2015, HCFC-142b is no longer being emitted from the SoCAB.

As a final check of the EPA rules, we can look at total HCFC emissions in the SoCAB over the study period. In 2007, the sum of emissions of the three most common HCFCs in the SoCAB was $4.47 \pm 0.94 \text{ Gg yr}^{-1}$. As of the first half of 2016, the summed emissions estimate was 2.08 ± 0.43 , a 54% reduction from the 2007 baseline study presented here. That reduction came from a 53% reduction in HCFC-22 emissions stemming from the 2010 ban on importation and the phase down in allowances sold to industry, most recently in 2015.¹³ While emissions estimates from prior to 2007 do not exist in the literature, the reduction since 2007 suggests the efficacy of the rules put into place by the EPA.

7.2.5 HCFC Replacements

With the continued need for refrigerants and foam blowing agents, industry has turned to third generation halocarbons which broadly fall into the category of hydrofluorocarbons (HFCs). These compounds do not contain chlorine giving them zero ozone depletion potential, but they do still act as powerful greenhouse gases. In response to the phaseout of HCFCs, the use of

HFCs has grown.¹⁵ HFC-134a is targeted as the main replacement for HCFC-22 in refrigeration uses. In 2007 in the SoCAB, emissions of HFC-134a were already at 2.19 ± 0.44 Gg yr⁻¹, which is roughly half of the sum of all HCFC emissions in that year. The emission of HFC-134a decreased slightly from 2007 as measured in 2014-2016 campaign (1.77 ± 0.36 Gg yr⁻¹) but remains within the margins of error of the 2007 value showing that HFC-134a is in continued use across the SoCAB.

HFC-365mfc is the main replacement for HCFC-141b in foam blowing uses. With a global warming potential of 804, it is important that emissions monitoring be continued to ensure minimal leakage while being used in industry settings. HFC-365mfc was detected and quantitated preliminarily during the 2014-2016 campaign, and a time series plot of its mixing ratios is shown in Figure 7.7. The average daytime enhancement for HFC-365mfc between August 2014 and May 2016 is 0.47 ± 0.02 ppt which is significantly higher than the local background showing that it is actively being emitted from the SoCAB. The gas has also been measured at remote locations and background levels have increased to over 1 ppt since monitoring began in 2005.⁷

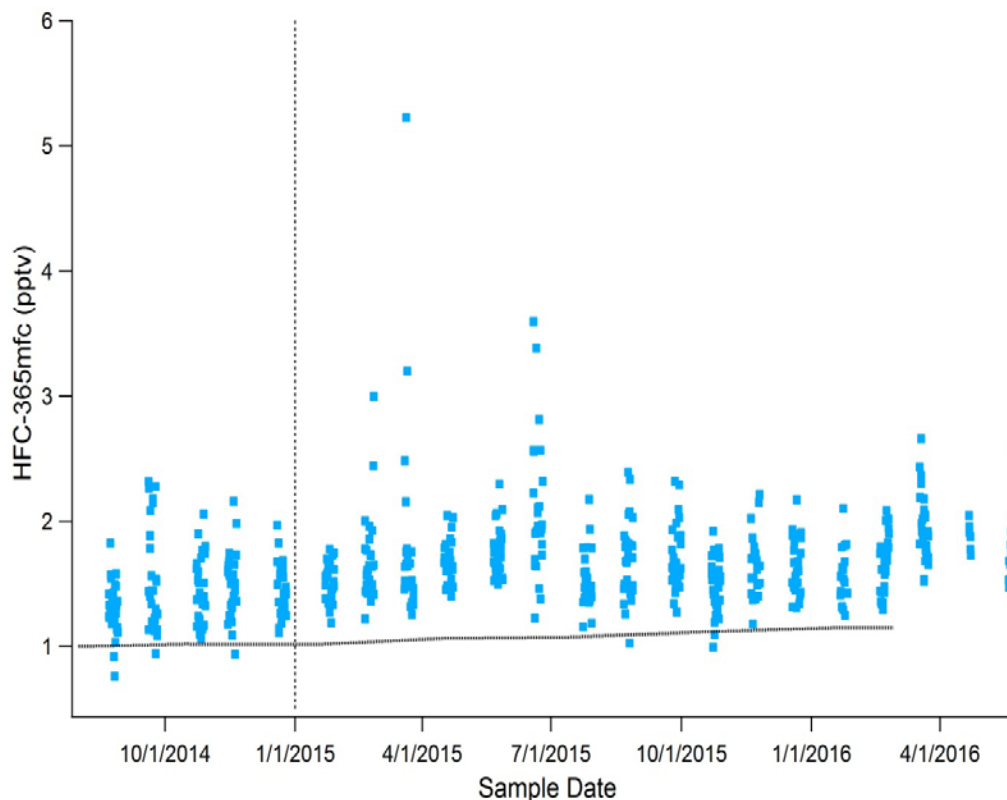


Figure 7.7 Temporal patterns in the mixing ratios of HFC-365mfc at Mt. Wilson during the 2014-2016 campaign. HFC-365mfc is the main industrial replacement for HCFC-141b. The results presented here are still exploratory, and so error on any given data point is $\pm 50\%$. The vertical dotted line denotes the beginning of the lowered cap on HCFC consumption by the EPA, and the black horizontal line is the seasonal average seen at Trinidad Head, CA, part of the AGAGE Network.

7.3 Conclusions

Hydrochlorofluorocarbons are currently undergoing phase out in the United States due to their ozone depletion potential. Over the past fifteen years, several rules have been put in place to limit the production and consumption of these gases with the goal of complete phaseout. Using data from two field campaigns in the South Coast Air Basin over a nine year time period between 2007 and 2016, we have shown that the rules put into place by the EPA are working towards limiting the emission of the three most emitted HCFCs. HCFC-22 emissions have decreased over 50% since 2007; however it appears that future decreases might occur more

slowly. Phase out of HCFC-141b began prior to the first SoCAB study, but our data show that the ban on production and importation is being followed as the emission rate of the gas has not changed since 2007. Finally, HCFC-142b has seen a dramatic decrease in daytime enhancements when comparing the two campaigns. It was shown that it is no longer emitted in the SoCAB as of 2015 in response to a decrease in the cap on allowances for HCFCs. As these gases are phased out of use, a newer generation of HFCs must be monitored as they are potent greenhouse gases, whose emissions will continue to increase. This study shows the importance of national rule making on environmental policy as, once enacted, the rules do get followed and immediate improvements are seen.

7.4 References

- (1) Newman, S.; Jeong, S.; Fischer, M. L.; Xu, X.; Haman, C. L.; Lefer, B.; Alvarez, S.; Rappenglueck, B.; Kort, E. A.; Andrews, A. E.; et al. Diurnal tracking of anthropogenic CO₂ emissions in the Los Angeles basin megacity during spring 2010. *Atmos Chem Phys* **2013**, *13* (8), 4359–4372.
- (2) Hsu, Y.-K.; VanCuren, T.; Park, S.; Jakober, C.; Herner, J.; FitzGibbon, M.; Blake, D. R.; Parrish, D. D. Methane emissions inventory verification in southern California. *Atmos. Environ.* **2010**, *44* (1), 1–7.
- (3) Gorham, K. A.; Blake, N. J.; VanCuren, R. A.; Fuelberg, H. E.; Meinardi, S.; Blake, D. R. Seasonal and diurnal measurements of carbon monoxide and nonmethane hydrocarbons at Mt. Wilson, California: Indirect evidence of atomic Cl in the Los Angeles basin. *Atmos. Environ.* **2010**, *44* (19), 2271–2279.
- (4) Wunch, D.; Toon, G. C.; Hedelius, J. K.; Vizenor, N.; Roehl, C. M.; Saad, K. M.; Blavier, J.-F. L.; Blake, D. R.; Wennberg, P. O. Quantifying the loss of processed natural gas within California's South Coast Air Basin using long-term measurements of ethane and methane. *Atmos Chem Phys* **2016**, *16* (22), 14091–14105.
- (5) Barletta, B.; Nissenson, P.; Meinardi, S.; Dabdub, D.; Sherwood Rowland, F.; VanCuren, R. A.; Pederson, J.; Diskin, G. S.; Blake, D. R. HFC-152a and HFC-134a emission estimates and characterization of CFCs, CFC replacements, and other halogenated solvents measured during the 2008 ARCTAS campaign (CARB phase) over the South Coast Air Basin of California. *Atmos Chem Phys* **2011**, *11* (6), 2655–2669.
- (6) California Air Resources Board. 2008 Almanac of Emissions- Emissions Calculator. 2009.
- (7) Prinn, R. G.; Weiss, R. F.; Krummel, P. B.; O'Doherty, S.; Fraser, P. J.; Muhle, J.; Reimann, S.; Vollmer, M. K.; Simmonds, P. G.; Maione, M.; et al. *The ALE / GAGE AGAGE Network*; Carbon Dioxide Information Analysis Center (CDIAC), Oak Ridge National Laboratory, U.S. Department of Energy (DOE), 2016.

- (8) Xiang, B.; Patra, P. K.; Montzka, S. A.; Miller, S. M.; Elkins, J. W.; Moore, F. L.; Atlas, E. L.; Miller, B. R.; Weiss, R. F.; Prinn, R. G.; et al. Global emissions of refrigerants HCFC-22 and HFC-134a: Unforeseen seasonal contributions. *Proc. Natl. Acad. Sci.* **2014**, *111* (49), 17379–17384.
- (9) Gentner, D. R.; Miller, A. M.; Goldstein, A. H. Seasonal Variability in Anthropogenic Halocarbon Emissions. *Environ. Sci. Technol.* **2010**, *44* (14), 5377–5382.
- (10) Montzka, S. A.; McFarland, M.; Andersen, S. O.; Miller, B. R.; Fahey, D. W.; Hall, B. D.; Hu, L.; Siso, C.; Elkins, J. W. Recent Trends in Global Emissions of Hydrochlorofluorocarbons and Hydrofluorocarbons: Reflecting on the 2007 Adjustments to the Montreal Protocol. *J. Phys. Chem. A* **2015**, *119* (19), 4439–4449.
- (11) Saikawa, E.; Rigby, M.; Prinn, R. G.; Montzka, S. A.; Miller, B. R.; Kuijpers, L. J. M.; Fraser, P. J. B.; Vollmer, M. K.; Saito, T.; Yokouchi, Y.; et al. Global and regional emission estimates for HCFC-22. *Atmos Chem Phys* **2012**, *12* (21), 10033–10050.
- (12) Barletta, B.; Carreras-Sospedra, M.; Cohan, A.; Nissenson, P.; Dabdub, D.; Meinardi, S.; Atlas, E.; Lueb, R.; Holloway, J. S.; Ryerson, T. B.; et al. Emission estimates of HCFCs and HFCs in California from the 2010 CalNex study. *J. Geophys. Res. Atmospheres* **2013**, *118* (4), 2019–2030.
- (13) US EPA. Phaseout of Class II Ozone-Depleting Substances <https://www.epa.gov/ods-phaseout/phaseout-class-ii-ozone-depleting-substances> (accessed Jun 7, 2017).
- (14) Hodson, E. L.; Martin, D.; Prinn, R. G. The municipal solid waste landfill as a source of ozone-depleting substances in the United States and United Kingdom. *Atmos Chem Phys* **2010**, *10* (4), 1899–1910.
- (15) Simmonds, P. G.; Rigby, M.; McCulloch, A.; O’Doherty, S.; Young, D.; Mühle, J.; Krummel, P. B.; Steele, P.; Fraser, P. J.; Manning, A. J.; et al. Changing trends and emissions of hydrochlorofluorocarbons (HCFCs) and their hydrofluorocarbon (HFCs) replacements. *Atmos Chem Phys* **2017**, *17* (7), 4641–4655.

CHAPTER 8: Conclusions

In order to try and prevent climate change, work must be done to reduce global greenhouse gas emissions. The state of California has been a leader in policy and innovation aimed at protecting our climate and way of life. In this work, a study funded by the California Air Resources Board is described in which greenhouse gas concentrations in air masses influenced by the Los Angeles megacity were monitored. Each month for two years running from June 2014 to May of 2016, whole air samples were collected at Mt. Wilson, California which sits downwind of Los Angeles and the metropolitan portion of the South Coast Air Basin. These samples were analyzed via gas chromatography analysis for over seventy compounds including greenhouse gases, air toxics, and reactive species that can form tropospheric ozone. This very large data set was used to characterize, quantify, and apportion the emissions of short-lived greenhouse gases within the SoCAB.

The most emitted of these gases, methane, was the focus of most of this dissertation work. There are several different sources of methane within the region. Evidence of varying sources was seen in the analysis of the ethane to methane enhancement ratio seen in each sample. It was noted that there was significant variation in this ratio from sample to sample and the average ratio had increased as compared to previous studies in the region. Other tracer ratios were used to show that oil and gas production and distribution was playing a larger role in the region than previously thought.

To further study the role of natural gas in the region, the composition of delivered gas was monitored in the SoCAB. The composition was noted to vary significantly between November 2014 and October 2015. This was best described by the ethane to methane ratio which ranged from 2-5% during that time. This result had not been noted before. It had been previously

assumed that natural gas composition remained constant over long periods of time and one compositional data point could be used in a regional inventory. This work showed the importance of monitoring the composition of natural gas as using one data point could lead to a gross under or over estimation of total emissions from the sector.

Using the California Air Resources Board's carbon monoxide inventory, it was determined that total methane emissions to the region were 243 ± 49 gigagrams per year over the period studied. This result was found to be lower than the estimate put forward in older studies of the region suggesting an overall decrease in methane emissions. To further study where these remaining emissions were coming from positive matrix factorization analysis was employed. It was determined that over 60% of the methane emitted from the SoCAB stemmed from the leakage of unburned pipeline natural gas. This result was found to be in agreement with previous studies from the region that suggested natural gas, not landfills, was the predominant source of methane.

Combining these results with regulatory data showed that there is a significant gap between what is reported as lost gas by the local gas company and what is actually being emitted. If the gas company is to be believed, there must be another source of natural gas to the region. A preliminary study conducted at UC, Irvine showed that there is significant post meter leakage of natural gas. This leakage would not be accounted for by the natural gas company, and if it is widespread enough, could help close the gap between the top-down estimate calculated here and what is being reported as lost.

Finally, several classes of refrigerant gases that are potent greenhouse gases were studied in the SoCAB as well. Emissions estimates were calculated for the Mt. Wilson data set and compared to previous studies in the region. Data showed across the board reductions in annual

emissions of these gases. This result is encouraging and should be used as an example of what policy and phase out schedules for greenhouse gases can look like and the results that can be achieved.